



This work is protected by copyright and other intellectual property rights and duplication or sale of all or part is not permitted, except that material may be duplicated by you for research, private study, criticism/review or educational purposes. Electronic or print copies are for your own personal, non-commercial use and shall not be passed to any other individual. No quotation may be published without proper acknowledgement. For any other use, or to quote extensively from the work, permission must be obtained from the copyright holder/s.

**Changes in advanced glycation content, structural
and mechanical properties of vaginal tissue
during pregnancy and in prolapse**

Homayemem Kinikanwo Weli

Institute for Science and Technology in Medicine

Thesis submitted to Keele University for the degree of Doctor of Philosophy

June, 2018.

ABSTRACT

Introduction: Pelvic organ prolapse is present in up to 50% of women. It is commoner in older women, often above 50 years of age and associated with hormonal e.g. oestrogen decline, and stiffer vaginal tissue. Pregnancy, on the contrary is a physiologic condition with higher oestrogen level and exhibits reversible structural and mechanical changes in pelvic tissues. Advanced glycation products, the ageing markers, stiffen connective tissues. There has been no previous systematic study on the relationship and action mechanisms of oestrogen, glycation level and mechanical property of vaginal tissues.

Aim: The aim of this project was to study the ultrastructural and mechanical properties of vaginal tissues, and understand the relationship and possible mechanisms of accumulation of glycation (pentosidine), vaginal wall mechanics and oestrogen receptor (ER- α) expression in the vaginal tissues in both pregnancy and prolapse. It was hypothesised that prolapse is a disease of accelerated ageing and that mechanical and ultrastructural changes in prolapsed tissues and oestrogen decline are related to the elevation of glycation content in the tissues.

Methods: Following ethical approval, vaginal tissues from 49 women with prolapse and 16 controls were obtained and proformas containing information on known and suspected prolapse associations were completed for each participant. Female Sprague Dawley rats' vaginal tissues were used for the pregnancy study. Nano-scale, micro-scale and tissue level mechanical characterizations of the tissues were performed using ball indentation technique, scanning electron microscopy, peakforce nanomechanical property mapping atomic force microscopy, and optical coherence elastography, which was applied for the first time to the study of vaginal tissues. The glycation contents of vaginal tissues in pregnancy and prolapse were quantified by high performance liquid chromatography and values obtained were analysed in comparison to medical comorbidities. Tissues were qualified by histological and immunological staining for structure (haematoxylin & eosin, trichrome and picosirus red stainings), glyoxalase I, ER- α , elastin and neural stain. A sulphated glycosaminoglycan (sGAG)-collagen model was used to study the role of sGAG in collagen fibrillogenesis.

Results: Rat vaginal tissues in pregnancy contained significantly lower amounts of pentosidine, higher oestrogen receptor- α and glyoxalase I (antioxidant enzyme) expression with larger creep, lower elastic modulus, larger fibril diameter and higher sGAG content than their non-pregnant counterparts. Observed morphological changes of the collagen fibrils in pregnancy were attributed to sGAG, which was noted to influence collagen fibril aggregation and bundling. Skin pentosidine content was reflective of vaginal tissue pentosidine in the same subjects. Pentosidine was significantly higher in prolapsed tissues and increased with age; with more age-dependent increase observed in the prolapse population and also significantly different between the 6th and 7th decades. Glyoxalase I and ER- α were poorly expressed in the prolapsed tissues in comparison to controls. Prolapsed tissues had notably disorganized ultrastructure and higher collagen fibril modulus. At all levels of tissue organization, prolapsed tissues were stiffer than controls, with increased stiffening at the more superficial layers of the tissue. Hypertension and smoking were associated with higher glycation and prolapse. In both pregnancy and prolapse, higher expression of glyoxalase I and ER- α were associated with lower glycation content of the vaginal tissues and lower modulus. These observations have led to the suggestions that oestrogen plays an important role in increase or reduction of glycation through an oestrogen-gluthathione-glyoxalase (antioxidant) pathway, which directly affects vaginal tissues' mechanics.

Future implications: These findings have implications to the current understanding of how prolapse may occur and can inspire future translational research on improved treatment of women with prolapse. Oestrogen may significantly influence the temporary and permanent mechanics of pelvic tissues such as the vaginal wall through its modulation of glycation accumulation within the tissues. Oestrogen thus shows promise of a potential future medical treatment for early stages of prolapse. The knowledge of new prolapse comorbidities can aid the early detection and possible prevention of prolapse through a high index of suspicion.

CONTENTS

ABSTRACT	ii
FIGURES	xiii
TABLES	xxii
ABBREVIATIONS	xxiii
PUBLICATIONS	xxvii
ACKNOWLEDGEMENT	xxix
CHAPTER 1: BACKGROUND	0
1.1 STRUCTURAL AND FUNCTIONAL ASPECTS OF THE FEMALE PELVIS	1
1.1.1 OVERVIEW	1
1.1.2 BONY PELVIS	1
1.1.3 PELVIC DIAPHRAGM, LIGAMENTS AND FASCIA.....	2
1.1.4 LEVELS OF PELVIC ORGAN SUPPORT	3
1.2 VAGINAL CONNECTIVE TISSUE STRUCTURE AND BIOMECHANICS	6
1.2.1 HISTOLOGY OF THE VAGINA	6
1.2.2 VAGINAL MECHANICS	7
1.2.3 THE VAGINA AS A CENTRAL PELVIC SUPPORT	7
1.2.4 VAGINAL TISSUE EXTRACELLULAR MATRIX (ECM).....	9
1.3 PREGNANCY AND OESTROGEN EFFECTS ON THE VAGINAL WALL CONNECTIVE TISSUE.....	11
1.3.1 OVERVIEW.....	11
1.3.2 THE RELATIONSHIP BETWEEN COLLAGEN, MATRIX REMODELLING ENZYMES AND OESTROGEN	13

1.4	CONNECTIVE TISSUE AGEING.....	14
1.4.1	OVERVIEW.....	14
1.4.2	AGEING THEORIES AND GLYCATION MARKERS OF AGEING	15
1.4.3	FORMATION OF ADVANCED GLYCATION END PRODUCTS (AGEs)...	17
1.4.4	TYPES OF AGEs.....	18
1.4.5	ACCUMULATION AND REMOVAL OF AGEs <i>IN VIVO</i>	19
1.4.6	AGEs REACTION MECHANISM	20
1.4.7	EFFECT OF AGEs ON THE ECM	21
1.5	PELVIC ORGAN PROLAPSE.....	22
1.5.1	OVERVIEW.....	22
1.5.2	EPIDEMIOLOGY.....	24
1.5.3	GRADING OF DISEASE SEVERITY AND SYMPTOMS.....	24
1.5.4	CURRENT TREATMENT.....	26
1.5.5	KNOWN AND POTENTIAL RISK FACTORS.....	27
1.5.6	CONNECTIVE TISSUE CHANGES IN PROLAPSED TISSUE	31
1.6	VAGINAL WALL MECHANICS IN PREGNANCY AND PROLAPSE	35
1.6.1	PREGNANCY	35
1.6.2	PELVIC ORGAN PROLPASE.....	37
1.6.3	AGE AND MENOPAUSE.....	38

1.7	METHODS FOR CONNECTIVE TISSUE STRUCTURAL AND MECHANICAL ANALYSIS	39
1.7.1	CONNECTIVE TISSUE STRUCTURAL AND MORPHOLOGICAL ANALYSIS.....	39
1.7.2	MECHANICAL TESTS	46
1.7.3	QUANTIFICATION OF COLLAGEN	49
1.7.4	AGEs DETECTION.....	50
	CHAPTER 2: HYPOTHESES AND AIMS.....	53
2.1	HYPOTHESES.....	54
2.1.1	PROLAPSE IS A DISEASE OF ACCELERATED AGEING AND VAGINAL TISSUE ARE STRUCTURALLY AND MECHANICALLY ALTERED IN RELATION TO THEIR GLYCATION CONTENT	54
2.1.2	GLYCATION ACCUMULATION IN PELVIC TISSUES IS INFLUENCED BY OESTROGEN	55
2.2	RESEARCH AIMS	56
	CHAPTER 3: MATERIALS AND METHODS	58
3.1	TISSUES AND ETHICS.....	59
3.1.1	RAT TISSUES: ETHICAL APPROVAL AND DISSECTION.....	59
3.1.2	HUMAN TISSUES: ETHICAL APPROVAL, PARTICIPANT RECRITMENT, CONSENT TAKING AND DATA CHARACTERISTICS.....	60
3.2	STRUCTURAL AND MORPHOLOGICAL STUDIES	62
3.2.1	HAEMATOXYLIN AND EOSIN (H&E).....	62

3.2.2	ELASTIN STAINING	62
3.2.3	NEURAL STAINING.....	63
3.2.4	TRICHROME STAINING	63
3.2.5	SIRUS RED STAINING.....	64
3.2.6	SCANNING ELECTRON MICROSCOPY (SEM) OF VAGINAL TISSUES .	64
3.2.7	OPTICAL COHERENCE TOMOGRAPHY (OCT).....	65
3.2.8	AFM ANALYSIS	65
3.3	BIOCHEMICAL ANALYSES	66
3.3.1	SULPHATED GLYCOSAMINOGLYCANS (sGAG) AND WATER CONTENT.....	66
3.3.2	AGEING BIOMARKER DETECTION	67
3.3.3	COLLAGEN ASSAY	70
3.3.4	IMMUNOCHEMISTRY.....	70
3.4	BIOMECHANICAL TESTS.....	71
3.4.1	BALL INDENTATION MECHANICAL TESTING.....	71
3.4.2	NANOMECHANICAL MAPPING BY ATOMIC FORCE MICROSCOPY (PFNMAFM).....	82
3.4.3	OPTICAL COHERENCE ELASTOGRAPHY (OCE).....	83
3.5	MODEL STUDY OF THE EFFECT OF sGAG ON COLLAGEN FIBRILLOGENESIS.....	85

3.6	STATISTICS	87
-----	------------------	----

**CHAPTER 4: PHYSIOLOGICAL CHANGES OF VAGINAL TISSUE IN PREGNANCY-
EVALUATION OF ADVANCED GLYCATION PRODUCTS' LEVELS, TISSUE MECHANICS AND
STRUCTURE89**

4.1	GLYCATION, MECHANICS AND STRUCTURAL CHANGES OF NATIVE VAGINAL TISSUES IN PREGNANCY	90
-----	---	----

4.1.1	INTRODUCTION.....	90
-------	-------------------	----

4.1.2	AIMS.....	91
-------	-----------	----

4.1.3	METHODS.....	91
-------	--------------	----

4.1.4	RESULTS.....	91
-------	--------------	----

4.1.5	DISCUSSION	105
-------	------------------	-----

4.2	INFLUENCE OF SULPHATED GLYCOSAMINOGLYCANS ON COLLAGEN FIBRILLOGENESIS AND STRUCTURE- AN IN VITRO STUDY	111
-----	---	-----

4.2.1	INTRODUCTION.....	111
-------	-------------------	-----

4.2.2	AIMS.....	112
-------	-----------	-----

4.2.3	METHODS.....	113
-------	--------------	-----

4.2.4	RESULTS.....	113
-------	--------------	-----

4.2.5	DISCUSSION	119
-------	------------------	-----

4.2.6	CONCLUSION.....	122
-------	-----------------	-----

4.3	THE CORRELATION OF GLYCATION CONTENT IN THE SKIN AND VAGINAL TISSUE IN PREGNANCY	123
-----	---	-----

4.3.1	INTRODUCTION.....	123
-------	-------------------	-----

4.3.2	AIM.....	124
4.3.3	METHODS.....	124
4.3.4	RESULTS.....	124
4.3.5	DISCUSSION	126
4.3.6	CONCLUSION	129
CHAPTER 5: GLYCATION CHANGES OF VAGINAL TISSUES IN PROLAPSE IN RELATION TO KNOWN AND POTENTIAL RISK FACTORS		130
5.1.1	INTRODUCTION.....	131
5.2	AIMS	132
5.3	METHODS.....	133
5.4	RESULTS.....	133
5.4.1	VALIDATION TESTS FOR TISSUE STORAGE AND DRYING METHOD 133	
5.4.2	OVERVIEW OF RECRITUTED PATIENT CHARACTERISTICS	136
5.4.3	PENTOSIDINE QUANTITY IN PROLAPSED AND CONTROL GROUPS AND ITS POTENTIAL RELATIONSHIP WITH RISK FACTORS, PROLAPSE GRADE AND SYMPTOM PERCEPTION	143
5.4.4	ER- α AND GLO-I EXPRESSION	154
5.5	DISCUSSION.....	158
5.5.1	INFLUENCE OF TISSUE STORAGE ON PENTOSIDINE CONTENT OF TISSUES.....	158

5.5.2	GLYCATION IN PROLAPSED VAGINAL TISSUES	159
5.5.3	GLYCATION AND AGE IN PROLAPSED VAGINAL TISSUES.....	160
5.5.4	OESTROGEN INFLUENCE ON GLYOXALASE AND GLYCATION (INFLUENCE OF MENOPAUSE AND AGE)	161
5.5.5	THE ASSOCIATION OF GLYCATION IN PROLAPSED TISSUES TO HYPERTENSION, DM, CHOLESTEROL AND SMOKING	163
5.5.6	THE ASSOCIATION OF SEVERITY/ICIQVS AND PROLAPSE GRADE TO GLYCATION OF PROLAPSED TISSUES AND PROLAPSE TYPES	165
5.6	CONCLUSION	166
CHAPTER 6: A STUDY OF THE STRUCTURAL AND MECHANICAL PROPERTIES OF PROLAPSED VAGINAL TISSUES		168
6.1	INTRODUCTION	169
6.2	AIM	170
6.3	METHODS.....	170
6.4	RESULTS.....	171
6.4.1	HISTOLOGY (STRUCTURE AND COMPOSITION AT THE MICRO SCALE) 171	
6.4.2	COLLAGEN CONTENT.....	180
6.4.3	AFM (STRUCTURE, MECHANICS AND ORGANIZATION AT THE MICRO AND NANO SCALE)	182
6.4.4	RELATIONSHIP BETWEEN GLYCATION AND PROLAPSED TISSUE MECHANICS (FROM BALL INDENTATION DATA)	194

6.4.5	OCE (MECHANICS AT TISSUE SCALE).....	196
6.5	DISCUSSION.....	201
6.5.1	HISTOLOGY	201
6.5.2	STRUCTURE AND COMPOSITION	204
6.5.3	MECHANICS AND GLYCATION	208
6.6	CONCLUSION	213
6.6.1	MAIN FINDINGS.....	213
6.6.2	STUDY IMPLICATIONS	215
	CHAPTER 7: GENERAL DISCUSSION AND CONCLUSIONS.....	216
7.1	OVERVIEW.....	217
7.2	NOVEL APPLICATION OF MECHANICAL MEASUREMENT MODALITIES IN THE STUDY OF THE VAGINAL TISSUE	218
7.3	RELATIONSHIP BETWEEN AGEs, GLYCATION AND THE PRESENCE OF PROLAPSE.....	219
7.4	NEW UNDERSTANDING ON THE RELATIONSHIP BETWEEN GLYCATION LEVEL, OESTROGEN AND GLYOXALASE I EXPRESSION.....	220
7.5	CORRELATION OF GLYCATION AND VAGINAL TISSUE MECHANICS IN PREGNANCY AND PROLAPSE.....	221
7.6	NEW CO-MORBIDITIES IN PROLAPSE: HYPERTENSION, SMOKING, CHOLESTEROL.....	222

7.7	IMPROVED KNOWLEDGE OF HISTOPATHOLOGY AND ULTRASTRUCTURAL CHANGES IN THE VAGINAL WALL IN PREGNANCY AND PROLAPSE	223
7.8	MECHANICAL CHANGES IN PROLAPSED TISSUES: NEW INSIGHT ON HETEROGENEITY OF PROLAPSED TISSUES	225
7.9	CONCLUSIONS AND FUTURE CONSIDERATIONS	226
	REFERENCES	230
	APPENDICES	271
	APPENDIX 1: CAP STUDY PROFORMA	271
	APPENDIX 2: ICIQVS QUESTIONNAIRE.....	274
	APPENDIX 3: ETHICAL APPROVAL FOR STUDY	278

FIGURES

Figure 1.1: Female pelvic organs

Figure 1.2: Image of the bony pelvis showing attachment of pelvic diaphragm muscles and fascial condensations (tendinous arch and levator plate)

Figure 1.3: Levels of pelvic support

Figure 1.4: Superior cross sectional view of female lesser pelvis showing the urinary bladder (B), the uterine cervix (C), part of the vagina (V), the rectum (R) and the endopelvic fascia as a continuation of the adventitial layers of pelvic viscera

Figure 1.5: Haematoxylin and Eosin stained section of vagina showing mucosal, muscularis and adventitia layers

Figure 1.6: Illustration of collagen organization of mature collagen within the extra cellular matrix.

Figure 1.7: Illustration of advanced glycation of mature collagen fibers.

Figure 1.8: Formation of AGEs by reaction of reducing sugar with a lysine or arginine based protein segment.

Figure 1.9: Chemical structure of pentosidine.

Figure 1.10: Illustration of pelvic organ prolapse types

Figure 1.11: Scanning electron micrograph showing collagen fibrils

Figure 1.12: TEM image of an intact cell showing intracellular organelles.

Figure 1.13: Polarised microscopy image of human bone biopsy.

Figure 1.14: AFM image of collagen I fibrils.

Figure 1.15: Second harmonic generation image of airway collagen fibrils.

Figure 3.1: Dissection of Female Sprague Dawley rats.

Figure 3.2: Reproductive organs of Female Sprague Dawley rats isolated from the pelvic cavity.

Figure 3.3: HPLC chromatogram showing pentosidine elution at 9.6 minutes

Figure 3.4: Pentosidine standard curve

Figure 3.5: Schematic illustration of tissue sample holder for indentation ball instrument.

Figure 3.6: Mounted vaginal tissue segments within plastic O-rings secured within a metal screw and plate system.

Figure 3.7: Ball indentation deformation imaging system.

Figure 3.8: Displacement images of vaginal tissues at time 0 (t_0) and after 24 hours (t_{24}) obtained using the CCD camera.

Figure 3.9: Insertion of tubular vaginal wall over a cylindrical object to enable precise incising in the process of creating a rectangular flat sheet for mounting on mechanical test device.

Figure 3.10: Mechanical test load-stage designed to support tissue during slicing.

Figure 3.11: Design of mechanical test load stage with tissue cutter.

Figure 3.12: Slicing stage (final product).

Figure 3.13: Thickness measurement illustration T0 and T24 images of sliced vaginal tissue layers using method 1.

Figure 3.14: Slicing of slightly frozen tissue mounted on tissue stage using method 2.

Figure 3.15: OCT image of sliced tissue using method 2.

Figure 3.16: Sample location images (top) and histological images (bottom) of tissues studied using AFM.

Figure 4.1: Representative H&E stained images of pregnant and non-pregnant rat vaginal wall.

Figure 4.2: Low and high magnification images of representative SEM images of pregnant and non-pregnant vaginal tissues.

Figure 4.3: AFM measurement of collagen fibril morphology of pregnant and non-pregnant vaginal tissues

Figure 4.4: Quantification of collagen fibril dimensions of pregnant and non-pregnant vaginal tissues through AFM images

Figure 4.5: OCT imaging of rat vaginal tissues

Figure 4.6: Cross-sectional appearance and thickness of representative pregnant and non-pregnant vaginal tissues across longitudinal trough (lt), longitudinal peak (lp) and transverse.

Figure 4.7: Alcian blue staining of pregnant and non-pregnant vaginal wall.

Figure 4.8: Glycosaminoglycan (GAG) content per dry weight of pregnant and non-pregnant rat vaginal tissues

Figure 4.9: Water content per dry weight of pregnant and non-pregnant rat vaginal tissues

Figure 4.10: AGE marker level measured from HPLC for the pentosidine content in vaginal tissues from pregnant and non-pregnant rats.

Figure 4.11: Mechanical property (24 hour creep) of intact vaginal tissue segments from pregnant and non-pregnant rats measured by the ball indentation technique

Figure 4.12: Correlation between pentosidine and vaginal tissue creep

Figure 4.13: Mechanical property (Elastic modulus) of intact vaginal tissue segments from pregnant and non-pregnant rats measured by the ball indentation technique

Figure 4.14: AFM measurement of mechanical property by peakforce quantitative nanomechanical mapping mode.

Figure 4.15: Average modulus of collagen fibrils in the pregnant and non-pregnant vaginal tissues

Figure 4.16: Immunostaining images of vaginal tissue sections showing representative images of ER- α receptor expression

Figure 4.17: Immunostaining images of vaginal tissue sections showing representative images of glyoxalase I expression

Figure 4.18: Illustration of AGEs formation inhibition by oestrogen

Figure 4.19: Turbidity assay result showing effects of sGAG and collagen concentration on collagen fibrillogenesis in real time.

Figure 4.20: Light microscopy images of type I collagen fibers formed in the absence (A) and presence (B) of sGAG

Figure 4.21: Polarisation microscopy imaging of the polymerized type I collagen fibrils formed in the presence and absence of sGAG.

Figure 4.22: Clustering of type 1 collagen fibrils formed in the presence and absence of sGAG by quantification of fibril per unit area

Figure 4.23: SEM images of polymerized type I collagen fibrils obtained in the presence and absence of sGAG

Figure 4.24: Pentosidine in pregnant and non-pregnant skin tissues

Figure 4.25: Correlation between Skin and vaginal tissue pentosidine

Figure 5.1: Average age of women studied in control and prolapsed groups

Figure 5.2: Parity in prolapsed, control groups and total population studied.

Figure 5.3: Pentosidine in prolapse and control tissues.

Figure 5.4: Pentosidine and age in vaginal tissues from entire study population.

Figure 5.5: Pentosidine amounts by age groups in vaginal tissues of controls.

Figure 5.6: Pentosidine amounts in prolapsed vaginal tissues by age groups.

Figure 5.7: Pentosidine in prolapsed and control tissues based on menopausal status.

Figure 5.8: Amounts of pentosidine in vaginal tissues of hypertensive and non-hypertensive patients in the entire study group

Figure 5.9: Pentosidine in vaginal tissues of women with hypertension in control and prolapsed groups

Figure 5.10: Pentosidine amounts in vaginal tissue of women with DM

Figure 5.11: Pentosidine content in the vaginal tissue of smokers and non-smokers.

Figure 5.12: Pentosidine content of vaginal tissues in prolapse involving the anterior and posterior walls of the vagina.

Figure 5.13: Pentosidine amounts in tissues in relation to grade of prolapse.

Figure 5.14: Scatter plot showing relationship between pentosidine amounts in the tissues in and the grade of prolapse.

Figure 5.15: Scatter plot of tissue pentosidine content with ICIQ-VS score

Figure 5.16: Symptom severity perception (ICIQ-VS) and prolapse grade

Figure 5.17: Representative images showing ER- α expression in age-matched prolapsed and control tissues

Figure 5.18: ER- α receptor count control and prolapsed tissues.

Figure 5.19: Representative images showing GLO I expression in age-matched prolapsed and control tissues.

Figure 6.1: Low magnification images of representative control and prolapsed samples showing histological layers and structure overview of vaginal tissues.

Figure 6.2: Medium magnification images of control and prolapsed tissues showing epithelial and sub-epithelial regions.

Figure 6.3: Cell count at basal lamina of age-matched control and prolapsed groups

Figure 6.4: Elastin stain with and without counter staining in representative age-matched prolapsed and control tissues

Figure 6.5: Higher magnifications of regions within tissue sections stained for elastin in representative age-matched Prolapsed and control tissues

Figure 6.6: Neural stain (red) in representative age-matched Prolapsed and control tissues..

Figure 6.7: Trichrome stained images of control and prolapsed tissues.

Figure 6.8: Higher magnifications of regions within tissue sections stained with trichrome stain in representative age-matched prolapsed and control tissues

Figure 6.9: Representative picrosirius red stained images of age-matched control and prolapsed vaginal wall sections

Figure 6.10: Total collagen in prolapsed and control vaginal tissues,

Figure 6.11: Total collagen in age-matched premenopausal and menopausal prolapsed and control vaginal tissues

Figure 6.12: Representative PF AFM images of control and prolapsed vaginal tissue sections viewing collagen from $1 \times 1 \mu\text{m}$ LP regions showing collagen modulus range.

Figure 6.13: Representative PF AFM images of control and prolapsed vaginal tissue sections (Adventitial layers) viewing collagen from $5 \mu\text{m}^2$ areas showing collagen modulus range.

Figure 6.14: Average collagen fibril modulus extracted using the nanoscope analysis software from $1.4 \mu\text{m}^2$ and $5.0 \mu\text{m}^2$ areas of LP and Adventitial zones of Control and prolapsed tissues

Figure 6.15: Representative AFM height images showing collagen fibril organization in $5 \mu\text{m}^2$ areas of prolapsed and control tissues within the LP region.

Figure 6.16: Representative AFM images showing collagen fibril organization in $1.4 \mu\text{m}^2$ areas of prolapsed and control tissues within the LP region.

Figure 6.17: Representative 3-D AFM images illustrating ultrastructural organisation within the LP region of prolapsed and control tissues. $5 \mu\text{m}^2$ and $1.4 \mu\text{m}^2$ images are shown on the left and right respectively

Figure 6.18: Representative AFM height images showing collagen fibril organization in $5.0 \mu\text{m}^2$ areas of prolapsed and control tissues' adventitial region

Figure 6.19: Representative AFM height images showing collagen fibril organization in $1.4 \mu\text{m}^2$ areas of prolapsed and control tissues in the adventitial regions.

Figure 6.20: Representative 3-D AFM images illustrating ultrastructural organisation within the adventitial region of prolapsed and control tissues. $5 \mu\text{m}^2$ and $1.4 \mu\text{m}^2$ images are shown on the left and right respectively

Figure 6.21: Average gap between collagen fibrils in $1.4 \mu\text{m}^2$ areas of control and prolapsed vaginal tissue sections.

Figure 6.22: Average collagen fibril diameter in $1.4 \mu\text{m}^2$ areas of prolapsed and control vaginal tissues.

Figure 6.23: Collagen fibril count in $1.0 \mu\text{m}^2$ per unit area in prolapsed and control samples

Figure 6.24: Collagen fibril alignment in control and prolapsed tissues

Figure 6.25: Thickness of tissues obtained using the two methods of slicing

Figure 6.26: Correlation of creep and modulus of adventitial layer of prolapsed tissues sliced using method 1 with pentosidine content.

Figure 6.27: Correlation of creep and modulus of adventitial layer of prolapsed tissues sliced using method 2 with their pentosidine content

Figure 6.28: OCE tissue set up with and without embedding in agar for image acquisition

Figure 6.29: Elasticity map of Control and Prolapsed tissues imaged in air. Cross-sectional views along the y-axis of horizontally placed tissues are shown.

Figure 6.30: Elasticity map of prolapsed and control tissues imaged immersed in agar.

Figure 6.31: Illustration of glycation stiffening in prolapsed tissues and potential to initiate prolapse.

Figure 7.1: Proposed relationship between glycation, oestrogen, GLO-I antioxidant, accelerated ageing, altered tissue mechanics and pelvic organ prolapse.

TABLES

Table 5.1: Pentosidine content of different non-contiguous regions of the same piece of tissue

Table 5.2: Pentosidine content of the same tissues before and after storage at -20°C

Table 5.3: Pentosidine content of the same tissues dried in a 60 degree oven or lyophilisation overnight.

Table 5.4: Table showing the age distribution within the prolapse, control and entire study population

Table 5.5: Table showing number of women with parities of 0-6 in both groups

Table 5.6: Overview of participant characteristics in prolapsed and control groups

ABBREVIATIONS

ACTG2 - SM gamma-actin

AFM - Atomic force microscopy

AGE - Advanced glycation end product

AGEs- advanced glycation end products

BMI - Body mass index

CALD 1- caldesmon

CCD - Charge coupled device

DAPI - 4',6-diamidino-2-phenylindole

DM - Diabetes Mellitus

DMMB - Dimethylmethylene blue

DMT - Derjaguin–Muller–Toporov

DNA - Deoxyribonucleic acid

DS - Dermatan sulphate

ECM - Extracellular matrix

EDTA - Ethylenediaminetetraacetic acid

ER- α – Oestrogen receptor-alpha

ERK - Extracellular Signal Regulate Kinases

FTIR - Fourier transform infra-red spectroscopy

GA - Glutaraldehyde

GFAP - anti-glial fibrillary acidic protein

GLO-I - Glyoxalase I

GSH - Gluthathione

HPLC - High performance liquid chromatography

HRA NRES - Health Research Authority, National Research Ethics Service

HRT - Hormone replacement therapy

H&E - Haematoxylin and Eosin

ICIQ-VS - International Consultation on Incontinence Vaginal Symptoms Questionnaire

LP- Lamina propria

MAPK - Mitogen-Activated Protein Kinases

MHY11 - SM-myosin heavy chain

MMPs - Matrix Metalloproteinases

NFκB - Transcription factor nuclear Factor Kappa B

OCE - Optical coherence elastography

OCT - Optical coherence tomography

OD - Optical densities

OsO₄ - Osmium tetroxide

PDGF - Platelet-Derived-Growth-Factor

PFQNM - PeakForce Quantitative Nanomechanical Mapping

Prolapse - Pelvic organ prolapse

RAGE - Receptor for advanced glycation end products

REC – Research Ethics Committee

RNA - Ribonucleic acid

sGAG - Sulphated glycosaminoglycans

SEM- Scanning electron microscopy

TEM - Transmission electron microscope

TIMPs - Tissue inhibitors of matrix metalloproteinase

TPM1 - tropomyosin

UHNM NHS Trust - University Hospital of North Midlands National Health Service

UV - Ultraviolet

α -SMA - α -Smooth Muscle Actin

2-D -2 dimensional

3-D- 3 dimensional

PUBLICATIONS

Journals

Homayemem Weli, Riaz Akhtar, Zhuo Chang, Wen-wu Li, Jason Cooper, Ying Yang
Advanced glycation products' levels and mechanical properties of vaginal tissue in pregnancy.
European Journal of Obstetrics and Gynaecology and Reproductive Biology (2017) 214: 78-85
(<https://doi.org/10.1016/j.ejogrb.2017.04.037>)

Homayemem Weli, Jason Cooper and Ying Yang Skin advanced glycation content reflects
vaginal tissue glycation in relation to pregnancy. Medical Hypotheses (2017) 104: 84-87
(<http://dx.doi.org/10.1016/j.mehy.2017.09.016>)

Conference Abstracts

Homayemem Weli, Zhuola Zhuola, Kanheng Zhuo, Wen-wu Li, Jason Cooper, Ying Yang
“The alteration of structural organisation, nano-mechanical property and glycation content of
prolapsed vaginal tissues” at the Royal Society Discussion meeting (OBSTRACT: interpreting
the abstraction of tissue regeneration and re-engineering of female pelvic floor disorders)
London, UK 16th October 2017

Homayemem Weli, Riaz Akhtar, Zhuo Chang, Jason Cooper, Ying Yang “Influence of
sulphated glycosaminoglycans on ultrastructure of vaginal tissues during pregnancy” Royal
College of Obstetricians and Gynaecologists world congress, Cape Town, South Africa 21st
March 2017

Homayemem Weli, Riaz Akhtar, Zhuo Chang, Wen-wu Li, Jason Cooper, Ying An advanced
glycation product level and mechanical properties of vaginal tissue during pregnancy in

female Sprague Dawley rats. Royal College of Obstetricians and Gynaecologists, London, UK
3rd March 2017

Homayemem Weli, Zhuola Zhuola, Kanheng Zhuo, Wen-wu Li, Jason Cooper, Ying Yang
The alteration of structural organization, Nano-mechanical property and glycation content of
prolapsed vaginal tissues. Bell Blair Research Society and Royal College of Obstetricians and
Gynaecologists, London, UK 3rd March 2017

Homayemem Weli, Jason Cooper and Ying Yang Correlation of ageing, hypertension and
oestrogen receptor expression with advanced glycation content in prolapsed tissues. British
Society of Urogynaecologists and Royal College of Obstetricians and Gynaecologists annual
research meeting 11th November 2016

Homayemem Weli, Jason Cooper and Ying Yang Relationship between ageing and oestrogen
receptor expression gives insight into development. UK Molecular Epidemiology Group
(UKMEG) winter meeting Newcastle University 1st December 2015

ACKNOWLEDGEMENT

I am immensely grateful to God almighty and my very supportive and encouraging family (Minini, dad, mum Adi, Ola, Keme) whose presence, relentless care and encouragement have been indispensable in both good and difficult times. I say a special thank you to my parents, Dr and Mrs. Weli, my first teachers and academic mentors. To my husband, Minini and my mum, thank you for always keeping me on track, and for the listening ears. I thank my friends and church family for the prayers and encouraging words.

I say a very big thank you to my Supervisors, Professor Ying Yang and Mr. Jason Cooper for the consistent academic supervision, corrections and mentoring through the PhD. Thank you for giving me the opportunity to learn new techniques and hone new skills and for always making time out of your very busy schedules to review my work or chat about our project and the way forward. Your expertise and guidance have been extremely important for the completion of this work and I remain grateful.

I particularly thank Keele University for giving me the opportunity to study and research in a field I was very passionate about.

I say thank you to Rivers State Sustainable Development Agency and University Hospital of North Midlands Charitable fund for research funding.

I thank Dr. Wen-wu Li and Dr. Fidelia Uche for teaching me how to use the HPLC device. Many thanks to Dr. Fola Dandare and Dr. Fidelia Uche for the moral support through the PhD. Thanks Sudeshna Bhunia for making the ‘regular days’ in the laboratory interesting; having initially been the only student in GHRC studying a gynaecology disease, it was great to finally have another student researching in a related field (obstetrics). Thanks to my sister, Dr.

Wanwuri Akor, mum and Margaret Nkonde for helping edit some aspects of my work. I thank my collaborators at Liverpool University and University of Dundee. It was a pleasure working with you all. Special thanks to Zhuola for patiently working with me through the second round of AFM experiments. I thank the Electron Microscope unit and the Keele University Animal House staff, especially Dr. Stephanie Jones for their immense support. Thank you to Dr. Paul Roach's group for kindly letting me use some of their rats for research. I thank all the UHNM urogynaecology surgical and theatre staff for their support in providing the test samples. Special thanks to Mr. Cooper, Ms Purwar, Mr Redman, Mr. Todd and Mr Misra. I thank all my colleagues at GHRC, particularly Prof. Ying's group. I enjoyed sharing the lab with you all.

CHAPTER 1: BACKGROUND

1.1 STRUCTURAL AND FUNCTIONAL ASPECTS OF THE FEMALE PELVIS

1.1.1 OVERVIEW

The female pelvis contains the organs of reproduction (ovaries, fallopian tubes, uterus, and vagina), storage and excretion (urinary bladder, and rectum) (1) as shown in figure 1.1. The uterus (horn, body and cervix), ovaries and vagina have reproductive functions i.e. mating, egg production, fertilization, implantation and growth and delivery of the fetus. Physiologically, these are all involved in various degrees of load bearing.

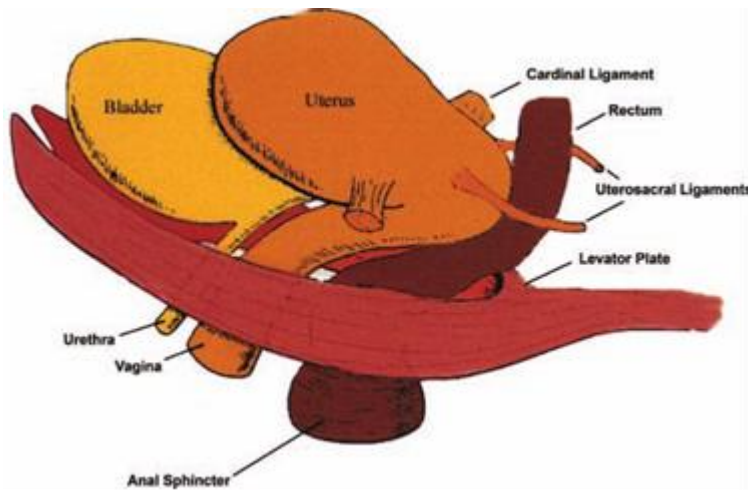


Figure 1.1: Female pelvic organs(2)

1.1.2 BONY PELVIS

The pelvic organs are supported by an intricate layout of muscles and ligaments connected to a bony frame work (Figures 1.1 and 1.2). This frame work of pelvic bones comprises of the two innominate bones fused to the spinal sacrum posteriorly and anteriorly. They are joined by the

pubic symphysis (3). The innominate bones are made up of the iliac, ischium and pubis. These give shape to the pelvic basin (greater and lesser), which is wider and more circular in females than in males (4).

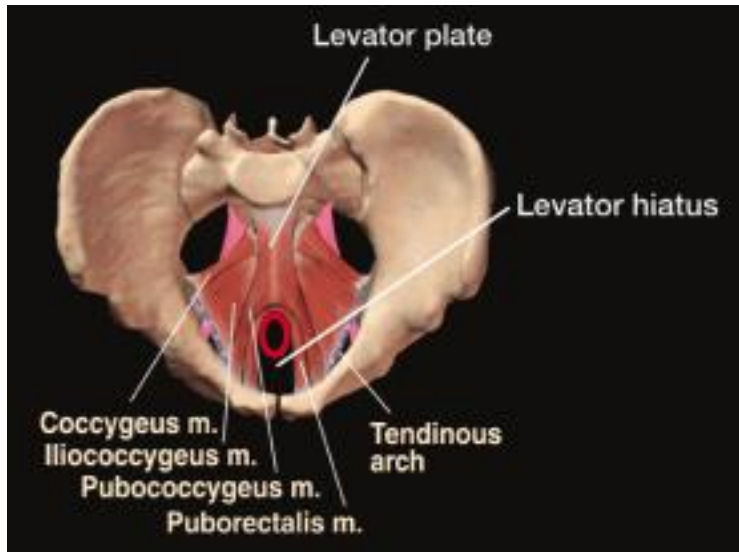


Figure 1.2: Image of the bony pelvis showing attachment of pelvic diaphragm muscles and fascial condensations (tendinous arch and levator plate) (3)

1.1.3 PELVIC DIAPHRAGM, LIGAMENTS AND FASCIA

Muscles, ligaments and fascial layers within and around this bony frame work constitute the pelvic support; preventing prolapse when intact and directly or indirectly maintaining faecal and urinary continence (5).

The pelvic diaphragm (Figure 1.2) is the deepest layer of muscular support on which the pelvic organs rest directly (1). It comprises of the paired coccygeus, levator ani and the two muscles that originate in the pelvis but attach to the femur (obturator internus and piriformis muscles). The coccygeus and levator ani are innervated by the branches of the anterior rami of the 4th and 5th sacral nerve roots (S2 - S4) and the S2 to S4 pudendal nerve branches (3). The

coccygeous muscle makes up the posterior aspect of the pelvic diaphragm and its inferior surface is the sacrospinous ligament. The levator ani muscle is made up of the pubococcygeus and iliococcygeus muscles (6). These originate and attach within the lesser pelvis.

Different parts of the most medial muscle, the pubococcygeus, form the periurethral muscles that insert into the vagina walls and loop around the rectum, sub dividing the muscle into the pubo urethralis, pubovaginalis and puboanalis respectively. Fibers also insert into the perineal body and the external anal sphincter (3). The iliococcygeous is the thinner and more lateral aspect of the levator ani muscle and its paired fibers fuse with fibers of the pubococcygeous posteriorly to form the levator plate, on which the pelvic organs rest. This plate regulates the diameter of the urogenital hiatus, an external opening for the lower pelvic visceral. When a female is in the standing position, it remains horizontal if undamaged and in this way, closes the urogenital hiatus, preventing prolapse.

1.1.4 LEVELS OF PELVIC ORGAN SUPPORT

Three levels of ligamentous support and suspension of the pelvic viscera shown in Figure 1.3 have been described (4,7). These anchor the uterus and, upper, middle and lower third of the vagina to the pelvic wall. Level I support involves the uterosacral ligament that suspends the uterus to the sacrum. It is continued downward as the paracolpium, which attaches the vaginal apex to the pelvic wall.

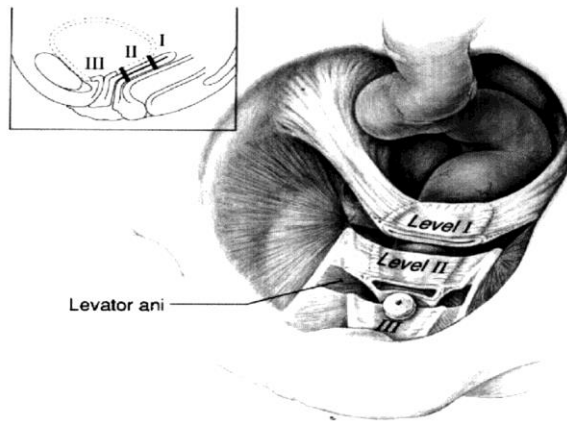


Figure 1.3: Levels of pelvic support (4)

Endopelvic fascia attaches the middle third of the vagina to the pelvic sidewall. It is a layer of connective tissue comprising structural proteins (1). Like ‘cling-film’, this fascia encompasses the organs and muscles with differential thickening in the arcus tendineus region (6). It links with supporting pelvic ligaments such as the cardinal ligament and fuses to form the adventitia layer of the viscera, enforcing strength and enclosing the pelvic structures as a discreet unit (Figure 1.4).

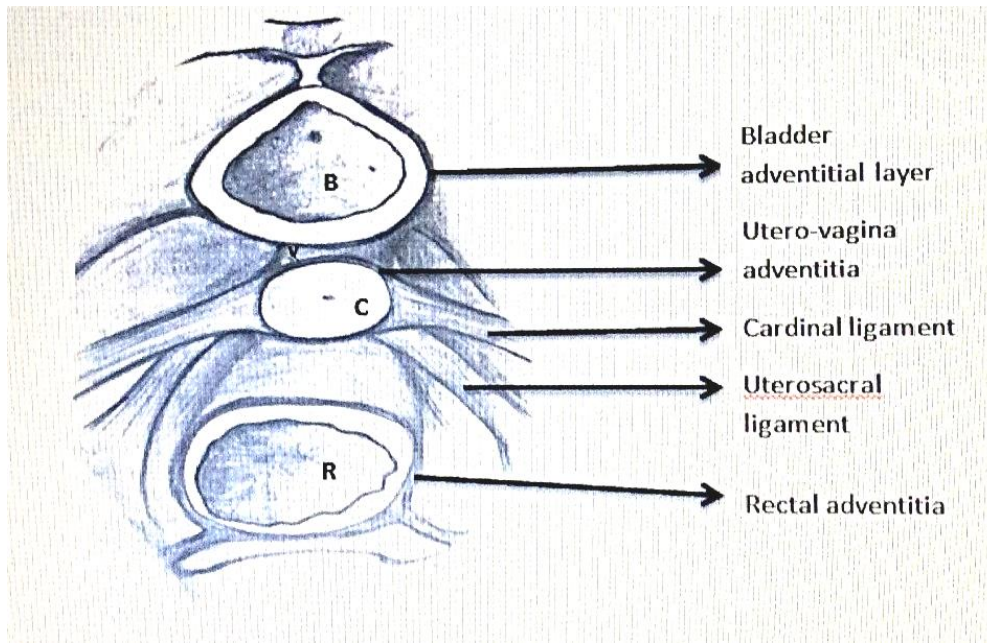


Figure 1.4: Superior cross sectional view of female lesser pelvis showing the urinary bladder (B), the uterine cervix (C), part of the vagina (V), the rectum (R) and the endopelvic fascia as a continuation of the adventitial layers of pelvic viscera.

Ligamentous continuations (uterosacral and cardinal ligaments are shown)

More superficial layers of pelvic support comprise the urogenital membrane or perineal membrane, ischio-carvenosus and bulbocavernosus muscles and the superficial transverse perineal muscle (3). They support the region between the perineal body and the inferior pubic rami, providing extra support for the anterior and lower pelvic viscera (urethra and vagina). This is the third level of support.

The fibromuscular perineal body is located between the vagina and anus, and serves as an attachment to vaginal, perineal and anal sphincter muscles (3). It is a convergence point of some muscles of the pelvic diaphragm and structures of the perineal membrane (8). It plays an important role in maintaining pelvic organ support and also in changing the elasticity of the

pelvic cavity during childbirth. Damage to or weakness of this structure typically predisposes to prolapse.

1.2 VAGINAL CONNECTIVE TISSUE STRUCTURE AND BIOMECHANICS

1.2.1 HISTOLOGY OF THE VAGINA

The vagina has an inner mucosal layer, a sub-mucosal dense connective tissue layer, an intermediate muscularis layer and outer adventitia or loose connective tissue layer as shown in Figure 1.5 (3,9). The mucosa is made up of a layer of stratified squamous epithelium. Underneath this is the thick lamina propria (LP) or dense connective tissue layer comprising mainly of collagen and elastin fibers which gives the vagina its elastic and tensile characteristic alongside the observable longitudinal folds and rugae of the entire mucosal layer (8).

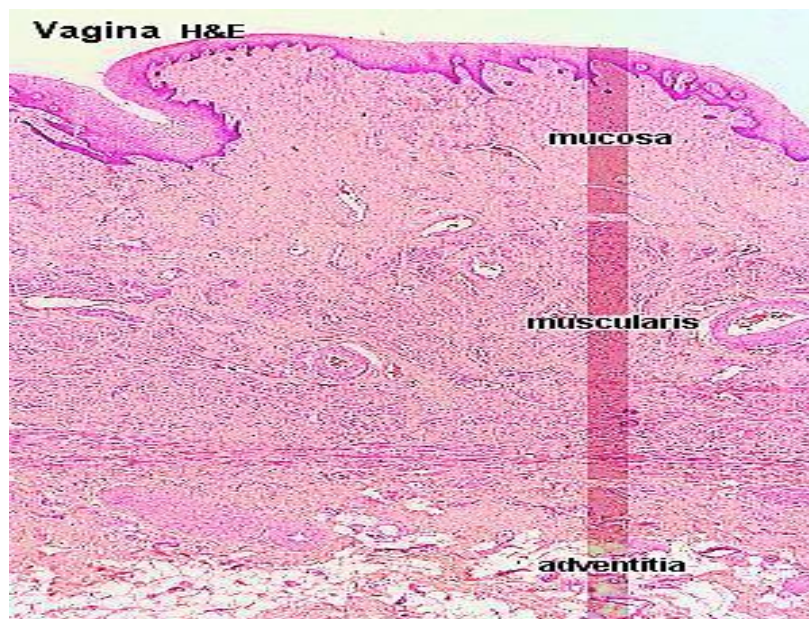


Figure 1.5: Haematoxylin and Eosin stained section of vagina showing mucosal, muscularis and adventitia layers. (9)

Within the muscular layer is an inner, less defined circular and outer longitudinal layer (1). The LP and muscularis layer make up the fibromuscular supporting layer. This lies adjacent to the fibrous connective tissue layer –the adventitia.

Mast cells, adipocytes, myocytes and fibroblasts are the constituent cells of the vagina and they are few in number. Fibroblasts are responsible for producing the extracellular matrix (ECM), which includes the fibrous structural proteins (collagen and elastin) and an amorphous ground substance made up of glycoproteins, hyaluronan and proteoglycans (8). Production and degradation of fibrillar proteins are maintained in equilibrium in an on-going remodeling process. Imbalance in this process may lead to loss of tissue integrity which may predispose to prolapse.

1.2.2 VAGINAL MECHANICS

The vagina, like many other soft tissues, is anisotropic, that is, its mechanical property changes with changes in the direction of applied force (10,11). It also exhibits visco-elastic and temporary plastic properties. It stretches in response to applied force and has the ability to return to its original length immediately (12), demonstrating its elasticity. Plasticity, on the other hand, is observed in preparation for childbirth, where it distends progressively to accommodate delivery of fetus. It is a physiological effect lasting only during labour. In some mammals, it stretches to approximately 3 times its original size to accommodate the delivery of the fetus (13).

1.2.3 THE VAGINA AS A CENTRAL PELVIC SUPPORT

The vagina is a pivotal point of attachments for pelvic support, involved in the development or non-development of prolapse. It has a central location within the pelvic cavity and serves as

the communication of the female reproductive tract with the exterior as well as providing an outlet to excess intra-abdominal pressure (4). It is a hinge point for the three levels of pelvic support (Levels I, II and III, previously described in Figure 1.3) (3). It is thus susceptible to intra-pelvic pressure changes and the integrity of its fibromuscular walls plays a vital role in preventing development.

In a study carried out to assess the influence of levator ani muscle damage on prolapse, transection of the levator ani nerve resulted in atrophy of the muscles but not loss of support in the nulliparous monkeys (14,). This finding suggests that, aside from the levator ani, other supporting structures such as the vagina may play a role in the development of prolapsed. Furthermore, in women with prolapse, structural protein composition of the vaginal wall are significantly altered (16). These suggest the involvement of the vaginal wall in maintaining pelvic support and preventing or limiting.

The vagina offers indirect active and passive mechanical support to the pelvic organs. Having smooth muscle cells, it cannot generate force but can transmit applied force (6). It is closely associated with the arcus tendineous fascia, which is largely comprised of striated muscle cells that have the capacity to generate contractile forces to control vagina wall motion (1). The overall mechanical function of this pivotal tissue is enabled by its mechanical constituents at the histological level and the nano-level organization of the same. This forms the unique spatial arrangement of an organ that can distend to accommodate physiologic load demands, withstand periodic stresses and recoil to its original state.

1.2.4 VAGINAL TISSUE EXTRACELLULAR MATRIX (ECM)

1.2.4.1 OVERVIEW

Collagen and elastin are structural proteins produced by fibroblasts (8). Collagen constitutes over 80% of the structural proteins of the vagina connective tissue (11). It can stretch to 4% its original length before failure. Elastin fibers, comprising about 13% of the structural proteins in the tissue, can distend to double their original length without permanent deformation (5). Mature elastin comprises an inner region of amorphous cross-linked elastin surrounded by a microfibrillar scaffold (17). Elastin is formed following deposition of its secreted soluble precursor, tropoelastin on a fibrillin-rich microfibril template (18). Elastin gives the tissue its elastic recoil property whereas tensile strength is largely maintained by structural collagens. After extensive tissue deformation, elastic recoil would typically occur, utilising minimal energy (19). Elastic fibers are synthesized continuously in the female genital tract for a lifetime with degradation and re-synthesis occurring post-partum (20). Due to the higher composition of collagen fibers in the vaginal tissue, the present study has focused on collagen ultrastructure. Therefore, its formation and crosslinking is discussed further in the following section.

1.2.4.2 COLLAGEN FORMATION AND MATURATION

Differential arrangements of collagen in connective tissues give them their specific unique morphologies and strength. Collagens are formed by triple α -chain helices linked together by hydrogen bonds as well as covalent bonds, which reflect protein maturation and tensile strength (8). Each helix comprises of repeats of Glycine-X-Y monomers where X and Y could be any amino acid but are typically hydroxyproline or proline (21). Extracellular assembly of

hydrogen bond-linked procollagen into tropocollagen fibrils via action of peptidases and a further self-assembly of the tropocollagen gives rise to collagen fibers and bundles. The covalent crosslinks and arrangement of collagen fibers within the vagina tissue, determine to a large extent the innate tensile strength of the tissue (19). Lysly oxidase is involved in formation of crosslinks that stabilize collagen fibers during maturation process, enabling them withstand increasing load (22). Divalent crosslinks, dehydro-hydroxylysino-leucine (Δ -HLNL) and hydroxylysino-keto-norleucine (HLNL), are first formed and subsequently reinforced by conversion to trivalent crosslinks, histidinohydroxylysino-leucine (HHL) (23) as shown in Figure 1.6. These crosslinks are present to lesser degrees in elastin and in both cases are formed via oxidative deamination of an amino group of lysine to form a reactive lysyl aldehyde. Cross linkages generally prevent gliding between collagen fibers, imparting optimal tissue stiffness whereas in elastin cross-linkages prevent excessive stretching of tissue.

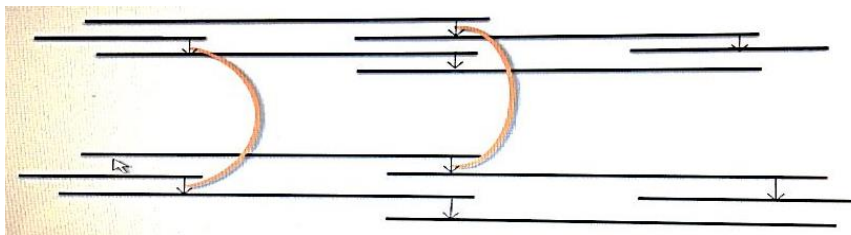


Figure 1.6: Illustration of collagen organization of mature collagen within the ECM.

Immature divalent crosslinks (black vertical arrows) are stabilized by mature divalent crosslinks (brown arcs).

The fibrillar collagens, type I, III and IV are present in the vagina with a predominance of Type I in healthy tissues. Type I collagen imparts toughness and resilience to deformation to the tissue (16). It is responsible for the tensile properties whereas type III is present where there is room for tissue distension and growth (5,24). Both are structural, fibril-forming

collagens. Collagens type III and V associate with type I to produce smaller collagen fibers with reduced mechanical strength (11,25). Optimal strength of the tissue is, thus, maintained via a balance between synthesis and degradation of these collagen types by various Tissue Inhibitors of Matrix Metalloproteinases (TIMPs) and Matrix Metalloproteinases (MMPs).

1.2.4.3 GROUND SUBSTANCE

Proteoglycans bind all cellular and acellular components of the connective tissue matrix together. These include aggrecan, perlecan, versican, lumican, fibromodulin, chondroadherin and decorin (11). Amongst other functions, this amorphous aspect of the connective tissue confers visco-elasticity to the tissue and modulates its nano-architecture (5,26). The higher molecular weight glycoproteins have brush-like structures which by trapping water, ensure tissue hydration, hence enabling its resistance to compressive force. This implies that basic factors such as tissue hydration influence tissue mechanics. sGAG are known to be involved in collagen fibril formation or parallel association with other fibrils without the involvement of chemical or physical crosslinks, and this is another mechanism by which they indirectly influence the mechanical property of tissues (27). They modulate collagen fibril diameter. For example, dermatan sulphate (DS) can increase collagen fiber diameter but decorin has the opposite effect (28).

1.3 PREGNANCY AND OESTROGEN EFFECTS ON THE VAGINAL WALL CONNECTIVE TISSUE

1.3.1 OVERVIEW

Pregnancy is a unique time in which the female reproductive tract undergoes rapid physiological changes and pelvic floor adaptation. Interestingly, despite high strain undergone

by the pelvic floor muscles during pregnancy, the majority of women do not have obvious pelvic floor injury during pregnancy (29,30). It is therefore useful to study some pregnancy adaptations alongside changes in prolapse in order to understand prolapse pathology.

Pregnancy influences the metabolism of pelvic tissues. The collagen content of the uterus and cervix change during pregnancy (31). Oestrogen, relaxin and progesterone are pregnancy hormones with direct effects on connective tissue protein breakdown and re-synthesis. Research reveals that there is a loss of pelvic tissue collagen during pregnancy due to a paracrine effect of relaxin. To effect softening and relaxation, relaxin may cause collagen degradation and restructuring in the vagina and uterus during pregnancy (32).

Oestrogen and progesterone are, however, more notable pregnancy hormones whose metabolic effects on pelvic tissues have been more widely studied. Oestrogen and progesterone are modulated not only in pregnancy but also during the normal menstrual cycle, resulting in a more continuous effect on pelvic tissues. They are maintained at a higher level in pregnancy by hypothalamic-pituitary-gonadal axis control (33). Whilst progesterone helps to maintain pregnancy and prevent preterm labour (34) oestrogen appears to directly influence pelvic tissue metabolism in pregnancy. For example collagen induced arthritis and rheumatoid arthritis are significantly improved with oestrogen treatment and temporarily remitted in pregnancy, a state of high oestrogen levels (35). Another study carried out using Female Sprague-Dawley rats noted that ovariectomy resulted in reduced epithelial height which responded to treatment with oestradiol, which influenced vaginal epithelium and nonvascular smooth muscle (36). Progesterone did not have such an effect.

1.3.2 THE RELATIONSHIP BETWEEN COLLAGEN, MATRIX REMODELLING ENZYMES AND OESTROGEN

Results from studies investigating effects of oestrogen on the pelvic tissue of women with pelvic floor disorder are varied. Some findings suggest that oestrogen is associated with increased break down and reduction in total amounts of collagen (37). On the contrary, oestrogen treatment has also been associated with fibroblast mitotic activity, increased turnover of collagen and other structural proteins (38,39). Similarly, increased activity of tissue inhibitors of matrix metalloproteinase (TIMPs), inhibitors of collagen breakdown have been observed with oestrogen therapy (40). In a 6 month prospective study, oestrogen treatment was associated with both increased breakdown and neo-synthesis of collagen in vaginal tissues (41). A significance of this observation is the potentially lower amounts of older collagen and higher amounts of newer collagen due to the influence of oestrogen. An understanding of this matrix remodeling effect would be useful in explaining findings from past studies regarding the effects of oestrogen on pelvic connective tissue collagen metabolism.

Many studies showing improvements in pelvic tissues' properties with oestrogen treatment have been associated with premenopausal and healthy states (39,40). Transient symptomatic improvement with oestrogen therapy has been observed in pelvic floor dysfunction as well as worsening of the condition in post-menopausal women (42–44). These pelvic floor problems in women are associated with altered vaginal connective tissue metabolism (8,45). Up-regulation of genes encoding matrix metalloproteinase (MMPs) and tissue inhibitors of matrix metalloproteinase (TIMPS) was observed to occur during the proliferative and secretory phases of the normal menstrual cycle, respectively (46). In the same study, the cyclical change

in expression of genes encoding pelvic tissue metabolic enzymes was noted to be absent in post-menopausal states, which were associated with up-regulation of TIMPs. Female steroid receptors are expressed in most urogenital tissues with cyclical expression and down regulation of these occurring in the vaginal epithelium in response to hormonal changes occurring during the menstrual cycle (47). The vaginal tissue is thus metabolically susceptible to cyclical variations in female hormones during the menstrual cycle and subsequent changes at menopause. Due to the higher composition of collagen (81%) in the vaginal wall compared to other pelvic tissues (48), changes in collagen metabolism would significantly influence the vaginal wall's mechanical properties. These changes therefore need to be studied in depth in order to understand pregnancy adaptations and pelvic floor disorders.

1.4 CONNECTIVE TISSUE AGEING

1.4.1 OVERVIEW

Macroscopically, ageing is observed (in external organs such as skin) as the development of fine wrinkles, loss of elasticity and reduction in tissue thickness. Functionally, the ageing process has been associated with various age-related diseases (49). Microscopically, there are various alterations linked with these visible effects. Cellular, biochemical and genetic changes have been noted but there is still an uncertainty as to what triggers the overall process, the onset of which apparently varies from person to person.

Ageing cells have reduced proliferative capacities and productive abilities. Fibroblasts, for example, have been shown to have a lifespan equivalent to about 50 passages *in vitro* (50). Cellular changes in ageing connective tissue are largely reflected in resulting biochemical changes such as altered synthesis and modification of cellular products by differentially active

cell organelles such as lysosomes (19). The result is alteration in quality and quantity of cellular products that make up the ECM (ground substance and fibril-forming proteins).

With increasing age, constituents of the ground substance such as hyaluronic acid, versican, neutral and acid mucopolysaccharides reduce significantly (51). Decreased amounts of versican, a molecule involved with maintaining viscosity and elasticity suggests affectation of the viscoelastic property of ageing connective tissues (52). In view of the moisture retention function of the ground substance, its alteration with age implies a loss of cushioning effect in older connective tissues.

Elastin and collagen are fibril-forming proteins that decrease with age in connective tissues (53). These changes have the potential to influence tissue behavior under passive loading (19). Collagen, a cellular product is the most abundant protein in the body and is responsible for maintaining connective tissue form and shape (54). Ageing changes are particularly observed in collagen, reflecting the altered shape and form of organs grossly observable in older superficial connective tissue such as aged skin (19).

1.4.2 AGEING THEORIES AND GLYCATION MARKERS OF AGEING

Several ageing theories have been adduced to attempt to explain the ageing process. These range from the free radical theory to the theories of telomere shortening, oxidative stress and mitochondrial DNA changes, although none entirely explains all known age-related changes in biological tissues (22). Investigations have thus recently shifted to cellular and extracellular modifications through glycation reaction as markers of ageing. The resultant substances are called advanced glycation end-products (AGEs) (55). Glycation is a process in which proteins, fats and nucleic acids in body tissues get modified non-enzymatically with reducing sugars, it

typically occurs over months or years (56). It predominantly affects ECM collagen and elastin because they have slow turnover rates within the ECM (55). Glycation results in stiffer, less digestible proteins and can permanently alter connective tissue properties (57). Advanced glycation is implicated in ageing and many diseases including gynecological disorders such as prolapse and urinary incontinence (4, 5). Pelvic tissue glycation has been further studied since the observation of higher amounts of insoluble collagen or glycation products in prolapsed pelvic tissues by Jackson et al in 1996 (23).

Age-related crosslinking of cellular components such as proteins, lipids and nucleic acids upon prolonged contact with reducing sugars has been noted (58). These modifications change the properties of affected cellular components and hence, the overall cellular function. Of particular interest to ageing is the crosslinking of long-lived structural proteins such as collagen and elastin. Crosslinking of collagen (Figure 1.8) reduces its solubility, significantly influencing connective tissue property since collagen is the main structural protein of connective tissues (59).

Older connective tissues contain glycated proteins, nuclei and fatty acids formed by prolonged contact of reducing sugars with susceptible amino acids of proteins (8). Glycation occurs by a maillard reaction in which reducing sugars covalently bind to amino acids. Intermediate products of oxidation formed are rearranged over months or years into AGEs. Within tissues, this process is non-enzymatically regulated. Collagens are prime targets for the glycation process because of their long half-life that leads to prolonged contact with reducing sugars. They also contain significant amounts of susceptible lysine and arginine residues along their chains for the reaction (9–11).

This added crosslinks confer higher resistance to proteolytic degradation to the collagens (57). While there has been no change in amounts of enzymatic crosslinks of aged collagen, non-enzymatic crosslinks have been greatly increased in aged connective tissue collagen (19). This increase is thought to contribute significantly to increased stiffness of ageing tissue. Notably, elastin is less susceptible to non-enzymatic glycation due to presence of reduced amounts of lysine residues per molecule compared with collagen (19,60).

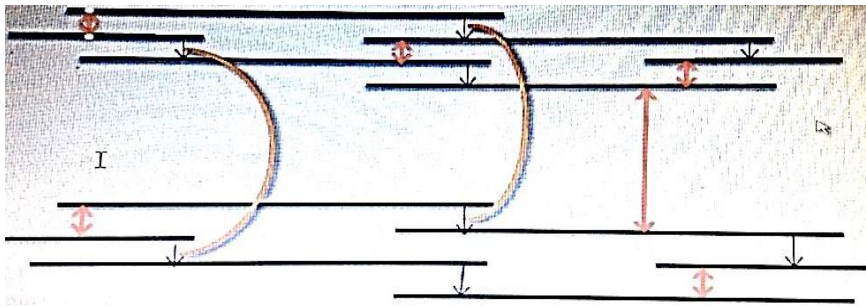


Figure 1.7: Illustration of advanced glycation of mature collagen fibers. Mature and immature enzymatic crosslinks are shown by black single arrows and brown arcs respectively. The double arrows (red) represent advanced glycation.

1.4.3 FORMATION OF ADVANCED GLYCATION END PRODUCTS (AGEs)

AGEs are produced in a maillard reaction which was first described in 1912 (61). The carbonyl group of a reducing sugar reacts with free amino groups in proteins leading to the formation of an unstable Schiff base which may rearrange to form a ketoamine (amadori) product (62) as shown in Figure 1.8. These undergo oxidative changes to form the unstable AGEs. Stable crosslinks may form after years of contact of amadori product with amino acids, leading AGEs formation. Slow turn over proteins such as collagen, elastin and fibronectin are

therefore particularly susceptible to this process (19,22). AGEs are found in increased quantities ageing tissues and have become markers of ageing.

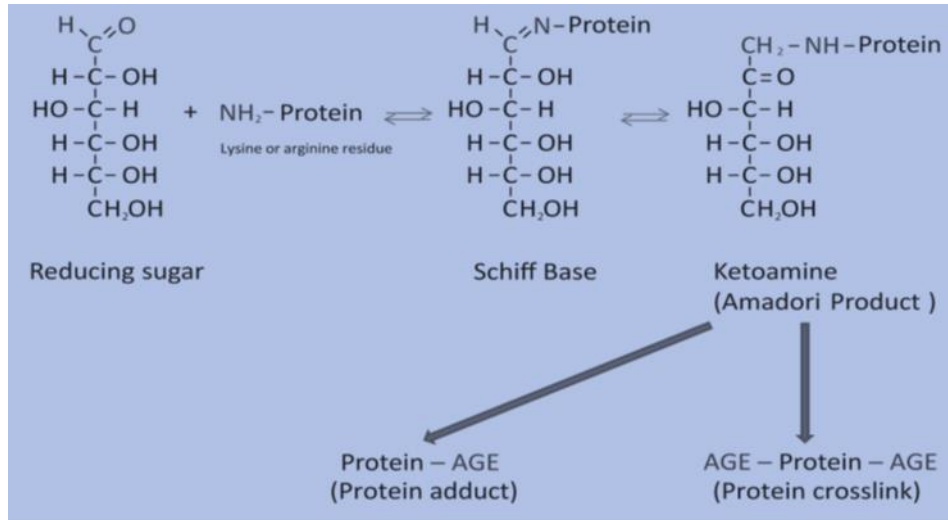


Figure 1.8: Formation of AGEs by reaction of reducing sugar with a lysine or arginine based protein segment. After series of rearrangement of the unstable ketoamine product, advanced glycation may occur over months or years

(55).

1.4.4 TYPES OF AGEs

There are various types of AGEs. The glycated hemoglobin was the first discovered AGEs and has since been used to monitor the treatment progress and compliance of diabetes mellitus patients (55). Others are Carboxymethyl-lysine (CML) (the most prevalent AGE in the human body), glucosepane, fructo-lysine, methyl-lysine, hydroimidazolones, pyrrolidine, Carboxy ethyl-lysine (CEL) and pentosidine. Of the aforementioned, only pentosidine forms auto-fluorescent protein cross-links. Pentosidine can thus be detected by UV or fluorescent wavelengths (63), making it a useful analytical tool for ageing studies.

Pentosidine (Figure 1.9) is formed by the reaction of a pentose sugar with arginine and lysine (64). The involvement of free radical oxygen species in its formation makes it a fluorescent glycoxidation product. It was first identified and characterized by Sell and Monnier (65). Since then it has been extensively used as a marker of ageing. Its fluorescent property is exploited for detection and quantification of ageing in mammals (66,67).

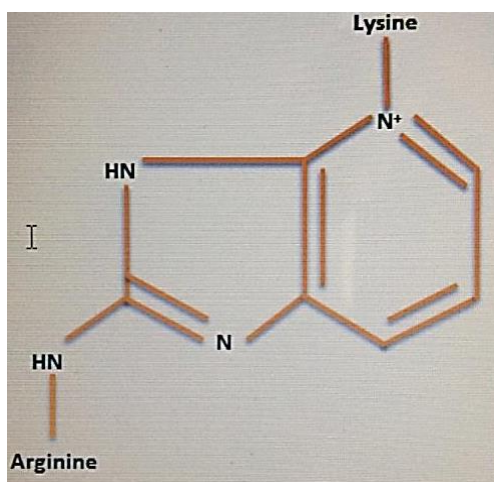


Figure 1.9: Chemical structure of pentosidine

1.4.5 ACCUMULATION AND REMOVAL OF AGEs *IN VIVO*

Various factors promote or inhibit the glycation process. Indeed the amounts of AGEs *in vivo* are determined by a balance between factors promoting their accumulation and factors involved in their removal. AGEs can be produced within the body as earlier described or directly ingested from foods. The method of production of foods is important in accumulation of AGEs. Frying and baking favour AGE production in contrast to boiling or steaming foods (56). AGEs are known to impart a brown colour to foods. Smoking and exposure to Ultra Violet radiation also favour the formation of AGEs through suggested oxidation stress mechanisms and increased expression of AGEs receptors (55).

Genetic susceptibility in the accumulation or otherwise of AGEs has also been observed (68). Ascorbic acid counters the glycation process. Reduced dietary intake of AGE-promoting compounds (reducing sugars) or foods rich in AGEs such as roasted coffee and fried foods might thus be useful in limiting the accumulation of AGEs *in vivo*.

Contrary to previously held beliefs, AGEs, once formed, can be removed by cells. Cells have innate detoxification pathways to prevent accumulation of AGEs. These mechanisms have been noted to be attenuated with physiological ageing. The enzyme systems, glyoxalase I and II (GLO-I and II (glutathione-dependent glyoxalase system) and fructosamine kinases are involved with the removal of AGEs from cells (69,70). They break down ketoamine products and some are widely expressed in various tissues of the human body. Glutathione, for example, converts glycoxal methylglycoxal α -oxoaldehyde to a less toxic compound, lactate. AGE receptor systems, AGER 1, 2 and 3 promote the internalization of AGEs into cells for subsequent degradation (55).

1.4.6 AGEs REACTION MECHANISM

AGEs promote deleterious effects via the RAGE group of receptors. These are encoded on chromosome 6 near the Major Histocompatibility Complex III (68). The binding of AGEs to their receptors signals various metabolic pathways including Mitogen-Activated Protein Kinases (MAPK), Extracellular Signal Regulate Kinases (ERK) and P21 (56). Transcription factor nuclear Factor Kappa B (NFkB) is activated and pro-inflammatory genes are transcribed. This fosters a positive feed-back regulatory mechanism that overrides the natural autoregulatory negative feedback loop. Inflammatory signals and enzymes accumulate and

protective mechanisms such as super oxide dismutase are deactivated, leading to oxidative damage.

1.4.7 EFFECT OF AGEs ON THE ECM

The ECM is the major target of the glycation process. There are notable age-related changes in the diameter of collagen fibers. These may become thicker and coarse (71). Reflecting this structural changes are altered mechanics. Glycated collagen is increasingly stiff and less flexible with higher vulnerability to mechanical load (72). Affected proteins have less available domains for cellular interaction, leading to distortion of ECM rearrangement (19). Additional glycation of the collagen increases their molecular weight and viscosity (73), making them less soluble. These insoluble, 'aged' collagen are more resistant to degradation by MMPs, preventing replacement by newer ones (74). Thus mechanical changes in connective tissue may appear permanent. Glycation of elastin has been associated with tissue wrinkling (actinic elastosis) (51). CML-modified elastin is associated with this process (75). The elastins lose their elasticity and are also more resistant to degradation.

Cells are also affected by the glycation process. Since nucleic acids are susceptible (76), the viability of cells significantly reduces. This is associated with early cell death. There is also a decline in the production of ECM proteins. The overall effect is an ECM with mechanically altered structural proteins resistant to degradation and having less efficient interaction with cells.

1.5 PELVIC ORGAN PROLAPSE

1.5.1 OVERVIEW

Pelvic organ prolapse (Figure 1.10), also known as utero genital or uterovaginal prolapse, is a debilitating condition with severe effects on the quality of life of those affected. This is the downward descent or protrusion of the female pelvic organs below or away from their anatomical position and often visible through the vaginal wall (6) Although not life threatening, prolapse affects the quality of life of individuals with the disease. The first surgery was self-performed by a female sufferer in 1697. Faith Ratworth was so distressed by the debilitating symptoms that she pulled down on her uterus and cut it with a knife, surviving severe haemorrhage but remaining incontinent for life (77). Multiple pelvic organs that surround the vaginal wall are typically involved in prolapse. Cystocele involves urinary bladder and sometimes the urethra, rectocele accommodates the rectum and utero-vaginal involves a direct descent of the uterus or vagina vault (in patients who have had hysterectomy) (77).

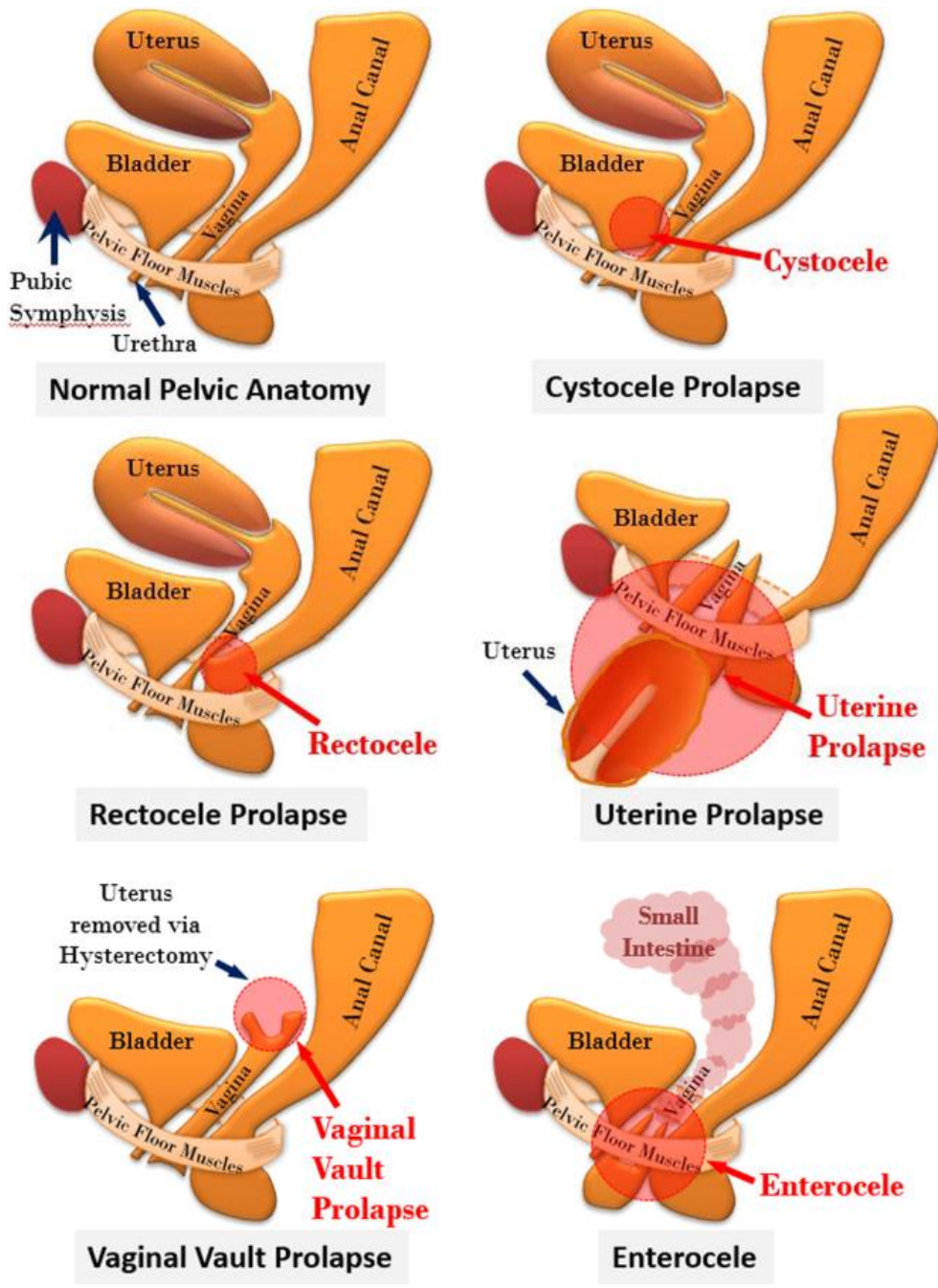


Figure 1.10: Illustration of pelvic organ prolapse types (78). Anterior (cystocele) and posterior (rectocele) vaginal wall prolapse, uterine prolapse, vaginal wall prolapse and enterocele (prolapse involving the small intestine) are illustrated.

1.5.2 EPIDEMIOLOGY

Prolapse is present in up to 50% of women presenting for routine gynecological visits (79), with symptoms in the general population of 8.4% (80). In the United Kingdom (UK), prolapse is the commonest indication for hysterectomy in post-menopausal women. Approximately 20% of women undergoing major gynecological surgery present with prolapse. Up to 76% of women seen for routine gynecological visits in developed countries were noted to have lost some degree of vagina support (81,82). Prolapse is found to result in 18 percent of all gynecological surgical procedures in all age groups. Its prevalence is higher in the aged population with a 41% prevalence in those aged 50-79 years (6). The commonest of the three kinds of prolapse is the cystocele (34% prevalence). Rectocele and uterine prolapse account for 19% and 14% of cases, respectively (83). The high prevalence of this disease translates to a high economic burden on society; in the United States it costs over \$1 billion dollars yearly (79). With increased longevity, finding the cause of and proffering a solution to prolapse would not only lead to improved quality of life in affected individuals but also, indirectly improve the economies of many countries.

1.5.3 GRADING OF DISEASE SEVERITY AND SYMPTOMS

As previously noted prolapse either involves the protrusion of the urinary bladder into the anterior wall of the vagina (cystocele or urethrocele), an outpouching of the anterior rectal wall into the posterior wall of the vagina (rectocele) or a downward descent of the uterus or vagina vault (in patients who have undergone hysterectomy) known as uterovaginal prolapse (77). This is the traditional anatomical site and vaginal wall-based classification. The various types of prolapse result in the different symptoms that are typically associated with the

disease. Although, an understanding of this means of classification gives insight to the origin of the various presenting symptoms, many clinical cases do not exactly fit into the groups.

Rectocele is associated with faecal incontinence, constipation, tenesmus, faecal urgency and straining (6). In some cases, manual pushing within the vagina is required to achieve defaecation. Cystocele is associated with urinary incontinence, urinary hesitancy, frequency, urgency and the feeling of incomplete voiding. As with rectocele, manual pushing against the anterior vaginal wall might be required to ensure voiding. Uterine or vaginal prolapse might result in a feeling of fullness within the vagina, the sensation of downward descent and dyspareunia (84).

For surgical grading and treatment purposes as well as the assessment of quality of life, various grading systems have been developed. Originally, assessment was simply made based on level of prolapse in relation to the hymen. More objective and detailed scoring systems have since then been developed.

The Baden-Walker grading system directly references the descent of prolapsed tissue from the ischial spine to the hymen and beyond, with half-way points to and from the hymen (85). Its advantage is that it is quick and encodes a lot of information. 4 grades of prolapse are described:

grade 0 which implies no evidence of prolapse, grade 1 (prolapse halfway to hymen), grade 2 (prolapse up to the hymen), grade 3 (prolapse halfway past hymen), and grade 4 (maximum descent). This method has been criticized as permissive of intra and inter-observer variations as well as making no note of the severity of individual patient symptoms as it is purely an

anatomical measurement. This has resulted in the search for grading systems that better assess the severity of symptoms and impact on the quality of life (86).

The Pelvic organ prolapse quantification (POP-Q) system is a more widely accepted scoring system than the Baden-Walker half way system (87). Using the hymenal ring as a fixed reference point (0), there are six defined points and 3 other reference points, measured and assigned a positive number when located above or a negative number when below the hymen. Although not routinely used in most clinical practices due to time constraints of taking 9 measurements, it is said to be more objective and reliable, having little variations across various observers. The International Consultation on Incontinence Vaginal Symptoms (ICIQ-VS) questionnaire on prolapse scoring gives insight into the quality of life of sufferers. It asks questions on the impact of the disease symptoms on the patient's activities with attention to the social aspects of the disease impact (86). It comprises of 9 vaginal symptoms questions with corresponding symptom severity assessment on a scale of one to ten with one denoting least severity and ten, very severe symptom. It further contains 4 sexual matters question also assessed based on severity and a grading of the impact of prolapse on the sufferer's quality of life on a scale of 1-10 (86). Vaginal symptoms and quality of life scores obtained reflect disease severity. Properly categorizing the disease is vital for research and can be used to assess differences in ageing and the various sub-groups of prolapse.

1.5.4 CURRENT TREATMENT

Symptomless prolapse is treated by conservative management. When there are debilitating symptoms, palliative methods such as vaginal pessaries can be used (85). Various surgical methods are in use from removal of redundant vaginal wall and support of the underlying

tissue, to suspensory operations such as sacrocolpexy and sacrospinous fixation procedures. In these later procedures the prolapsed tissue is respectively suspended with an artificial mesh to the sacrum or fixed to the sacrospinous ligament (6). Synthetic meshes such as polypropylene have been used in the treatment of prolapse but with significant side effect in up to 20% of patients (88). Although these therapeutic techniques offer symptomatic relief, they do not cure the underlying disease process. Despite various measures to improve the quality of life of women prolapse, a definitive solution is yet to be found. Up to 30 percent of those treated surgically require repeat surgery (81,89) suggesting non-reversal of any prior underlying connective tissue alterations that led to the prolapse in the first instance. Unraveling key points in disease pathology would be a step towards more lasting therapies.

1.5.5 KNOWN AND POTENTIAL RISK FACTORS

1.5.5.1 REPEATED VAGINAL DELIVERIES

Vaginal delivery has been associated with the highest risk of developing prolapse (1,82,90) and has been categorized as an independent risk factor (80,91,92). Since fetal passage during delivery is one of the vagina's main functions, suggesting it to be a cause of prolapse would be synonymous with saying cardiac failure, for example, is the direct result of the hearts normal physiologic function of pumping blood around the body. Furthermore, prolapse has been noted to occur in a few nulliparous individuals (93). This observation and findings from studies carried out to assess the postpartum mechanics of the vagina are challenges to the widely held concept of vaginal delivery being the major cause of prolapse.

In a study carried out using rodent models, it was revealed that the vagina and other pelvic tissues demonstrated significant changes in mechanical properties during the middle and late

stages of pregnancy but these returned to normal 4 weeks post pregnancy (94). It has also been observed that following vaginal delivery; there was no significant change in vaginal strength (95). The innate function of an organ can scarcely be said to be the cause of its failure. Rather, abnormal functioning or excessive use beyond its limit of functionality could result in organ failure. This, however, would be determined and to a large extent, modified by genetic and lifestyle factors. So, a more likely risk factor would be repeated and traumatic vaginal deliveries. Additional deliveries have been noted to increase the chances of prolapse by 10-20 percent up to a maximum of 5 deliveries (6). Repeated vaginal delivery potentially exposes the pelvic organs, nerves and blood vessel to traumatic damage. Expectedly, the reproductive organs in their healthy states are well adapted to withstand the birth process, expanding where necessary and returning back to their resting states afterwards (8). Disruption in this mechanism may result in prolapse.

Instrumental deliveries and prolonged labour are direct traumatic events associated with higher risk of prolapse. Forceps delivery has been associated with a higher risk of prolapse (6). This could be due to direct damage to the pelvic structures or the primary indication for the use of forceps. Vaginal delivery of macrosomic babies (>4.5kg birth weight), for example, could result an obstructed labour leading to intervention by the use of forceps. In this case, both indication and intervention predispose to pelvic organ damage that may lead to future prolapse (82).

1.5.5.2 FACTORS LEADING TO RAISED INTRA-ABDOMINAL PRESSURE

Factors that raise the intra-abdominal pressure have been linked with the development of the disease is increasing body-mass-index. Obesity, which also raises the intra-abdominal pressure

is one of the three major risk factors associated with prolapse (96). Women with lower body mass index (BMI) are less likely to undergo surgery for prolapse when compared with those with higher BMI. The odds ratio of developing prolapse is high in overweight women (2.51; 95% CI 1.18–5.35) and higher in obesity (2.56; 1.23–5.35) (83). Heavy weight lifting, chronic cough and repeated constipation may also lead to prolapse via a similar mechanism. Studies have shown that a higher percentage (61%) of women with prolapse have reported straining while stooling as young adults than women without prolapse (4%) (97). Individuals with stage II or greater prolapse had an increased risk of constipation (odds ratio 3.9; 95% CI 1.4–11.9) compared with women with stage 0 or 1 prolapse (98). Furthermore, women who perform more physical work or occupations involving heavy lifting are more at risk for prolapse than those whose job are less physically demanding(99).

1.5.5.3 AGEING

Ageing, previously discussed in 1.4.2 is a known risk factor of pelvic organ prolapse. The risk of developing prolapse is noted to increase with increase in age (6). In a study in the United States, a 40% risk increase per decade of life was observed. Studies carried out in other parts of the world have also observed an increase in prevalence of the disease in the older population, even in regions with a relatively low incidence of the disease (95). Prolapse is rarely seen amongst women less than 30 years of age but thereafter, there appears to be a consistent increasing prevalence with age up till age 80 (82). In some populations, over two-fifths of women aged 50 to 79 years have some form of prolapse.

A study carried out to determine the incidence of pelvic floor muscle trauma during delivery found more damage in association with higher maternal age (30). Ageing influences the

composition, mechanics and metabolism of pelvic tissues as well as relevant hormones (100). Age also influences the tissues' regenerative ability, which is particularly useful when injury is sustained. Research has shown that vaginal fibroblasts decrease with age (101). This may influence their capacity to maintain the pelvic tissue in a healthy state. Furthermore, tissue glycation, which alters its mechanical property, increases with age. While age may appear to be a non-modifiable risk (100), its study is relevant as the effects of ageing on tissues can be slowed down by lifestyle changes (102).

1.5.5.4 OTHER POTENTIAL RISKS AND DISEASE ASSOCIATIONS

Other risk factors, including previous hysterectomy and wider pelvic inlet, have been associated with prolapse (93). This is believed to occur as a result of wider outlet for transmission of raised intra-abdominal pressure, leading to more pressure on the pelvic viscera and subsequent prolapse. The incidence of prolapse in women who have undergone previous hysterectomy is slightly higher than in the control population (91,103,104). This risk is higher in women who underwent hysterectomy for prolapse. The prolapse however, when it does occur, takes place many years after hysterectomy (104).

Ethnic and familial factors appear to have a role in the development of (82,83,105). Studies also show that women with first degree relatives having prolapse have a higher risk of disease occurrence than those without this familial association (99). A study carried out involving genetically matched women with a known family history of prolapse revealed the presence of a minimum of 6 nucleotide repeats in association with the disease, most of which are directly involved in maintaining connective tissue structure and function (106). This suggests that development of prolapse may result from connective tissue alteration.

1.5.6 CONNECTIVE TISSUE CHANGES IN PROLAPSED TISSUE

1.5.6.1 OVERVIEW

There is a paucity of information detailing exact connective tissue that may lead to prolapse. In many aspects where knowledge exists some contradictory evidence is also present. No consensus has been reached regarding the exact role of all connective tissue components and sex steroid hormones in the aetiology of the disorder. Unraveling this may be the key to understanding the complex interplay between known risk factors and more certain triggers of the disease. Despite this observed lack of consistency in findings regarding pelvic connective tissue cells, certain aspects such as ageing of connective tissue structural proteins, repair after damage, ECM remodeling and hormonal effects show remarkable trends. This lights the path for new research linking connective tissue ageing, remodeling and development of prolapse.

Conditions affecting the integrity and elasticity of the connective tissue also influence the development of the disease. The increased occurrence of prolapse in patients with connective tissue disorders such as Ehlers Danlos syndrome and cardiomyopathy has been observed (6). In cases where prolapse has been noted in nulliparous individuals, the presence of a genetic connective tissue defect has been suggested (8).

1.5.6.2 COLLAGEN

Pelvic supporting ligaments from women with prolapse have shown decreased amounts of total collagen (23) but collagen Type III, which is associated with reduced fiber size and low mechanical strength of the connective tissue is generally increased in prolapsed vaginal tissues (6). Type III collagen is present in the skin of babies at birth whereas mature skin has collage

type I (11,25). Its presence at early stages of development suggests that it is relevant in enabling connective tissues to expand to accommodate growth. Its increase in prolapsed tissues is a pointer to prolapse being a response to increased vaginal tissue loading. Findings on the levels of collagen I and collagen I/III ratios in prolapse tissues have been inconclusive (8,23,107).

Studies on collagen I mRNA in vaginal fascia and immunofluorescence of collagen in full thickness vagina apex tissue revealed no significant change between controls and test subjects (108,109). Another study comparing the total collagen content of the vaginal apex and parametrium of women with and without prolapse revealed a reduction of collagen in the parametrium where prolapse was present but no significant differences in the vagina apex (110). Others carried out on the arcus tendinous fascia and periurethral fascias showed decreased collagen type I (111,112). Differences observed could be the result of use of varied tissue types and different analysis techniques. It is however noteworthy that similar observations of low levels of collagen I have been noted in vagina tissue where disease is present (8).

1.5.6.3 MATRIX REMODELING ENZYMES

An increase in matrix metalloproteinase (MMP)-2 and MMP-9 has been consistently noted in prolapse tissues (23,108,113). Despite the use of different analytical methods, research suggests higher activity of these fibrillar collagens' degrading enzymes in various regions of the vaginal tissue and uterosacral ligaments. A congruent decrease in associated TIMPs activity has also been noted (45). Increase in tenascin, a marker of wound healing (113) and the aforementioned markers of collagen degradation suggests that prolapse reflects an on-

going remodeling or tissue healing process with loss of homeostasis of this remodeling process. Overall, studies on amounts of collagen subtypes and regulatory enzymes suggest a dysfunctional regulation of collagen that results in its qualitative decline and quantitative imbalance in prolapsed tissues.

1.5.6.4 FIBROBLASTS

Fibroblasts are the predominant cells of the vagina connective tissue (3). These slow growing cells have been shown to change morphology and biochemistry in response to applied force. They are mechanosensitive (114). They undergo mechanotransduction like other mechanosensitive cells in load bearing tissues of the body (96). They are also responsible for the production of matrix remodeling enzymes (115). The mechanical function of fibroblasts can be hindered by abnormal underlying matrix architecture and in disease states they may produce abnormal ECM. For example, fibroblasts in prolapsed tissues were also noted to produce stiffer connective tissue matrix (116). Ageing also has an impact on vaginal tissue fibroblasts. It has been revealed that the fibroblasts show a numerical decline and reduced contractile ability (109) and reduced MMP-2 production (115) with age. The ageing fibroblasts showed decreased wound healing abilities as well as a lack of ability to maintain tissue architecture.

Oestrogen can also influence vaginal fibroblasts behaviour and modulate its biochemical and mechanical activities. Repeated stretching of the fibroblasts correlates with production of matrix degrading enzymes (96). This effect can be modulated by the reproductive hormones, such as oestrogens via pro-trophic mechanisms (117). Oestrogen may increase cellularity but has no overall effect on maintaining tissue structure (8). Studies reveal the role of oestrogen in

stimulating collagen turnover stress urinary incontinence (38,41), and this process can influence pelvic tissue ageing and remodeling. ECM genes associated with breakdown and resynthesis are altered during the female reproductive cycle and menopause (46). The pelvic tissues also change mechanically in response to cyclical changes in the hormones as well as during menopause (118). Further suggestive of the influence of ovarian hormones such as oestrogen on vaginal fibroblasts is the observation that the vaginal wall, like other pelvic tissues, undergoes remodeling during pregnancy (119). Although, there are few studies on fibroblasts in pregnancy, it is known that there is a control of the vaginal wall cell numbers by a poorly understood homeostatic balance between apoptosis and cellular proliferation. The apoptotic process is noted to decline in the second trimester (120). This is suggestive of increasing cell numbers and potentially increased vaginal tissue remodeling in pregnancy (120).

1.5.6.5 NON ENZYMATIC CROSSLINKING OF COLLAGEN

The most consistent connective tissue findings are the development of new crosslinks in prolapsed tissues (8). This is in keeping with the early hypothesis by Jackson suggesting prolapse to be the result of increasing trivalent non-enzymatic crosslinks gradually dominating slow turn-over proteins ultimately leading to an older, stiffer connective tissue (23). Notably, he found higher amounts of an AGE, pentosidine, in the tissues. Since then a few other studies have reiterated this finding, showing no change in divalent, enzymatic pyridinoline crosslinks but an increase in advanced glycation of pelvic connective tissue collagen (8,45). This, as well as the presence of disorganized collagen structure in prolapsed tissues correlates with the increasing incidence of the disease observed with increasing age.

1.6 VAGINAL WALL MECHANICS IN PREGNANCY AND PROLAPSE

1.6.1 PREGNANCY

Various studies have been carried out in attempts to understand the mechanical behaviour of the vagina under various conditions. Known prolapse risk factors such as pregnancy have been studied to understand their effects on mechanical changes that may lead to prolapse. Both pregnancy and prolapse affect pelvic tissues' metabolism and mechanical property. Pregnancy-induced mechanical changes occur during a relative short period of time and under a female reproductive hormone rich condition in contrast to prolapse, which may take years to develop. Understanding pelvic tissue mechanical changes in pregnancy will therefore provide useful insight into what may occur in prolapse.

Pregnancy is associated with increased elasticity and reduction in stiffness of these tissues prior to delivery (13) Pregnancy influences structural and functional components of the ECM. Collagen alignment, for example has been noted to reduce in pregnancy. Decreased stiffness in the vagina and its supporting structures (to about 50% less than in non-pregnant states) was noted in mice models during second and third trimesters of pregnancy (11). It resolved post-partum. This finding is congruent with similar observations in another research carried out using non-pregnant and pregnant (late stage) using *Fibulin 5* knock-out mice, pelvic tissue. Pregnant rodents were found to distend up to 3 times their original size in the last two trimesters of pregnancy. Reduced tissue strength has also been noted in association with maximum distension at delivery (121). A study by Feola et al also noted reduced tangent modulus of the vaginal wall in mid and late pregnancy and immediate peuperium when compared with virgin rats. These normalised 4 weeks postpartum although the tissue was more sensitive to active stimulation in pregnancy (122).

The findings imply that pregnancy alters vaginal tissue mechanics in preparation for distension during delivery but this returns to normal post-partum (13). The return to normal post-partum (11) correlates with findings in other studies showing no observable residual mechanical change in the vagina of women post-partum (95).

Another study recorded increased vaginal weight and length through pregnancy with progressive decline in ultimate load and stress capacity occurring with repeated pregnancies (123). Altered vaginal mechanics observed during pregnancy are said to be similar to observed changes in prolapsed tissue (13). Pregnancy however, is followed by healing and re-synthesis of structural proteins in the vaginal and pelvic tissues.

An age-dependent hormonal effect was observed in rat models. The ultimate load and linear stiffness properties of younger rats with surgically induced menopause was lower than in rats with active hormones (124). The same effect was noted in older rats. Hormone replacement therapy (HRT) or MMPs reduced this effect in younger but not older rats. This observation highlights a possible age-dependent hormonal benefit of HRT and a different mechanism by which ageing influences tissue mechanics.

There is significant remodeling of the vaginal wall during pregnancy as a delivery adaptation (122). These changes in vaginal tissue mechanics are the result of underlying qualitative, organizational and quantitative changes in the extracellular matrix (ECM), with passive mechanics more influenced by the fibrillar component (122,125). The vaginal wall is noted to have the capacity to distend up to 4-11 times its original size in pregnancy (13) but the underlying mechanisms leading to this are not fully elucidated. More is known about these biomechanical changes in the vaginal wall than the underlying connective tissue or biochemical modifications that effect such mechanical changes. The stiffness of the vaginal

wall, tensile strength and maximum load at failure is known to be reduced in pregnancy while maximum elongation increases (121). Vaginal wall smooth muscle cell phenotype and characteristics change during pregnancy. The smooth muscles have been shown to change into a less contractile phenotype and further studies show reduced contractility of the cells in pregnancy (48).

1.6.2 PELVIC ORGAN PROLAPSE

Human studies on vaginal wall mechanics in prolapse have shown great variations between mechanical properties. In a study to determine the tensile and bending properties of the vaginal tissue of 16 post-menopausal women with or without prolapse, tissues from women without prolapse were noted to have higher strength (126). Another study compared the properties of vaginal tissue from women with prolapse with cadaveric specimens without evidence of prolapse, showed no significant differences in stress, strain and load at failure. A wide variability in the mechanical parameters was noted within the test groups (127). Rahn et al observed increased distensibility in prolapsed vaginal tissues compared with controls when the tissues were strained to failure (13) but Jean-Charles et al observed significantly higher stiffness in anterior and posterior prolapsed vaginal walls (128). Furthermore, there is a contrast in results of tests carried out in vitro and in vivo. While many in vitro tests have revealed increased modulus and stiffness of the isolated prolapsed vaginal tissue, in vivo tests note the contrary. Two in vivo studies using a suction technique and 10 mm orifice probe respectively noted more extensible vaginal tissue in (129,130). The inconclusive findings necessitate further studies on the mechanics of prolapsed vaginal wall.

1.6.3 AGE AND MENOPAUSE

Age and menopause are other factors that may influence the vaginal tissue's mechanical properties, with many studies noting increased stiffness and elastic modulus of the vaginal tissues in association with both factors (118). An experiment aimed at determining the visco-elastic property of vaginal tissue showed that pre-menopausal vaginal tissues were more resistant to shear force while menopausal vaginal tissue from women without prolapse had a higher complex modulus, an indicator of reduced elasticity (12). In the same experiment, hormonal therapy in post-menopausal women was associated with higher tissue stiffness when compared with post-menopausal tissue without hormonal therapy. A study by Chantereau et al comparing mechanical properties of vaginal wall in young female cadavers with data from literature on mechanical properties of the vaginal wall in older women revealed significant differences in keeping with increased stiffness occurring with age (131). Overall decreased tissue elasticity or increased stiffness has been associated with both age and menopause.

These studies give insight into the mechanical properties of prolapsed tissues compared with non-prolapsed ones but make no direct link to exact micro-structural connective tissue changes responsible for the observed altered mechanics. Also, many studies have made use of animal models, which despite their usefulness; do not represent the *in vivo* human system. Researches performed using human tissue samples either had constraints of small tissue sizes or sample inconsistencies.

1.7 METHODS FOR CONNECTIVE TISSUE STRUCTURAL AND MECHANICAL ANALYSIS

1.7.1 CONNECTIVE TISSUE STRUCTURAL AND MORPHOLOGICAL ANALYSIS

The function of a biological tissue is determined by its physical and chemical structure. Abnormal functioning thus reflects altered structure. Characterization techniques have been developed and are continuously being developed to detect these alterations. Available methods have their benefits and limitations. A non-destructive, fast, multi-parameter technique is required to holistically characterise connective tissue.

1.7.1.1 ELECTRON MICROSCOPY

1.7.1.1.1 SCANNING ELECTRON MICROSCOPY (SEM) AND TRANSMISSION ELECTRON MICROSCOPY (TEM)

In this technique, an electron beam strikes the surface of structures being observed and is reflected to a screen for viewing after signal amplification (132). It is useful for viewing structures at the cellular level (133). By observing the relationship between cell and matrix proteins information can be obtained on the ultrastructural organization of connective tissues. It enables visualization of the alignment and dimensional properties of fibrillar proteins like collagen (132). Although it achieves good ultrastructural resolution, it has the disadvantage of requiring stringent sample preparation steps, with the potential of introducing artefacts to images (132).

Scanning electron microscopy (SEM) is useful for surface analysis of tissues. The electron beams generated in the SEM scan the surface of the object so it has the advantage of

bombarding the sample less than would occur with transmission electron microscope (TEM) (134). This however results in imaging of structures at the surface of the specimen only (Figure 1.11). This limitation is overcome by the TEM which uses a transmission beam; which penetrates the surface of objects (135) making it more suitable for tissue ultrastructural analysis (Figure 1.12). It however requires the preparation of very thin (5-100 nm if using 100 KeV voltage) tissue slices to permit adequate penetration of electron beams (132).

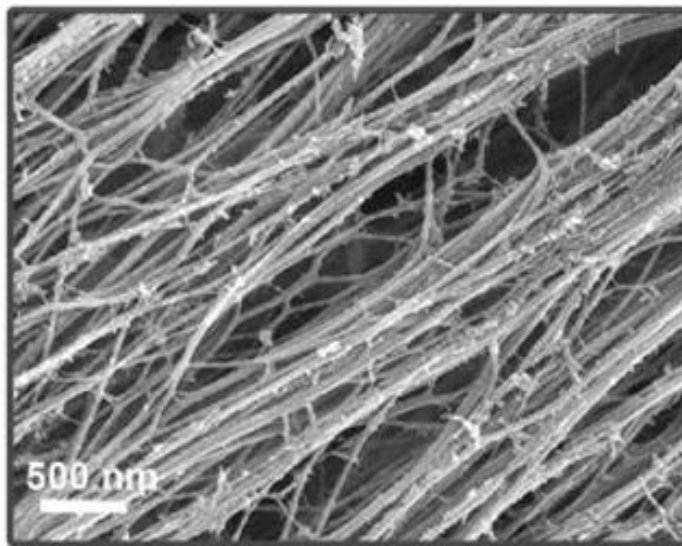


Figure 1.11: Scanning electron micrograph of collagen fibrils (136).

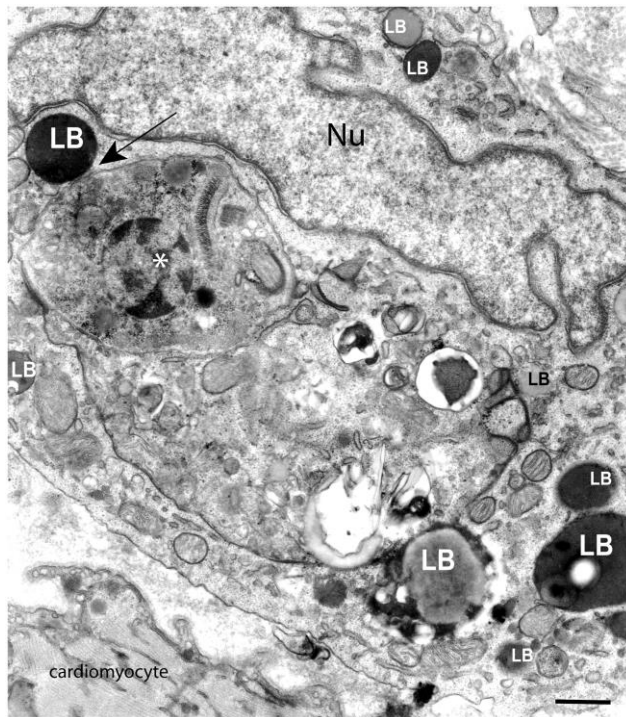


Figure 1.12: TEM image of intracellular organelles within an intact cell (137). Scale bar= 1 μ m

1.7.1.1.2 IMMUNOGOLD LABELLING

This is a staining technique useful in electron microscopy. Various sizes of gold particles are conjugated to antibodies, which target antigens on different biological structures (138). It gives detailed resolution of ultrastructure and the density of gold particles targeted at a specific antigen can be used to quantify the antigen or substrate it represents (139,140). It is useful in distinguishing protein components in biological specimens, hence improving sensitivity and specificity of electron microscope imaging.

Drawbacks of this technique include the requirement of specific fixation of samples in order to preserve their antigens for antibody binding and the likelihood of non-specific antigen

binding occurring (141). These specialized fixation or antigen preservation methods differ depending on the target antigen for preservation and can alter ultrastructure (142).

1.7.1.2 POLARISED LIGHT MICROSCOPY

This is an optical imaging technique to reveal the alignment features in tissues. A transverse light wave with directional vibrations (polarised light) strikes the surface of an object and birefringence is measured (143). Polarized light can be produced by applying a polarising filter plate to natural light (144). The birefringence of a polarised light gives insight into the structural properties of the object being imaged. Collagen birefringence changes with increasing age so this characteristic can be exploited for ageing studies (145). A linearly or circularly polarised light can be used to highlight differential characteristics of an anisotropic tissue, e.g. revealing the alignment of structural fibers (Figure 1.13). This alignment can be semi-quantified (146). It however, has the disadvantage of a low resolution and magnification typical of light microscopy causing errors in semi-quantitative image interpretation (147).

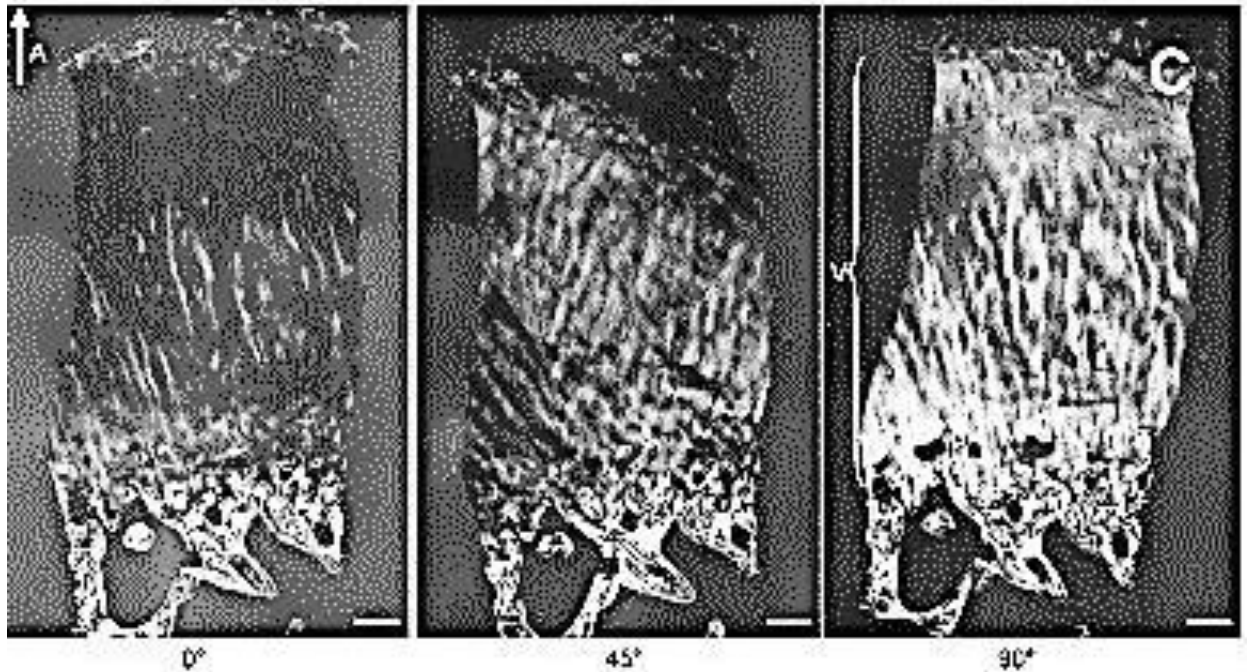


Figure 1.13: Polarised microscopy image of human bone biopsy. The amount of birefringence reflects the alignment (0° , 45° and 90°) of collagen fibers in the different specimens (148). Scale bar $250 \mu\text{m}$

To improve the quality of the images, picosirus red is frequently used as a contrast enhancement agent made from picric acid and sirius red dye. It has the unique property of staining both thin and thick collagen fibers (149). Fiber hue reflects density in a particular region of the sample. It can be used with polarized light microscopy to achieve semi-quantitation of collagen fiber and its orientation in a tissue sample (150). Also, the spatial distribution of structural proteins can also be obtained by employing image-subtraction software techniques to remove regions of little interest and reveal the arrangement of structures being viewed (150).

1.7.1.3 ATOMIC FORCE MICROSCOPY (AFM)

AFM is a type of scanning probe microscopy which uses a sharp-tipped solid probe to scan the surface of the object being assessed (151). The force between the probe's tip and sample is measured over the entire surface of the object being imaged (152). This gives a topographic view of the objects surface, showing the vertical relationship of surface structures to each other (Figure 1.14). AFM can be used in non-touch mode and repeated scanning can be minimized to make it suitable for biological specimens (153).

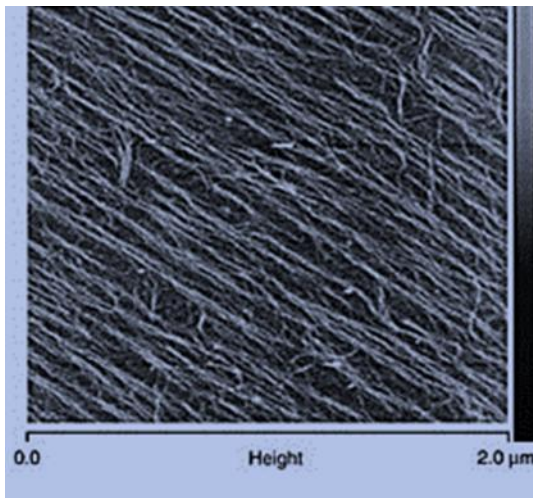


Figure 1.14: AFM image of collagen I fibrils (154)

1.7.1.4 SECOND HARMONIC GENERATION (SHG)

Imaging in second harmonic generation is achieved by generating more energetic photons from photons striking a nonlinear material, yielding better image resolution than optical methods (155). This makes SHG suitable for imaging thick specimens down to nano-scale resolutions (156). It is a particularly useful technique for fibrillar collagen imaging because such collagens generate bright second harmonic signals (157) as shown in figure 1.15. This lends it as a potentially important tool for tracking connective tissue changes. It is useful for

imaging both fresh and fixed tissue samples. Interpretation of generated image however requires some level of expertise (155)

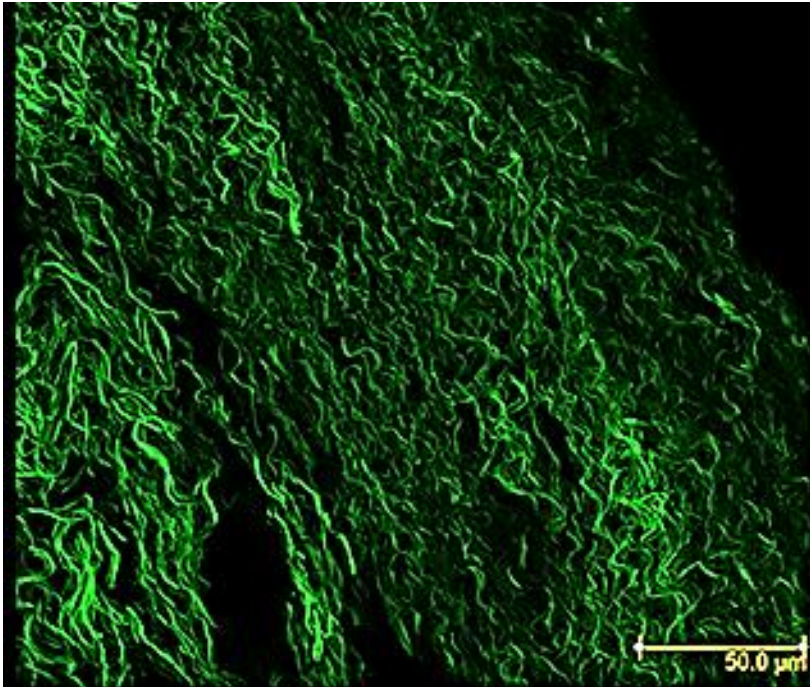


Figure 1.15: Second harmonic generation image of airway collagen fibrils (157).

1.7.1.5 FOURIER TRANSFORM INFRA-RED SPECTROSCOPY (FTIR) AND RAMAN SPECTROSCOPY

The infra-red spectrum or Raman scattering of collagen gives insight to its native structure as well as structural alterations (158). FTIR has been used in the attenuation mode and also on a complementary basis with Raman spectroscopy to detect glycation-induced changes in collagen structure (158,159). These microspectroscopic methods are non-invasive and particularly useful for *in vivo* and diagnostic studies. They also do not require prior protein or peptide hydrolysis or tissue labeling lending them useful in non-destructive *in vitro* studies (160). Expertise is however, required for data analysis and interpretation and, the result obtained is semi-quantitative (158).

1.7.2 MECHANICAL TESTS

Connective tissues are load bearing. Mechanical characterisation reflects their function. To characterise human soft tissue *in vivo*, limitations of system complexity and technique invasiveness are considered (161). For this reason, *in vitro* studies are relevant first steps. *In vitro* studies are particularly important in cause and effect and, correlation studies. In addition, they enable tissue characterisation that is important in the ultimate design of ideal *in vivo* diagnostic devices. *In vitro* mechanical tests for soft tissues involve simple manual devices as well as automated bioreactors and computational models (162,163).

There are few studies and techniques available for the mechanical characterization of prolapsed tissues (5). Some of these have been used in prolapse studies but with inherent limitations. Most *in vitro* mechanical studies of the vaginal wall have used destructive methods which are often adaptations of tensile or compression tests (11–13,127,164,165). The forces applied using such methods are dissimilar to what is experienced by the tissue *in vivo* and such tests prevent simultaneous assessment of within tissue properties as the tissues are destroyed during testing. Some of the techniques used in mechanical assessment may be adapted or improved for use in the study of prolapsed tissues and hence are discussed below

1.7.2.1 COMPRESSION TEST

The compression test involves compressing test tissues or materials in between two plates with or without confinement of the tissues in a chamber that restricts its lateral deformation (166,167). The compressive force (applied load) and corresponding tissue deformation give mathematical insight into tensile properties of assessed tissue (168).

Using the compression method, the viscoelastic property of prolapsed vagina tissue has been assessed (115). Information on the altered mechanical characteristic of prolapsed tissue can be obtained but the tissue is destroyed in the process and the method gives no insight into the cause of disease development. When testing biological tissue, factors such as tissue inhomogeneity and anisotropism should be considered (169). For this reason, a non-destructive method is preferred.

1.7.2.2 TENSILE TEST

The tensile test has also been used to study prolapse tissue mechanics (11,94). Tissue anchorage devices such as wires or sutures, are loaded until the tissues' break point is attained (13,170) or devices are adapted for use with tissue biopsies (5). The test is based on the changes in force required to deform the test tissue at a constant rate of elongation. The force per cross-sectional area of the tissue is used to obtain tensile stress and strain values for calculation of Young's modulus, and determine both yield and ultimate tensile strength (171). Despite its usefulness, the tissue is also destroyed in the process and there is increased strain at tissue anchorage points (168). Testing to breaking point is an un-natural test of prolapse and does not simulate disease outcome. It is important to develop a mechanical test that would highlight the mechanical property of the prolapsed tissue that reflects or closely simulates disease outcome.

1.7.2.3 BULDGE TEST

This is another method for determining the mechanical characteristic of soft tissues (172). It is useful for testing membrane compliance. Liquid is passed through an opening at a constant

rate to deform the tissue (168). Applied force is more symmetrically distributed to the tested material but leakage can occur, making it less suitable for many biological tissues (168)

1.7.2.4 NON-DESTRUCTIVE AND MINIMALLY DESTRUCTIVE TESTS

1.7.2.4.1 CUTOMETER-LIKE MEASUREMENT (IN VIVO STUDIES)

Some *in vivo* studies on prolapsed tissue with non-destructive modes have been reported. The tests used are tactile imaging (10), suction technique and skin probe method (128,130). In the skin probe method 1.5 mm skin probe was adapted for use in the study of vaginal wall tissue's mechanical property (128). The suction method developed by Chuong et al was an adaptation of Cutometer-like technique. It involves the application and release of suction pressure to the vaginal wall (130). These are of diagnostic use but require significant adaptation for use in understanding prolapse. An ideal prolapse research method should have a set up that closely mimics the disease pathology, that is, vaginal wall deformation. Considering the central role of pelvic support played by the vagina tissue (4), descent of pelvic organs may occur as excess pressure is consistently transferred to the central vagina tissue. Therefore, the load-dependent creeping property of vaginal tissue may reflect, in an *in vitro* setting, prolapse. A mechanical test to assess tissue load deformation over time (creep) in a non-destructive way is thus required.

1.7.2.4.2 IN VITRO STUDIES

These include spherical ball indentation and optical coherence elastography (OCE), which are discussed in 3.4.1 and 3.4.3.

1.7.3 QUANTIFICATION OF COLLAGEN

To accurately quantify AGEs in connective tissues, especially in collagen, it is important to first quantify collagen to enable analysis of the relationship between the presence of these markers and amounts of tissue collagen. Collagen quantitative assay methods have been limited by the extensive crosslinks formed by collagen molecules (173). Methods that exist for its quantitation include: the use of precipitating dyes for in-situ measurement of soluble collagen (174) the use of HPLC or colorimetric methods to analyse the hydrolysed protein. HPLC and colorimetric methods are based on collagen quantification in relation to the amino acid, hydroxyproline (173).

1.7.3.1 HYDROXYPROLINE ASSAYS

Hydroxyproline is a collagen-specific amino acid oxidation product constituting approximately 14 percent of collagen (175). It is a post-translational modification of collagen. Collagen, which is comprised of tri-peptide repeat sequence, has hydroxyproline often recurring at the Y position of its glycine-X-Y repeat (176). Thus assaying hydroxyproline enables collagen quantification in the presence of other protein types.

Hydrolysis of collagen is pre-requisite to obtaining hydroxyproline. This is the cleavage of peptide bonds of proteins and peptides to obtain constituent amino acids. Various technical variations exist for tissue hydrolysis but in principle, heating a solution of proteins or polypeptides 110°C in concentrated hydrochloric acid over 18 to 24 hrs results in cleavage of the amino acid bonds within polypeptide chains (177).

Colorimetric methods have been used to quantify hydroxyproline. The principle is the formation of a chromophore by an oxidation reaction with hydroxyproline (178). This method

is cheaper, less laborious and less time consuming than HPLC. The intensity of the chromophore directly relates to the amount of hydroxyproline present in the hydrolysed tissue sample (173) .

1.7.3.2 HIGH PERFORMANCE LIQUID CHROMATOGRAPHY (HPLC)

HPLC can be utilized in the extraction of hydroxyproline following sample hydrolysis in hydrochloric acid (179). Hydroxyproline, derived from proline (using phenyl isothiocyanate) can be separated and isolated from other amino acids using reverse-phased HPLC. It is then detected at its absorption wavelength (180). Variations in the column size and HPLC settings determine the elution or separation time of amino acids (179).

1.7.3.3 HISTOCHEMISTRY - PICROSIRUS RED ASSAY

The picrosirus red dye stains specifically for collagen. The dye intensity after staining is directly proportional to the amount of collagen present in the sample hence stained biological sample can be dissolved and assessed colorimetrically (181). The OD reflects the amounts of collagen present in a biological sample. Although this assay method permits simultaneous structural and quantitative assessment of tissue samples, sirus red stains some collagen fiber types less intensely giving a less accurate representation of the amount of collagen in a sample than the oxidative colorimetric assays (174).

1.7.4 AGEs DETECTION

1.7.4.1 IMMUNOHISTOCHEMISTRY

Antibodies to AGEs receptors have been used to detect the presence of AGE in tissues (182). Antibodies to AGE scavenger receptors or polyclonal antibodies to RAGE enable visualization

of concentrations of the markers within tissues. This method can be employed *in vivo* by using anti-sera but it cannot be used for absolute quantification of the ageing marker (183). Also, quantifying these receptors does not give an accurate picture of the amount of AGEs present in the biological sample.

1.7.4.2 HPLC

HPLC requires complete hydrolysis of the proteins to be analyzed as earlier described. Pentosidine, a fluorescent ageing marker is detected via HPLC coupled with an ultraviolet (UV) or fluorescent detector (184). UV detection has been achieved at 325 λ while fluorescent detection occurs at excitation and emission spectra of 335 and 385 nm respectively (185). An online screen display gives a graphical representation (chromatogram), showing peaks of the amounts of various amino acids. Running various known concentrations of a stock solution of the ageing marker and comparing with relative amounts of unknown test samples gives absolute amounts of the ageing marker in the tissue (177). Furthermore, the HPLC can be coupled to a mass spectrometer which takes advantage of the mass shift conferred on amino acids by glycation for a mass-based detection (186). HPLC, unlike immunohistochemistry for AGEs detection enables absolute quantification of the amount of AGEs present in a tissue. Although it has cumbersome and time-consuming sample preparatory steps and cannot be used *in vivo*, the same hydrolysed tissue can be used for both collagen and pentosidine quantification.

1.7.4.3 COLLAGEN ALIGNMENT CAPACITY

The alignment of collagen fibril monomers under a magnetic field has been noted to change with age. In a study carried out using extracted collagen (from new born to 24 month old rats),

the degree of re-alignment of procollagen monomers reflected fluorescence due to AGEs (73). Younger collagen with lesser AGE-specific fluorescence had better alignment than older collagen. The less anisotropic AGEs were suggested to inhibit the re-alignment of collagen monomers in older collagen. This quantification of collagen monomer alignment can be exploited for future *in vitro* quantitation of fluorescent AGEs in collagen extracts.

2 CHAPTER 2: HYPOTHESES AND AIMS

2.1 HYPOTHESES

2.1.1 PROLAPSE IS A DISEASE OF ACCELERATED AGEING AND VAGINAL TISSUE ARE STRUCTURALLY AND MECHANICALLY ALTERED IN RELATION TO THEIR GLYCATION CONTENT

There is an increased prevalence of prolapse in the aged population and minimal occurrence in younger women (82,91). Prolapse, once thought to be a disease of the multiparous has been observed in some nulliparous women (45). This is a challenge to some widely held concepts about its aetiology. In view of this lack of clarity it is important to further investigate another notable risk factor, ageing. Considering the above observations and striking similarities between ageing connective tissues in other parts of the body and prolapsed tissue and the observed associations of the disease with ageing, prolapse could be another disease of ageing. There is a need to investigate the relationship between presence of ageing markers and development of disease, an understanding that may be beneficial in future prediction of prolapse even before disease becomes apparent.

The structure of tissues dictates their function in healthy and disease states. Chronic disorders are typically the result of multiple cellular and tissue level changes, which accumulate to result in the disease phenotype appreciable at the organ level. (187). It is therefore expected that the vaginal wall, a major adaptable tissue in pregnancy and prolapse, would exhibit notable ultrastructural changes in keeping with functional changes.

Most studies on prolapse have only focused on biochemical or ageing changes of the prolapsed tissues or mechanical properties (8). This leaves a gap in understanding the exact relationship between these two properties. There is a need for a combined comparison of

mechanical and biochemical changes. Markers of ageing are known to be present in higher quantities in prolapsed tissues compared with controls (8,23,45). The prolapsed vaginal tissues have shown significantly different mechanical properties from normal tissues. Despite rising interest in the mechanics of prolapse, much remains to be done. A recent review of the state of pelvic tissue biomechanics reveals a need for the collection of more mechanical data to add to the body of knowledge and potentially aid the creation of useful study models (118).

The ageing process is believed to be a key determinant of prolapse. It is hypothesized that age-related changes correlate directly with mechanical changes of vagina tissue. This correlation may reflect prolapse occurrence and severity. In other words, ageing can predict vaginal tissue mechanics, and development. In addition, since physical ageing is a global phenomenon occurring in all cells to varying degrees, these changes are also reflected in other parts of the body. Therefore, it is expected that there should be correlation between the progression of ageing in various body tissues, both superficial and deep.

2.1.2 GLYCATION ACCUMULATION IN PELVIC TISSUES IS INFLUENCED BY OESTROGEN

Oestrogen is associated with pelvic tissue remodelling, involving breakdown and re-synthesis of the key structural proteins (188). Pregnancy, a high oestrogen state is known to cause increased elasticity of pelvic tissues (13,121). It is also thought that glycation of structural proteins leads to stiffer, less elastic connective tissues, an effect noted in prolapsed tissues with higher glycated proteins (12,55). Understanding that pregnancy is associated with higher amounts of oestrogen than in non-pregnant states and that pelvic tissues are sensitive to oestrogen (47) leads to the hypothesis that a state of high oestrogen such as pregnancy is

associated with breakdown of structural crosslinks of collagen and elastin in the vaginal ECM, resulting in reduced amounts of glycation products and reduced tissue stiffness. Gestation and delivery are associated with pelvic tissue remodeling, involving breakdown and re-synthesis of the key structural proteins (188). Pregnancy is known to cause increased elasticity of pelvic tissues, and high oestrogen level (13,121). It is also thought that glycation of structural proteins leads to stiffer, less elastic connective tissues, an effect noted in prolapsed tissues with higher glycated proteins which occur more frequently in aged women who have low oestrogen level (12,55). Considering the modulations in oestrogen levels during pregnancy and in preparation for delivery of the foetus and, the sensitivity of vaginal tissue to the hormonal changes (47), it is hypothesised that high oestrogen levels correlates with breakdown of structural crosslinks of collagen and elastin in the vaginal ECM, resulting in reduced amounts of glycation products. This may enhance the loss of older stiffer collagen and cause improved compliance of the female pelvic tract to accommodate passage of the fetus. This implies a potential relationship between vaginal tissue oestrogen expression and glycation content.

2.2 RESEARCH AIMS

The aims of the research were:

1. To investigate the relationship between vaginal wall mechanics and glycation content during pregnancy, understanding the association between ER- α expression in the tissues with the process, to understand a possible mechanism where present and to investigate vaginal tissue ultrastructure in pregnancy as well as the influence of sGAG on the same and to study the relationship between skin and vaginal tissue glycation in the same subjects. These have been studied in Chapter 4 under sections 4.1, 4.2 and 4.3 respectively

2. To quantify and study the glycation compound, pentosidine in prolapsed tissues and study this in relation to known and suspected risk factors and glycation associations including age, hypertension, smoking, cholesterol level and diabetes. A further aim was to understand the reason for glycation increase in prolapsed tissues by studying the glycation changes, ER- α expression and the expression of a glycation lowering antioxidant, glyoxalase I in the tissues. Chapter 5 addresses this aim.
3. To mechanically characterize the vaginal tissue in prolapse at nanoscopic, microscopic and macroscopic scales using multiple new techniques in the study of prolapse, and to assess vaginal tissues' structural properties with a view towards understating prolapse pathology. This has been studied in chapter 6. A further goal was to correlate the glycation content of the vaginal tissue in pregnancy and prolapse with observed mechanics. This has been addressed in chapters 4 (4.1) and 6 in pregnancy and prolapse, respectively.

3 CHAPTER 3: MATERIALS AND METHODS

3.1 TISSUES AND ETHICS

3.1.1 RAT TISSUES: ETHICAL APPROVAL AND DISSECTION

Outbred 6-8 month old female Sprague Dawley rats were used following local ethical approval by the Animal Welfare & Ethical Body Review, in accordance with the Animal act of 2006. From these, non-pregnant and E15-E18 (last trimester) pregnant rats were humanely culled by a Schedule 1 method. Both fresh and defrosted tissues frozen at -20°C were used after the Schedule killing. Following midline dissection of abdominal wall and location of pelvic tissue complex in rats (shown in Figure 3.1), full thickness vaginal tissues were obtained by blunt dissection and separation of posterior vaginal wall from rectal tissue and detachment of anterior wall from urethral tissue.

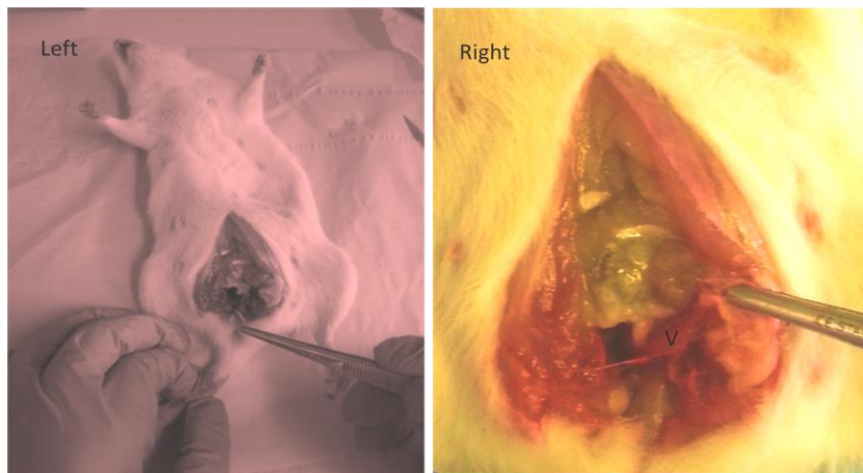


Figure 3.1 Dissection of Female Sprague Dawley rats. A mid-line abdominal section was made followed by blunt dissection to locate the pelvic tissues. Dissection of the abdominal wall with intact viscera is seen on the left, while the image on the right shows the vagina (V) lifted off from the rectum following blunt dissection.

The vaginal wall was subsequently separated from the bicornuate uterus and surrounding pelvic tissue complex shown in figure 3.2.



Figure 3.2: Reproductive organs of Female Sprague Dawley rats isolated from pelvic cavity. The vaginal wall (V), uterine horns (H), cervix (C), urinary bladder (B), and an ovary (O) are shown.

3.1.2 HUMAN TISSUES: ETHICAL APPROVAL, PARTICIPANT RECRITMENT, CONSENT TAKING AND DATA CHARACTERISTICS

National and local ethical approval was obtained. National ethical approval was sought from the Health Research Authority. The approved Research Ethics Committee (REC) reference number was 13/LO/1655. National Research Ethics Service London and local approval was

obtained from the University Hospital of North Midlands (UHNM) Research and Development department. Information sheets and proformas were designed by participating scientists and clinicians with the approval of the University Hospital of North Midlands National Health Service (UHNM NHS Trust) Research and Development department prior to study commencement. Women 41 years and above were recruited. Clinicians obtained informed consent from women scheduled for elective prolapse and other relevant gynecological surgery. Redundant vaginal tissues excised during surgery and otherwise discarded were collected and used for study. Prolapsed regions of the vaginal wall were obtained from women undergoing surgery for prolapse. Control samples were vaginal tissue obtained by surgeons from participants undergoing surgery for conditions such as gynecological or urological cancers. Sixty-five samples were obtained (49 prolapse and 16 controls). Full thickness vaginal tissue segments were obtained from upper middle zones (prolapse) and apical regions (controls) of the vaginal wall based on surgical availability. Samples not containing vaginal tissue segments were excluded. Proformas were created to obtain data on age, parity, mode of deliveries, presenting symptoms, type of prolapse, comorbidities such as hypertension, diabetes, smoking, etc, type of surgery, grade of prolapse based on Baden-Walker half way system and (International Consultation on Incontinence Questionnaire-Vaginal Symptoms) ICIQ-VS score described in 1.5.3, diagnosed incontinence and prolapse types and grades, and previous prolapse surgery. Proformas were completed by the research student and participating surgeon from clinical notes' data and patient interviews with information obtained logged onto Microsoft Excel spreadsheet. Known and potential risk factors were compared against pentosidine amounts in the tissue.

3.2 STRUCTURAL AND MORPHOLOGICAL STUDIES

3.2.1 HAEMATOXYLIN AND EOSIN (H&E)

Histological sections were obtained to confirm the presence of the various histological zones and for structural assessment. 4-6 µm cryosections were cut from middle zones of vaginal wall segments by a microtome cryostat (Leica Biosystems) after proper orientation of the tissues anatomically. They were fixed with 4% formalin or 4% paraformaldehyde for routine histology. Samples were supported in optimal cutting temperature embedding medium from CellPath Ltd. Samples were rehydrated and stained with Weigert's haematoxylin (Sigma-Aldrich) for 8 minutes followed by bluing in tap water for 10 minutes. They were subsequently stained with eosinophilic eosin (Sigma-Aldrich) for 3 minutes followed by dehydration in two changes of 95% alcohol for 30 seconds each time, clearing with histoclear (Fisher Scientific) for 5 minutes and mounting with a xylene based mounting medium (distyrene, tricresyl phosphate plasticiser and xylene, DPX from Fisher Scientific). For the human tissues, cell counts from routine H&E staining were performed in each x20 image obtained using image J and comparisons were made between prolapse and control samples.

3.2.2 ELASTIN STAINING

For elastin staining, a modified Verhoff's stain (kit from abcam, UK) was used with and without counterstaining. Hydrated sections were placed in working elastic solution for 15 minutes, dipped 15 times in a differentiating solution, rinsed briefly in tap water and placed in Sodium thiosulphate solution for 1 minute. For counterstaining, slides were rinsed in running tap water and placed in Van Gieson's Solution for 5 minutes. They were subsequently rinsed

twice in 95% alcohol and dehydrated in 100% alcohol and mounted with a xylene based resin prior to light microscopy imaging.

3.2.3 NEURAL STAINING

For neural stain, tissue sections were washed in phosphate buffered saline (PBS) and fixed in 4% PFA for 10 minutes. These were subsequently washed thrice in tris buffered saline (TBS) and blocked using 5% Normal Goat Serum (NGS) in TBS-T for an hr at 4°C. Primary antibody, 2.4 g/L anti-glia fibrillary acidic protein (GFAP) purchased from Dako, UK was diluted in TBS-T at ratio 1: 100. And added to tissue sections and left overnight at 4°C. Samples were counterstained with goat anti-mouse fluorophore 547H at dilution ratio 1:300 in TBS-T. The experimental set up was placed in a dark room for 2 hours, followed by washing in TBS. Coverslips were introduced to samples using DAPI containing mounting medium and left to stand for 2-3 hours at room temperature covered in aluminium foil prior to imaging under a inverted fluorescent microscope (Nikon Eclipse Ti-SR, Japan).

3.2.4 TRICHROME STAINING

4 µm thick cryosections of the vaginal tissues were stained using Masson-Goldner-trichrome staining kit from CarlRoth, Germany. Sections were rehydrated and stained with Iron haematoxylin (a 1:1 ratio mix of solutions A and B) for 3 minutes. They were rinsed with 1% acetic acid solution for 30 seconds followed by 10-15 minutes bluing in tap water. Slides were stained with Goldner's counter stain I for 10 minutes, rinsed with 1% acetic acid solution and subsequently placed in Goldner stain II for 20 minutes. Following rinsing, counterstain with Goldner stain III for 2-5 minutes and a further 1% acetic wash step was performed. Dehydration in alcohol, clearing in xylene and mounting using resin based mounting medium

followed. Results were interpreted as follows: green for connective tissue areas, orange for erythrocytes, red for cytoplasm and muscular layers.

3.2.5 SIRUS RED STAINING

Picrosirius red solution was prepared with 0.5 g Sirius red (sigma Aldrich, direct red 80) and 500 ml aqueous solution of picric acid. Hydrated 4 μm tissue sections were placed in picrosirius red solution for a minimum of one hour to attain equilibrium and thereafter washed twice in acidified water, dehydrated in three changes of 100% ethanol, cleared in xylene solution and mounted as described in 3.2.1 for viewing.

3.2.6 SCANNING ELECTRON MICROSCOPY (SEM) OF VAGINAL TISSUES

Freshly dissected whole vaginal tissues from pregnant and non-pregnant rats were segmented to obtain whole tubular rings. These were fixed with glutaraldehyde (GA) and washed with sodium cacodylate buffer. Critical point drying of the tissues occurred in a chamber filled with dry ethanol. This was gradually replaced with carbon dioxide over few hours at 31⁰C and ~ 73 atm. And subsequently anchored to metallic stubs by carbon stickers, further coated with a metallic paint to improve conductivity. Improved specimen conductivity was achieved by incubation in osmium tetroxide (OsO₄). Specimens were then gold coated within a vacuum in a sputter gold coating chamber in preparation for imaging. Low and high (1k- 15k) magnification images were obtained for native tissues and collagen gels fluids and gels using a field emission SEM (Hitachi S4500) of resolution 1.5 nm.

3.2.7 OPTICAL COHERENCE TOMOGRAPHY (OCT)

Freshly dissected vaginal tissues of pregnant and non-pregnant rats were imaged using OCT prior to mechanical testing and for assessment of structure and cross-sectional thickness measurement. OCT can provide useful information about the internal structure of a biological tissue. Its longitudinal resolution depends on the coherence length of its light source and some devices are unsuitable for use to determine thickness of larger tissue samples due to a limited field of view in the mm range (189). An OCT instrument (TELESTO-II, Thorlabs) was used. The instrument can achieve up to 3.5mm depth penetration. Near-infrared light at 1300 nm wavelength was transmitted through specimens placed flat on clear petri dishes. The intensity of the backscattered light produced 2-D images of cross sectional images of the tissues across selected areas from screen displays of the tissues.

3.2.8 AFM ANALYSIS

AFM was conducted using a Bruker Multimode instrument (Nanoscope VIII MultiMode AFM, Bruker Nano Inc., CA) equipped with a 150 x 150 x 5 μ m scanner (J-scanner) operated with PeakForce Quantitative Nanomechanical Mapping (PFQNM) modality. For PFQNM measurements, the spring constant of the cantilever and deflection sensitivity were measured on a clean sapphire sample and then, the set up was calibrated with a polymer of known elastic modulus (PSI, Vishay Measurements Group, UK) (190). 4 μ m thick vaginal tissue cryosections of pregnant and non-pregnant rats without fixation were collected onto coverslips and stored at -20⁰C until testing. The coverslips were glued to metal support stubs prior to testing. To obtain high resolution images air dried sections were used. A silicon nitride tip (Bruker Bruker TAP150) with a nominal tip radius of 8 nm and a 5 N/m spring constant was used for imaging.

2-D and 3-D height images were obtained from the Nanoscope software (version 1.5) for structural analysis. Data on collagen fibril size, count and alignment were obtained using image J software.

3.3 BIOCHEMICAL ANALYSES

3.3.1 SULPHATED GLYCOSAMINOGLYCANS (sGAG) AND WATER CONTENT

The sulphated glycosaminoglycan (sGAG) content in both pregnant and non-pregnant rat vaginal tissues was determined by staining of 4-6 μm vaginal tissue sections using alcian blue. To prepare the staining solution (0.1% w/v alcian blue solution), 0.1g of alcian blue powder from Sigma-Aldrich, UK was dissolved in 3% acetic acid prepared from 3ml glacial acetic acid (Sigma-Aldrich,UK) and 97 ml 97mL dH₂O. Rehydrated tissue sections were placed in the resulting solution of pH 2.5 for 30 mins, then washed in running tap water for 2 mins. Following distilled water rinse, dehydration occurred in two changes of absolute ethanol. Clearing and mounting of coverslip preceded light microscopy imaging of samples. A strong blue stain was indicative of the presence of sGAG. For sGAG quantification, DMMB (1, 9-dimethylmethylene blue) method was used. In brief, lyophilized and weighed rat vaginal tissues were digested in papain enzyme solution (50 ml of 200 mM phosphate buffer containing 1 mM ethylenediaminetetraacetic acid (EDTA) at (pH 6.8), 25 mg papain from papaya latex and 48 mg N-acetylcysteine) (191). Three hundred μl of digestion solution was added to 6-12 mg dried and weighed tissue samples and incubated for 16 h at 60°C. Thereafter, 200 μl of DMMB solution (DMMB solution prepared by dissolving 4mg of DMMB dye (Sigma-Aldrich, UK) in a 250 mL solution comprising of 0.58g NaCl and 0.75g glycine (both from Sigma-Aldrich, UK) and 2.08 ml of 0.1M HCL (Fisher Scientific, UK) was

added to each well of 96 well-plate containing 50 µl of samples or standard solution aliquots, followed by immediate absorbance reading at 530 nm (BioTec Synergy 2). The standard curve was made by using serial dilutions of bovine chondroitin sulphate stock solution. For the measurement of water content, the freshly dissected vaginal tissues were weighed initially and then dried to constant weight. Water content of the tissues was determined as the difference between wet and dry tissue weights tissues and expressed as a percentage of the wet weights.

3.3.2 AGEING BIOMARKER DETECTION

The glycation product, pentosidine, which is formed by the reaction of arginine and lysine with a pentose sugar (19) was chosen for detection (192) by an ultraviolet detector. Freshly dissected vaginal tissue portions from aged-matched pregnant and non-pregnant rats were hydrolysed in 6 M hydrochloric acid at 110°C over 20 hours. Hydrolysed samples, following removal of hydrochloric acid in a lyophiliser, were redissolved in deionised water at a concentration of 0.1mg/µl and separated using high performance liquid chromatography (HPLC, Agilent 1220 LC, USA). Separation occurred in a C-18 250 x 4.60 analytical column and detection at 325 nm wavelength by an ultraviolet detector. Pentosidine eluted at 9.6 minutes in a 30 minute run (figure 3.3) using 0.1% trifluoroacetic acid made from 1ml of HPLC grade trifluoroacetic acid (Sigma-Aldrich) and 1L distilled water and 80% acetonitrile made from 800 ml of HPLC grade acetonitrile (Fisher Scientific) and 200ml water as solvents A and B, respectively at a flow rate of 1 ml/min with gradient of 0-18% from 0 to 12 minutes and 100% for 12 to 18 minutes for solution B and 100% - 82% from 1 to 12 minutes of solution A.

Serial dilutions of pure pentosidine compound (Caymann Chemical, USA) was used for standard quantification. A linear standard curve, figure 3.4 ($r^2=0.99$) was obtained from serial dilutions of the pure pentosidine compound and areas of peak which were proportional to pentosidine content. For human tissues, full thickness prolapse and control tissues were analysed.

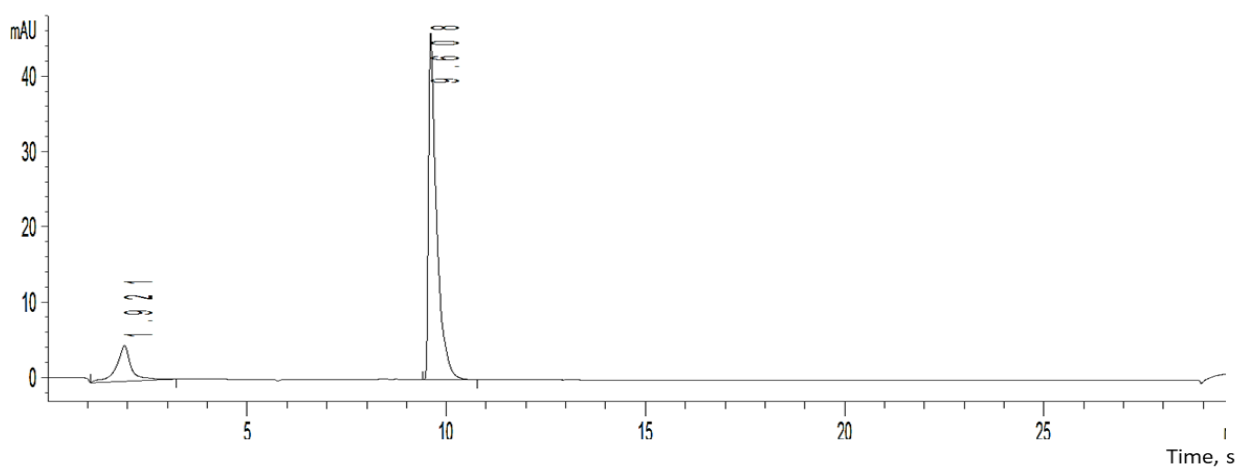


Figure 3.3: HPLC chromatogram showing pentosidine elution at 9.6 minutes.

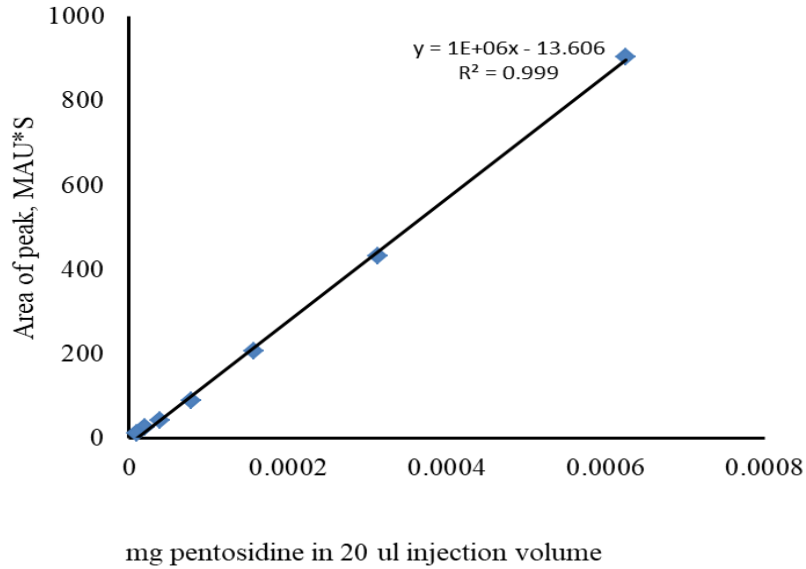


Figure 3.4: Pentosidine standard curve.

3.3.2.1 VALIDATION TESTS FOR PENTOSIDINE ANALYSIS

Validation tests were carried out on the human samples. The tests were designed to test the effect of the use of different locations of the same tissue for pentosidine analysis, stored versus freshly obtained tissues for analysis and lyophilisation versus oven drying methods. For sample validation, full thickness tissue bits from 3 non-contiguous regions of each randomly selected samples were obtained and tested for pentosidine content to determine repeatability of pentosidine testing on the same tissue. In order to examine the impact of sample storage on pentosidine content, repeat testing of samples stored at -20 degree C for more than 12 months using the same protocol was carried out. Two types of sample drying methods prior to hydrolysis were assessed. The same samples were dried using a 60 degree oven and lyophilisation overnight and tested for pentosidine content.

3.3.3 COLLAGEN ASSAY

A colorimetric assay was used to detect hydroxyproline for collagen quantification in age-matched control and prolapsed tissues, n=8 per group. The assay kit was purchased from Sigma-Aldrich (St. Louis, MO). 100 mg full thickness tissue sections were weighted and the homogenized inside PTFE capped glass vials. To each of these 100 ul deionized water and 100 ul 12 M (37%) HCL were added and hydrolysis took place at 110 °C oven over 3 hours. Hydroxyproline standard was diluted in deionized water and standards, ranging from 0-1.4 ug were made prepared in a 96 well plate. 20 ul of diluted test solutions were inserted in wells of a 96 well plate and left to dry in a 60 degree oven. After drying, each well was incubated with 6 µL of Chloramine T Concentrate and 94 L of Oxidation Buffer for 5 minutes at room temperature, followed by 100 L of the Diluted DMAB Reagent (within the kit) and subsequent incubation at 60 degrees for 90 minutes. Following colour development, reading was carried out at 560nm for standards and samples in a 96-well plate on a spectro-photometer. Conversion of OD readings to amount of hydroxyproline in the solutions was made using standard curve equation which were subsequently converted to total collagen content using a factor of 14 (193).

3.3.4 IMMUNOCHEMISTRY

6 µm-thick sections of vaginal tissues were cut in a cryostat machine, fixed by 4% paraformadhyde and rehydrated for ER- α and Glo-I immunostaining. For oestrogen (ER- α) receptor detection, sections were permeabilised with triton-X after blocking for 4 hours with 5% bovine serum albumin, BSA soluton made by dissolving 5mg of BSA powder in 100 ml phosphate buffered saline, PBS. Following incubation with mouse monoclonal IgG antibody

to ER- α (from Santa Cruz Biotechnology) directed against the intranuclear steroid receptors, goat anti-mouse IgG (Life Technologies) was incubated against the primary antibody. The primary antibody (1:100 dilutions in 1% bovine serum albumin, BSA solution) was incubated with the tissues overnight at 4⁰C. and thereafter washed thrice with phosphate buffered saline. The tissue sections were incubated at room temperature with secondary antibody solutions at the same dilution ratio. For negative control samples, the primary antibody was not added to tissues. For the antioxidant staining, rabbit polyclonal IgG against glyoxalase I antibody (Abcam, UK) was used to detect its expression with mouse anti-rabbit IgG as the secondary antibody. Three wash steps (to remove non-specific staining) were followed by cover slip mounting with 4',6-diamidino-2-phenylindole (DAPI) coated mounting medium for nuclei counterstaining and fluorescent microscopy.

3.4 BIOMECHANICAL TESTS

3.4.1 BALL INDENTATION MECHANICAL TESTING

Ball indentation method is a minimally destructive method that enables *in vitro* characterization of soft tissues and can provide information on tissue creeping and modulus (168). The deformation of the test tissue over time can be imaged in real-time. This technique incorporates advantages of the tensile test and the blister test; there is even distribution of applied force and the tissue remains intact through the test. In addition, it achieves a high resolution of 10 μ N and 10 μ m for force and displacement respectively (168). Briefly, the mechanical test device consisted of two transparent plastic O-rings held securely in place by stainless steel screwed plates as shown in figure 3.5 below. Prior to testing, tissues were

mounted between the O-rings and the set up was screwed securely in place (Figures 3.5 and 3.6)

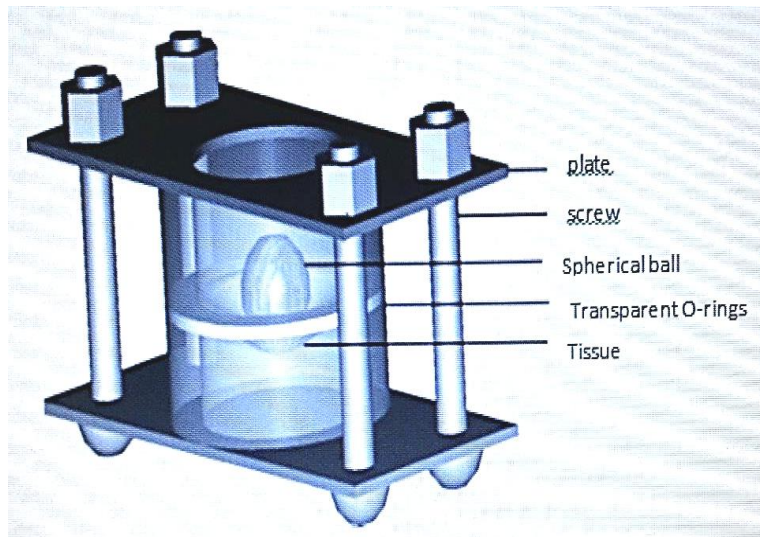


Figure 3.5: Schematic illustration of tissue sample holder for indentation ball instrument

(168).



Figure 3.6: Mounted vaginal tissue segments within plastic O-rings secured within a metal screw and plate system.

Distension of tissues was achieved by central displacement, produced by a spherical Teflon or stainless steel balls of weights 0.027 g and 0.27 g for creep and modulus testing respectively. The deformation images were acquired using a microscope with a long focal distance connected to a charge coupled device (CCD) camera (XC-ST50CE, Sony, Japan) and computer as shown in figure 3.7. To obtain creep data, time 0 and 24 hour deformation images (deformation image pictured below, Figure 3.8) were taken with the tissues deformed and incubated in a moist chamber at 37°C and 5% CO₂. Image deformation profiles were recorded on an image acquisition software, the Labview program (National instruments,UK).

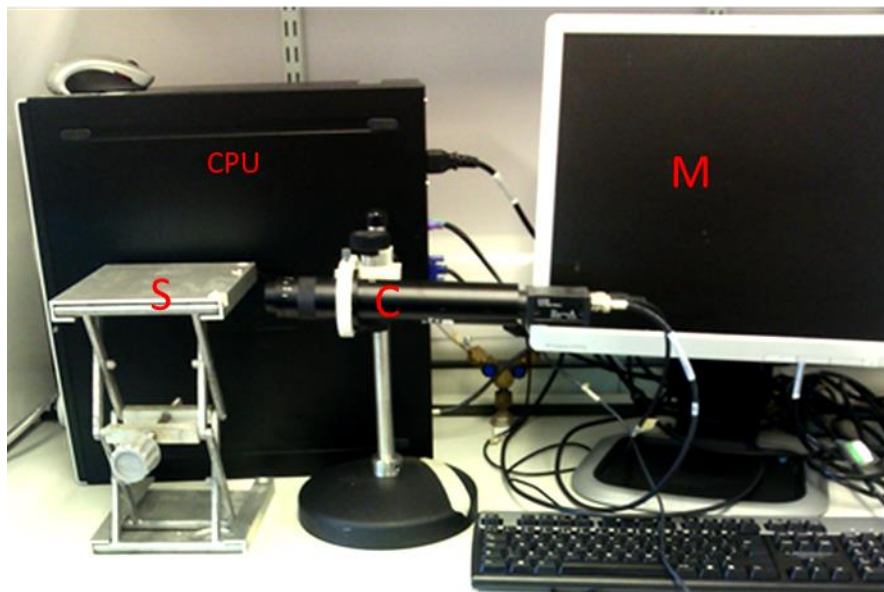


Figure 3.7: Ball indentation deformation imaging system. The CCD camera (C), the stage (S) for sample placement and computer monitor and central processing unit are shown.

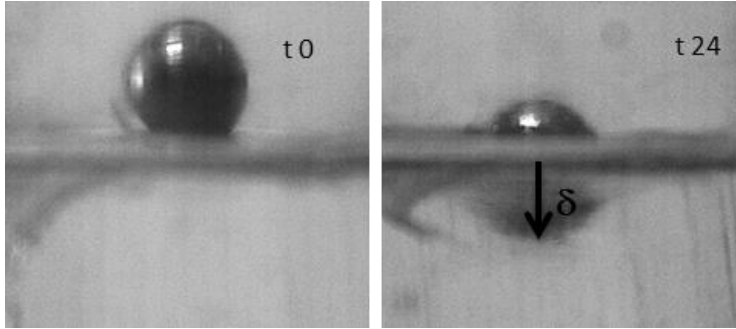


Figure 3.8: Displacement images of vaginal tissues at time 0 (t 0) and after 24 hours (t24) obtained using the CCD camera

The following equation based on the initial displacement, δ , was used for elastic modulus, E , measurement (168):

$$6w/EhR = 0.075(\delta/R)^2 + 0.78(\delta/R) \quad [1]$$

where 'h' represents the tissue's thickness, measured by optical coherence tomography, 'R' is the radius of the spherical ball (4 mm) and 'w' is the weight of the ball.

3.4.1.1 RAT TISSUE TESTING

Using the ball indentation method, the 24 hour creep deformation and modulus of the intact vaginal tissue segments were measured following pre-established protocol (168). Whole intact tubular vaginal organs from the rats were placed in cylindrical tubes as shown in figure 3.9 and carefully dissected by a mid-line incision and opened up into a rectangular flat piece prior to mounting between the O-rings secured within a plate and screw system as previously described.



Figure 3.9: Insertion of tubular vaginal wall over a cylindrical object to enable precise incising in the process of creating a rectangular flat sheet for mounting on mechanical test device. The arrow indicates the tissue's location.

3.4.1.2 HUMAN TISSUE TESTING

Ball indentation testing of prolapsed vaginal tissues was carried out for assessment of the relationship between glycation and tissue-level creep and modulus. Prolapsed tissues with a diameter of 12 mm or more were selected for ball indentation testing. This enabled adaptation of tissues tested to the mechanical testing device. The test was carried out using the method described in 3.4.1. For the human samples, central displacement was produced by a spherical stainless steel ball of weight 0.27g. Image acquisition and calculations were performed as previously described. Human vaginal wall tissues were much thicker than rat tissues. They

could not directly be mounted in the ball indentation ring and generate detectable deformation. Furthermore, thicker samples do not meet the dimensional criteria for modulus calculation by the equation [1]. Two slicing tools have been developed to prepare samples with appropriate thickness for the testing.

3.4.1.2.1 CREATION OF TISSUE SLICING TOOL

To enable slicing of isolated human vaginal tissue segments with appropriate thickness for the mechanical testing, a load stage (Figure 3.10) was conceptualized. The aim was to achieve secure tissue holding and simultaneously apply downward load to stabilize tissue during horizontal slicing motion in the z-plane. The design consisted of a biologically inert block made of poly tetrafluoroethylene (Teflon) and moveable stainless steel tissue holders.

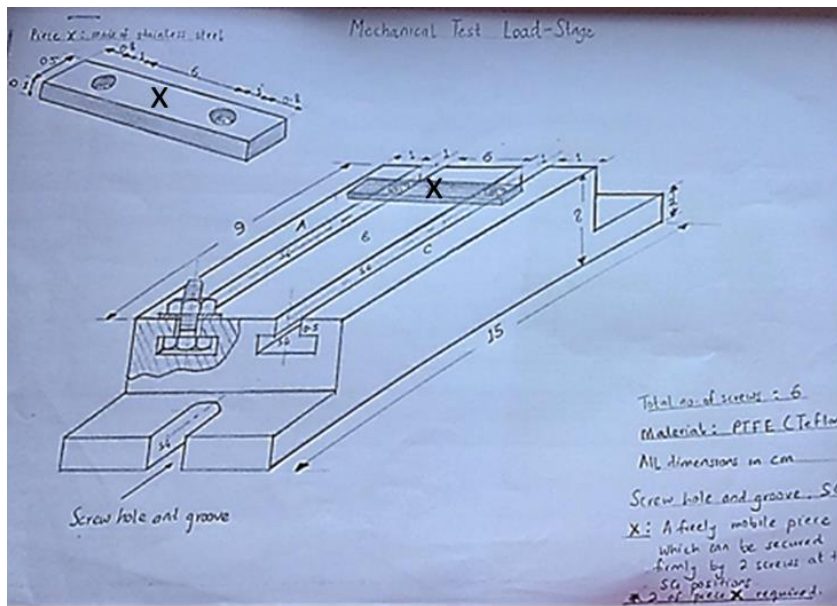


Figure 3.10: Mechanical test load-stage designed to support tissue during slicing.

Design improvement (Figure 3.11) was made with the aim of controlling tissue thickness with minimal dependence on the dissecting skill of the user.

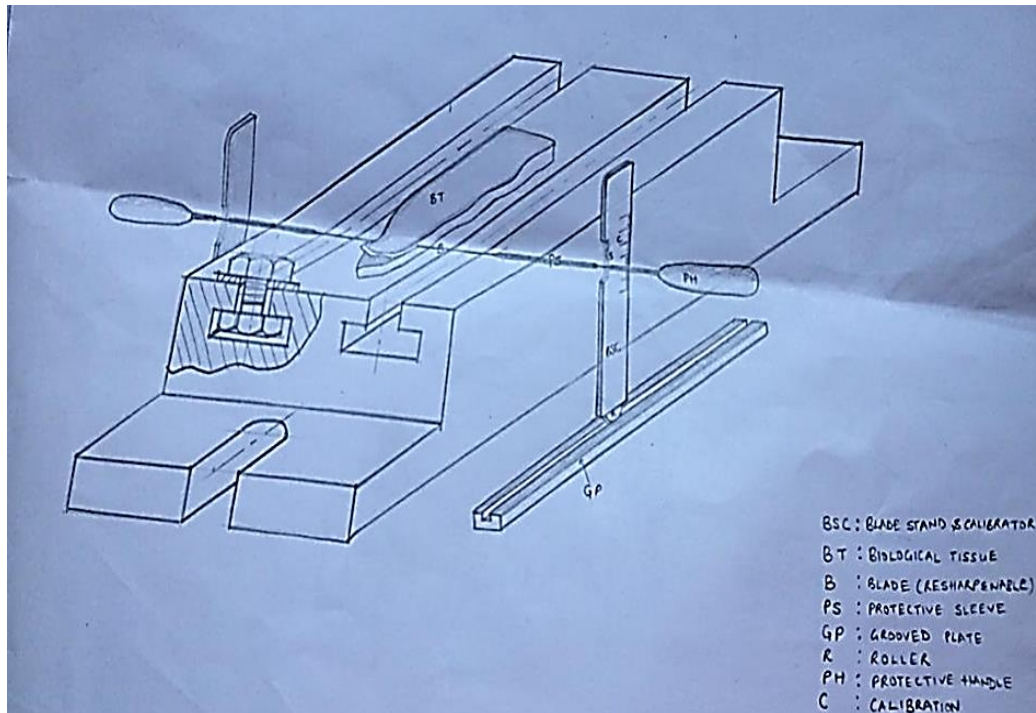


Figure 3.11: Design of mechanical test load stage with tissue cutter.

Sliding movement through affixed tissue (with piece x, a mobile but fixable piece made of stainless steel (figure 3.11) was to be enabled by rollers on the blade stand and calibrator (BSC,). The calibration was to ensure accurate choice of sliced tissue thickness while the grooved plate is firmly affixed to an underlying platform to ensure uniformity of sliced tissue thickness along its entire length. Rollers, blade stand and calibrator, grooved plate and supporting platform would be non-compressible.

The blade region was to be a thin ($<0.25\text{mm}$) segment that can be regularly re-sharpened or a disposable blade for safety reasons. A significantly sharp blade would produce a cut upon contact with biological tissue with minimal saw-like motion (which moves the soft tissue out of place). A protective sleeve (PS in figure 3.11) to which the blade is fixed was incorporated into the design for safe handling. PS would have a thinner segment which fits into calibration

grooves to regulate thickness. The grooved plane, GP (in Figure 3.11) would have elevated vertical platforms that extend to one third the lower region of the blasé stand and calibrator, BSC in the same figure. These would support BSC bilaterally, guiding sliding movement during tissue cutting. BSC can be fitted with vertically oriented locks at grooved region to secure thinner segment of PS when in working position. This would prevent slipping of blade during cutting.

A more cost-effective preliminary design (Figure 3.12) was however adopted with a compromise on automation of dissection. It consisted of a 1 mm groove created on the superior surface of the originally designed Teflon block to guide slicing of 1 mm thin tissues after downward fixing unto block. It was useful however in producing approximately 1.6 -2.3 mm thick tissue slices. Due to this variation in thickness, Young modulus calculations were carried out for each sample.

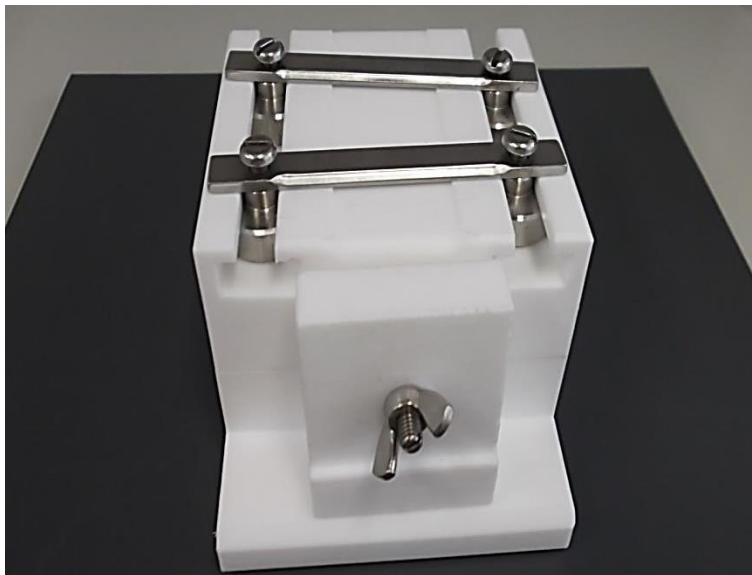


Figure 3.12: Slicing stage (final product).

The stage produced was a fixed polytetrafluoroethylene (Teflon) block with moveable stainless steel clamps over a 1mm groove for mounting and slicing of tissue. A detachable front piece of Teflon block was anchored by a screw and used for additional tissue support.

3.4.1.2.2 TISSUE SLICING PROTOCOLS

Vaginal tissue segments were sliced using 2 methods to adapt the tissues to the ball indentation device. The first method was manual slicing of tissues at room temperature by placing tissues on slicing stage. This was an improvised technique developed using readily available instruments. Sliced adventitial layers of the tissues were mounted on the ball indentation sample holder and imaged as previously described (3.1.7, obtaining t0 and t24 images (section 3.1.7), obtaining T0 and T24 images. The imaging of a ruler was also carried out alongside tissues to enable thickness determination (figure 3.13). Measurement of tissue deformation and thickness was performed using image J calibrated by the image of the ruler as the reference.

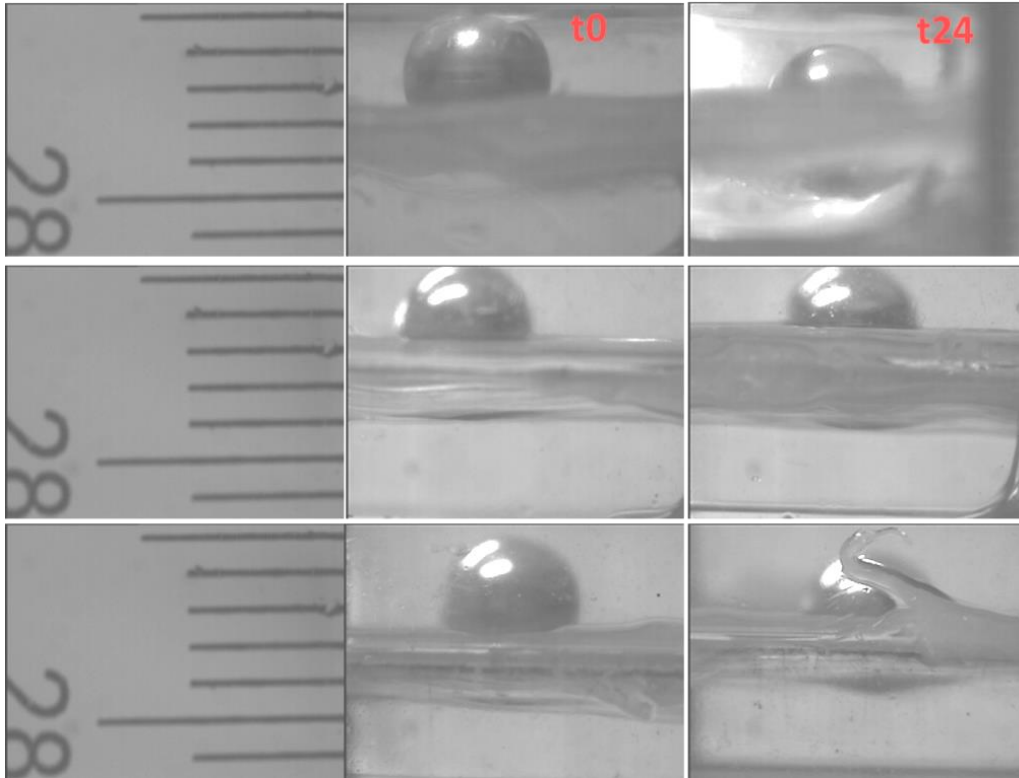


Figure 3.13: Thickness measurement illustration on T0 and T24 images of sliced vaginal tissue layers using method 1. The imaged ruler alongside tissues has been illustrated. Each division in the ruler (left panel) was 1 mm.

A second method of tissue slicing was developed to obtain thinner tissue slices. Whole tissue segments were mounted and secured on the slicing tool and the entire set up was kept at -80°C for 30 minutes. Thereafter the system was removed and the slightly frozen, firm tissues were sliced, by first removing the epithelial layer and then the subsequent layers (figure 3.14).

An optical coherence tomography instrument (OCT, section 3.2.7) was used for determination of the thickness of the tissue slices via obtained cross-sectional images as shown in figure 3.15. Measurements were taken at 3 points on each image and the average obtained.

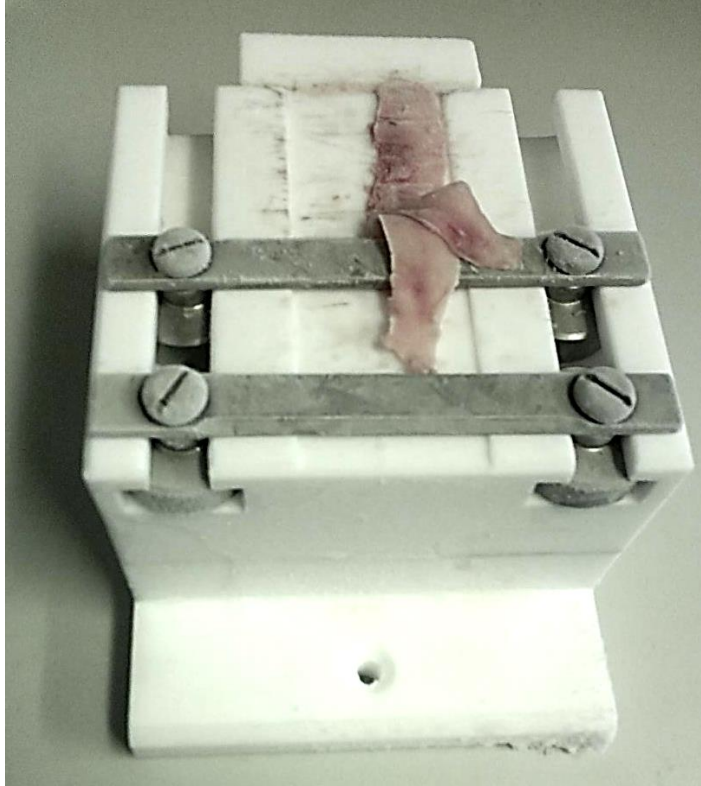


Figure 3.14: Slicing of slightly frozen tissue mounted on tissue stage using method 2. The short freezing resulted in easier slicing of tissues.

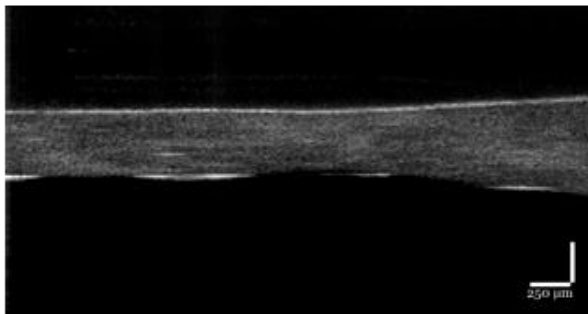


Figure 3.15: OCT image of sliced tissue using method 2. The thickness of the resulting tissue slices were obtained from the OCT image. Scale bar = 250 μm.

3.4.1.3 CORRELATION CALCULATION OF GLYCATION MARKER AND TISSUE MECHANICS

The creep and modulus of sliced prolapse tissue layers obtained as described above using ball indentation method were compared with known pentosidine content of the corresponding tissues by calculating the Pearson's r^2 correlation coefficient. Mechanical data by slicing methods 1 and 2 have been calculated respectively. Human control samples were too small in size to obtain the mechanical measurement data for correlation coefficient calculation.

3.4.2 NANOMECHANICAL MAPPING BY ATOMIC FORCE MICROSCOPY (PFNMAFM)

5 μ m thick cryosections of non-fixed prolapse and non-prolapsed vaginal tissues were obtained. With the use of routine laboratory protocols, contiguous sections of each tissue tested was stained with Haematoxylin-Eosin stains, imaged and used as pictographic guides for orientation of sections and location of LP zones for AFM imaging as shown in figure 3.16. Sample location was carefully selected and a photograph of the region obtained for reference as shown in figure 3.16. AFM testing occurred as previously described using the nominal radius silicon nitride tip and a 5 N/m spring constant for imaging. To observe tissue architecture at the micro level, 5 micron squared regions were sampled in the LP and adventitial zones of the tissues. Within each 5 micron area, three 1.4 micron areas were imaged to obtain a better view of the individual collagen fibrils. The elastic modulus for each imaged region of the samples was extracted using the Derjaguin–Muller–Toporov (DMT) model (194) to extract image raw mean from Nanoscope analysis software version 1.5.

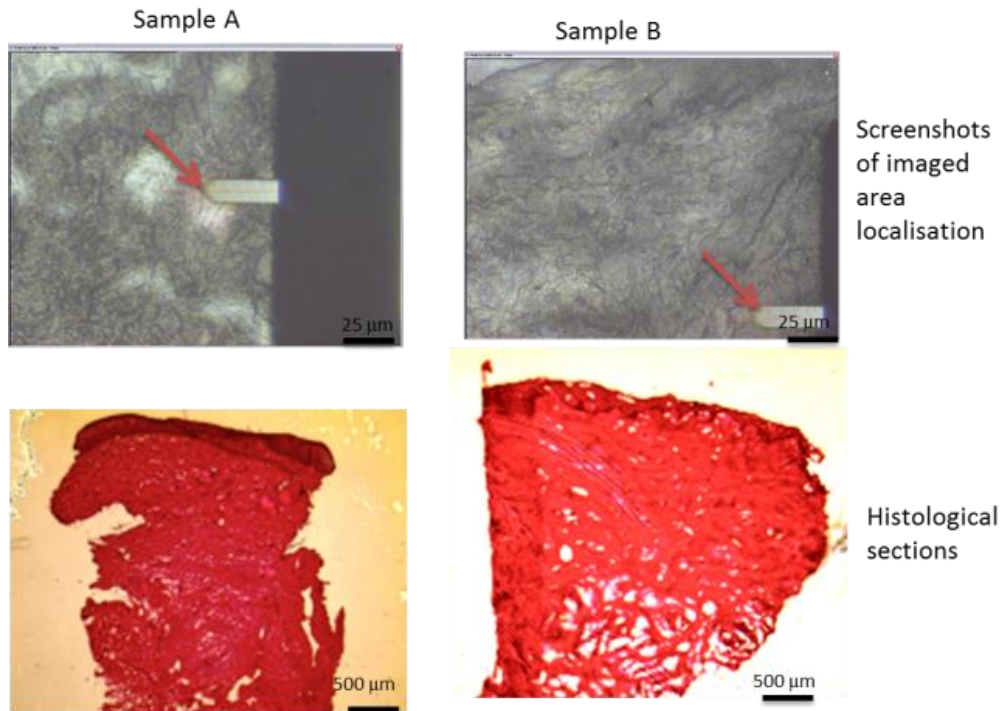


Figure 3.16: Sample location images (top) and histological images (bottom) of tissues studied using AFM. Real time images of tissues being assessed with the AFM probe were compared with histological images of contiguous tissue sections. (bottom) H&E stained images of contiguous sections of tissues imaged with AFM

3.4.3 OPTICAL COHERENCE ELASTOGRAPHY (OCE)

Whole tissue segments of some prolapsed and control tissue sections were further imaged by OCE. OCE is a method for non-invasive cross sectional assessment of biological tissues and it is useful in the determination of thickness and mechanics of the tissue (195). It has been widely used in the study of body tissues such as skin, blood vessels and retina. OCE can distinguish between properties of a normal and diseased tissue. For example, it has been noted to reveal differences between normal and atherosclerotic tissue (189,195). It utilizes optical reflections of infrared lights from tissues to determine thickness and structural organization.

OCE is useful for both cross sectional imaging of biological tissues and non-destructive mechanical characterisation (196). First introduced in 1988 by Schmitt, OCE utilizes tissue deformation or displacement to provide information on its stiffness (197). The displacement of the tissue in response to an internal or externally applied load gives information about its mechanical property (196). By utilising Phase resolved OCT detection which has resolutions in the Nano scale, OCE can accurately analyse and extract tissue deformation parameters to give information about its mechanical property with high accuracy (198).

This part of the study was a collaborative research conducted in Prof. Huang's lab. in Dundee University following the same system set up described by Guan G et al (199). The OCE system comprised of a phase sensitive OCT (Ph-S-OCT) and vibration stimulation. Ph-S-OCT detected the vibration signal using a superluminescent diode light source with a wavelength of ~1310 nm and band width of ~85 nm. In vibration stimulation, an electromagnetic actuator driven by a sine-wave modulated signal was used. The driving voltage was 500mV, the sampling frequency was 46 Hz and the driving frequency was 8 kHz. ~1 μm actuator displacement was applied to the specimens. Light delivery to the specimens occurred through an objective lens of of ~30mm. Axial and transverse resolution of the system were ~8.9 μm and ~15 μm in air respectively. The acquisition rate was ~46,800 A-scans/s. The OCT probe beam scanning was controlled by a software created using LabVIEW language. It performed 512 repeat scans at 256 locations with repeated application of the stimulus to enable 2-D image acquisition, with a resulting B scan comprising of 512×256 A-scans. A total number of 12 age-matched tissues (6 control and 6 prolapsed) tissues were studied. Control and prolapsed samples were imaged in air and immersed in 2% agar prepared at 29 $^{\circ}\text{C}$ and cooled to room temperature prior to imaging. Images of specimen set up were obtained for an understanding

of sample orientation during data interpretation. Data was processed as described by Guan G et al (199) and the 3D stiffness of each tissue was estimated. This was based on the rationale that the tissue vibration amplitude is related to the tensile strain and elasticity of the tissue and within the same tissue, the vibration amplitude varies with changes in regional strain. The stiffer the tissue, the less the displacement in relation to its original length (strain), whereas the softer tissues or softer regions of the same tissue would undergo more strain if the same stress was applied. The OCE hinges on the assumption that the same force is applied to an area. Therefore a relative modulus of the tissues can be obtained. To obtain absolute modulus 2% agar with a modulus of 193 kPa was used as the reference.

3.5 MODEL STUDY OF THE EFFECT OF sGAG ON COLLAGEN FIBRILLOGENESIS

3.5.1.1 COLLAGEN TURBIDITY ASSAY

To study the effect of sGAG on collagen fibrillogenesis, 0.1 mg/ml, 0.2 mg/ml, 0.5 mg/ml type I collagen solutions were prepared with and without introduction of sGAG. Corning 100mg Rat tail type I collagen stock solution (3 mg/mL), sterile 10X phosphate buffered saline (PBS), sterile distilled water (dH₂O), and 1M NaOH were placed in an ice during the process.

The volume of reagents required were calculated using the following formulas:

Volume of collagen required (Va) =

(Target concentration of collagen solution) × (Total Volume of collagen solution (Vt))

Concentration of collagen stock solution

Volume of 10X PBS needed (Vb) =

Total Volume of collagen solution (Vt)/

10

Volume of 1N NaOH required(Vc) = (Va) × 0.025

Volume of dH2O required(Vd) = (Vt) – (Va + Vb + Vc)

dH₂O, 1N NaOH, and 10X PBS were mixed in a sterile tube. Collagen was slowly pipetted into the tube, and then the solution was gently mixed. The resulting mixture was at a neutral pH. The collagen solutions were retained in 5 ml bijoux tubes on ice for immediate introduction of sGAG. Chondroitin sulphate and over sulphated dermatan sulphate (purchased from Sigma Aldrich) was the sGAG used in the study. The physiologic ratio of sGAG to collagen was calculated to be 1:50 (165). To maintain near physiologic environment but allow for observation of changes where present, 200 µm of collagen monomer solutions – controls and samples containing sGAG in the ratio 1:50 and 1:100 were transferred to a 96 well plate and induced to fibrillogenesis by incubating at 37⁰C. In order to track collagen fibrillogenesis in real time, optical densities of the samples in the well plates containing test and control samples were obtained by placing plates in a BioTek Synergy 2 multi-mode microplate reader and obtaining readings at 560 nm. To achieve uninterrupted reading at 5 minute intervals, the Gen5 software was pre-set for a 96 well plate at 37⁰C in a 1 hour kinetic run with 5 minute intervals.

3.5.1.2 MORPHOLOGY OF COLLAGEN HYDROGEL BY LIGHT MICROSCOPY AND POLARISATION MICROSCOPY

After collagen fibrillogenesis, samples with higher collagen concentrations were lyophilised, gold coated and imaged using SEM. Semi-solid gels, were frozen in optical cutting medium and cryosectioned to obtain 8-12 μm sections on poly-L-lysine coated slides. Collagen solutions containing sGAG were stained for confirmation of the presence of sGAG using alcian blue staining process and subsequent sections stained for collagen using picrosirius red solution made from 0.5g of sirius red dye (Direct red 80, Sigma-Aldrich, UK) and 500 ml aqueous solution of picric acid (Sigma-Aldrich, UK). Acidified water was prepared by adding 5ml of glacial acetic acid (Sigma-Aldrich, UK) to 1 liter of tap water. Formalin fixed tissue sections were rehydrated in ascending series of ethanol and immersed in picrosirius red solution for 1 hour. Tissues were rinsed in two changes of acidified water. Stained sections were imaged by light and polarization microscopy.

3.5.1.3 SEM IMAGING OF COLLAGEN HYDROGELS

Drying of the collagen hydrogels took place in a lyophilisation chamber with controlled release of pressure in chamber after sample drying. Samples were anchored to tubular stubs in a plastic pot with regulated air spaces prior to dehydration and gold coated as previously described in section 3.2.6 prior to imaging.

3.6 STATISTICS

Unpaired t-tests were performed for comparison of means between prolapsed and non-prolapsed groups and pregnant and non-pregnant groups, after determination of data normality

using D'Agostino and Pearson omnibus normality tests. Data have been expressed as mean and standard error of mean.

For the prolapse study, Gpower 3.1.9.2 software was used for calculation of effect sizes from means and standard deviations of prolapsed and control groups and post hoc power calculated based on difference between two independent groups. To compare multiple groups a single factor ANOVA was performed at 95% confidence interval. A p-value below 0.05 indicated statistical significance. In the graphs, statistical significance has been indicated at three levels: * $p \leq 0.05$, ** $p \leq 0.01$, and *** $p \leq 0.001$ respectively. Standard error of the means were used to measure variability. Powers of 85% were obtained for comparison of data between prolapsed and control groups' pentosidine and the blood pressure study. Pearson's correlation coefficient was calculated for determination of relationship between prolapsed vaginal tissue mechanical properties and pentosidine as well as vaginal and skin pentosidine.

**4 CHAPTER 4: PHYSIOLOGICAL CHANGES OF VAGINAL
TISSUE IN PREGNANCY-EVALUATION OF ADVANCED
GLYCATION PRODUCTS' LEVELS, TISSUE MECHANICS
AND STRUCTURE**

4.1 GLYCATION, MECHANICS AND STRUCTURAL CHANGES OF NATIVE VAGINAL TISSUES IN PREGNANCY

4.1.1 INTRODUCTION

It is known that ageing is associated with increased tissue glycation where it alters the mechanical properties of the connective tissues, resulting in stiffer tissues and diseases such as atherosclerosis (12). Age-related pelvic floor disorders in women such as prolapse and urinary incontinence are more common after the menopause when oestrogen levels are low. Since oestrogen may influence amounts of old and new collagen in pelvic tissues, and older connective tissue contains more glycation products, oestrogen therefore has the potential to affect the mechanical properties of the tissue by altering glycation content.

Pregnancy, marked with high levels of female hormones including oestrogen, confers unique alterations to the mechanical properties of pelvic connective tissues in order to meet the physiological performance. However, there are few studies on glycation content and its influence on the mechanical properties of pelvic connective tissues during pregnancy. It was hypothesized that a relationship exists between oestrogen, glycation content and mechanical properties of pelvic tissues.

It is expected that the glycation content in pelvic tissues will change with a corresponding change in their mechanical properties, and that these changes are influenced by hormone levels. Currently few studies correlate hormone level and glycation content of pelvic tissues during pregnancy and reveal relevant mechanisms.

4.1.2 AIMS

This study aimed to investigate the correlation of vaginal wall mechanical properties with glycation content during pregnancy, in association with the expression of a key pregnancy hormone (oestrogen) receptor, and an antioxidant enzyme, glyoxalase I and investigate the possible mechanisms for observed correlations, where present, by utilising multiple new approaches in a rat tissue model.

4.1.3 METHODS

Samples were obtained as described in 3.1.1. Morphological and mechanical assessments were carried out using histological staining techniques, SEM imaging, AFM analysis, OCT imaging and ball indentation testing as described in 3.2.6, 3.2.7, 3.2.8, 3.4.1 and 3.4.2 respectively. Pentosidine was detected and quantified in the tissues as described in 3.3.2 and immunostaining of the tissue sections was carried out as described in 3.3.4.

4.1.4 RESULTS

4.1.4.1 STRUCTURE AND ORGANIZATION OF NATIVE PREGNANT AND NON-PREGNANT VAGINAL TISSUES

4.1.4.1.1 H&E STAINING

Three distinct zones were notable in the vaginal tissues from both groups as shown in figure 4.1. The epithelial cells were spindle shaped particularly at the superficial regions and neatly and more compactly arranged in the non-pregnant vaginal wall but in the pregnant vagina, cells were arranged in multiple layers and appeared rounded and swollen with many detached and present in the luminal region. Nuclei of non-pregnant tissues were darker in contrast to

pale appearance of pregnant vaginal nuclei. In all zones of the tissues, spindle shaped cells were seen in the non-pregnant tissues but in the pregnant tissues a more rounded appearance is appreciable. Darker and denser tissue architecture is notable in the non-pregnant tissues in contrast to the pale, loose architecture of the pregnant tissue. Physiologic ruggae was present in the luminal surfaces of tissues from pregnant and non-pregnant groups. This however is more pronounced in the non-pregnant tissue with deeper or more compact folds.

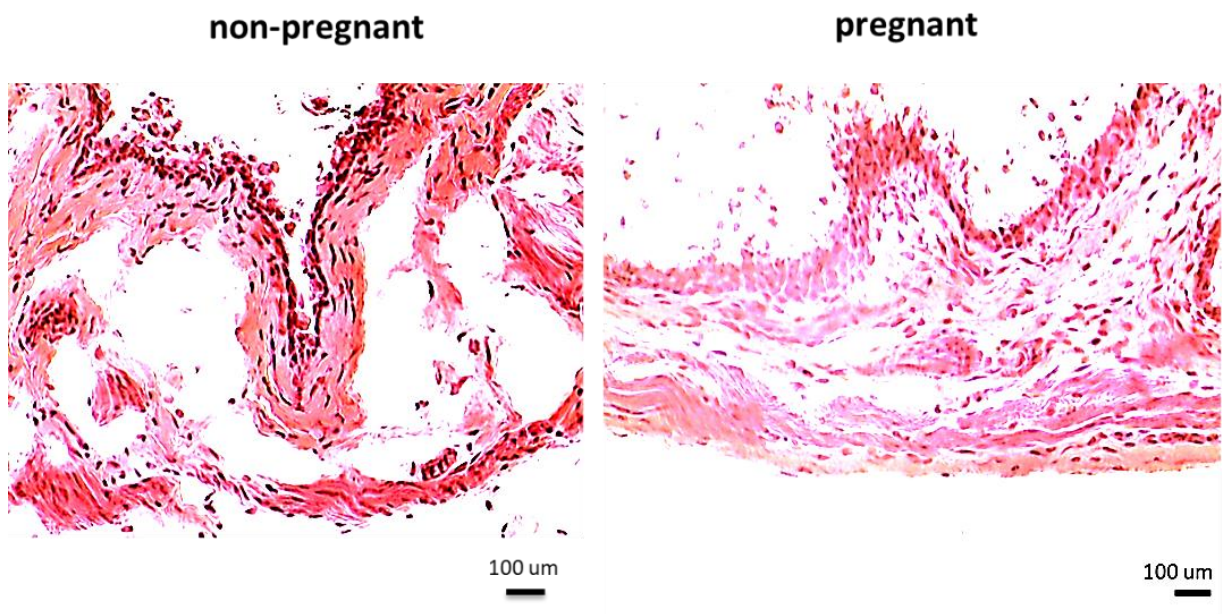


Figure 4.1: Representative H&E stained images of pregnant and non-pregnant rat vaginal wall. More compaction and staining is notable in the non-pregnant vaginal wall.

4.1.4.1.2 SEM IMAGING

Scanning electron microscope revealed further ultrastructural differences between the groups (figure 4.2). In the low magnification images, full-thickness segments of the vaginal walls were appreciable. These were wider in the pregnant tissues. Notable compaction was present in the epithelial regions of the non-pregnant tissues in contrast to the loose appearance of the

tissues in pregnancy. Higher magnifications of the lamina propria (LP) regions showed that cells were more abundant and arranged in close proximity to each other in the non-pregnant tissues. Epithelial regions of the pregnant rat were covered with randomly arranged and loose collagen fibrils. The muscularis and adventitial layers of the non-pregnant tissues displayed sheet-like appearance with apparently thinner fibrils. The sheet-like appearance or compaction was altered in the pregnant tissues and more detached collagen fibrils are present. They appeared swollen or wider and in spirals projecting out of intact bundles.

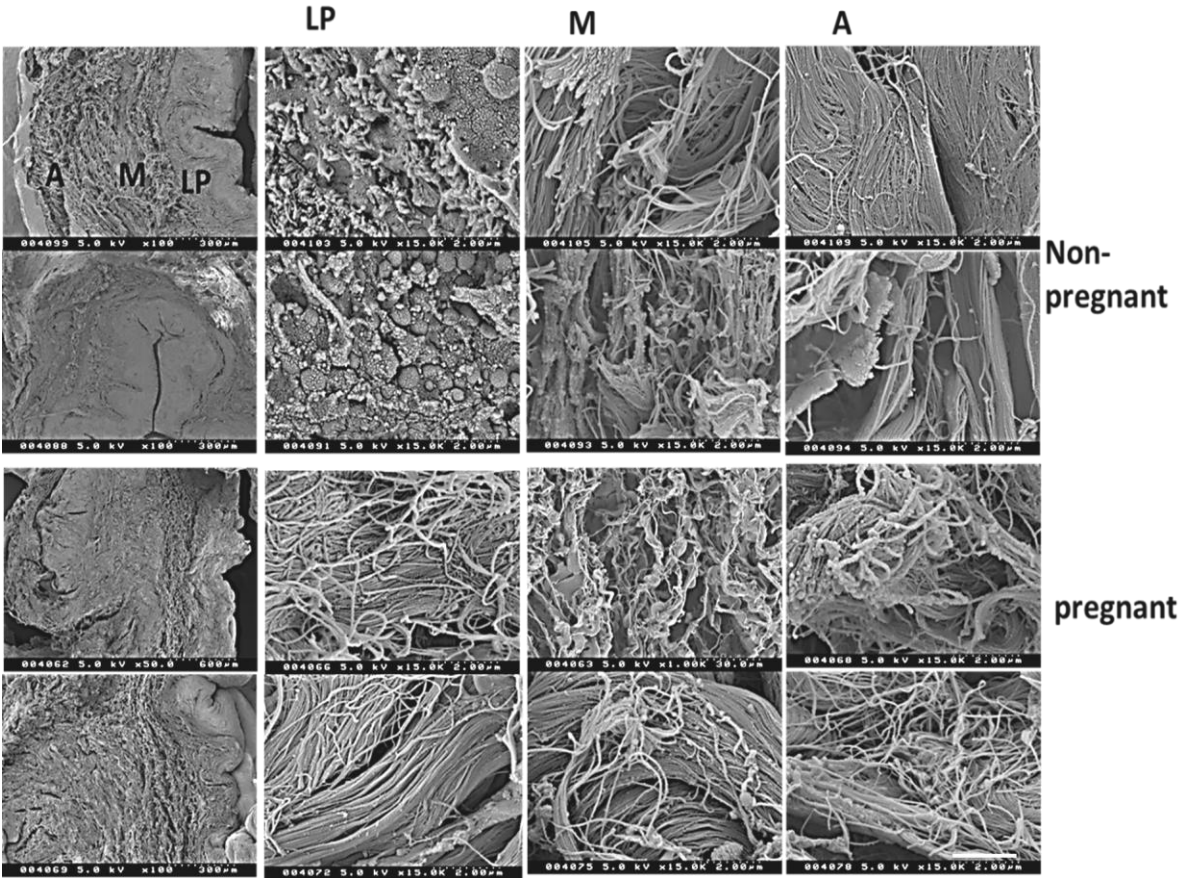


Figure 4.2: Low and high magnification images of representative SEM images of pregnant and non-pregnant vaginal tissues. LP=Lamina Propria, M=muscularis, A= adventitia. Scale bar =2 μ m

4.1.4.1.3 AFM ANALYSIS

Fibrils within the pregnant tissues appeared wider and merged as shown in the 2-D and '3-D' images (Figure 4.3). They also exhibited more frequent banding, in contrast to the distinctly separated fibrils of the tissues in the non-pregnant group. The average fibril diameter of tissues in the pregnant tissue was significantly greater than that of the non-pregnant group (Figure 4.4). Fibrils of the tissues in the pregnant group appeared flatter and often merged to form wider 'fibers' unlike the fibrils in the non-pregnant group, which had more separated individual collagen fibers as shown in figure 4.3.

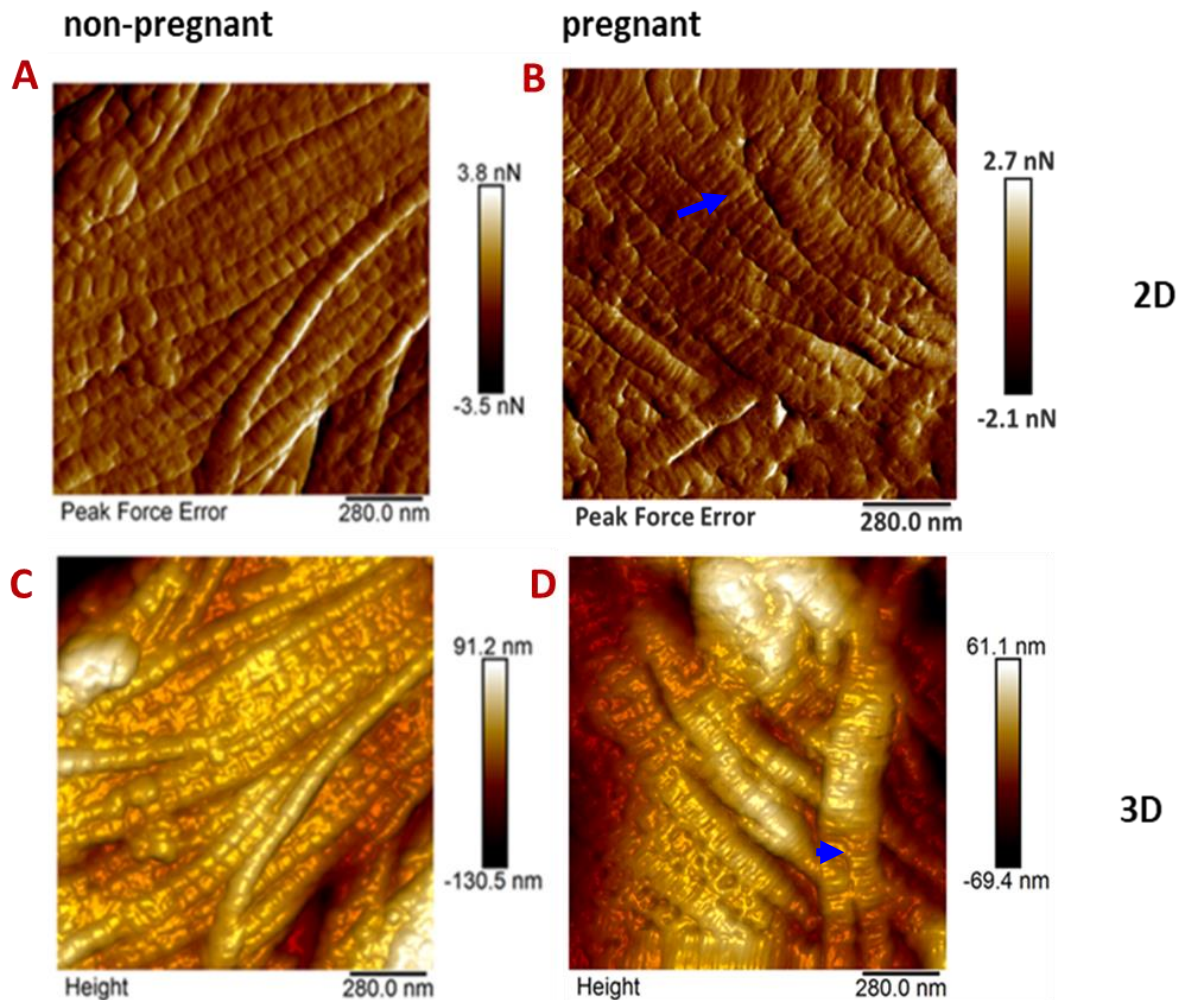


Figure 4.3: AFM images showing collagen fibril morphology of pregnant and non-pregnant vaginal tissues. Representative 2-dimensional (A and B) and 3-dimensional (C and D) images of collagen fibrils are shown. Blue arrows point to merged, wider collagen fibrils.

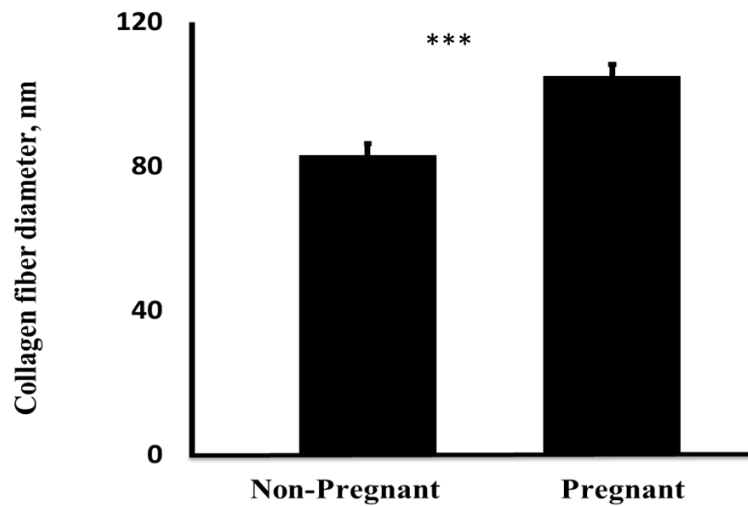


Figure 4.4: Quantification of collagen fibril dimensions of pregnant and non-pregnant vaginal tissues through AFM images. The mean diameters of 15 collagen fibrils from 3 x 1.4 μm^2 regions of 3 x 5 μm thick sections have been analysed (n=3 per group).

*****P=0.000**

4.1.4.1.4 OCT IMAGING

2-D images of cross sectional views of the tissues were obtained across selected areas from screen displays of the tissues (Figure 4.5). Some structural changes were appreciable using OCT (Figures 4.5 and 4.6). Non pregnant tissues exhibited more rugae and increased opacity. Pregnant tissues were thicker and less opaque, with a well-hydrated appearance. Due to the

presence of rugae, the thicknesses of the non-pregnant tissues were variable across the whole length unlike the more uniformly thick pregnant vaginal wall.

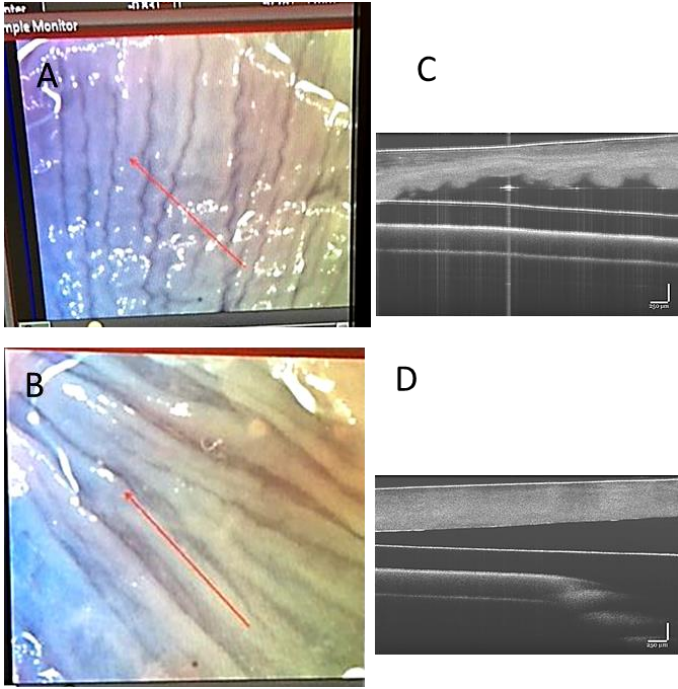


Figure 4.5: OCT imaging of rat vaginal tissues. Red arrows in A and B (on screen visible images) show areas of cross sectional imaging to obtain images C and D (OCT images) from which thickness measurements can be obtained. Scale bar = 250μm

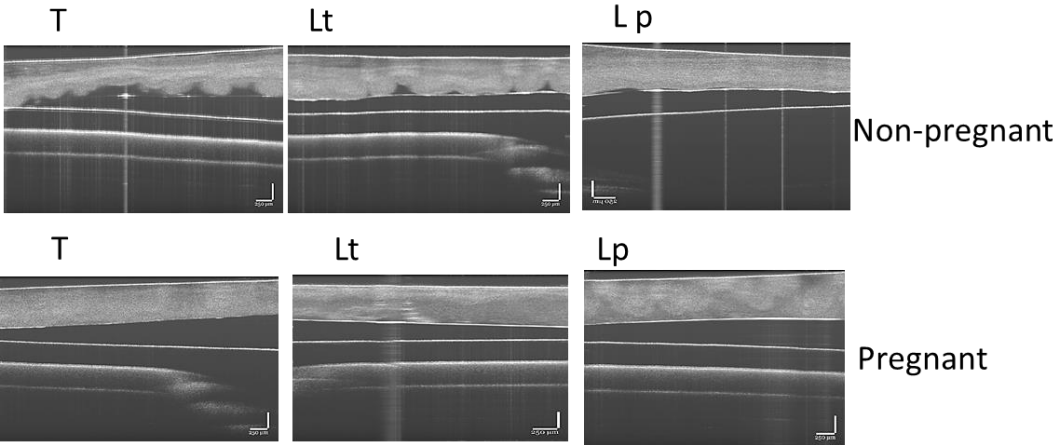


Figure 4.6: Cross-sectional appearance and thickness of representative pregnant and non-pregnant vaginal tissues across longitudinal trough (Lt), longitudinal peak (Lp) and transverse areas (T) of the rugae. Scale bar = 250µm

4.1.4.2 sGAG CONTENT

4.1.4.2.1 sGAGs STAINING BY ALCIAN BLUE

sGAG staining of the vaginal tissues revealed higher staining intensity in the pregnant tissues than non-pregnant one (figure 4.7). The stain was confined to top and lower regions of the tissues with minimal stain taken up in the middle muscularis regions of the non-pregnant tissues. For the pregnant tissues, a more generalized staining was appreciable. This necessitated quantification of sGAG in the tissues.

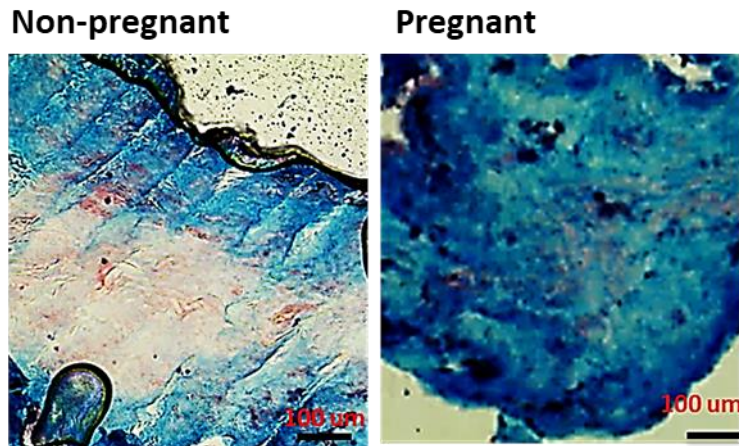


Figure 4.7: Alcian blue staining of pregnant and non-pregnant vaginal wall.

4.1.4.2.2 QUANTIFICATION OF sGAG BY DMMB ASSAY

DMMB assay revealed that sGAG content was significantly higher in the tissues from pregnant rats ($p=0.02$) than in the non-pregnant (Figure 4.8) group with corresponding significantly higher water content in the tissues from the pregnant rats (Figure 4.9).

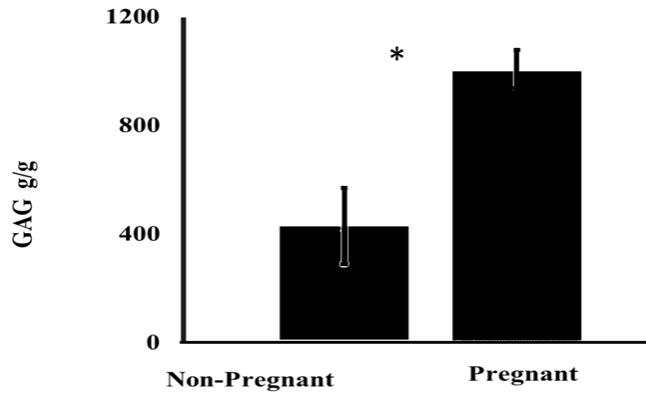


Figure 4.8: Glycosaminoglycan (sGAG) content per dry weight of pregnant and non-pregnant rat vaginal tissues (n=3 per group). *P= 0.015

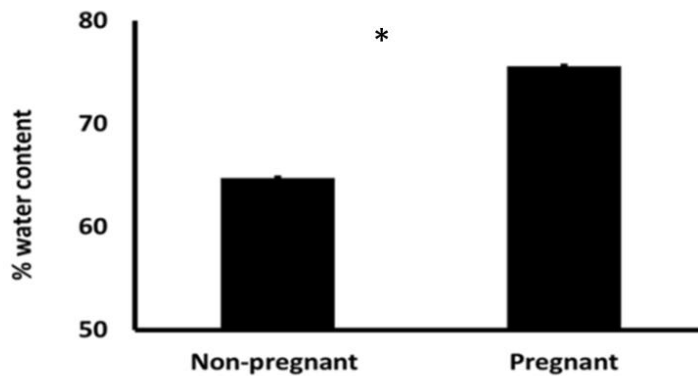


Figure 4.9: Water content per dry weight of pregnant and non-pregnant rat vaginal tissues (n=3 per group). *P=0.047

4.1.4.3 PENTOSIDINE LEVELS

Pentosidine contents per gram of the dry tissues for both groups are shown in Figure 4.10. Vaginal tissues from pregnant rats contained an average of 0.02 mg pentosidine per gram of tissue while tissues from non-pregnant rats contained 0.04 mg pentosidine per gram of tissue. These differences were found to be statistically significant ($P = 0.04$).

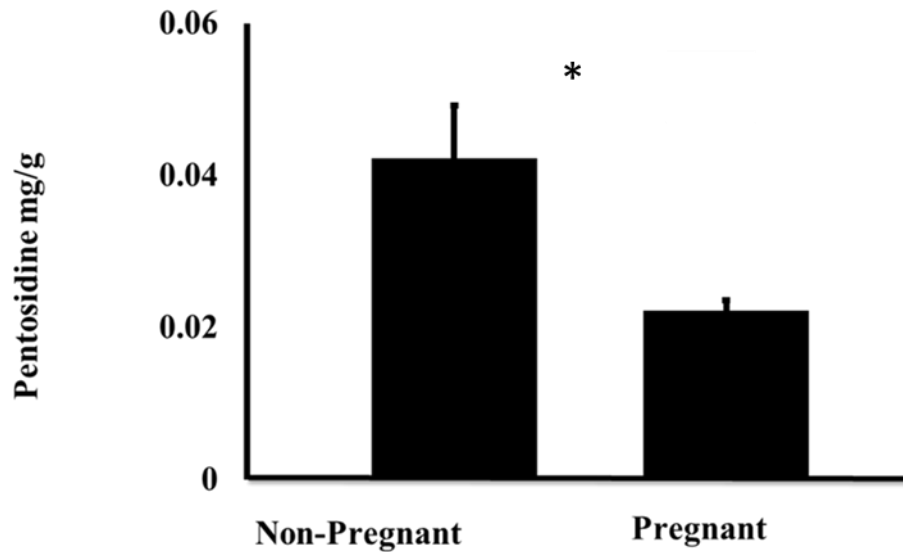


Figure 4.10: AGE marker level measured by HPLC showing the pentosidine content of vaginal tissues from pregnant and non-pregnant rats (n=5 per group). *P=0.042

4.1.4.4 CREEP BEHAVIOR AND CORRELATION WITH PENTOSIDINE

Using the ball indentation technique, tissues were deformed over 24 hours with a constant weight. Significantly higher deformation was observed in tissues from pregnant rats ($p=0.003$) as compared with non-pregnant rats tissues (Figure 4.11). There was a negative correlation ($r^2 = -0.50$) noted between 24 hour creep and tissue pentosidine content of the same rats (Figure 4.12).

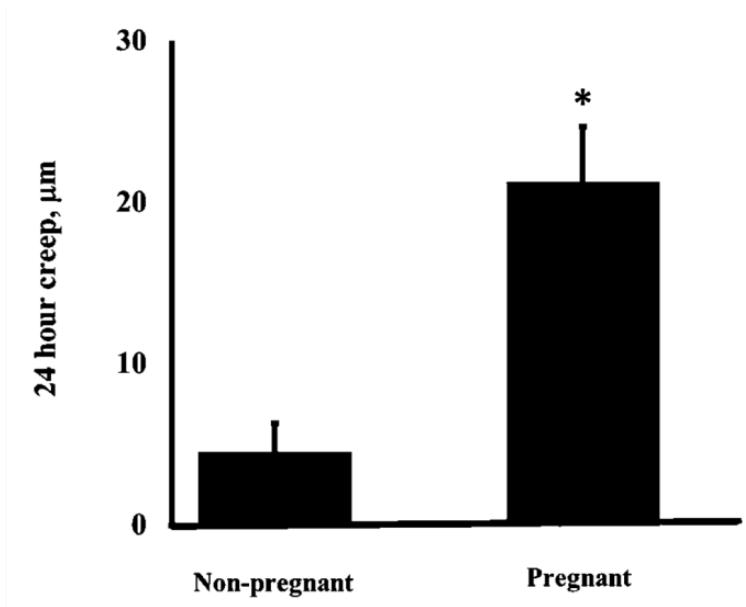


Figure 4.11: Mechanical property (24 hour creep) of intact vaginal tissue segments from pregnant and non-pregnant rats measured by the ball indentation technique (n=5 per group). *p=0.003

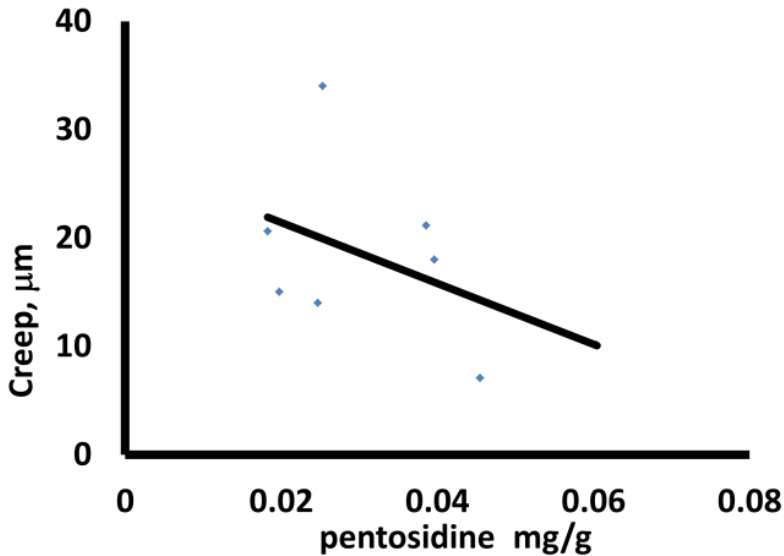


Figure 4.12: Correlation between pentosidine and vaginal tissue creep ($r^2 = -0.50$)

4.1.4.5 VAGINAL TISSUE MODULUS AT THE NANOSCALE AND TISSUE LEVEL

The ball indentation test results showed that approximately five times more deformation and 200% percent lower apparent elastic modulus were observed for the pregnant rat vaginal tissues compared with non-pregnant rats vaginal tissues (Figure 4.13). Collagen fiber modulus have been determined by peakforce quantitative nanomechanical mapping AFM. The mapping images shown in Figure 4.14 demonstrated a trend towards a higher elastic modulus in non-pregnant rats. By quantification of 15 fibers per image, the nano-scale measurements showed distinct differences between the two groups (Figure 4.15). It is clear that these tissue-level mechanical properties were consistent with nanoscale elastic modulus measurements obtained with AFM.

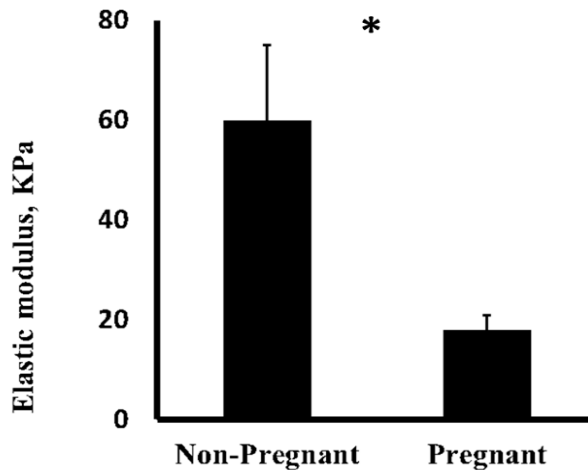


Figure 4.13: Mechanical property (Elastic modulus) of intact vaginal tissue segments from pregnant and non-pregnant rats measured by the ball indentation technique (n=5 in each group), *P=0.047.

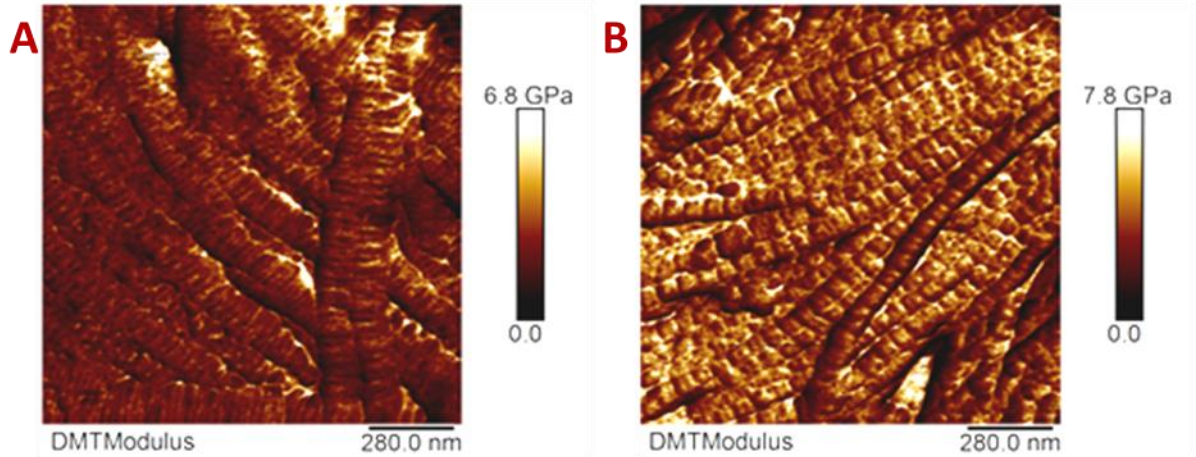


Figure 4.14: AFM measurement of mechanical property by peakforce quantitative nanomechanical mapping mode. Representative maps showing modulus range over a 1.4 μm^2 area of vaginal tissue sections from pregnant (A) and non-pregnant (B) rats. The color bars alongside the images indicate the modulus values.

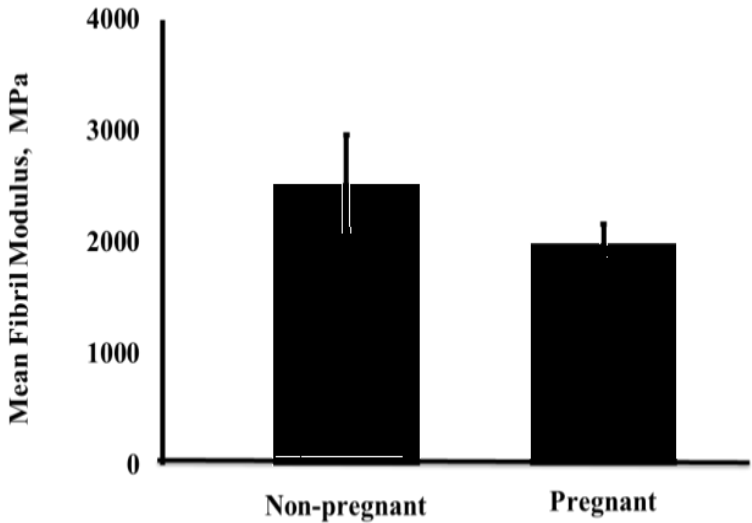


Figure 4.15: Average modulus of collagen fibrils in the pregnant and non-pregnant vaginal tissues derived from mapping images shown in Figure 4.14. (n=3 per group, P=0.355)

4.1.4.6 OESTROGEN RECEPTOR AND GLYOXALASE EXPRESSION IN PREGNANT AND NON-PREGNANT VAGINAL TISSUES

ER- α and anti-oxidant enzyme, glyoxalase I expression in both tissue groups were determined by immunostaining assays as shown in Figures 4.16 and 4.17. Tissue sections from both groups were well nucleated as shown by DAPI staining in Figures 4.16 and 4.17 whilst the intranuclear oestrogen receptors were much more strongly expressed in the tissues from pregnant rats than the non-pregnant tissue (Figure 4.16). Location of glyoxalase I enzyme was predominantly sub-epithelial and more expressed in the tissues from pregnant rats (Figure 4.17).

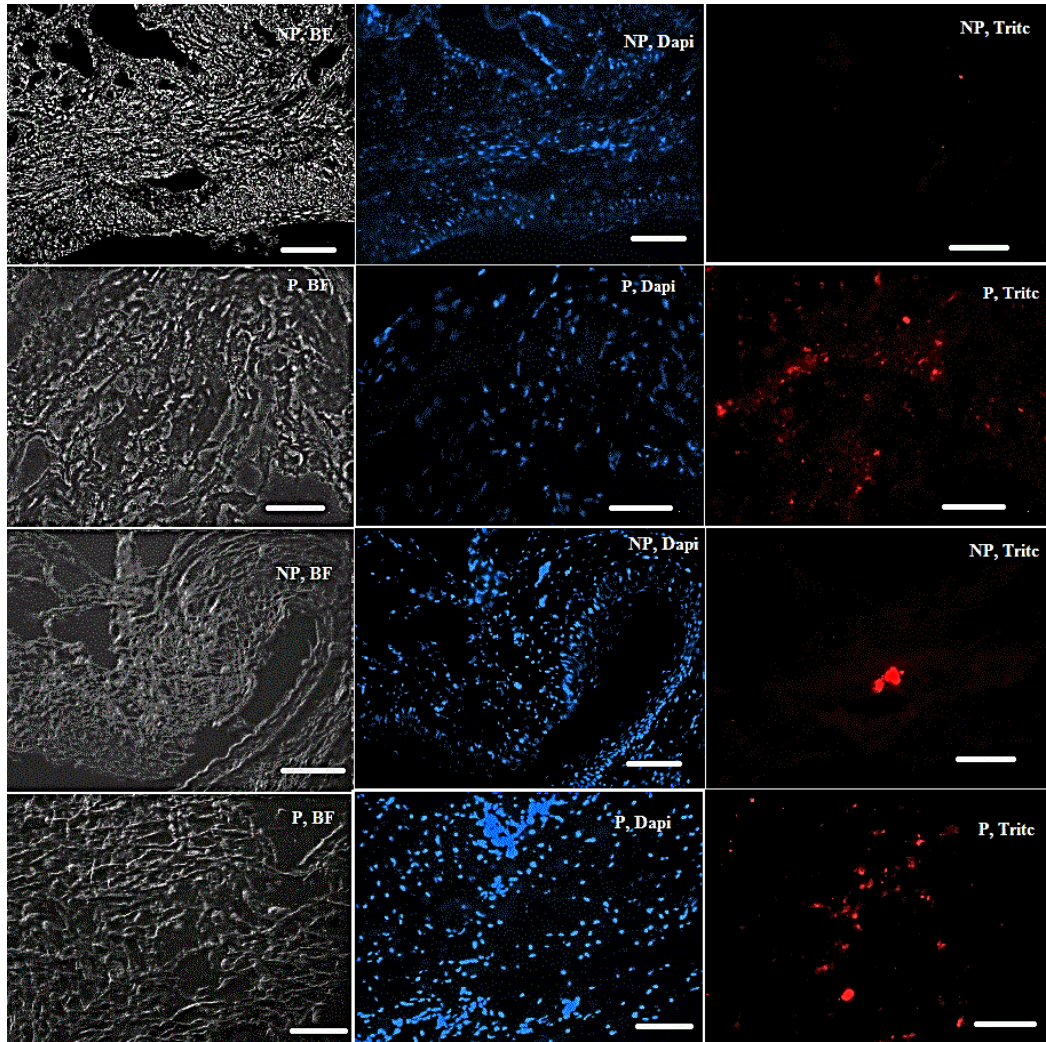


Figure 4.16: Immunostaining images of vaginal tissue sections showing representative images of ER- α receptor expression; P: pregnant; NP: non-pregnant; Tritc (red): ER- α receptor; BF: bright field and Dapi (blue): nuclei. Scale bars = 50 μ m.

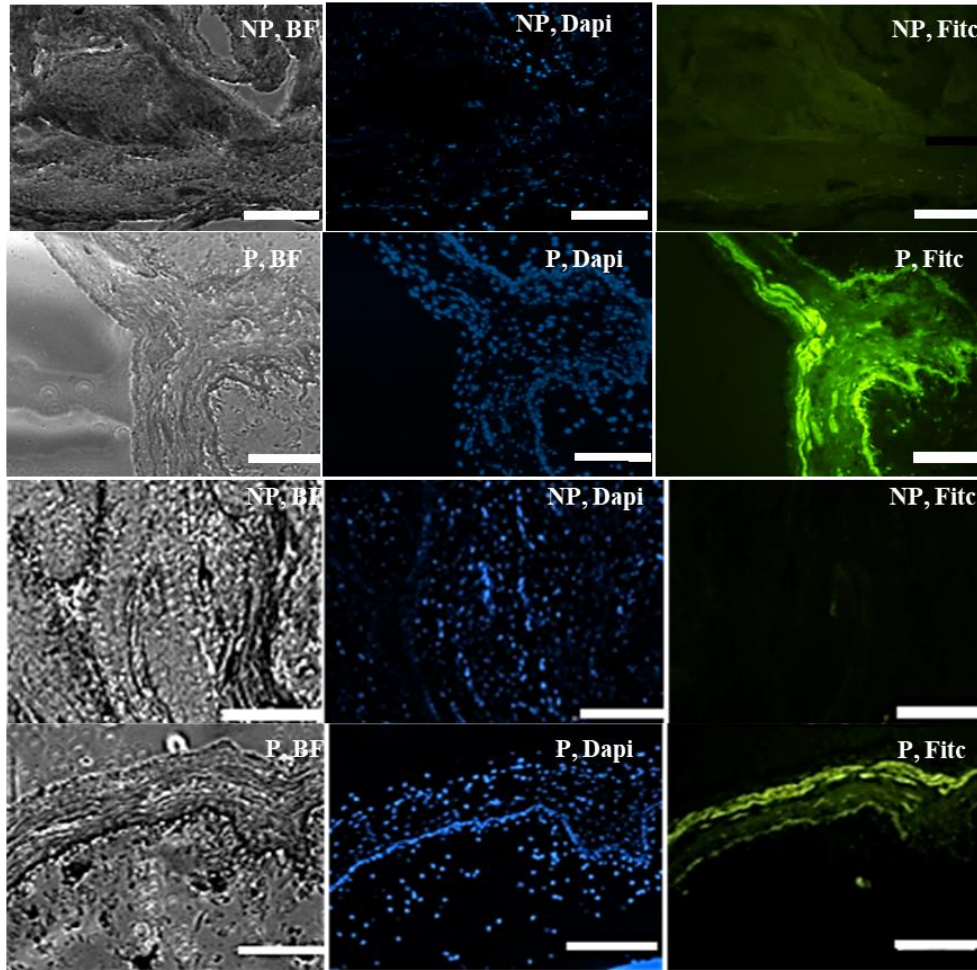


Figure 4.17: Immunostaining images of vaginal tissue sections showing representative images of glyoxalase I expression. P: pregnant; NP: non-pregnant; FITC (green): glyoxalase-1; BF: bright field and Dapi (blue): nuclei. Scale bars = 50 μ m.

4.1.5 DISCUSSION

Studies on pregnancy induced changes in the middle and last two trimesters of pregnancy have mostly focused on cervical changes rather than the vaginal wall changes. This study revealed for the first time that a glycation product, pentosidine, was significantly reduced during pregnancy, a high oestrogen state; and that this reduction in glycation correlated with higher mechanical creep. Vaginal tissues in pregnancy also expressed higher levels of the antioxidant

enzyme, GLO-I, than did tissues from the non-pregnant rats. The higher creep behaviour of whole vaginal tissue segments in pregnant rats correlated inversely with their modulus and glycation content. Nano-scale examination of the collagen fibers in pregnant tissue by AFM supported the change in bulk mechanics. The morphology and chemical composition changes were observed as significantly thicker collagen fibril diameter and higher sGAG content in pregnant tissues. The regulatory relationship between oestrogen and glycation content in pregnancy was evidenced in this study.

AGEs accumulate in tissues, typically increasing with age and causing connective tissue stiffening (14). Although AGEs are associated with many pathologic states, their accumulation within tissues is not always permanent. Macrophages within the body may bind to and scavenge AGEs (201). The high oestrogen state in pregnancy associated with reduced AGEs in the vaginal wall is congruent with other research. Previous findings have noted a decrease in skin autofluorescence (a reflection of advanced glycation) during pregnancy (202). A 50% reduction of pentosidine has also been observed in blood vessels under chronic oestradiol therapy (203). Oestrogen treatment of vascular endothelial cells reduced advanced glycation-induced inflammation (204). This suggests on-going physiologic changes in pregnancy such as modifications of connective tissues by pregnancy-related hormones. Pregnancy or states of high oestrogen expression may therefore involve mechanisms resulting in AGE cleavage and reduced formation. Relationships between glycation products and stiffening of other body tissues such as tendon, intervertebral discs, skin and arteries have been studied but for the first time a relationship is demonstrated in vaginal tissues during the pregnancy (205–207). Other studies have similarly reported the association of high glycation with tissue stiffness (205,208).

By a constant load procedure a significantly higher creep and lower stiffness of pregnant vaginal tissues was observed in this study. This is congruent with previous studies. The fibromuscular vaginal wall has been previously noted to increase in circumference during pregnancy with apparent collagen reduction (4). The vaginal wall and supporting tissues are more distensible during pregnancy, with a decrease in stiffness, or modulus in preparation for delivery with minimal injury (1,2,4). Collagen fibrils within the vaginal wall also undergo progressive disorganisation and remodelling through the middle and later stages of pregnancy (48). Although there was associated apparent thickening of the collagen fibrils in this study, other research suggest that individual fibril diameter may not account for overall tissue modulus (209). Higher tissue modulus typically is the result of crosslinking between fibrils with both enzymatic and non-enzymatic (glycation) crosslinks and is reflected in increased stiffness of the collagen fibers and tissues (19). The significance of reduced glycation crosslinks observed in pregnant tissues may therefore be correlated with altered mechanical properties of the tissues - reduced stiffness and enhanced creep.

Crosslink changes were unlikely to account for the increased collagen fibril diameter observed in pregnant tissues in our study, leading to consideration of another possible mechanism for the observed wider fibrils. Type I collagen fibrils could increase diameter by lateral fusion of fibrils, possibly aiding fiber performance at high strain (210). Our AFM images revealed collagen fibrils which appeared fused to form the wider fibrils. To further understand the observation, sGAG contents were measured and were notably higher in the pregnant rats' tissues. Previous studies have also noted a progressive increase in sGAG content of pelvic tissues during pregnancy and its loss at delivery (48,211). Certain proteoglycans also modulate fibrillogenesis and fiber alignment (212). Studies have shown that removal of sGAG results in

disorganization of collagen fibrils (213). sGAG present between collagen fibrils in connective tissues may aid their arrangement, resisting complete fiber disorganisation during stretching. sGAG influence collagen fibril association through methods other than direct chemical or physical crosslinking (27), causing apparent increased fiber diameter and resisting complete deformation during sliding. Thus, the higher expression of sGAG in pregnancy may serve as a protective measure during tissue stretching by preventing complete disorganisation of fibrils

In pregnancy, oestrogen may influence tissue glycation by modulating the oxidative stress pathway. Glycation is associated with oxidative stress and reactive oxygen species have been shown to trigger AGE formation (214,215). Excessive production of reactive oxygen species within the mitochondria of cells inhibits glyceraldehyde-3-phosphate dehydrogenase and diverts substrates from glucose breakdown pathways to increased AGE formation (216). Oestrogen administration has been associated with reduced oxidative damage and glycation induced stress within connective tissues (203,217). Oestrogens cause increased expression and activity of antioxidant enzymes and their co-factors (218). Reduced oestrogen is associated with decreased amounts of the thiol antioxidant, glutathione (GSH) which is reversed by oestrogen administration (218). Oestrogen also influences the glutathione-dependent glyoxalase system through glyoxalase I which plays a role in the removal and prevention of AGEs accumulation by detoxification of methylglyoxal, a reactive dicarbonyl intermediate and AGE precursor (215,219). Deficiency in glyoxalase I enzyme has been implicated in increased AGE accumulation within tissues (220). In our study, we noted increased expression of glyoxalase I enzyme in the tissues from pregnant rats similar to findings in other studies (221). A high oestrogen level is also associated with increased activity of glutathione peroxidase, a potent antioxidant (222). This would lead to more removal of reactive oxygen

species and subsequent reduced glycation. Thus, in addition to on-going physiologic removal of AGE by macrophages within tissues (223,224), a decrease in glycation of tissues resulting in reduced formation of AGEs is expected. Therefore, states of higher oestrogen such as pregnancy or the proliferative phase of the female menstrual cycle would be associated with reduced AGEs through a proposed oestrogen-gluthathione-glyoxalase pathway as depicted in Figure 4.18.

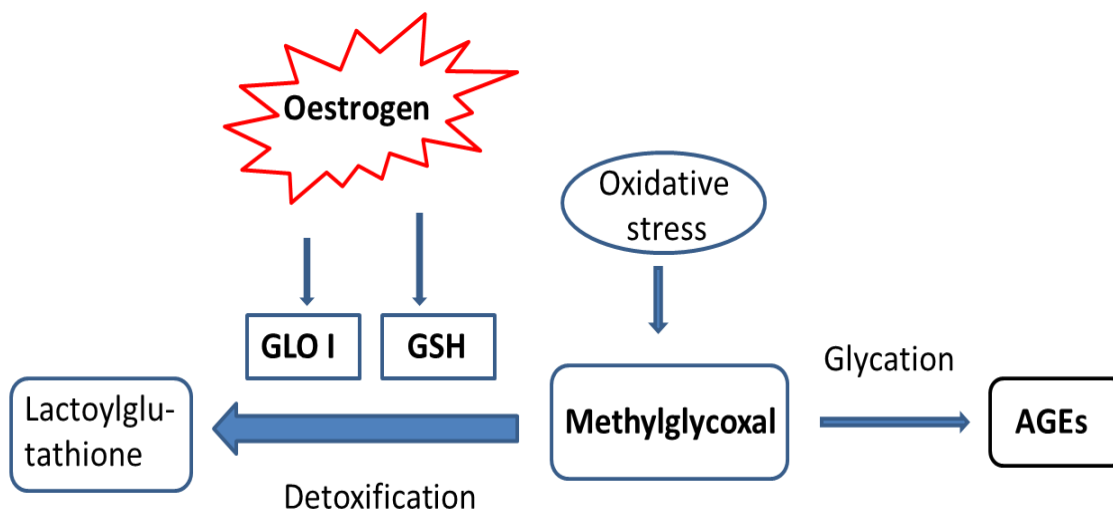


Figure 4.18: Illustration of AGEs formation inhibition by oestrogen. Oestrogen increases antioxidant enzyme (GLO-I) and co-factor (GSH). In the detoxification processes, intermediate AGE precursors e.g. methylglyoxal, are diverted to other pathways, leading to reduced AGE accumulation

As a result, whilst oxidative stress promotes AGEs formation, oestrogen increases the activity of glyoxalase and GSH leading to stronger detoxification, production of lactoylglutathione and decreased AGEs. This physiologic pathway would also be useful in understanding the pathogenesis of prolapse which occurs predominantly in older, menopausal women. During the years preceding the menopause oestrogen levels decline and this may halt the process of

cyclical removal of AGEs which should occur during the normal reproductive life of the female. Progesterone is another significant hormone during pregnancy. However there is minimal evidence for its influence on AGEs. Further investigation on the effects of progesterone on glycation may however be useful in obtaining a more robust understanding of the effect of pregnancy on AGEs in pelvic tissues.

This study used a minimally destructive technique for assessment of vaginal tissue bulk mechanical property and employed the AFM technique for the study of collagen fiber mechanics and morphology. In this way, assessment of the global and nano-scale mechanical and structural properties of vaginal tissues was achieved. The findings from this animal model study sets a foundation for to the study of human samples.

4.1.5.1 CONCLUSION

There was a reduction in vaginal tissue pentosidine in pregnancy with an associated increase in oestrogen receptor and glyoxalase I immunoexpression. Reduced glycation was associated with increased creeping of vaginal tissues. Oestrogen may therefore play a role in the increase in of the vaginal wall's capacity to stretch through glyoxalase I up-regulation and subsequent glycation reduction. This new insight into the correlation of women's oestrogen level, glycation reaction and pelvic tissue mechanical property from this study may enhance our understanding on some pelvic organ diseases.

This study is the first of its kind and highlights a relationship between mechanical changes observed in pregnancy and collagen fiber changes within the connective tissue. It confirmed that vaginal tissues in pregnancy contain lower levels of advanced glycation end products. Glycation reduction may contribute to the increased flexibility (high creep) of pregnant

vaginal tissues in association with increased sGAG levels and collagen fiber fusion. Pregnancy reduced vaginal wall glycation by increasing both the antioxidant enzyme, glyoxalase I, content and oestrogen. This is potentially is a major reason for the observed changes. These observations generate novel insights into other pathways for vaginal tissue mechanical changes during pregnancy and provide some evidence that the alteration of glyoxalase concentration by the elevation of oestrogen level correlates with a reduction in AGEs level and vaginal tissue flexibility.

4.2 INFLUENCE OF SULPHATED GLYCOSAMINOGLYCANS ON COLLAGEN FIBRILLOGENESIS AND STRUCTURE- AN IN VITRO STUDY

4.2.1 INTRODUCTION

While functional adaptations of the vaginal wall in pregnancy have been extensively studied, few studies have investigated ultrastructural changes (13,48). Although, the focus has been on cervical changes in pregnancy and parturition the vaginal wall plays a significant role in vaginal delivery (13,48,188,225). Collagen is the major structural protein in body tissues (226) and sulphated glycosaminoglycans (sGAG) are ECM components notable for their role in collagen formation (27,227). It is therefore useful to study the role of sGAG in vaginal tissue adaptation during pregnancy in order to gain deeper insight into ultrastructural changes of the tissue.

Commonly employed tissue engineering techniques such as collagen solution and gel synthesis are useful methods in the preliminary study of diseases and physiologic processes (228). The relative ease of producing a-cellular engineered collagen scaffolds in the laboratory in comparison to obtaining and investigating human or animal tissues with associated ethical

requirements (229) favours the use of engineered collagen gels for preliminary studies. In addition, the pH and temperature regulated trigger of collagen fibril formation enables real time observation or tracking of the simulated biological processes (226). At an alkaline or neutral pH or warm temperature, collagen monomers are induced to polymerize by a “nucleation” and elongation process. Collagen gels are used in 3-D cultures, with or without the introduction of cells to simulate the native tissue environment, in near physiologic studies with remarkable success in the understanding of normal biology and disease pathology (230). It was therefore hypothesized that an in vitro collagen fibrillogenesis model would be useful in understanding ultrastructural changes of the vagina wall in pregnancy.

4.2.2 AIMS

In 4.1., pregnancy induced changes in the ultrastructure of vaginal tissue and sGAG content of the native tissues were investigated. Although the findings strongly suggest that sGAG are responsible for the merging of the collagen fibrils observed in tissues from the pregnant vagina, they do not permit real-time observations of the process. This necessitated a study to investigate collagen fibrillogenesis in the presence of sGAG in real time for comparisons with observations in native vaginal tissues. The aim was to investigate the effect of the sGAG, Dermatan Sulfate on Type I collagen fibrillogenesis and ultrastructure for a better understanding of findings in 4.1. A further aim was to assess the effectiveness of a commonly used tissue engineering technique of collagen fibrillogenesis in replicating changes seen in native tissues as a step towards future application of tissue engineering methods in the study of pelvic tissues.

4.2.3 METHODS

Collagen gels of 0.1 mg/ml, 0.2mg/ml and 0.5 mg/ml concentrations were formed in the presence and absence of the sGAG, dermatan sulphate and oversulphated chondroitin sulphate. The process was tracked by monitoring the optical densities (OD) of the solutions in real time. The materials and methods used have been described in detail in 3.5.

4.2.4 RESULTS

4.2.4.1 ASSESSMENT OF FIBRILLOGENESIS BY TURBIDITY ASSAY

Through turbidity assay, real-time measurements of the optical densities (ODs) of formed collagen fibrils were obtained via regular tracking of ODs of the collagen monomer solutions during and after fibrillogenesis in a microplate reader. The OD values at the given incubation time and rate of change of OD during the incubation period are the two important parameters that indirectly reveal fibrillogenesis rate and fibrils' morphology. A consistent effect of sGAG on OD of polymerizing and final polymerized collagen hydrogel was noted as shown in Figure 4.19. Collagen gels without sGAG demonstrated higher turbidity during formation and also after completion of fibrillogenesis compared to test samples containing sGAG. The OD values were higher when collagen concentration was higher. There was a rapid OD value increase during the first 15 minutes of incubation then plateau was attained. A more gradual rate of change of OD was observable in less concentrated collagen solutions (0.1 and 0.2 mg/ml) in comparison to higher concentrations. The addition of the sGAG appeared to reduce the turbidity of formed fibrils. Both rate of change of ODs and ODs of final gel was less for 0.1 mg/ml, 0.2mg/ml and 0.5 mg/ml solutions containing the sGAG. The OD of the formed collagen polymer solution was also influenced by the concentration of the monomer solution.

The higher the collagen concentration of the solution, the higher the rate of polymerization and final OD of the resulting gel (red line graphs compared from top to bottom in figure 4.19). At the near physiologic ratio of 1:50 sGAG to collagen ratio, a similar finding was noted (blue line graphs in sGAG ratio 1:50 from top to bottom). The higher ratio of sGAG (1:50) led to lower rate of fibrillogenesis and lower final OD at 0.1mg/ml and 0.2 mg/ml concentrations (blue line graphs compared from left to right in figure 4.19). When sGAG was maintained at a steady concentration but collagen concentration was increased, the rate of fibrillogenesis and final OD was increased with higher collagen concentrations but still attenuated by sGAG (blue line graphs from top to bottom in figure 4.19). This was clearly observed at sGAG ration 1:50 but not 1:100.

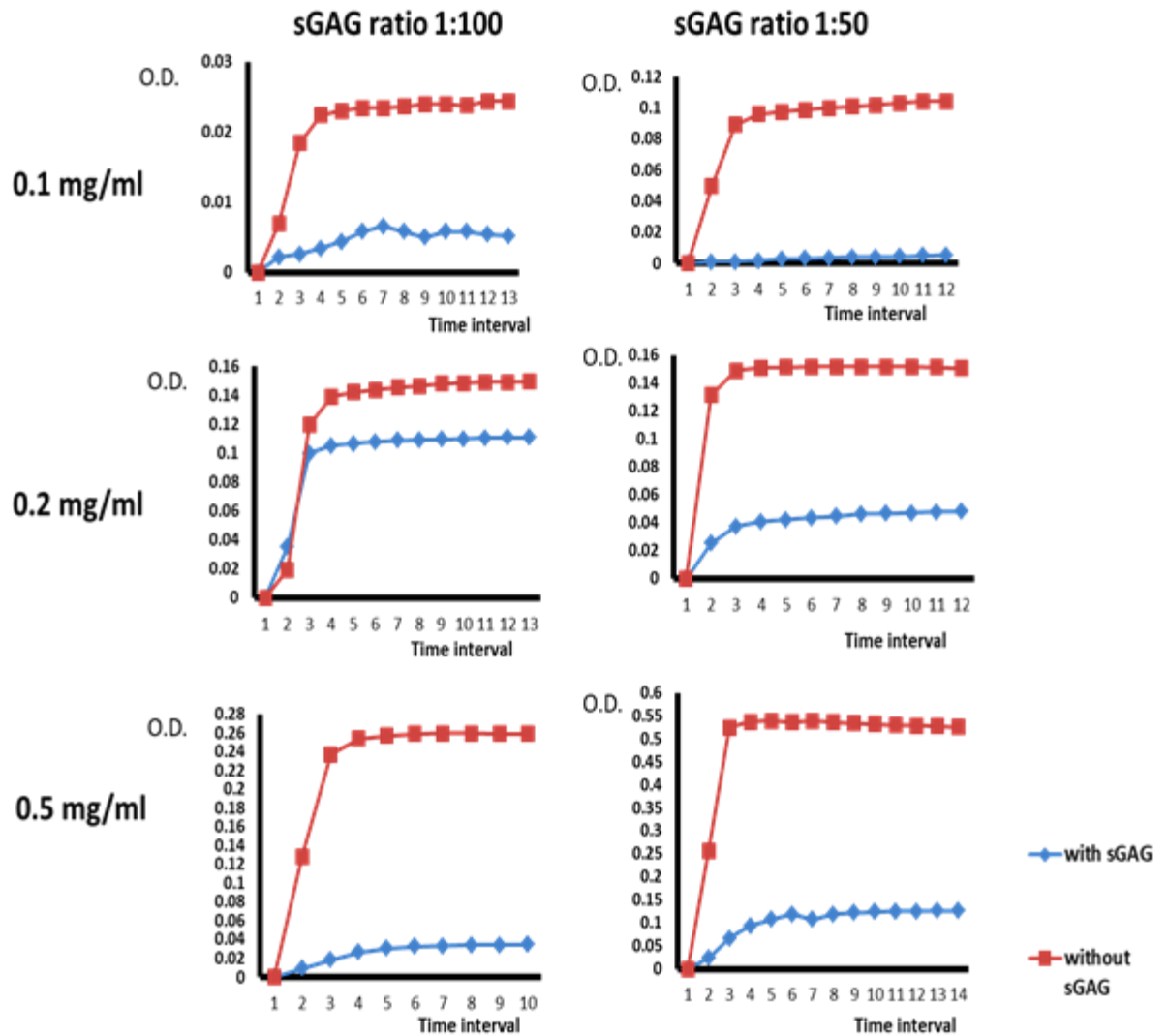


Figure 4.19: Turbidity assay results showing effects of sGAG and collagen concentration on collagen fibrillogenesis in real time. Results from collagen solutions of 0.1 mg/ml, 0.2 mg/ml and 0.5 mg/ml are shown. Time interval = 5 minutes

4.2.4.2 Assessment of fibril morphology by light and polarised microscopy

Light microscopy images of polymerized fibrils revealed loose, “cotton wool-like” fibrils formed in the absence of sGAG as shown in figure 4.20. Fibrils formed in the presence of

sGAG were more defined, compact in appearance and took up more picosirus red stain (Figure 4.20).

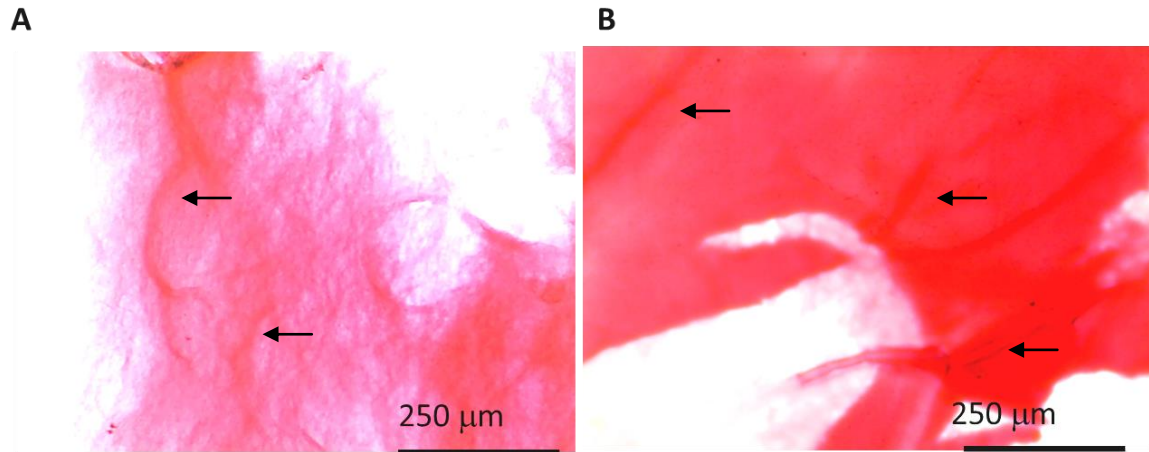


Figure 4.20: Light microscopy images of type I collagen fibers (1mg/ml collagen solution) formed in the absence (A) and presence (B) of sGAG (ratio 1:50). Arrows show collagen fibrils.

Further investigation using polarised microscopy confirmed that fibrils formed in the presence of sGAG were more compact as shown in Figure 4.21. In such images there were more fibrils per visualised area, suggestive of bundling. These changes were more appreciable in the polarised images than in the bright field images stained with picosirus red only. Polarisation images only revealed polymerised collagen in contrast to the light picosirus red stained images in which collagen monomers were visibly stained. Quantitative assessment (Figure 4.22) revealed significantly more ($p=0.00$) fibrils per unit area in samples formed with sGAG compared to controls.

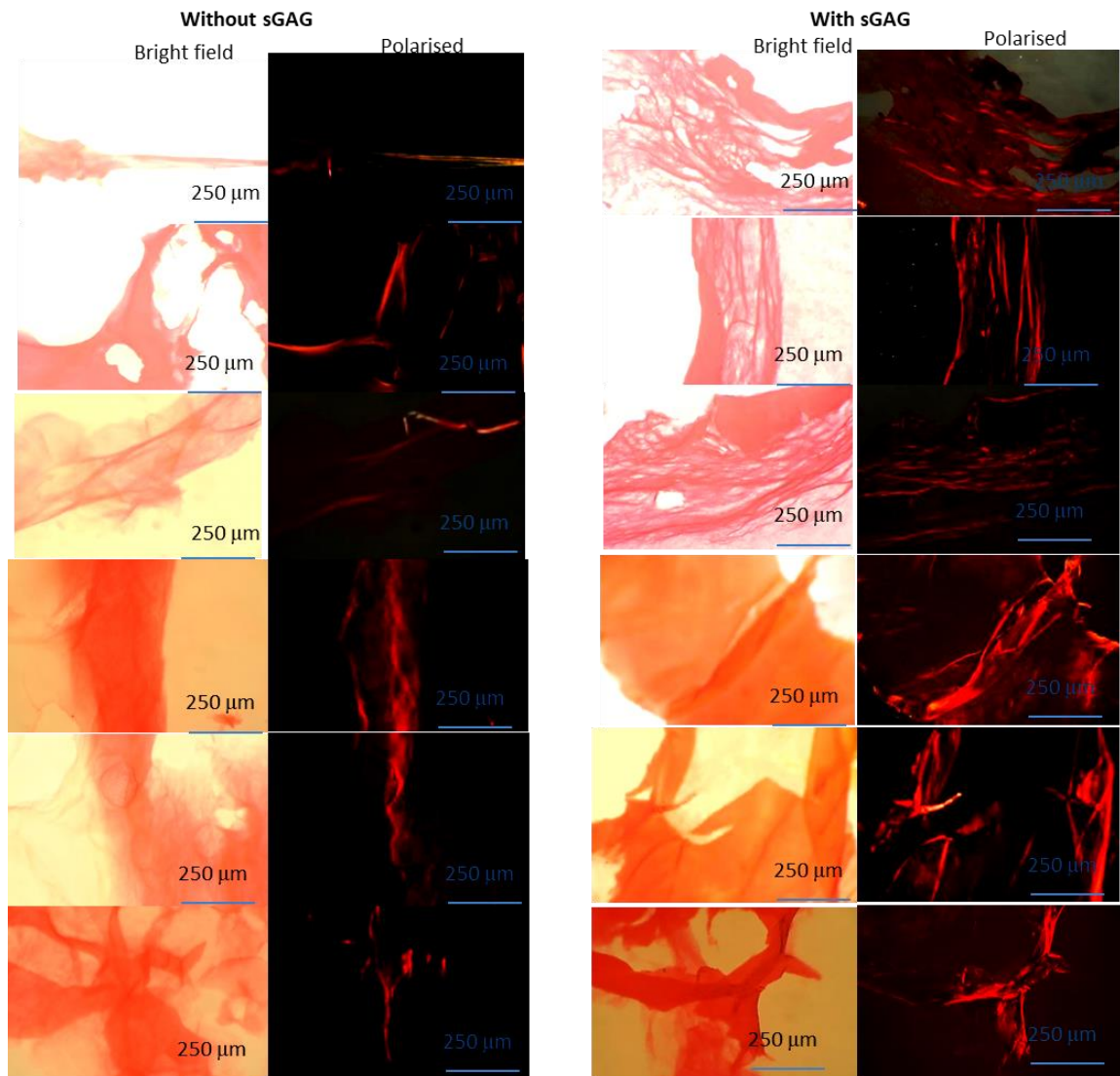


Figure 4.21: Polarisation microscopy imaging of the polymerized type I collagen fibrils (from 1 mg/ml solutions) formed in the presence and absence of sGAG (ratio 1:50).

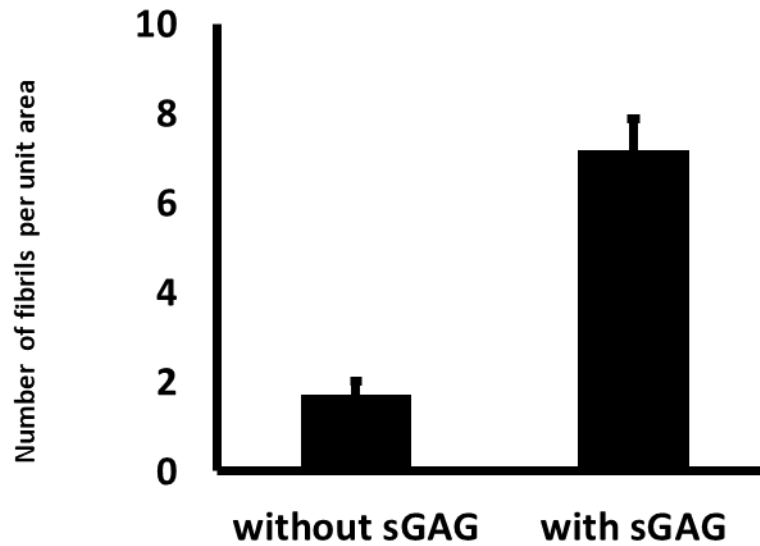


Figure 4.22: Clustering of type 1 collagen fibrils formed in the presence and absence of sGAG (n=6 per group) by quantification of fibril per unit area. *P=0.00**

4.2.4.3 Assessment of fibril morphology by SEM

SEM imaging revealed fibril interaction at the micron level and merged fiber diameter. There were aggregations of collagen fibrils and more obvious merging of fibers formed in the presence of sGAG leading to larger fiber bundles (Figure 4.23).

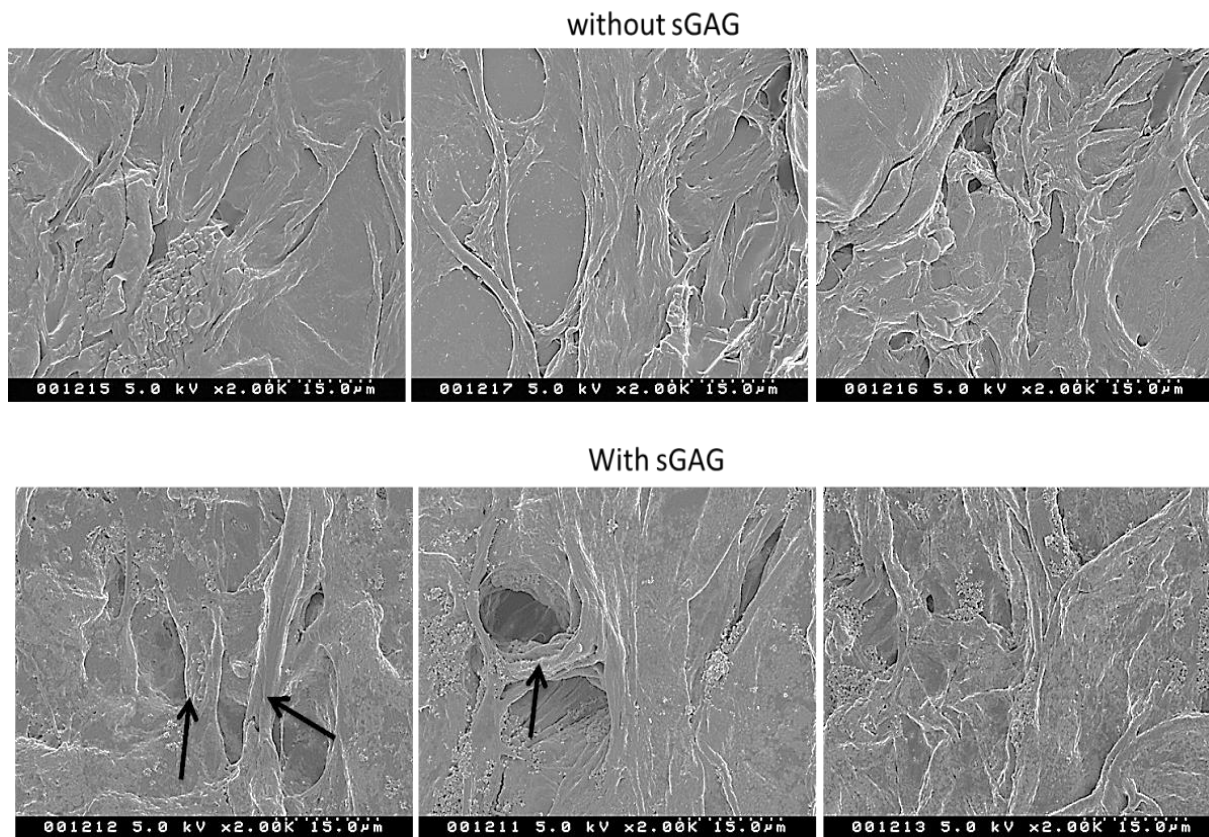


Figure 4.23: SEM images of polymerized type I collagen fibers obtained in the presence and absence of sGAG.

4.2.5 DISCUSSION

OD of a solution indicates its ability to absorb light or prevent its transmission. This property has been used to assess polymerizing collagen solutions to observe the kinetics of collagen fibrillogenesis (231) with the use of SEM and confocal reflectance microscopy to study the nature of formed fibrils (232). In collagen fibrillogenesis, the OD may be influenced by the collagen fibril diameter (233). As a result, lower concentrations of collagen solutions with soluble monomers have lower optical densities. In collagen fibrillogenesis the rising OD is a

reflection of the rate of fibril formation (226). Particle size can also affect the OD of a solution in an opposite way. When the particle size is significantly larger than the wavelength, there is less scattering of light, improved transmission of light and a consequent reduction in OD of the solution.

In the present study, the kinetics of type I collagen fibrillogenesis has been assessed by OD monitoring in real time and the appearance of resulting fibrils as well as the effect of sGAG has been studied using light microscopy and SEM. Both light microscopy and polarization microscopy of picosirus red stained images revealed compacting and definition of collagen fibers formed in the presence of sGAG. Qualitative assessment of the SEM images also revealed thicker, more aggregated fibers formed in the presence of sGAG. DS has been found to increase collagen fibril aggregation and bundling in other experiments (28). The OD of resulting polymerised type I collagen solutions were noted to decreased in the presence of the sGAG suggesting slower rate of type I collagen polymerisation in the presence of sGAG and wider, more light transmitting fibers formed. An initial lag phase at all concentrations in the presence of sGAG and significantly lower OD of 0.1 mg/ml solutions formed in the presence of sGAG was noted in the present study. Slower polymerization of collagen solutions formed in the presence of sGAG may have led to more soluble collagen monomers present per time and consequently lower OD. Collagen solutions formed from lower monomer concentrations also had lower ODs. With less collagen monomer concentration, the total number of insoluble fibers may be further reduced in the presence of sGAG, which causes fibril aggregation. These findings suggest that the rate of fibrillogenesis was influenced by interference from the sGAG (227) in a dose dependent manner and this effect was more pronounced at lower collagen

concentrations. At lower concentrations of collagen monomer solutions, a longer time is required for contact and interaction for fibril formation.

A study on the effect of chondroitin sulphate on fibrillogenesis of type II collagen revealed a pH dependent effect with a decrease in rate of fibrillogenesis at pH 7.3. Previous experiments by Reese et al (28), have shown that DS has a dose-dependent effect on collagen fibrillogenesis resulting in both reduction of the rate of reaction and turbidity of the final product. The change in fiber organization as a result of DS results in a decrease in turbidity of gels. Paderei et al (227) observed a dose-dependent delay in fibrillogenesis of type I collagen in the presence of DS. This was attributed to interference caused by interaction of the sGAG with the collagen monomers during polymerization. Such interference, though present in vivo, may be modulated by other factors influencing collagen fibrillogenesis. The present research has demonstrated effects of DS and chondroitin sulphate but decorin is also critical in collagen fibrillogenesis in vivo (234). Other minor collagen types, fibronectin, integrins, also modulate collagen fibrillogenesis (235). This study is therefore not an exact picture of the native process of type I collagen fibrillogenesis but demonstrates the usefulness of collagen models in studying the role of sGAG in collagen fibrillogenesis and ultrastructural formation the findings are better understood in the context of the previous study in 4.1, corroborating the effect of sGAG on native vaginal tissue ultrastructure in pregnancy.

It was also observed that even at low collagen concentrations, formed collagen fibers can be visualized inexpensively under light microscopes. We have further demonstrated the usefulness of polarization microscopy in studying the effect of sGAG on fibrillogenesis. Individual fibrils were not visualized under light (polarised and bright field) microscopy but

fibers were appreciable, sGAG resulted in the formation thicker fibers with better polarisation and spatial organisation which led to their visualisation under polarised light.

The merging or tendency towards collagen fiber bundling notable in the presence of sGAG is similar to observations seen in native collagen tissues in the vaginal wall of pregnant rats containing higher amounts of sGAG as detailed in 4.1.4.1.3 and 4.1.4.2. This confirms a role of sGAG in ultrastructural arrangement of connective tissues and an influence on pregnancy related vaginal tissue adaptation.

4.2.6 CONCLUSION

The sGAG-collagen model was useful in demonstrating the effect of sGAG on collagen fibrillogenesis *in vitro*, with results that mirror observations in the native tissue. sGAGs influence collagen fibrillogenesis *in vitro*. They may lead to clumping or apparent aggregation to form thicker fibers. The degree of influence of sGAGs on collagen fibrillogenesis is influenced by the concentration of the sGAG and the collagen solution. Observations of the effects of sGAG *in vitro* mirror observations in native vaginal tissues, with the added advantage of real time tracking. This study therefore also illustrates the relevance of *in vitro* tissue engineering studies in understanding *in vivo* processes. This model scan be considerably improved by clearly defining individual fiber dimensions for quantitative analysis and this might be more readily achieved with instruments such as the environmental SEM (236).

4.3 THE CORRELATION OF GLYCATION CONTENT IN THE SKIN AND VAGINAL TISSUE IN PREGNANCY

4.3.1 INTRODUCTION

The elevation of advanced glycation content in the vaginal wall in prolapsed tissues makes advanced glycation a significant association with the disease. Early detection of vaginal wall glycation could therefore be relevant in the prevention and management of prolapse. A vaginal wall biopsy to detect this would be ideal, but is invasive. Therefore the use of a more accessible organ, such as skin, would be beneficial. Our previous study suggests that conditions such as pregnancy, can induce a change in the vaginal tissues' glycation content (237).

There are currently no predictive tools for prolapse. The most common diagnostic techniques are based on physical pelvic examination (79,80,86,87). Due to the personal and private nature of pelvic problems and symptoms, diagnosis of prolapse often occurs when sufferers present with symptoms. As a result, more women have clinically evident prolapse than actually present with symptoms to their health care provider (79).

The consistent findings of higher vaginal wall glycation in women with prolapse in previous studies (8,23) suggest that the identification of vaginal wall glycation may be a useful tool for prediction, diagnosis and further management of prolapse. Vaginal tissue is poorly accessible and obtaining a vaginal biopsy is invasive and inconvenient for patients. The skin, on the contrary, is easily accessible and skin fluorescence can be measured non-invasively to reflect its advanced glycation levels (202). Since ageing is a generalized body process, it is expected that the various processes involved in ageing such as advanced glycation should occur at

similar rates in different body tissues. We therefore hypothesize that skin glycation would predict vaginal tissue glycation.

4.3.2 AIM

The aim of this study was to assess whether the skin glycation undergoes similar changes as observed in vaginal tissue glycation in the same subjects in order to evaluate the hypothesis that skin glycation would predict vaginal tissue glycation.

4.3.3 METHODS

Vaginal and skin tissues were obtained as described in 3.1.1 and pentosidine detection and quantification was carried out as described in 3.3.2.

4.3.4 RESULTS

The average skin pentosidine was obtained per gram dry tissue. Figure 4.24 shows that the average amounts of pentosidine were 0.007 mg/g and 0.014 mg/g in the pregnant and non-pregnant skin tissues respectively. There was minimal variability within groups and the difference was significant ($p = 0.0002$).

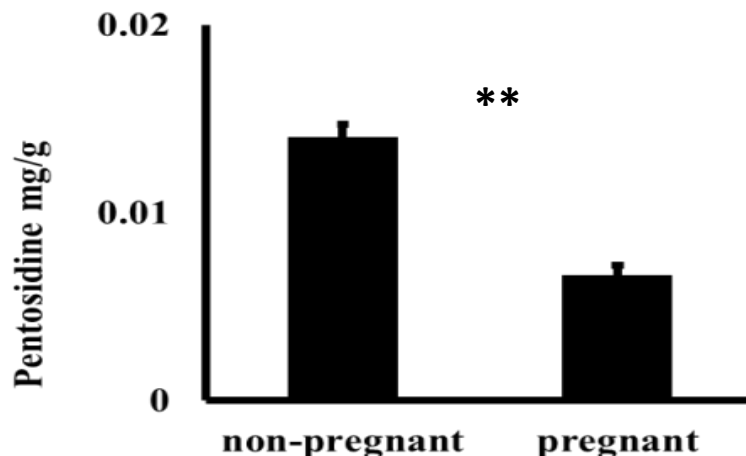


Figure 4.24: AGE marker (pentosidine) level measured via HPLC in pregnant (n=5) and non-pregnant (n=5) skin tissues. *P=0.000.**

Pentosidine in non-pregnant rat vaginal tissues was also significantly higher than in pregnant rat vaginal tissues ($P=0.042$) as shown in Figure 4.9, section 4.1.6. Although pentosidine levels in the skin were less than in the vaginal tissues, the pregnancy associated difference was more notable in the skin than in vaginal tissues. Pentosidine was higher in the vaginal tissue than in the skin of the same rats. Raised vaginal pentosidine was associated with raised skin pentosidine. A strong correlation ($R^2= 0.847$) was present between the pentosidine content of vaginal and skin tissues of the same rats (Figure 4.25).

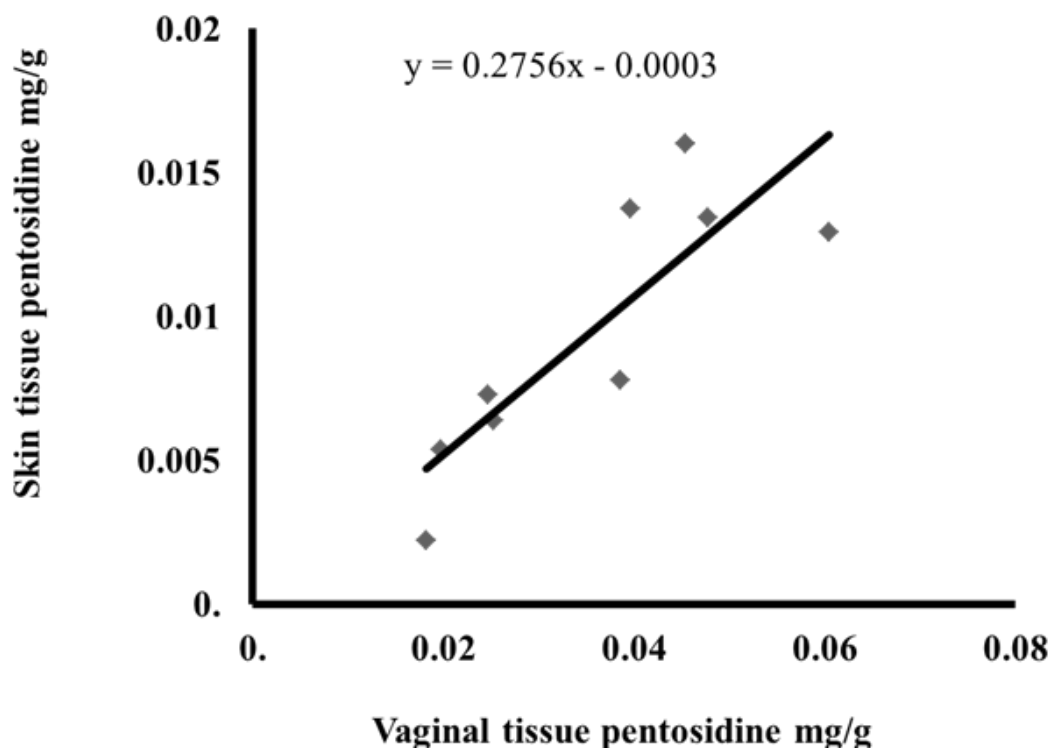


Figure 4.25: Correlation between Skin and vaginal tissue pentosidine. $R^2=0.847$

4.3.5 DISCUSSION

Advanced glycation is a cause of ageing that has gained significant attention in recent times (8). Glycation considerably affects the skin. It results in increased skin stiffness, decreased elasticity and higher resistance to MMP enzyme degradation (10) that enables connective tissue remodeling. Glycation induces inflammatory responses intracellularly and extracellularly (2). Advanced glycation end products can initiate DNA damage and stimulate cellular injury through their receptors; these are called the Receptor of Advanced Glycation End products, (RAGE) (11).

Ageing increases advanced glycation in body continuously. Other conditions can regulate glycation content of body tissues. For example, advanced glycation is facilitated by oxidative stress (201). As a result, increased oxidative stress such as occurs as a result of cigarette smoking and inflammation leads to highly glycation content (238). On the contrary, elevation of the female hormone, oestrogen causes the up-regulation of several antioxidants including a glycation reducing antioxidant, glyoxalase I. As a result, a lower glycation content has been observed in pregnant vaginal tissues in a rat model (237). Furthermore, it has been previously shown that skin glycation is lower during pregnancy (202). It is therefore expected that skin glycation would correlate with vaginal tissue glycation of the same animals because it is expected that hormone induced changes in vaginal wall glycation should be reflected in the skin in the same pregnant and non-pregnant states.

In this study, glycation was lower in the skin during pregnancy. This is congruent with a previous study noting reduced skin glycation-induced autofluorescence in pregnancy (202) and corroborates the tested hypothesis. An implication is that skin glycation assessment in women would be useful in the management of women with prolapse and a relevant predictive tool which may allow future prevention.

Recently, vaginal tissue glycation was noted to be lower in pregnancy through influences on ER- α and glyoxalase I, an AGE lowering antioxidant (237). Another study observed reduced glycation in vaginal tissues under oestrogen therapy (41). Oestrogen has also been found to influence blood vessel glycation. These, in conjunction with the present finding of reduced skin glycation in pregnancy suggest that pregnancy effects on glycation may be reflected in

multiple body tissues and organs. The observation of known glycation-associated illnesses should warrant checks for other conditions.

A positive relationship between vaginal and skin tissue glycation content was also noted in this study and supports the hypothesis that skin glycation reflects vaginal tissue glycation level. Advanced glycation content has been studied in different tissues in the body because it is believed to be global phenomenon occurring at reasonably similar rates in various sites of the body. Animal studies and human clinical trials have confirmed changes in advanced glycation content in other body tissues to be reflected in the skin (239–241). Mikulikova *et al* quantified pentosidine in tissues from rats with high fructose intake and found that pentosidine accumulation increased in tendon, skin and aorta occurred at different rates, with pentosidine increasing more in the skin and aorta than in tendons when 10% fructose was given (239). Skin advanced glycation level has been used to predict advanced glycation associated diseases in other tissues such as the retina and cardiovascular system (240–242) however no previous study has correlated advanced glycation levels between skin and vaginal tissues. We investigated glycation levels of vaginal and skin tissues in pregnancy, a physiological process, and found correlation between the collagen altering glycation product, pentosidine in both tissues in the same rats, implying that collagen changes in connective tissues across the whole body may provide vital information for physiological and pathological processes. The correlation of glycation products in skin and other tissues, and the ease of access of skin for sampling or biopsy, lays a foundation for future studies on the predictive value of skin glycation in relation to vaginal tissue glycation, and thus its potential role in the investigation, prevention and management of glycation related gynecological diseases. Our hypothesis is

also supported by a recent study which revealed that ultra-structural collagen changes in the skin of women with prolapse correlated with changes in pelvic tissues of the same women (243).

Further studies are required to determine whether the correlation of advanced glycation levels in skin and vaginal tissue are observed in human subjects during physiological and pathological processes. Furthermore, in pathological cases, it is important to note that changes in collagen metabolism may be the result or cause of a disease. For example, in prolapse, the alteration of collagen metabolism in the vaginal wall may be a result of prior tissue weakening or stretching but not necessarily the cause of the prolapse (244). In such a condition, collagen metabolism alterations or glycation levels may be more expressed locally in the vaginal wall than in skin tissues.

4.3.6 CONCLUSION

Our animal model study reveals that skin glycation correlates with vaginal wall glycation as both tissues respond similarly to a state of elevated oestrogen. This, in addition to previous literature demonstrating similar changes within the skin in response to changes in levels of the hormone, strongly suggests that skin glycation is reflective of vaginal tissue glycation, which is implicated in pelvic floor disorders. Skin glycation is a potentially useful marker in the prediction and diagnosis of glycation-associated pelvic floor diseases, with a view towards promoting preventive lifestyle. This understanding should guide future screening tests for early detection of detrimental levels of ageing in the vagina tissue.

5 CHAPTER 5: GLYCATION CHANGES OF VAGINAL
TISSUES IN PROLAPSE IN RELATION TO KNOWN AND
POTENTIAL RISK FACTORS

5.1.1 INTRODUCTION

Despite the high and increasing prevalence of prolapse in women, its aetiology and progression is unclear (8). There is no known cause of prolapse although several factors are implicated in its development. Common associations are vaginal delivery, particularly instrumental delivery, multiparity, obesity, elevated intra-abdominal pressure in conditions such as chronic straining and obstructive lung disease (6,104). Genetic and familial association of prolapse are also present, as is there the risk of occurrence in individuals whose first degree relatives are affected (99).

Ageing is also linked with prolapse development since its prevalence has been noted to increase with age (6). The association of age with prolapse has gained more attention in recent times as advanced glycation products are found to be present in higher amounts in prolapsed pelvic tissues (8,23). Advanced glycation is linked with chronological ageing and some endocrine and cardiovascular diseases (55,57,214). The difficulty in breaking down glycated proteins over time, results in the accumulation of such older proteins within the tissues and an ultimately mechanically altered connective tissue matrix. This change in connective tissue breakdown fostered by advanced glycation accumulation may be useful in understanding prolapse development. The physical and chemical properties of connective tissues are influenced by AGEs. AGEs have been associated with decreased cell proliferation, cell death, oxidative stress and inflammation (245). AGEs and AGEs receptors (RAGE) and the RAGE gene SNP change the metabolism of collagen and this leads to many disease states and ageing

of the body (246). RAGE triggers signal transduction for AGEs, cascading several signals including inflammation (57).

Glycation results in accumulation of older collagen. On the contrary, oestrogen treatment influences pelvic tissue collagen metabolism causing neosynthesis of collagen (23,41). Older, glycated collagen also may be difficult to degrade leading to retained changes in the pelvic tissues' mechanical property but factors influencing the accumulation of AGEs in the prolapsed tissues have not been well investigated. Although AGEs are known to be higher in prolapsed tissues with an influence on the tissues' mechanical properties by a possible effect on accumulation of old, MMP-resistant collagen and preferential degradation of newer collagen (23), the question of "cause or effect" still boggles the minds of many stakeholders. An understanding of previously poorly recognized glycation associations, its mode of glycation accumulation within prolapsed tissues and glycation associations (risks or habits) is required to better predict and prevent prolapse. In addition this would improve understanding of the role of glycation in prolapse development.

5.2 AIMS

The research in this chapter was aimed at investigating glycation changes in human prolapsed tissues in association with known and potential risk factors, such as age, hypertension, smoking, cholesterol level and diabetes, oestrogen changes and antioxidant enzyme level in the vaginal wall to understand glycation accumulation in the tissues. A further aim was to understand how glycation accumulates in tissues potentially leading to prolapse by studying the relationship between and glycation changes, ER- α expression and the expression of a glycation lowering antioxidant, GLO-I, within the tissues.

5.3 METHODS

To obtain human tissues for study, ethical approval was sought as described in 3.1.2. Participant recruitment and categorization based on data characteristics were subsequently carried out as described in 3.1.2. ER- α , and GLO-I immunostaining were performed as described in 3.3.4. Pentosidine quantification and validation tests were performed as described in 3.3.2.

5.4 RESULTS

5.4.1 VALIDATION TESTS FOR TISSUE STORAGE AND DRYING METHOD

To assess the reliability of pentosidine values obtained for each tissue piece, pentosidine was quantified for the different non-contiguous locations of the same tissue. There was no significant difference in pentosidine content of the different locations (A, B, C) of the same tissue piece as shown in table 5.1 ($p=0.97$). For the same tissue, the calculated maximum variation in pentosidine value was 0.001 mg/g.

Table 5.1: Pentosidine content of prolapsed samples from different non-contiguous tissue regions (p=0.97)

Sample ID	location A	location B	location C	Average	Standard deviation	Standard error of mean
H18	0.024	0.022	0.023	0.023	0.001	0.00056
H32	0.021	0.021	0.02	0.021	0.0006	0.00033
H30	0.016	0.014	0.015	0.015	0.001	0.00058

Pentosidine amounts were assessed for the same tissues before and after storage at -20°C . Although, post storage was slight lowering of pentosidine content, the difference was notably non-significant ($p=0.97$). The average standard deviation and standard errors of mean were 0.002 and 0.001 respectively and the maximum variation in reading was 0.003 as shown in table 5.2.

**Table 5.2: Pentosidine content of the same tissues before and after storage at -20⁰C
(p=0.97)**

Sample ID	Before storage	After storage	Standard deviation	Standard error of mean
H36	0.013	0.012	0.0007	0.0005
H40	0.022	0.025	0.0021	0.0015
H26	0.031	0.028	0.0021	0.0015
		Average	0.0016	0.0011

Freeze drying was compared with drying samples at 60⁰C (table 5.3). Following oven drying, pentosidine content of the tissue was the same or slightly increased. The difference was non-significant. The average standard deviation and standard error of mean were 0.003 and 0.002 respectively.

Table 5.3: Pentosidine content of the same tissues dried at 60⁰C in an oven or lyophilisation overnight. (p=0.66)

Sample ID	60 degree oven	Freeze drying	Standard deviation	Standard error of mean
H39	0.025	0.029	0.003	0.002
H38	0.017	0.014	0.002	0.001
H21	0.033	0.023	0.007	0.005
		Average	0.004	0.003

5.4.2 OVERVIEW OF RECRITUTED PATIENT CHARACTERISTICS

A total of 65 samples (49 prolapse, 16 controls) were studied (table 5.4). These were taken from women within the ages 41-91. There was a normal distribution of age. The modal numbers were 6, 12, 28, 15, 3 and 1 in the age groups 40-49, 50-59, 60-69, 70-79, 80-89 and 90-99 respectively (Table 5.4). Comparisons in pentosidine were therefore made using age groups containing 3 or more n number. The average, mode and median ages of the total population studied were 64.8, 67.0 and 64.0 respectively. The average ages of women in the prolapse and control groups were 57.82 and 66.65, respectively (Figure 5.1). There was less variation in age in women with prolapse compared with controls (standard error of mean of 2.89 and 1.21 respectively).

Table 5.4: Table showing the age distribution within the prolapse, control and entire study population

	Control	Prolapse	Total population
Age groups	Number (% of total)	Number (% of total)	Number (% of total)
40-49	5(83.33)	1(16.67)	6 (9.23)
50-59	4(33.33)	8(66.67)	12(18.46)
60-69	5(17.86)	23(82.14)	28(43.07)
70-79	2(14.29)	12(85.71)	15(23.07)
80-89	0(0)	3(6.12)	3(4.6)
90-99	0(0)	1(2.04)	1(1.53)

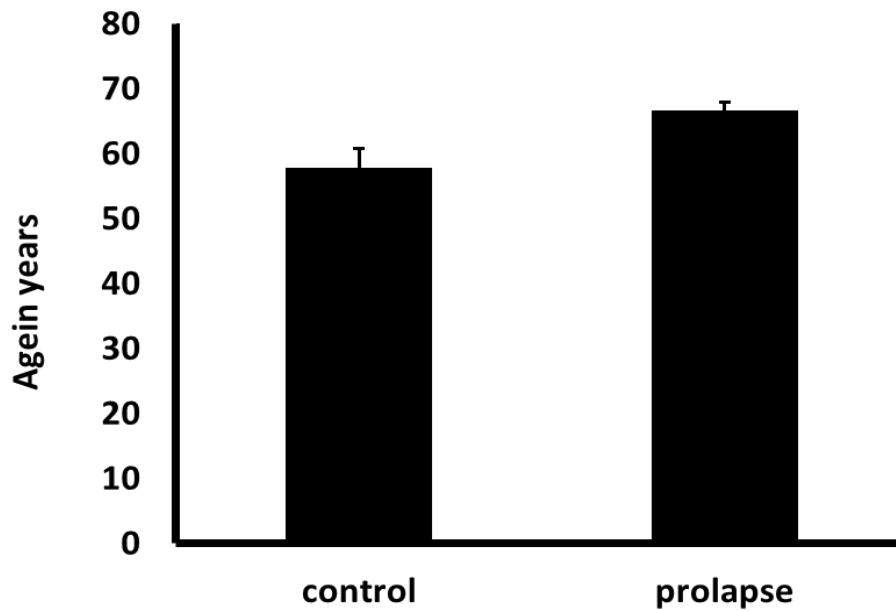


Figure 5.1: Average age of women studied in control (n=16) and prolapsed (n=49) groups.

The mean parity was 2.46 in the entire population studied and 2.3 and 2.5 in control and prolapse groups respectively (figure 5.2). Most women were parous but two women with prolapse had never been pregnant (Table 5.5). 2 women with prolapse and one woman without prolapse had parity of 0. The highest recorded parity in control group was 4 and in prolapse group, 6.

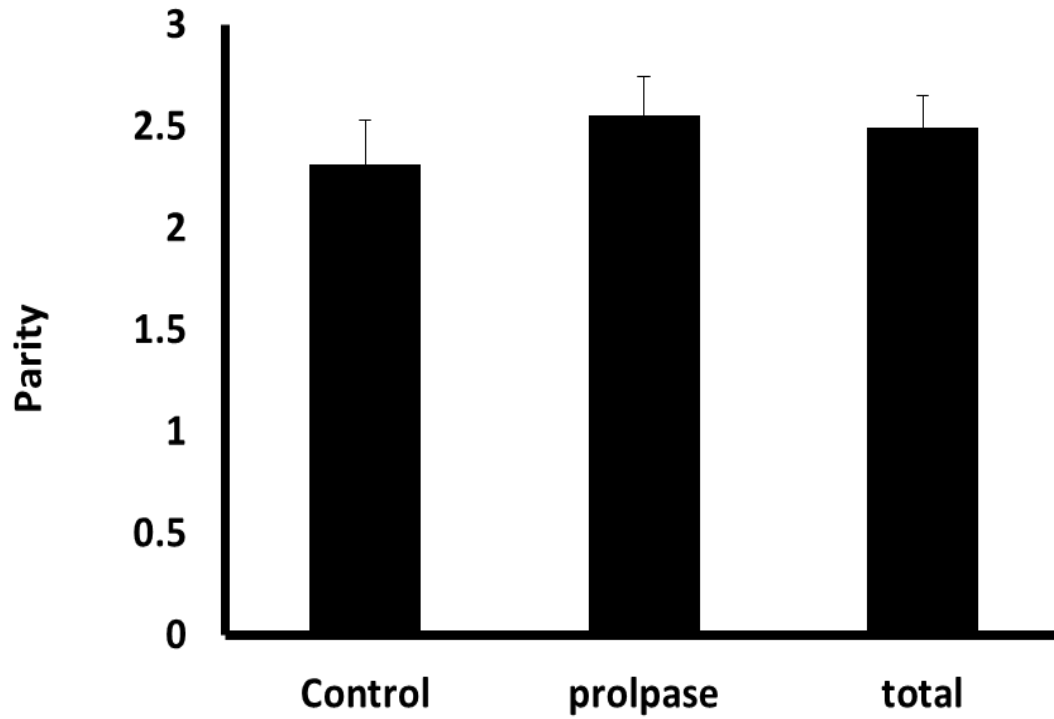


Figure 5.2: Parity in prolapsed (n=49), control groups (n=16) and total population (n=65) studied.

Table 5.5: The number of women with parities of 0-6 in both groups

Parity	Control	Prolapse
P0	1	2
P1	0	4
P2	9	13
P3	0	17
P4	5	6

P5	0	1
P6	0	3
No response	0	3

The predominant mode of delivery was vaginal delivery with 92% of the women having vaginal deliveries. This included 82.5% of the control population and 96.8% of women with prolapse. Of the control group, two women (5%) and 5 women with prolapse (4.6%) had at least one pregnancy with assisted delivery using forceps, ventouse or caesarean section (Table 5.6). Although the incidence of assisted delivery was low, the use of forceps or the performance of caesarean section was more likely than ventouse use.

12.5% and 10.2% of the control and prolapsed groups had taken HRT for at least five years (Table 5.6). Although none of the women in the control group had previous hysterectomies or removal of their ovaries, 32.6% of women with prolapse had reported prior hysterectomies and a quarter of these had associated oophorectomies. The commonest type of prolapse in this group was anterior prolapse (cystocele) with 67.34% of the women with prolapse presenting with this kind of prolapse. Rectocele was commoner than uterine prolapse. As expected, the most common group of symptoms were urinary symptoms. The most common complaint was a feeling of fullness within the vagina, a sensation of a lump in the vagina or a visible bulge from the vagina. Some women also experienced lower back or pelvic pain, and vaginal soreness and dryness. Grades II and III prolapse were more common than grades I and IV. Ten of the 49 women with prolapse had had previous surgery for prolapse resulting in a prolapse recurrence rate in the population studies of 20.4% as shown in Table 5.6.

There were a number of co-morbidities present in the population studied, predominantly cardiovascular problems such as elevated blood pressure. Thirty two women, representing 47.69% of the study population had hypertension as a co-morbidity. Of these 23 (74.19%) had prolapse and 7 (25.8%) were controls. 43.75% and 51.02% of the control group and women with prolapse had been diagnosed with hypertension. There was a lower prevalence of diabetes mellitus in the groups with 12.5% and 10.2% of the control and prolapsed groups having co-existing diabetes mellitus. More women with prolapse (40.8%) had co-existing diagnosis of elevated cholesterol than the control group (12.5%).

Table 5.6: Overview of participant characteristics in prolapsed and control groups.

CHARACTERISTICS	Sub classification	Control	Prolapse
Mode of delivery, <i>n</i> (%)	Normal vaginal delivery	15 (94.1)	46(94.0)
	Cesarean section	0(0)	1 (0.5)
	Forceps delivery	1 (5.9)	1 (0.5)
	Ventuosse	0(0)	1(0.5)
HRT, <i>n</i> (%)	HRT	2 (12.5)	5(10.2)
	No HRT	14 (87.5)	44(89.8)
Hypertension, <i>n</i> (%)	Hypertensive	7(43.7)	25(51.02)
	Non-hypertensive	9(56.3)	24(49.0)
Smoking, <i>n</i> (%s)	Smokers	2(12.5)	14(28.57)
	Non-smokers	14(87.5)	35(71.4)
DM, <i>n</i> (%)	Diabetic	2(12.5)	5(10.2)
	Non-diabetic	14(87.5)	44(89.8)

Cholesterol, <i>n</i> (%)	Elevated cholesterol	2(12.5)	20(40.8)
	Normal cholesterol	14(87.5)	44(89.8)
Prolapse types, <i>n</i> (%)	Cystocele	n/a	33(67.3)
	Rectocele	n/a	9(18.4)
	Uterine prolapse and proscendentia	n/a	6(12.2)
	Unrecorded	n/a	1(2.0)
Urinary symptoms, <i>n</i> (%)	Frequency	n/a	8(10.67)
	Urgency	n/a	6(8)
	Dribbling	n/a	5(6.67)
	Incomplete voiding	n/a	5(6.67)
	Stress leak/incontinence	n/a	9(12)
	Urinary retaintion	n/a	1(1.33)
	Nocturia	n/a	1(1.33)
Vaginal symptoms, <i>n</i> (%)	Vaginal lump/fullness	n/a	18(24)
	Drag in pelvis	n/a	2(2.67)
	Vaginal sore/dryness	n/a	6(8)
Bowel symptoms, <i>n</i> (%)	Constipation	n/a	6(8)
	Tenesmus	n/a	1(1.33)
Lower back pain, <i>n</i>	Lower back pain	n/a	7(9.33)

(%)			
Prolapse grade, <i>n</i> (%)	I	n/a	7(14.3)
	II	n/a	12(24.5)
	III	n/a	21(42.9)
	IV	n/a	7(14.3)
	Unrecorded	n/a	2(4.0)
Prolapse recurrence, <i>n</i> (%)	Frist time prolapse	n/a	39(79.6)
	Previous prolapse	n/a	10(20.4)

5.4.3 PENTOSIDINE QUANTITY IN PROLAPSED AND CONTROL GROUPS AND ITS POTENTIAL RELATIONSHIP WITH RISK FACTORS, PROLAPSE GRADE AND SYMPTOM PERCEPTION

Pentosidine was significantly higher ($p= 0.02$) in vaginal tissues in women with prolapse compared with controls as shown in figure 5.3. The average values of pentosidine per gram of tissue were 0.02 and 0.03 mg in controls and prolapsed vaginal tissues respectively.

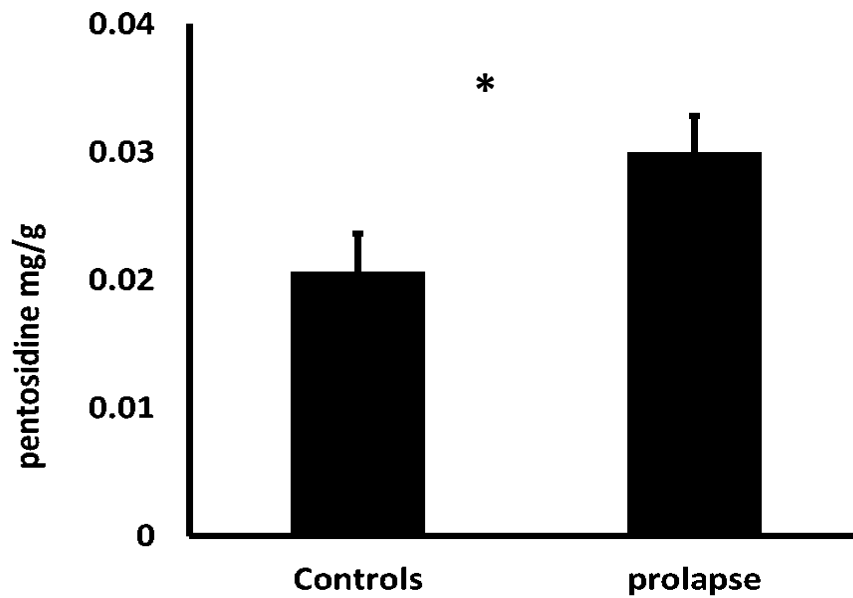


Figure 5.3: Pentosidine in prolapse (n=49) and control (n=16) tissues. (*p=0.02)

There was a steady increase of pentosidine with age in the entire population studied, ranging from 0.014 mg/g to 0.037mg/g. Age group 40-49 was significantly different from age groups 60-69 and 70-79 with p values of 0.00 and 0.01 as shown in figure 5.4. Age group 50-59 was significantly different from 60-69 with a p value of 0.04. The most significant differences were noted between age groups 40-49 and 60-69. Within the control population, there was a steady rise of pentosidine with age but this was non-significant between each age group (Figure 5.5). In the prolapse group, however the increase in pentosidine content with age was significantly different between age groups 50-59 and 60-69 with a p value of 0.012 (Figure 5.6).

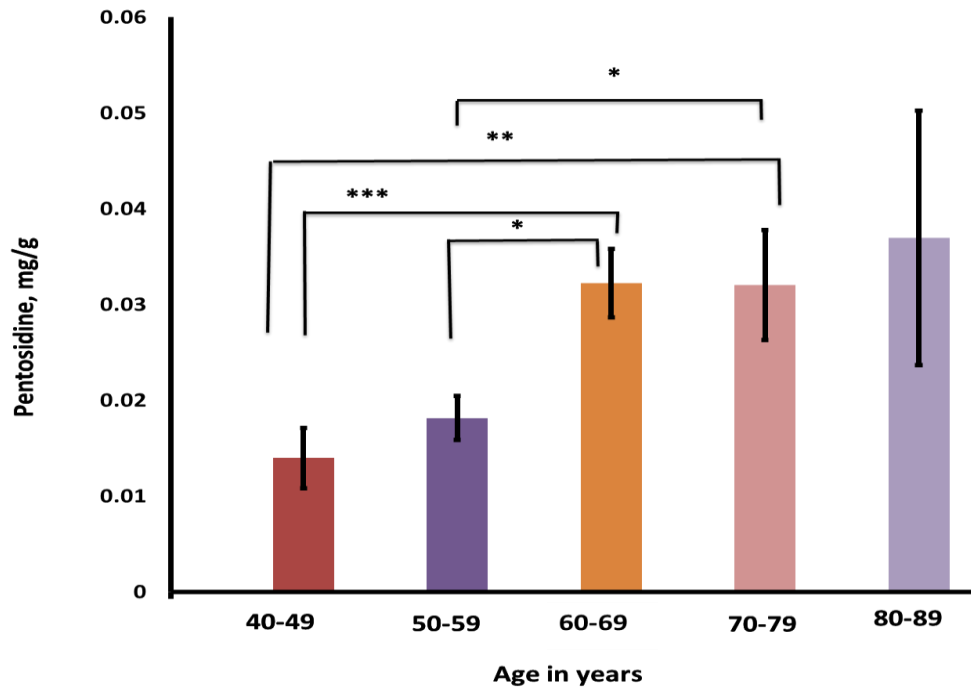


Figure 5.4: Pentosidine and age in vaginal tissues from entire study population. (n=6, 12, 28, 15 and 3 in age groups 40-49, 50-59, 60-69, 70-79 and 80-89 respectively)

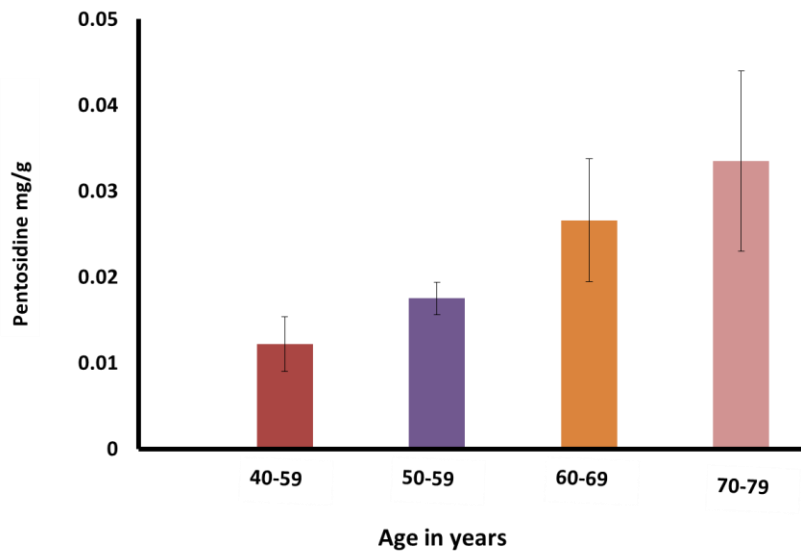


Figure 5.5: Pentosidine amounts by age groups in vaginal tissues of controls. (n=5, 4, 5 and 2 in age groups 40-49, 50-59, 60-69 and 70-79 respectively)

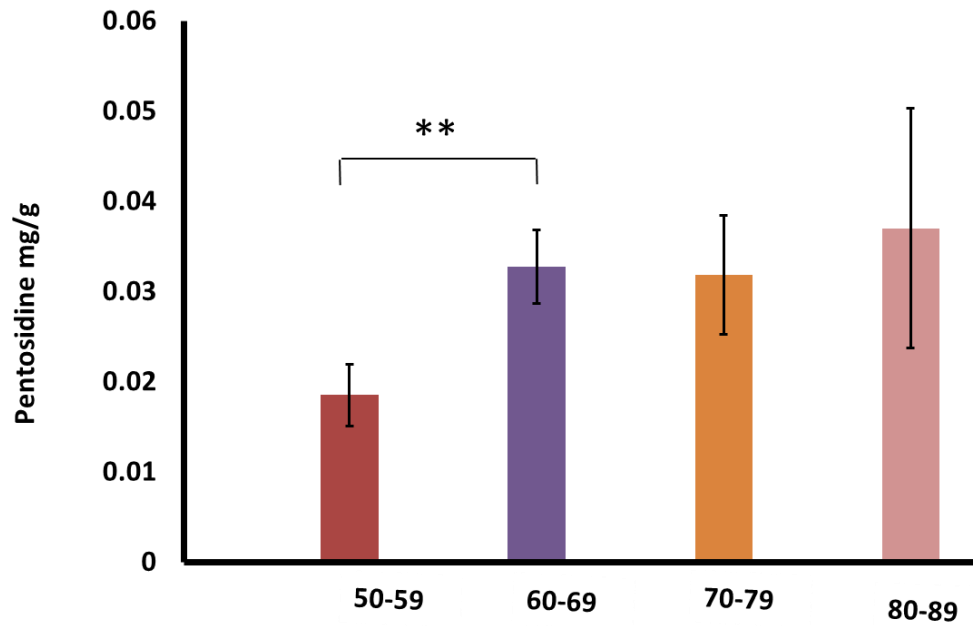


Figure 5.6: Pentosidine amounts in prolapsed vaginal tissues by age groups, $p=0.012$. (n=8, 23, 12 and 3 respectively for age groups 50-59, 60-69, 70-79 and 80-89)

Pentosidine was higher after the menopause in both prolapse and controls but this difference was non-significant in the prolapse group. Pentosidine was significantly different between premenopausal controls and menopausal controls but not between prolapse sub groups ($p=0.03$), figure 5.7.

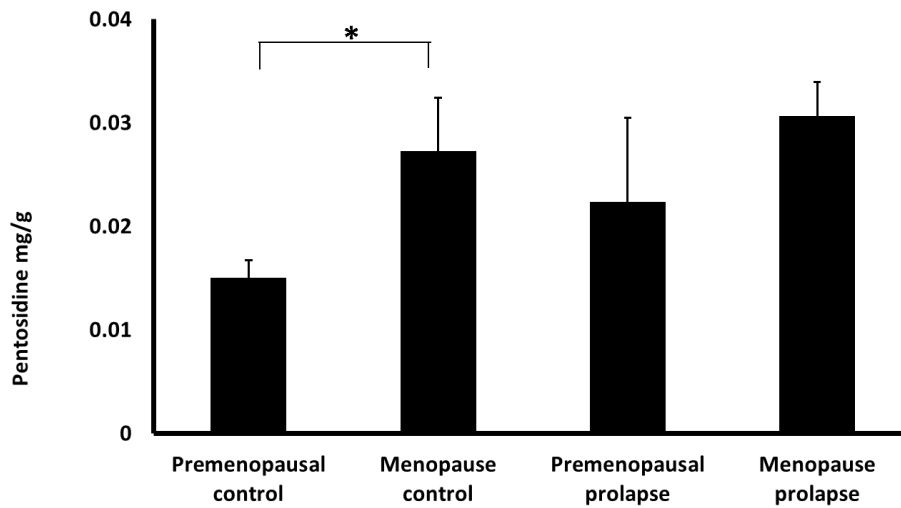


Figure 5.7: Pentosidine in prolapsed and control tissues based on menopausal status, *P=0.03. (n= 8, 9, 3 and 46 in premenopausal control group, menopausal control group, premenopausal prolapse group and menopausal prolapse groups respectively)

Pentosidine in the vaginal tissues of women with hypertension were significantly higher ($p=0.01$) than in women without hypertension (Figure 5.8). Amongst the prolapse and control groups, the vaginal wall pentosidine content was higher in women with co-existing hypertension with p values of 0.04 and 0.05 respectively (figure 5.9). Women with both prolapse and hypertension had the highest average pentosidine (0.036 mg/g) while women in the control group without hypertension had the least pentosidine content (0.014 mg/g).

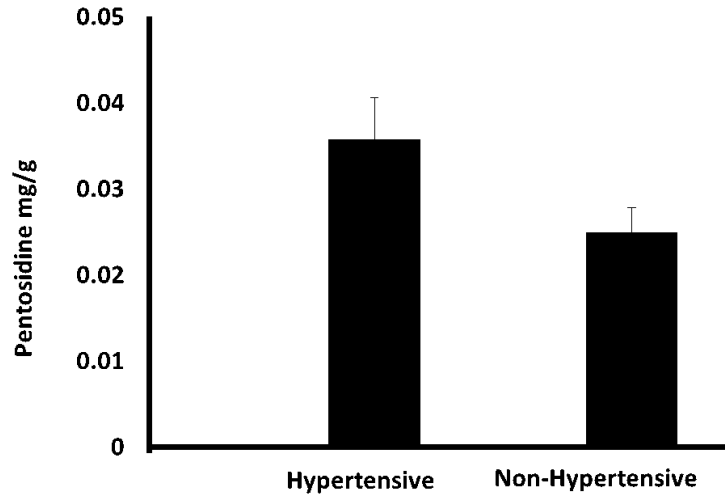


Figure 5.8: Amounts of pentosidine in vaginal tissues of hypertensive and non-hypertensive patients in the entire study group, *p=0.01. (n=32 and 33 in hypertensive and non-hypertensive groups)

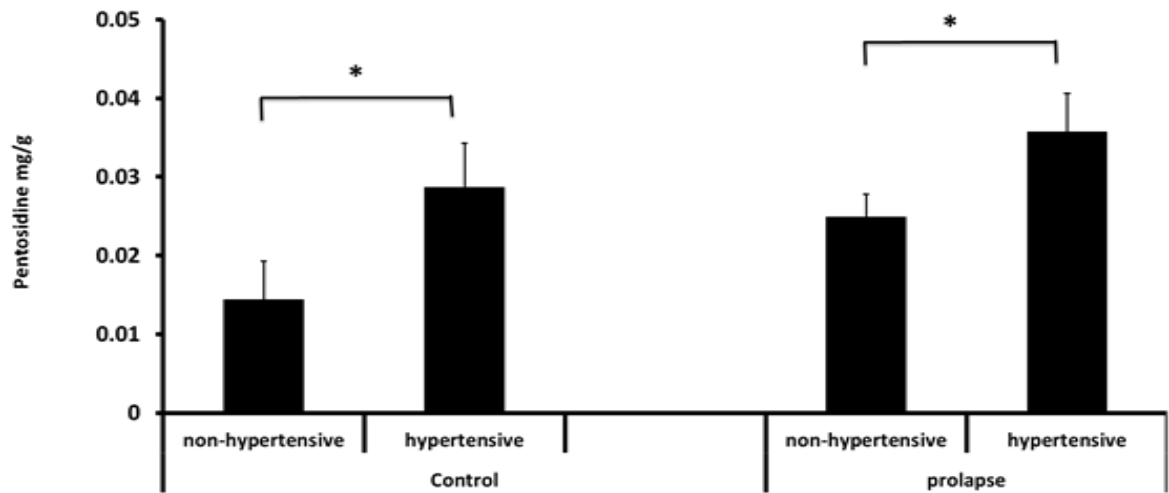


Figure 5.9: Pentosidine in vaginal tissues of women with hypertension in control and prolapsed groups, *p=0.04 and 0.05. n= 7 and 9 in control groups with and without hypertension; 24 and 25 in prolapse groups with and without hypertension respectively.

There was a non-significant increase in pentosidine content in the vaginal tissues of women with prolapse and DM, $p=0.4$, (Figure 5.10).

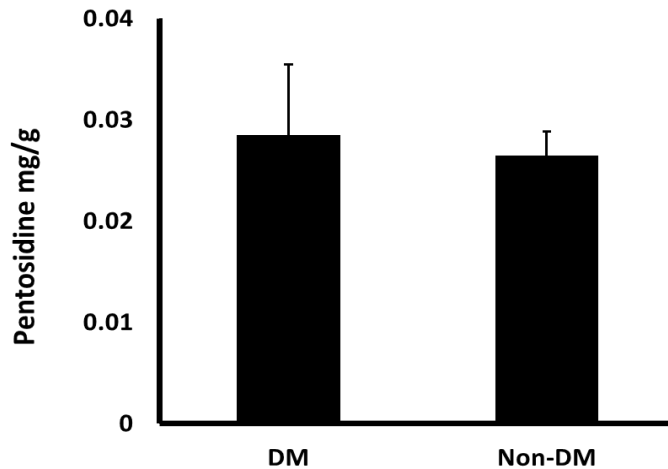


Figure 5.10: Pentosidine amounts in vaginal tissue of women with DM, $p=0.4$. (n=7 and 58 for the DM and non-DM groups respectively).

Twenty four percent (12.5% of controls and 28.57% of women with prolapse) of the population studied were current smokers (Table 5.6), of these 87.5% had prolapse. The smokers had a borderline significantly higher pentosidine ($p= 0.08$) in their vaginal tissues than the non-smokers (Figure 5.11). The average pentosidine level amongst smokers was 0.036 mg/g while non-smokers had an average pentosidine level of 0.026 mg/g.

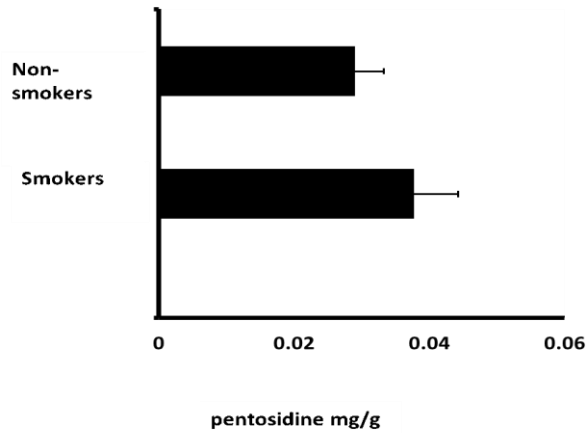


Figure 5.11: Pentosidine content in the vaginal tissue of smokers and non-smokers, $p=0.08$. (n=16 and 49 for smokers and non-smokers respectively)

An incidental finding of significantly higher amounts of pentosidine in the vaginal wall of women with anterior wall prolapse than in women with rectocele was made, $p=0.03$ (Figure 5.12).

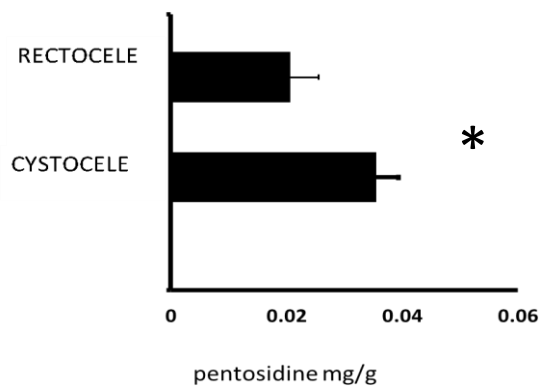


Figure 5.12: Pentosidine content of vaginal tissues in prolapse involving the anterior and posterior walls of the vagina, $*=0.03$. (n= 33 and 9 for cystocele and rectocele respectively)

There was a mild non-significant but steady increase in pentosidine with an increase in prolapse grade except for an unexpected decrease in pentosidine in tissues from grade 4 prolapse (Figure 5.13) based on clinical examination findings. Average amounts of pentosidine in the control group were lower than pentosidine in grade 1-3. A weak positive correlation was observed between grade of prolapse and pentosidine amounts of the tissue ($r^2=0.129602$), Figure 5.14. Higher amounts of pentosidine were observed in tissues from women with prolapse grade 3, with an average value of 0.034 mg/g.

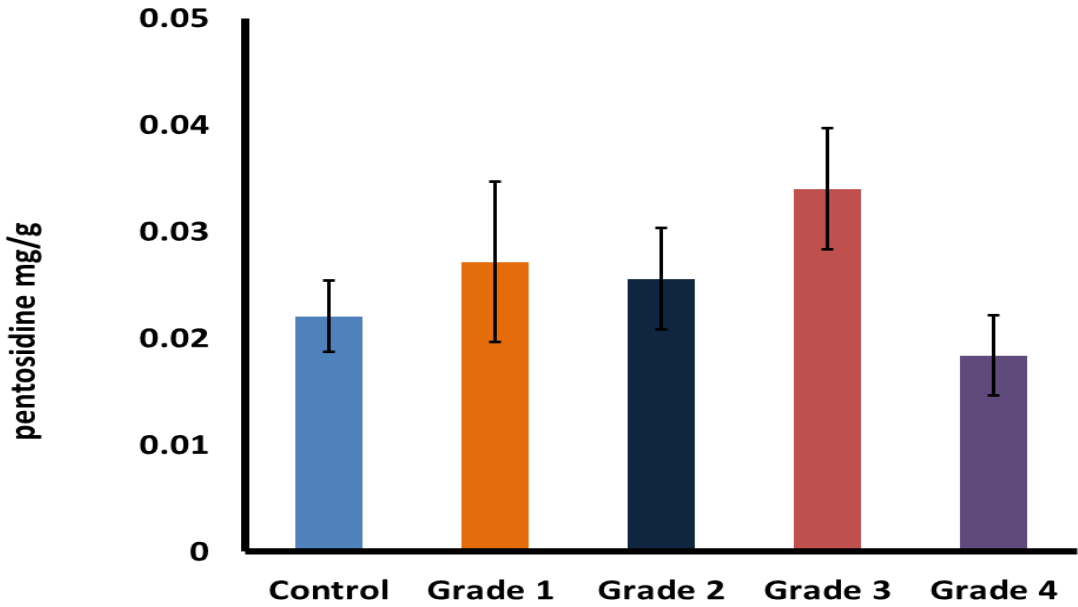


Figure 5.13: Pentosidine amounts in tissues in relation to grade of prolapse. (n=16, 7, 12, 21 and 7 for control, grade 1, grade 2, grade 3 and grade 4 prolapse stages respectively).

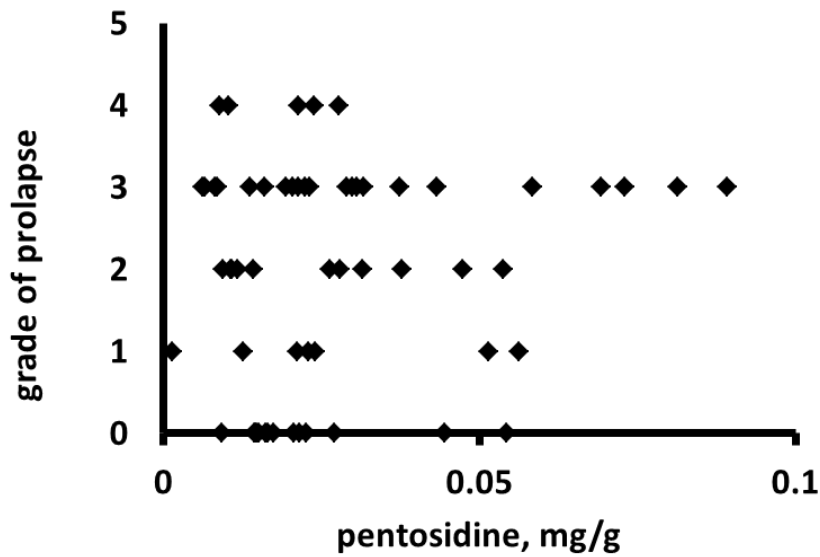


Figure 5.14: Scatter plot showing relationship between pentosidine amounts in the tissues and the grade of prolapse.

Perception of symptom severity and impact on quality of life by the patients themselves as assessed by ICIQ-VS correlated positively ($r^2=0.455747$) with pentosidine content of the tissues, shown in figure 5.15, and increased steadily from one grade to another with the exception of grade 1 (figure 5.16). Amongst women with grade 1 prolapse, perception of symptoms was unexpectedly high. An increase in the perception of symptom severity was however not significantly different between the prolapse grades ($p= 0.37, 0.38, 0.58$)

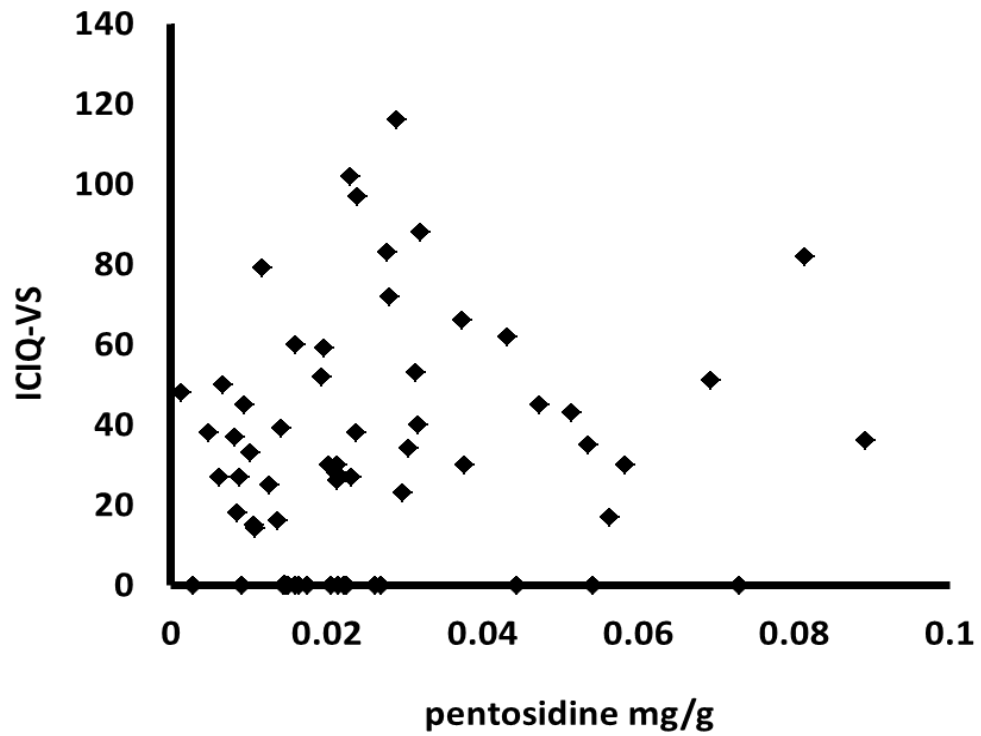


Figure 5.15: Scatter plot of tissue pentosidine content with ICIQ-VS score. Pearson's correlation coefficient, $r^2 = 0.4$

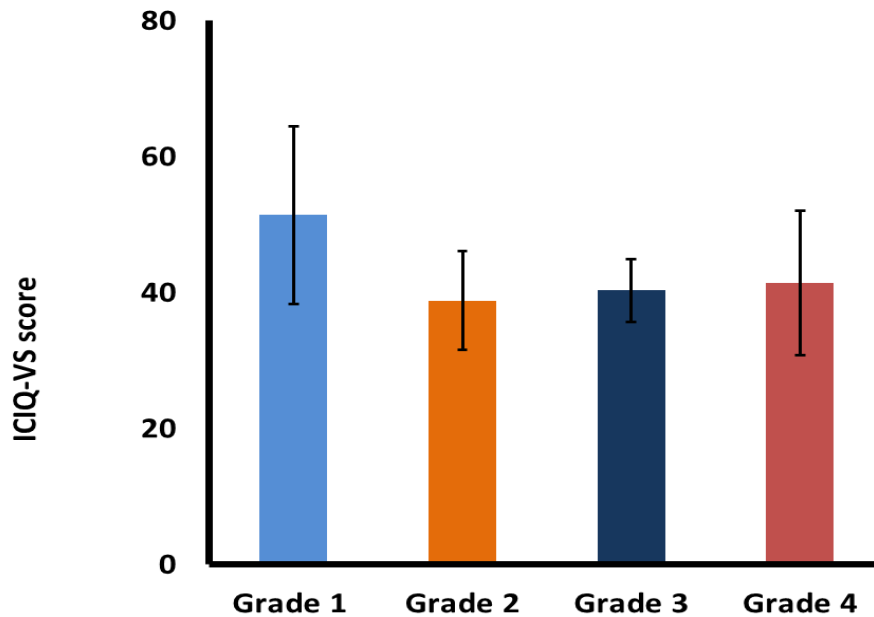


Figure 5.16: Symptom severity perception (ICIQ-VS) and prolapse grade (n= 7, 12, 21 and 7 for grade 1, grade 2, grade 3 and grade 4 prolapse stages respectively)

5.4.4 ER- α AND GLO-I EXPRESSION

Oestrogen receptors were expressed as nuclei-like spots located at the vicinity of the nuclei in both prolapse and control groups. Cellular nuclei were expressed in both groups. Oestrogen receptors were distinctively and more expressed in the control tissue sections than prolapsed tissues (Figure 5.17). There were few, diffusely expressed oestrogen receptors in the prolapsed group. The average number of visible receptors per image area was 95.5 and 19 for controls and prolapse respectively (Figure 5.18). The difference was significant ($p=0.013$).

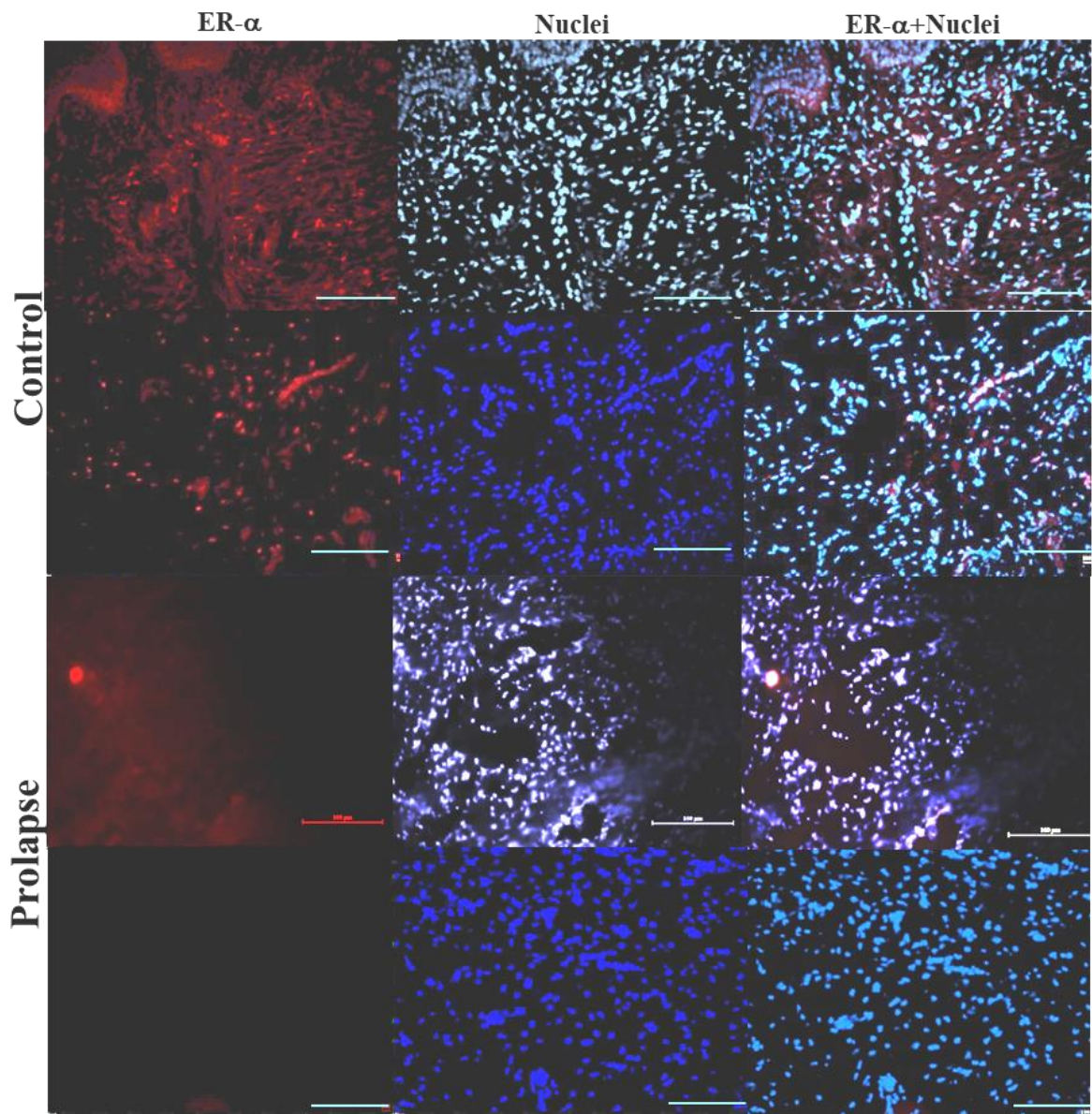


Figure 5.17: Representative images showing ER- α expression (red) in age-matched prolapsed and control tissues. Nuclei were counter-stained by DAPI (blue). Scale bar = 50 μ m

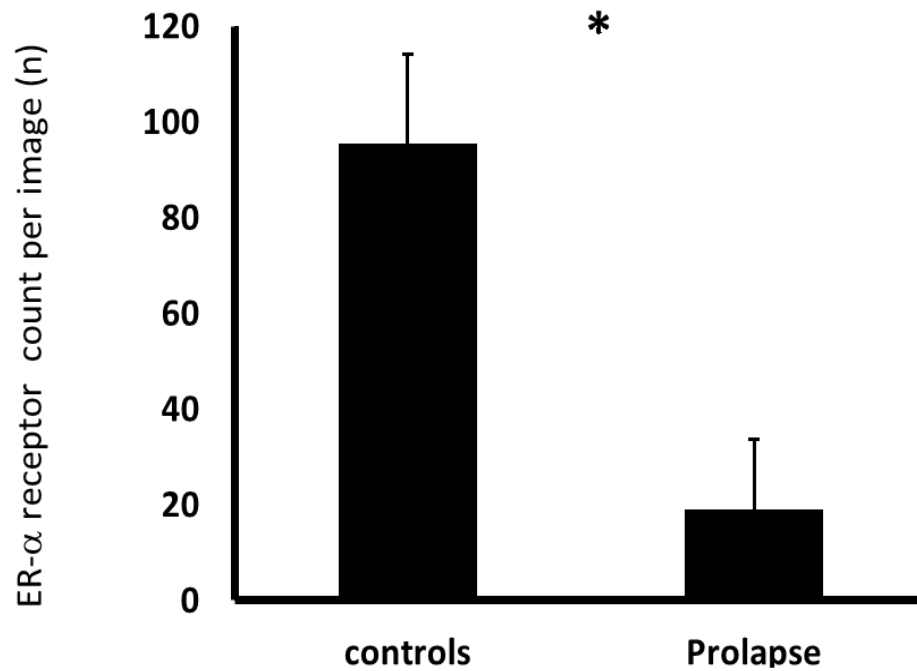


Figure 5.18: ER- α receptor count in control and prolapsed tissues based on image analysis, *p=0.013. n=3 per group

The expression of the antioxidant enzyme, glyoxalase I was diffusely spread within the tissue and sub-epithelial regions (figure 5.19). It was more expressed in the control tissues and minimally expressed in prolapsed tissues. Nuclei expression was noted in both groups.

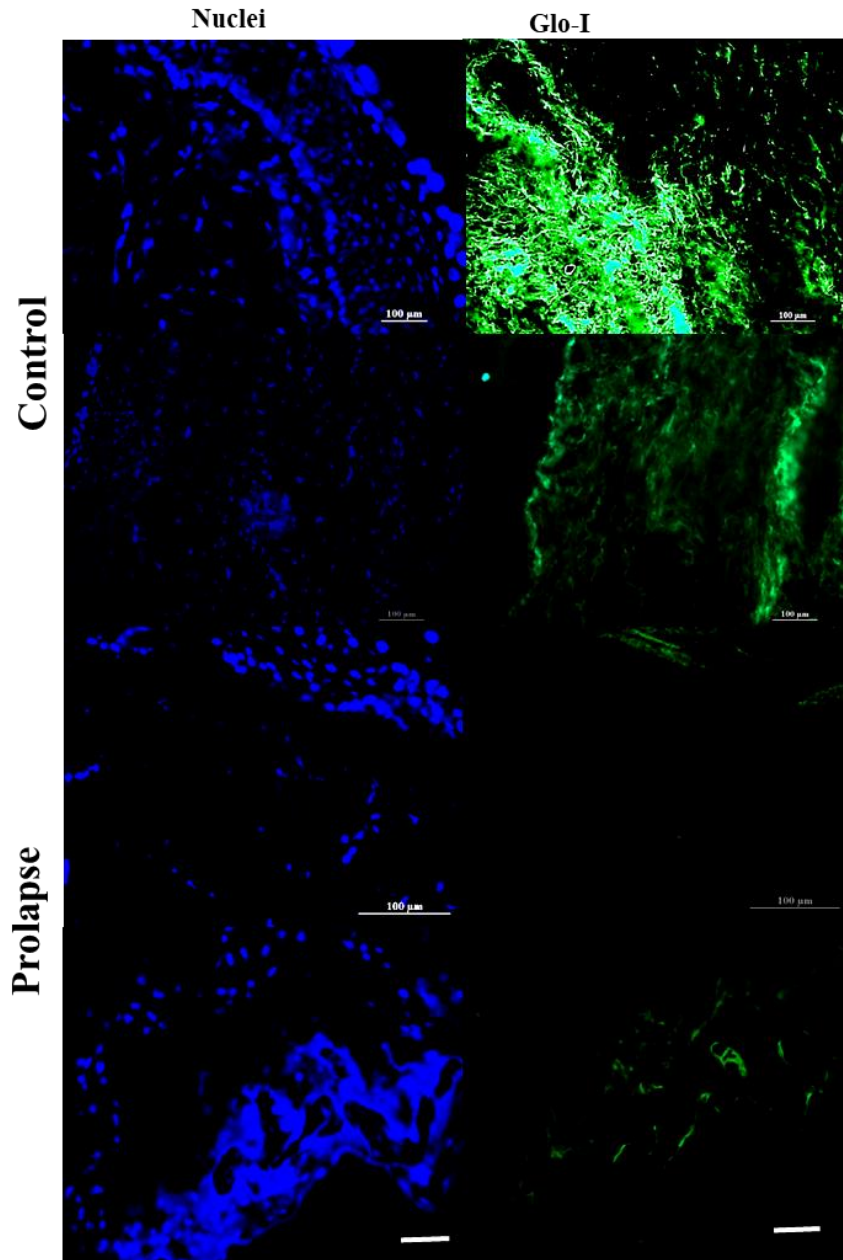


Figure 5.19: Representative images showing GLO-I expression (green) in age-matched prolapsed and control tissues. Sections counterstained by DAPI (Blue). Scale bar = 50 μm

5.5 DISCUSSION

5.5.1 INFLUENCE OF TISSUE STORAGE ON PENTOSIDINE CONTENT OF TISSUES

Various tissue components perform differently under storage conditions. DNA and protein, unlike RNA can be preserved in tissue stored at -80°C for up to 5 years and histologic staining of nuclei can confirm tissue integrity post-storage (247). Studies investigating storage conditions and tissue protein analysis have found that for tissues stored for up to 10 years at -80°C , reliable quantitative results can be obtained. For protein extracts, storage at 4°C for 24 h and repeated freeze-thaw cycles affected spot intensities in 2-D gels but did not alter quantification results. (248) This however is not the case with whole tissues which are better cryopreserved with cryoprotectants than stored at 4°C (249). Studies have also show that post-lyophilisation tissues can be stored at room temperature without significant changes to the protein activity after up to 2 weeks of storage (247). 0.2- 3 mm split thickness cadaveric skin obtained within 24 hours of death for surgical grafting can be stored for up to 7 days without loss of viability (250). The American association of tissue banks recommends that refrigerated skin and musculoskeletal human tissues can be stored for up to 14 and 5 days respectively, whereas frozen human tissue can be stored for up to 5 years at -40°C or less to maintain tissue viability. Previous studies have stored vaginal tissue prior to pentosidine content determination with no record of duration of storage or observed changes (41). An important factor in tissue cryopreservation is to avoid repeated free-thaw cycles (248). In the present study, no significant difference was noted in pentosidine, a glycated peptide content after 12 months of storage of full thickness vaginal tissues at -20°C .

We further studied the amounts of pentosidine in non-contiguous aspects of the same tissues and found no change in amounts of pentosidine. Another concurrent study in this project using rat vaginal and skin tissues (2.3.3) suggests that glycation is a generalized body process, affecting different tissues similarly. A study carried out using in rats suggest that the glycation process occurs in multiple tissues when exposed to high reducing sugar levels (239). The present study however for the first time notes similarity in glycation content from different aspects of the same prolapsed site, which is expected.

5.5.2 GLYCATION IN PROLAPSED VAGINAL TISSUES

Many studies have observed new crosslinks in prolapsed tissues (8). Early studies by Jackson et al suggested that prolapse may result from increasing trivalent non-enzymatic crosslinks gradually dominating slow turn-over proteins such as collagen and resulting in older, stiffer, connective tissue (23). In his study, higher amounts of pentosidine were present in prolapsed vaginal tissues. Since then similar findings have been noted in other studies (245). Divalent, enzymatic pyridinoline crosslinks may remain the same but the non-enzymatic advanced glycation of pelvic connective tissue collagen is notably higher in prolapsed tissues (8,251). In the present study, there were significantly higher amounts of pentosidine, a glycation compound in prolapsed tissues compared with controls, which is in keeping with the majority of published literature. These findings have raised the question of advanced glycations as a strong association and potential cause of prolapse. A recent study on the matrix produced by vaginal fibroblastic cells of prolapsed tissues noted that fibroblasts in prolapsed tissue produced matrix with stiffer collagen fibers (116). Advanced glycation leads to stiffening of tissues also noted in prolapsed tissues (201,208,252). There is thus a need to understand

glycation-induced mechanical property changes (tissue stiffening) as prelude to or following prolapse development.

5.5.3 GLYCATION AND AGE IN PROLAPSED VAGINAL TISSUES

Collagen has a slow turnover rate of about 15 years and this implies it is highly susceptible to glycation (253). As the predominant ECM protein, changes in collagen characteristics directly impact on connective tissue properties. With aging and an increase in tissue content of less soluble glycated collagen (23,254), there is reduced elasticity of tissues and increased stiffening. Formation of glycation products within tissues has been implicated in this process.

Pentosidine is regarded as a measure of chronological age as it is known to accumulate within tissues with increase in age (255). Pentosidine and other glycation products are implicated in age-related diseases including neurodegenerative diseases, osteoarthritis and hypertension. In a study carried out on human articular cartilage obtained from 11 and 19 year olds, pentosidine was found to increase linearly with age (192). Several other studies have noted an increase in pentosidine and other advanced glycation end products such as CML in skin with advancing age (55). The age-dependent accumulation of the glycation products within tissues may also be influenced by sun exposure (19).

Glycation accumulation in tissues result in altered mechanical properties and decreased elasticity (200,207). The Receptor of Advanced Glycation End Products (RAGE) mediate fibroblast apoptosis, a process directly proportional to amount of AGEs in the tissue (224,256). They are implicated in induction of inflammation within tissues and may influence the ECM remodeling (55). From studies on the pathophysiology of other glycation-induced or modulated diseases, they influence connective tissue properties through RAGE cascading or

instigating pro-inflammatory processes (57). In the present study, AGEs in the vaginal tissues were quantified and found to be higher in prolapsed tissues than in controls. This was consistent with other studies and suggests a potential role of AGEs in the pathophysiology of prolapse (8,23,245). We studied, for the first time, the increase in pentosidine with age in women with prolapse and compared this with age dependent increase in controls. A novel finding of a significant increase in vaginal tissue pentosidine in the transition between the 6th and 7th decade of life was noted. Although our results do not directly indicate that AGEs cause prolapse development, they strongly suggest that there is a significant difference in how AGEs accumulate in the tissues of women with prolapse as they age. We noted that the transition between the 6th and 7th decade was important in the accumulation of pentosidine and potentially prolapse development.

5.5.4 OESTROGEN INFLUENCE ON GLYOXALASE AND GLYCATION (INFLUENCE OF MENOPAUSE AND AGE)

No other studies have measured amounts of advanced glycation in human pelvic tissues and correlated this with oestrogen, its receptors, or a state with high oestrogen receptor expression such as pregnancy (237). In Chapter 4 (4.1.4.3 and 4.1.4.6), we studied glycation in the vaginal wall of pregnant and non-pregnant rats in relation to ER- α expression and found reduced glycation in pregnancy, which was also associated with higher ER- α expression. A study investigating cervical remodeling in mice in pregnancy noted a decrease in mature pyridinoline collagen crosslinks in relation to cervical wall softening (257). Oestrogen is a metabolic hormone and oestrogen treatment increases pelvic connective tissues' expression of newly synthesized collagen and reduces expression of older collagen (42). In a double-blind randomized trial of oestradiol valerate in women with pelvic dysfunction, oestrogen treatment

resulted in a decrease in advanced glycation end-products and increased immature crosslinks (41). Furthermore, oestrogen has been shown to improve the functionality (stretching) of fibroblasts, suggesting that it is a key player in the aetiology of prolapse (258).

GLO-I is a glutathione (GSH) dependent antioxidant enzyme system (69). GLO-I is part of the glyoxalase system present in the cytosol of cells (259). The glyoxalase systems catalyse the conversions of reactive acyclic α -oxoaldehydes into corresponding α -hydroxyacids. A dimeric Zn^{2+} metalloenzyme human glyoxalase I decreases concentrations of α -oxoaldehydes, important intermediates in the glycation reaction and this process is negatively affected by ageing (221,259). Its enzymatic sites bind methylglyoxal, glyoxal and other acyclic α -oxoaldehydes. It is thus useful in the detoxification of methylglyoxal, an intermediate glycolysis product, preventing its conversion to glycation products. Research has shown that GLO-I expression is influenced and regulated by oestrogen (218,219). The risk of prolapse is higher with age and menopause (12), when there is a decline in female hormones. In this study, there was reduced expression of antioxidant and oestrogen receptor- α in women with prolapse for age-matched samples. Noting that a previous study has also observed that oestrogen reduces glycation in prolapsed tissues (41), we propose that this effect occurs through the GLO-I system in pelvic tissues. We observed a significant increase in amounts of glycation at the transition between the 6th and 7th decade, suggesting significant changes in the metabolism at this point. Furthermore, we noted highest glycation in women with prolapse and menopause and elevated vaginal tissue glycation in premenopausal women with prolapse. Although this does not immediately answer the question of “cause or effect”, it sets a basis for understanding this. It is known that oestrogen decline precedes and leads to the state of menopause which is closely associated with ageing and changes within pelvic connective

tissues. This finding, on the role of oestrogen in advanced glycation accumulation can be better understood by studying the relationship between ageing and menopause. Finding out the “cause-effect” relationship between ageing and menopause would improve our understanding on the role of glycation in prolapse. Prolapse is commoner in menopausal and older women. The risk of prolapse development doubles with each decade of life (82). It is however unclear whether the development of prolapse is solely due to age or menopause alone. Studies have shown less advanced prolapse in premenopausal women with prolapse than in menopausal women with no hormone replacement (260). Since ageing in women cannot be separated from menopause, interplay between these factors may be pivotal to the understanding prolapse development.

5.5.5 THE ASSOCIATION OF GLYCATION IN PROLAPSED TISSUES TO HYPERTENSION, DM, CHOLESTEROL AND SMOKING

A study investigating women admitted over two and half years at Bulent Ecevit University hospital found the presence of hypertension and DM together to significantly increase the risk of prolapse (260). A observational study investigating 497 over a year and half found only the presence of hypertension significantly predictive of higher prolapse staging (260). Another case control study noted a significant association of hypertension but not DM with prolapse (261). In this study, we quantified amounts of pentosidine in the vaginal tissues of women with hypertension, diabetes, elevated cholesterol and current smokers in comparison to controls. We found that pentosidine is most elevated in women with both prolapse and hypertension; the glycation product being strongly associated with both diseases. Hypertension is a condition of elevated systemic blood pressure. For every increase in age there is stiffening of blood vessels and elevation of systemic blood pressure (262). Hypertension can be

associated with other diseases, in particular renal and metabolic disorders such as diabetes mellitus. Advanced glycation of blood vessels has been associated with stiffening of blood vessels and elevated blood pressure (263). Higher tissue glycation has been associated with higher skin autofluorescence and arterial stiffening (202). Hypertension and diabetes are described as a potential association or predictors of prolapse (260) but an exact understanding of the association between the diseases and prolapse has not previously been known. Although the finding in this study does not suggest a causal relationship between hypertension and prolapse, it reveals a potentially similar underlying pathology and strong association between both diseases. The same process, glycation, which is implicated in increased arterial stiffening and elevated blood pressure (264) may be implicated in prolapse pathogenesis. Since blood pressure is a routinely checked vital sign enabling early detection of hypertension, it may be a useful predictive tool of prolapse development and enable prevention.

Diabetic complications are associated with glycation of multiple proteins including fibrinogen, globulins and albumin and these result in many different advanced glycation products (201). The glycation process is involved in lens protein modification and cataract formation and immunoglobulin modification and immune suppression, making it a propagating agent in the systemic complications of diabetes (265). Pentosidine, a glycation product of collagen, is associated with accelerated blood vessel stiffening and atherosclerosis in patients with diabetes. Therefore our finding associating hypertension but not diabetes mellitus with glycation does not imply an exclusion of the glycation process in diabetes. Further studies to confirm elevation of other AGEs in prolapse tissues would be useful in understanding the relationship between diabetes and prolapse.

Few studies have investigated smoking association with prolapse. In a 5 year prospective observational study in women who had prolapse surgery, there was no significant risk of recurrence with smoking (89). Another retrospective cohort study involving 149, 554 women 20 years and above found that approximately half of those with prolapse were former or current smokers. Although cholesterol has not been previously studied in women with prolapse it is a component of metabolic syndrome, which also includes hypertension (81). In this study, amongst women with prolapse, pentosidine was higher in the presence of elevated cholesterol and smoking. Smoking and cholesterol are independent and associated risk factors for hypertension and type II DM, but no previous studies have associated smoking with elevated pentosidine levels in prolapsed vaginal wall. In the present study, this association is highlighted for the first time. Studies have shown higher chronic inflammatory cells in the anterior vaginal wall of women with prolapse (266). Smoking however promotes a systemic inflammatory state which can instigate glycation formation (81).

5.5.6 THE ASSOCIATION OF SEVERITY/ICIQVS AND PROLAPSE GRADE TO GLYCATION OF PROLAPSED TISSUES AND PROLAPSE TYPES

The ICIQVS questionnaire was developed to assess vaginal symptom and sexual matters' influence on quality of life in relation to prolapse from the patient's perspective (79,86). It was designed for routine clinical use, having being developed with the participation of 77 randomly selected women attending two urogynaecology clinics in the Southern part of England (86). The questionnaire was shown to be reliable and sensitive to change, with good validity and could identify changes in symptoms after surgical intervention (86). It comprises of a scoring system with nine symptom categories to reflect vaginal symptoms and three questions to investigate sexual life together with a quality of life score (80).

The development of the questionnaire is a reflection of the need for an objective and patient-based assessment of prolapse symptoms. Since its development, and the known association of glycation with prolapse, this study has for the first time made a comparison between glycation content and ICIQVS scoring showing a weak positive correlation. The pentosidine content of the tissues correlated similarly with symptom severity and prolapse grade. We observed a better relationship between ICIQVS scoring and the prolapse grade, with a steady increase in patient's perception of symptoms from grades 2 to 4, similar to findings noted during the development of the ICIQVS questionnaire in which symptom scoring decreased post-surgical intervention, which typically leads to elimination of prolapse or a lower grade of prolapse. These findings confirm that the questionnaire is a useful clinical tool in the management of women with prolapse and may further reflect underlying biochemical changes within the tissues.

5.6 CONCLUSION

Pentosidine increased with age in the entire population studied. This increase in age was significantly different between the 6th and 7th decade in the prolapse population. Hypertension was commoner amongst women with prolapse and it was associated with significantly more glycation. Although, incidence in the population studied was low, smoking and high cholesterol were commoner in women with prolapse and also associated with higher amounts of glycation. Parity was unrelated to pentosidine content of the tissues. Cystocele was the commonest type of prolapse in the group studied and associated with more glycation. There was however some relationship between pentosidine amounts, grade of predominant prolapse and symptom severity/effect of quality of life perception. Glycation was also a good predictor of prolapse stage and symptom severity. Parity and the percentage of vaginal deliveries was

not significantly different in prolapse and control groups. There was a low incidence of instrumental deliveries in the groups studied but this was slightly commoner in those with prolapse. There was a low incidence of HRT use in the groups studied.

Menopause, hypertension, smoking and cholesterol levels were strongly associated with glycation content of vaginal tissues in women with prolapse. Decreased ER- α was associated with decreased glyoxalase I and increased glycation in prolapsed tissues. These findings suggest that women with higher glycation content in their vaginal wall may be more predisposed to developing prolapse than others. Smoking, which also increases systemic oxidative stress is associated with increased glycation. The mechanism for glycation accumulation in prolapsed tissues may include an affectation of antioxidant-dependent inhibition of glycation related to decrease in ER- α expression. The presence of hypertension in association with glycation and prolapse is suggestive of similar underlying pathology for prolapse and systemic hypertension. Knowledge of this association can improve prolapse management by promoting screening, early detection and potentially, prevention.

6 CHAPTER 6: A STUDY OF THE STRUCTURAL AND
MECHANICAL PROPERTIES OF PROLAPSED VAGINAL
TISSUES

6.1 INTRODUCTION

Before the manifestation of diseases that are appreciable at the organ level, several cellular and tissue-level changes take place and accumulate to result in visible organ damage. This is particularly evident in chronic disorders (187). Therefore, the sole use of an organ level imaging technique to study the cause of prolapse can be likened to taking a snap shot of an individual in motion without knowing what triggered the motion. The problem is the absence of a clear understanding of what changes led to the overall disease picture - in this context prolapse.

Few studies however have investigated the structural and mechanical changes in prolapsed tissues (5). The mechanical testing of soft tissues has particularly posed a significant challenge for *in vitro* studies. Many of the readily available tests are destructive, and do not simulate the *in vivo* environment (12,13,164). This is clearly evident in some of the early studies that attempted to mechanically characterize prolapsed tissues. These have inconclusive results (5,13,164). Therefore the current understanding of prolapse aetiology has not been significantly improved over the past decade. There is thus a need for a non-destructive or minimally destructive *in vitro* test to mechanically assess prolapsed tissues.

Chapter 5 has revealed that DM and hypertension, ageing and the presence of biochemical markers of tissue ageing, advanced glycation end products have been consistently noted to be associated with prolapse (245). Glycation is known to affect tissue mechanical property but no study carried out in humans has demonstrated a correlation between glycation and the altered mechanics in pelvic tissues.

The vaginal wall directly supports the pelvic structures (1). Considering the central and supportive role of the vaginal wall (as described by Delancey's levels of support) in the pelvis (267) and being the tissue through which the pelvic organs prolapse, it is expected that a strong vaginal wall should be useful in limiting the prolapse of surrounding pelvic organs. There are however limited studies on vaginal tissue mechanical properties and a need for improvement on the current state of knowledge on female pelvic tissue biomechanics (118). Furthermore, the vaginal wall in prolapsed tissues is known to be stiffer with resulting higher modulus. Higher modulus is expected to result to superior mechanical properties but does not appear to be the case with prolapsed tissues.

6.2 AIM

The study aimed to investigate the structural and mechanical property of vaginal wall at nanoscopic, microscopic and macroscopic scales in prolapse and controls and also correlate mechanical properties with glycation content. The purpose was to assess vaginal tissues' structural properties with a view towards understating prolapse pathology.

6.3 METHODS

H&E, elastin, trichrome staining, picosirus red staining, neural immunostaining and hydroxyproline colorimetric assay have been used to determine structure and collagen composition of the prolapsed and control tissues. Detailed methods of AFM have been described in section 3.2.8. PFNMAFM as described in sections 3.4.2 has been used to analyse tissue ultrastructure, mapping of nanomechanical property. Ball indentation and OCE techniques described in sections 3.4.1 and 3.4.3 have been used to assess tissue level mechanics characteristics.

6.4 RESULTS

6.4.1 HISTOLOGY (STRUCTURE AND COMPOSITION AT THE MICRO SCALE)

6.4.1.1 H&E

Figure 6.1 shows that the distinct histological layers were present in the tissues. The connective tissue was more organized in control tissues and the transition between the epithelial and sub epithelial regions appeared more subtle than in prolapsed tissues. Vacant spaces were observed in LP and muscularis zones of many prolapsed tissue sections. Dense, hypercellular epithelial layers were also present with remarkably thickened (41) or shrunken (9) appearance in some tissues. There was a distinct or sharp transition between the epithelial and sub epithelial regions of prolapse tissues compared with controls.

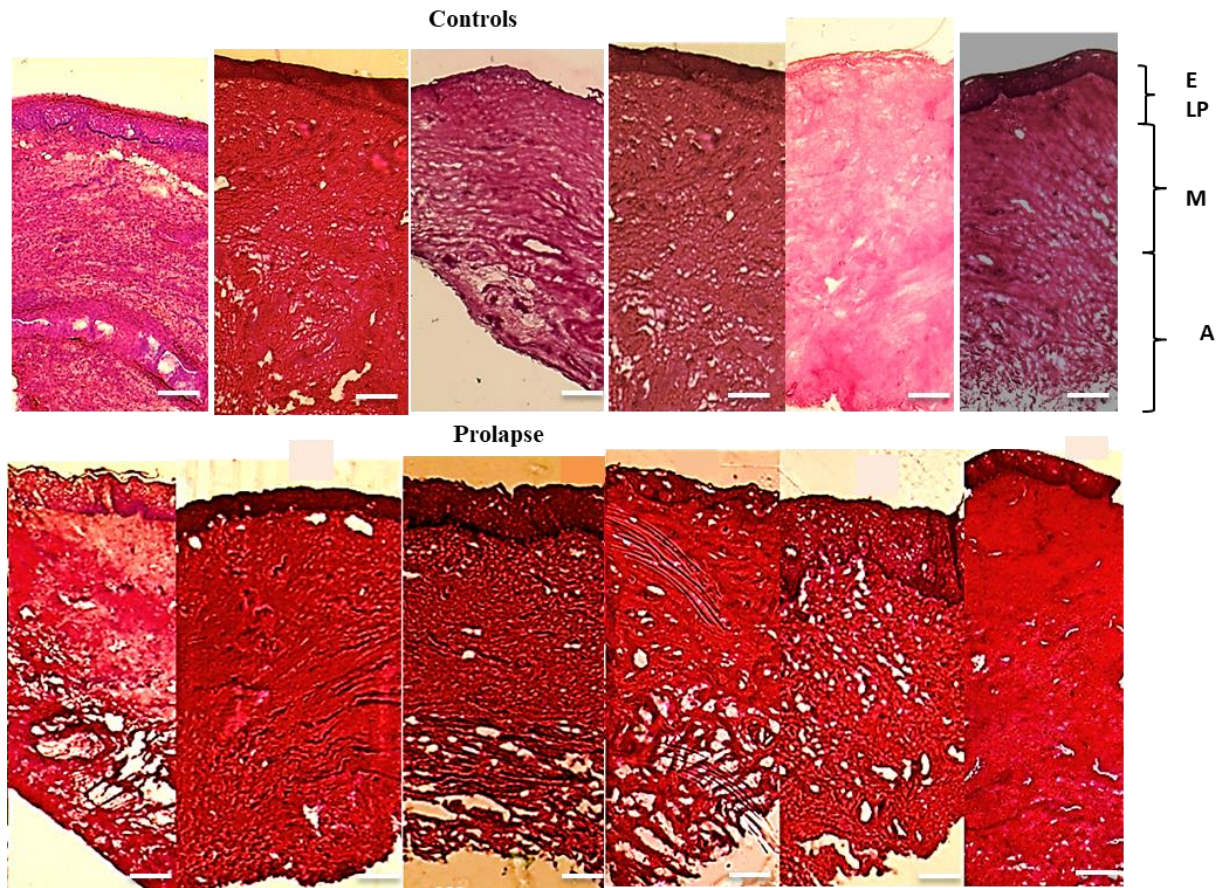


Figure 6.1: Low magnification images of representative control and prolapsed samples showing histological layers and structure overview of vaginal tissues. E=epithelial layer, LP=Lamina Propria, M=muscularis, A=Adventitia. Scale bars = 250 μ m

At higher magnifications (Figures 6.2) variable thickness of the epithelia was seen with more cellularity or apparent pigmentation in the basal lamina of prolapsed tissues. More dilated vessels were observed in the prolapsed tissues than in controls (Figure 6.2). The superficial stratified squamous layer of the epithelium observed in controls was thinned out (atrophied) or lost in the prolapsed tissues. Collagen densifications (observed as dark horizontal lines) were present in sub mucosa of some prolapsed tissues (figure 6.2). Spherical clusters of

macrophage-like cells were visible in the prolapsed tissues. The cell count per unit area of basal lamina was significantly higher in prolapsed tissues as shown in figure 6.3.

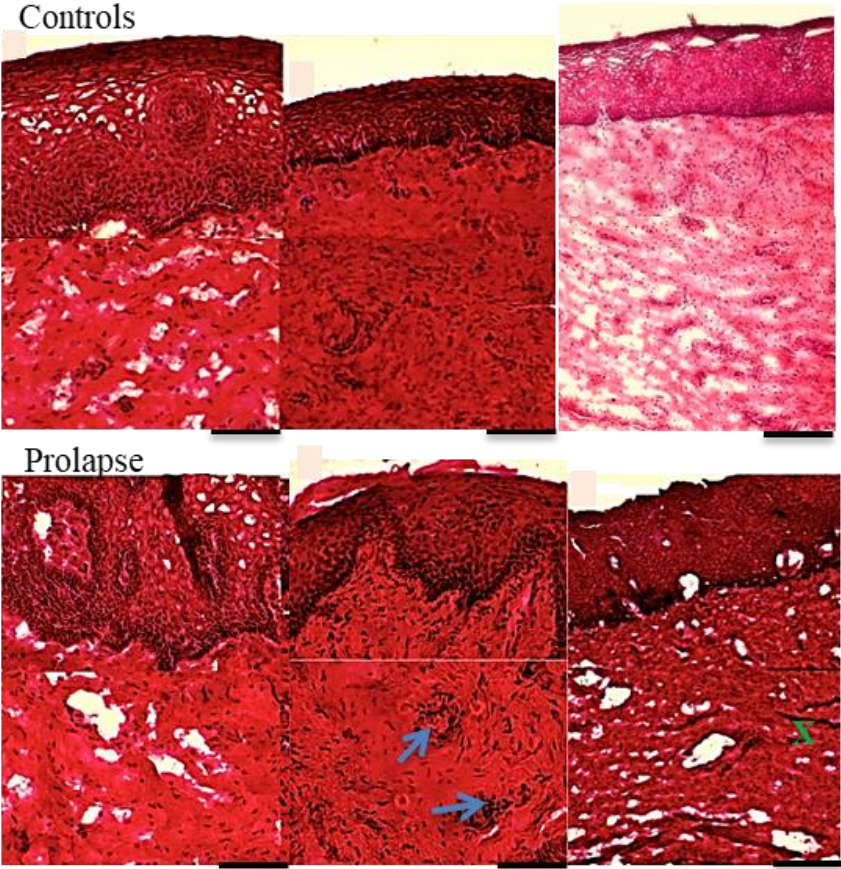


Figure 6.2: Higher magnification images of control and prolapsed tissues showing epithelial and sub-epithelial regions. Vacant spaces, areas of denser tissue (X) and cell clusters (blue arrow) visible in prolapsed tissues at LP and muscularis zones. (scale bars = 500 μ m)

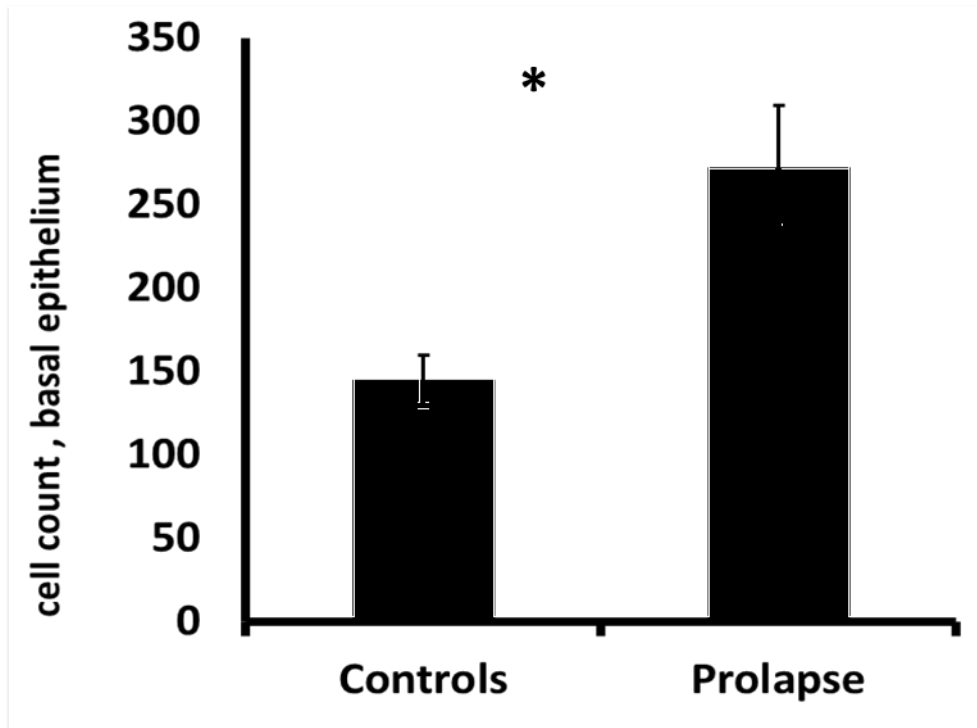


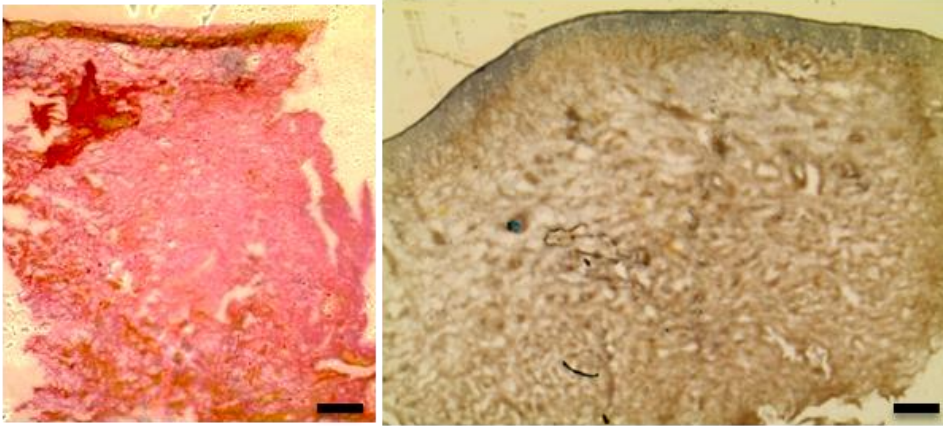
Figure 6.3: Cell count at basal lamina of age-matched control and prolapsed groups.

There is significantly higher cell count in prolapsed tissue sections, *P=0.02.

6.4.1.2 ELASTIN

There was expression of elastin in both prolapsed and control tissues (figures 6.4 and 6.5). Elastin was expressed in all 4 histological zones but mostly noted in the muscularis layers, epithelial zones and around blood vessels. The prolapses tissues appeared to stain for elastin more than controls.

Controls



Prolapse

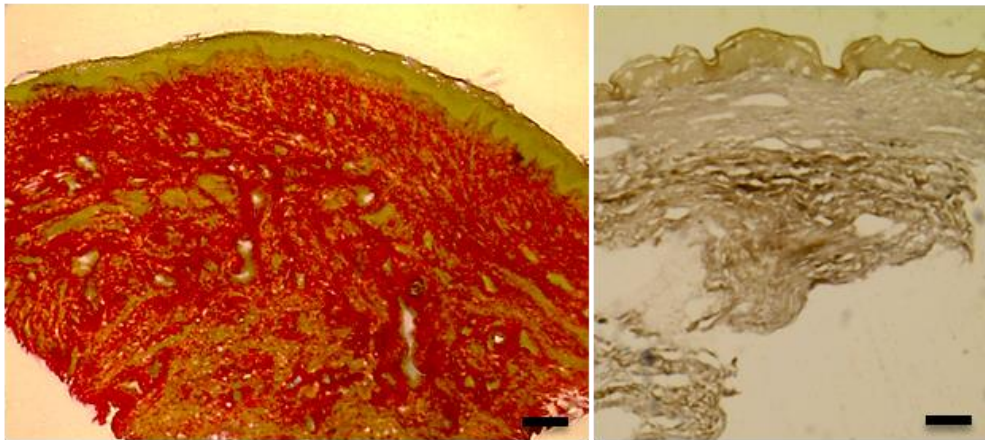


Figure 6.4: Elastin stain with and without counter-staining by Van Gieson's Solution in representative age-matched prolapsed and control tissues (scale bars: 250 μ m). Light brown and dark brown areas in counter-stained and non-counter-stained images represent elastin distribution within the tissues.

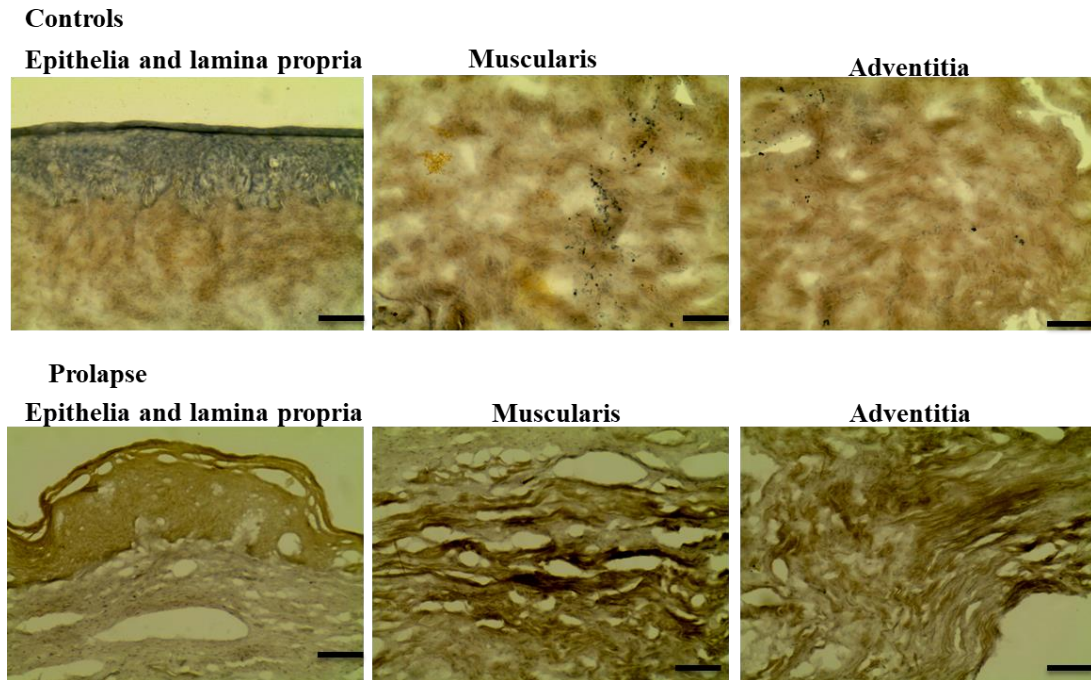


Figure 6.5: Higher magnifications of regions within tissue sections stained for elastin in representative age-matched prolapsed and control tissues (scale bars: 250 μ m)

6.4.1.3 NEURAL STAIN

Neural parts were observed within tissue cross sections as rounded dots with a few elongated processes, apparently cross sections of axons and dendritic processes (Figure 6.6). These were more expressed in the control tissues than in prolapsed vaginal tissues.

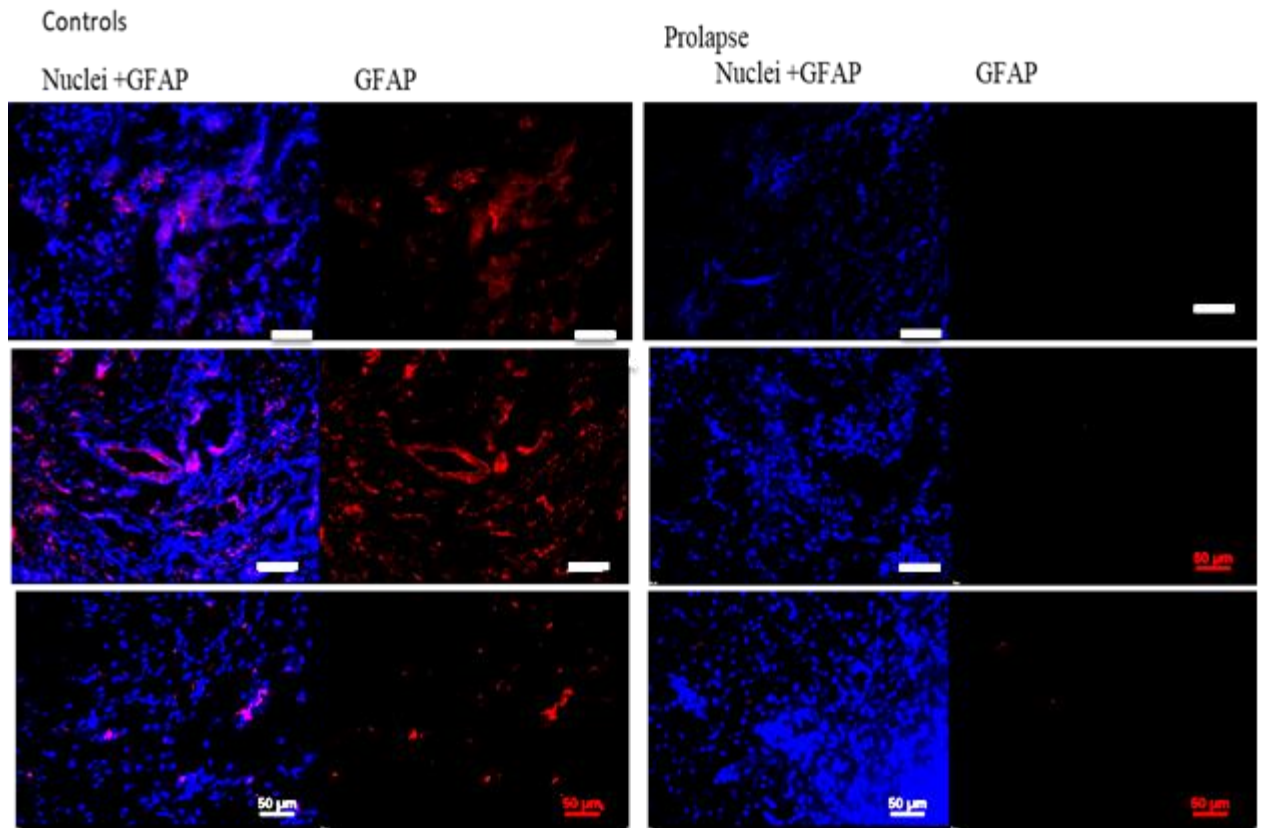


Figure 6.6: Neural stain (red) in representative age-matched prolapsed and control tissues. Images on the left (Nuclei+GFAP) show DAPI stained nuclei images (blue) superimposed on glial fibrillary acidic protein (GFAP) stained images (red). (scale bars: 50 μm)

6.4.1.4 TRICHROME STAINING

Differential staining (trichrome) of the tissue sections was carried out to observe different constituents of the layers of the tissues. Epithelial, LP and muscularis layers were visible in control and prolapsed tissues. A more extensive muscularis layer was evident in the control samples whereas prolapsed tissues appeared shrunken. A less organized structure was also evident in the prolapsed tissue in this region. Figure 6.7 shows that prolapsed tissues when

observed in full thickness contained more connective tissue (green) and less muscularis layer (red). Muscularis layers were filled with vacant spaces. Control tissues however contained more muscularis layer and less connective tissue as shown in Figures 6.7 and 6.8. The connective tissue layers of the prolapsed tissues are quite extensive through all tissue layers, particularly notable in the lower adventitial layers. At both low and higher magnification, Figure 6.8, the prolapsed tissue muscularis zone appeared infiltrating with connective tissue (blue), with remnants of muscular layer present.

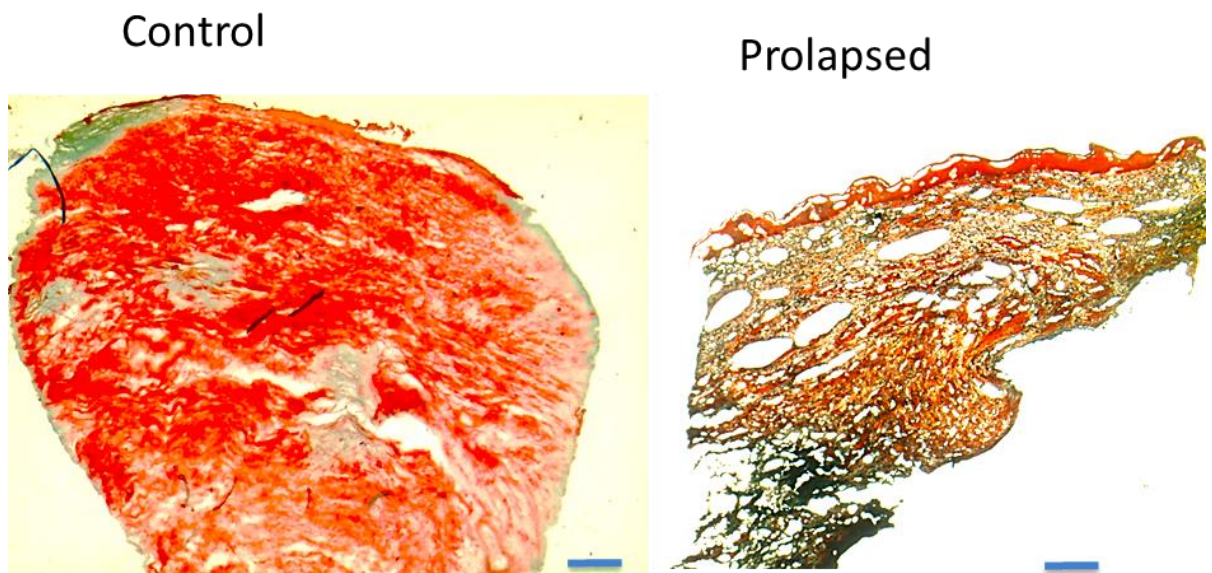


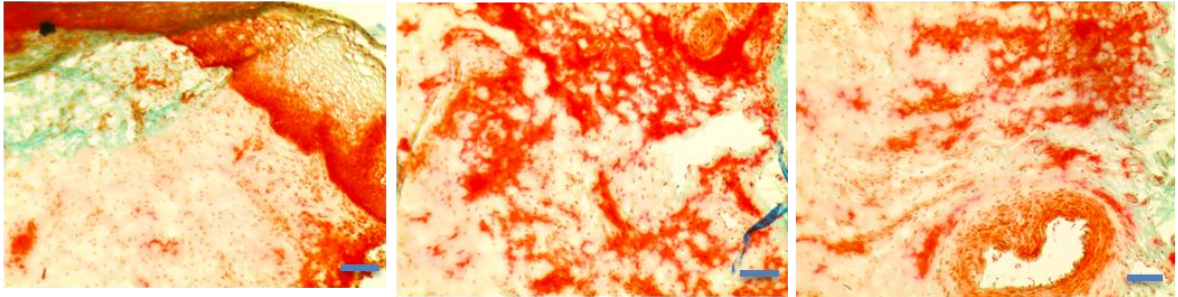
Figure 6.7: Trichrome stained images of representative age-matched control and prolapsed tissues. Blue/green= connective tissue, Red= muscular layer, orange= erythrocytes. Scale bars = 250 μ m. More intact and extensive muscular layer is notable in the control tissues compared to prolapsed tissues. The muscularis region in the prolapsed tissue appears patchy and infiltrated with connective tissue (green).

Controls

Epithelia and lamina propria

Muscularis

Adventitia



Prolapse

Epithelia and lamina propria

Muscularis

Adventitia

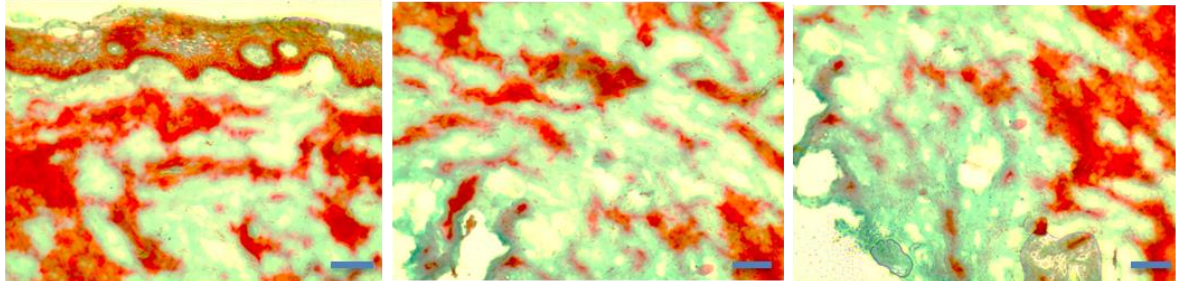


Figure 6.8: Higher magnifications of regions within tissue sections stained with trichrome stain in representative age-matched prolapsed and control tissues (scale bars: 250 μ m). Muscularis layer and erythrocytes are more notable in the control tissues compared to prolapsed tissues, which have extensive connective tissue also infiltrating the muscularis layer. Blue/green= connective tissue, Red= muscular layer, orange= erythrocytes. Scale bars = 250 μ m. More intact muscular layer is notable in the control tissues compared to prolapsed tissues.

6.4.2 COLLAGEN CONTENT

Further evaluation of the muscularis region was carried out using picosirus red staining aided by light and polarized microscopy (Figure 6.9). This was used to observe tissue structure for the presence of and rough estimate of amounts of collagen in the tissues. Collagen was present in both control and prolapsed vaginal tissue sections but denser collagen fiber groups were observed in the prolapsed tissues, which stained brighter red, more appreciable in the polarized images. Control tissues appeared to contain less collagen fibers but had a more organised architecture.

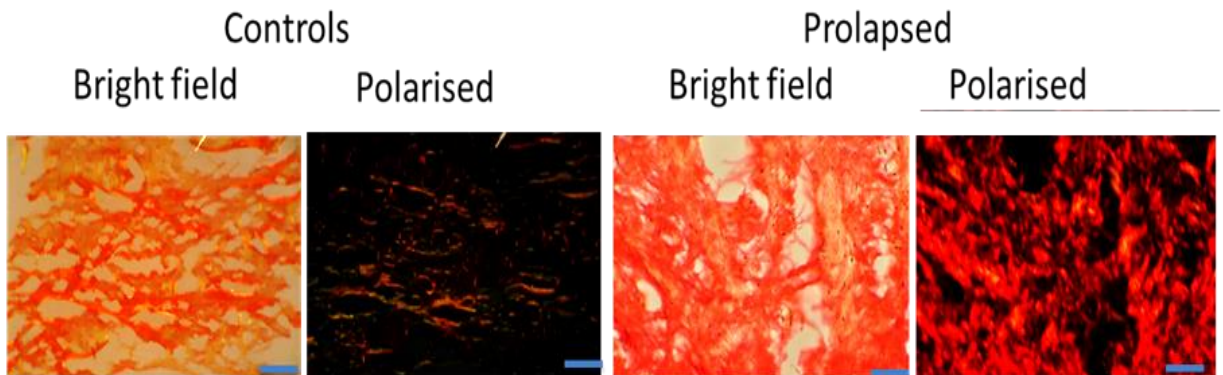


Figure 6.9: Representative picosirus red stained images of age-matched control and prolapsed vaginal wall sections. Bright field and polarized microscopy images are pictured. Scale bar= 100 μ m

Quantification of total collagen was carried out to confirm observations. The total collagen was significantly higher in prolapsed tissues compared with controls (Figure 6.10). Further comparison based on menopausal status revealed that the average amounts of collagen were highest in the prolapsed menopausal group with an average of 1.3 μ g/mg and lowest in the control menopausal group (0.86 μ g/mg tissue, Figure 6.11. Within the menopausal group this difference between vaginal tissue pentosidine content in prolapsed and control tissues was also

significant. The p values were 0.02 for comparison between prolapsed and control groups and 0.036 between control and prolapsed menopausal groups. In the entire study population, total collagen was higher in the menopausal group, $p=0.02$, figure 6.11

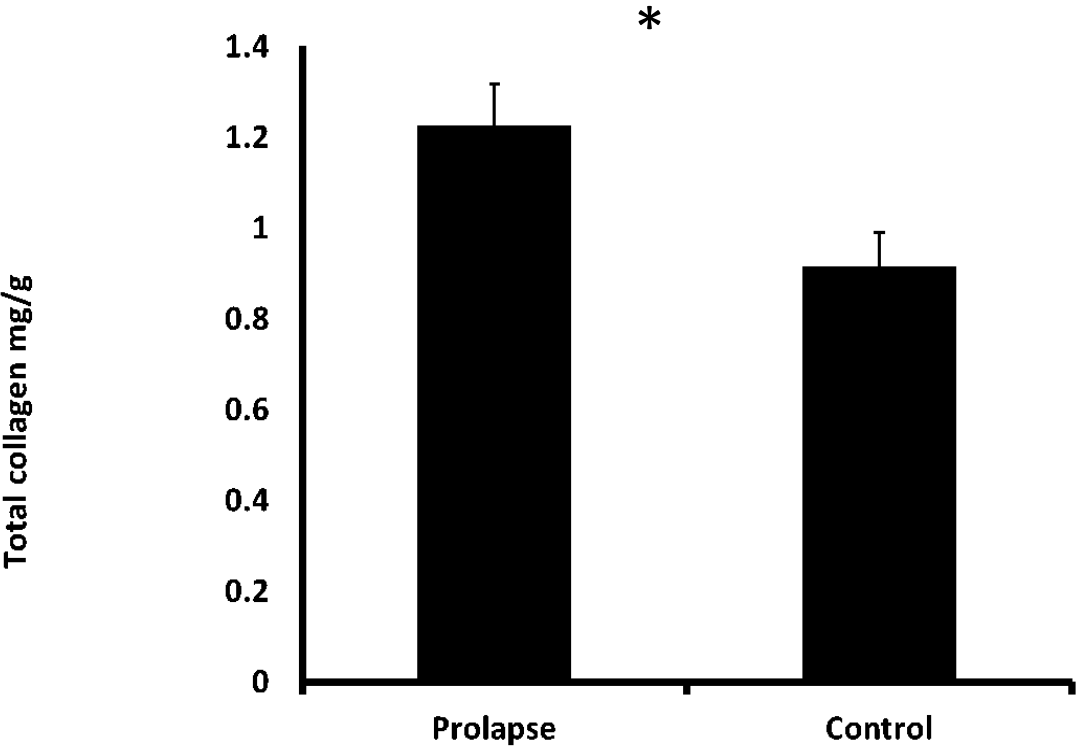


Figure 6.10: Total collagen in prolapsed and control vaginal tissues, $*p=0.02$ (n=8 per group).

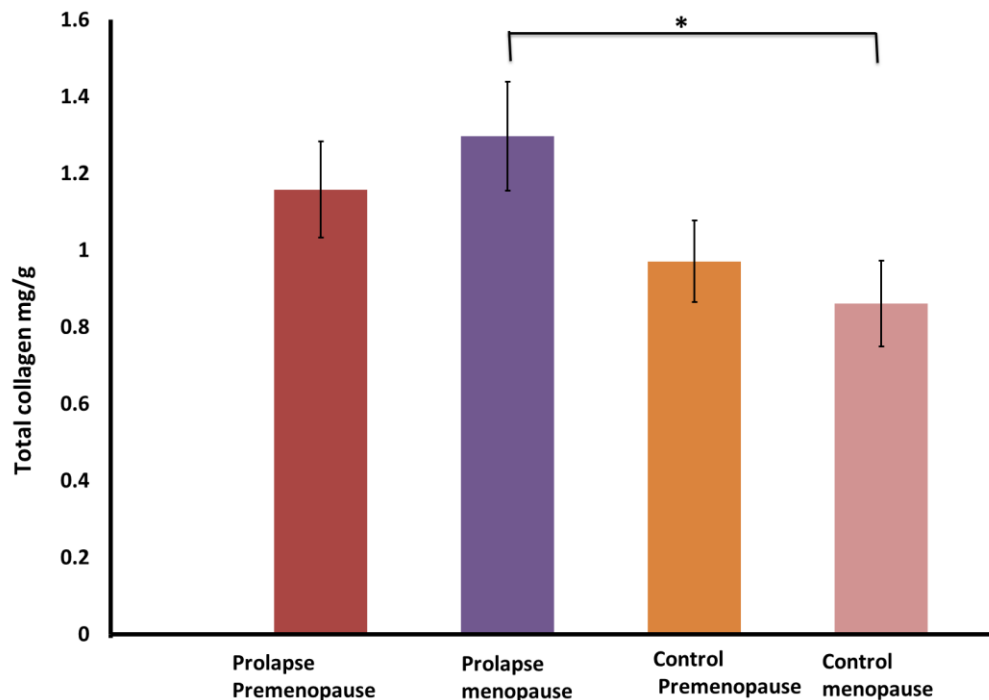


Figure 6.11: Total collagen in age-matched premenopausal and menopausal prolapsed and control vaginal tissues, *p=0.036 (n=4 per group)

6.4.3 AFM (STRUCTURE, MECHANICS AND ORGANIZATION AT THE MICRO AND NANO SCALE)

The structural and nanomechanical property of LP and adventitial layers of the tissues were investigated by measuring the collagen fibril modulus per unit area and observing fibril morphology using peakforce quantitative nanomechanical mapping (PF) AFM. Within a micron region there was varying range of modulus in both control and prolapsed tissues but average modulus of prolapsed tissues appeared higher than control tissues in the LP region as shown in figure 6.12. The same variable range of modulus was observed in adventitial regions

of prolapsed and control tissues, with higher upper modulus limit in control tissues (figure 6.13).

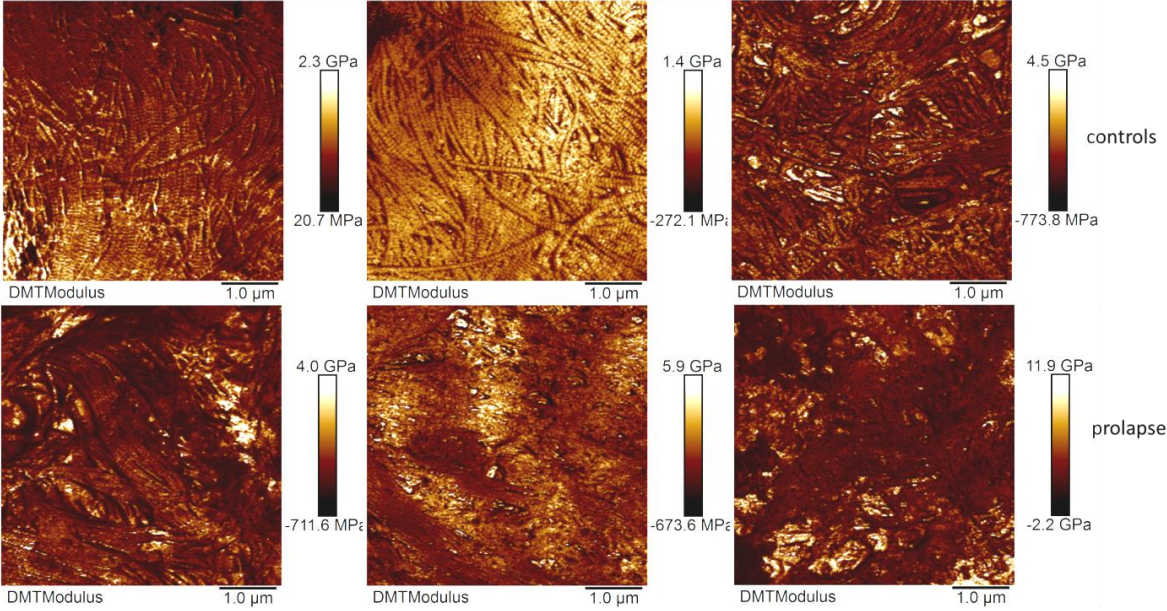


Figure 6.12: Representative PF AFM images of control and prolapsed vaginal tissue sections viewing collagen from 1x1 μm LP regions showing collagen modulus range.

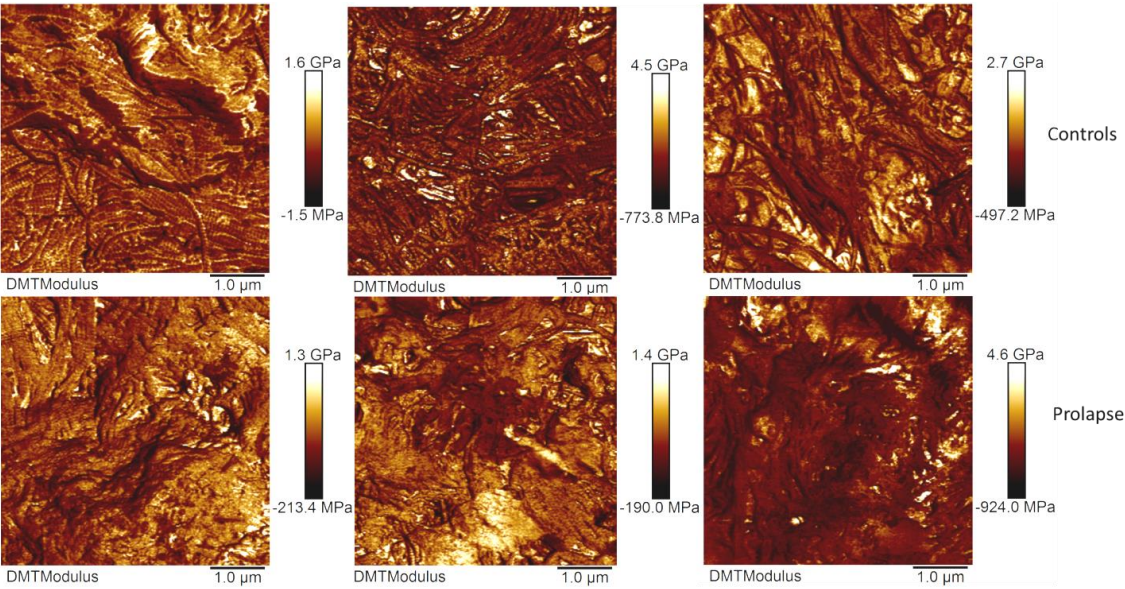


Figure 6.13: Representative PF AFM images of control and prolapsed vaginal tissue sections (Adventitial layers) viewing collagen from $5 \mu\text{m}^2$ areas showing collagen modulus range.

Objective measurement and quantification of the average modulus of 12 aged matched control and prolapsed tissues taking the average modulus of three images per tissue, revealed a significantly higher modulus in the prolapsed tissues at the LP regions compared with prolapsed tissues, $p=0.02$ (figure 6.14). In the prolapsed tissues, the LP was significantly stiffer than the adventitial region ($p=0.01$).

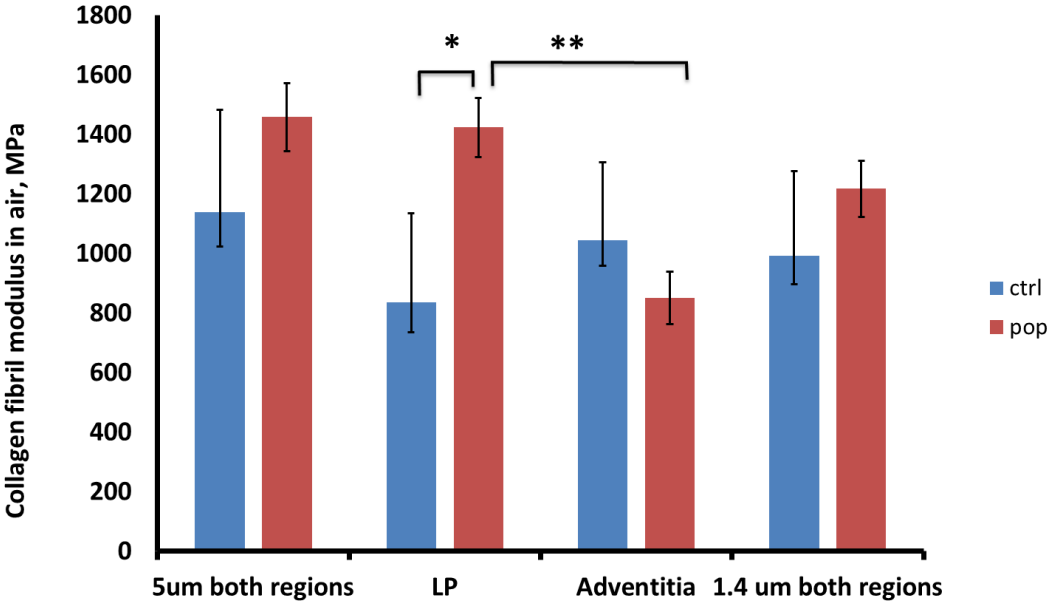


Figure 6.14: Average collagen fibril modulus extracted using the nanoscope analysis software from $1.4\mu\text{m}^2$ and $5.0 \mu\text{m}^2$ areas of LP and Adventitial zones of Control ($n=8$) and prolapsed ($n=8$) tissues. The average moduli (image raw mean) have been extracted from images represented in 6.4 and 6.5 using the nanoscope analysis software. Significant

differences are noted between LP zones of control and prolapsed tissues (p=0.02) and the different zones within the prolapsed tissues (p=0.01).

On the contrary, the prolapsed tissues adventitial layer had slightly lower average modulus than the controls but this was not significantly different. Within the control tissues there was more homogeneity as the modulus was not significantly different between the LP and adventitial layers (p=0.7). In the prolapsed tissue however there was a sharp reduction in modulus from the LP layer to the adventitial layer (figure 6.15). This difference was significant (p=0.01).

The 5 μm^2 images as shown in figure 6.15 enabled visualization of tissue architecture and an overview of the collagen bundles at the micron level. Control vaginal tissues showed the different ECM architecture at the micro scale. Clear bundling of collagen fibrils is visible in control samples with a somewhat “basket weave, appearance of the bundles. “Swirl-like” or twisting patterns were also noticed in some of the collagen bundles of control samples. There is intertwining or parallel arrangement of these bundles with occasional gaps in the control samples but in the prolapse tissues a complete loss of bundling is evident in some samples while others have very few bundles. A webbed or net appearance is seen in some of the prolapsed tissues. Some amorphous compound, likely glycosaminoglycan, is visible over fibrils.

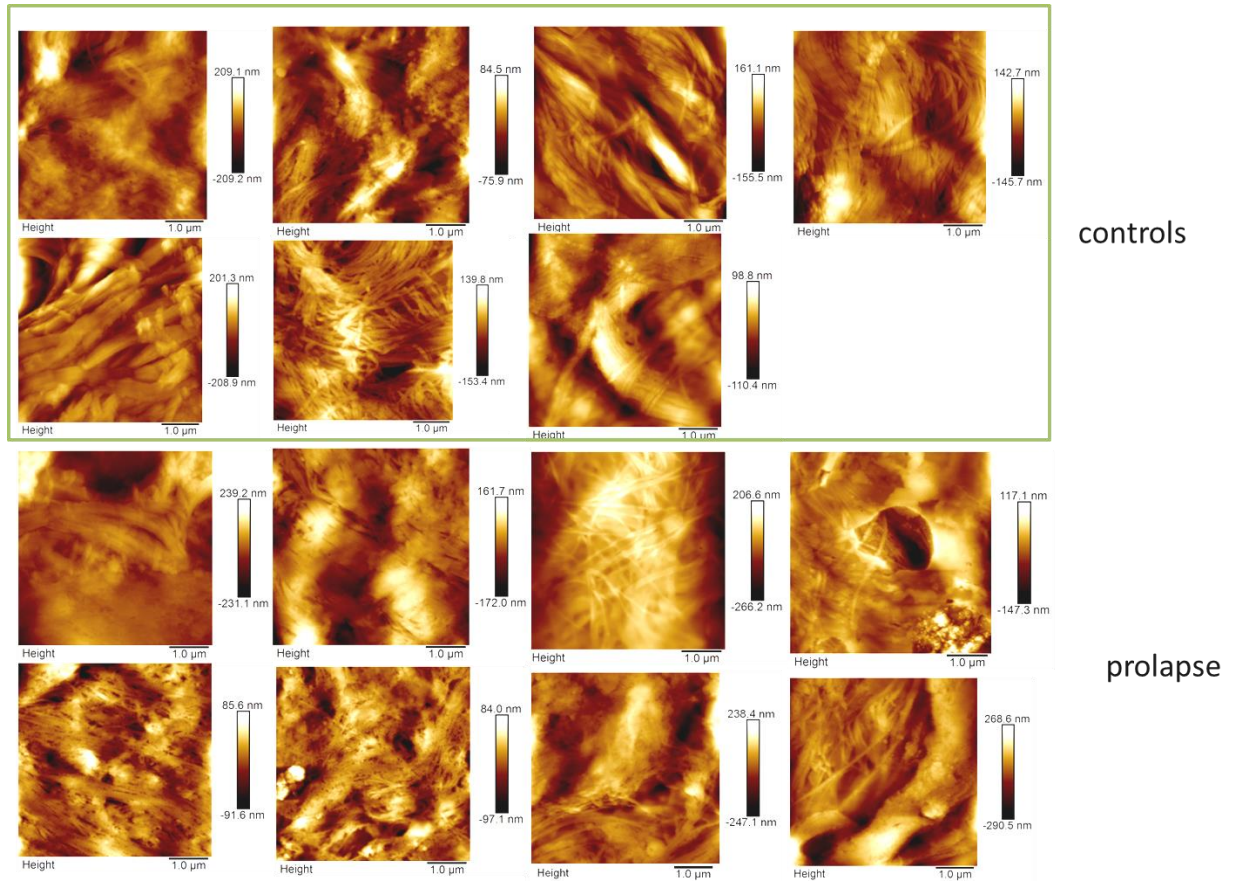


Figure 6.15: Representative AFM height images showing collagen fibril organization in 5 μm^2 areas of prolapsed and control tissues within the LP region.

Further visualization of the arrangement of collagen fibrils within the bundles in the LP region was observed in the 1.4 μm^2 images as shown in figure 6.16. Collagen fibrils displayed the characteristic D period banding pattern in this region. Fibrils in the control tissues appeared more compacted and aligned with a predominant axis while fibrils in the prolapsed tissues were disorganized with most exhibiting large spaces between fibrils. These changes were more appreciable in 3-D images as shown in figure 6.17.

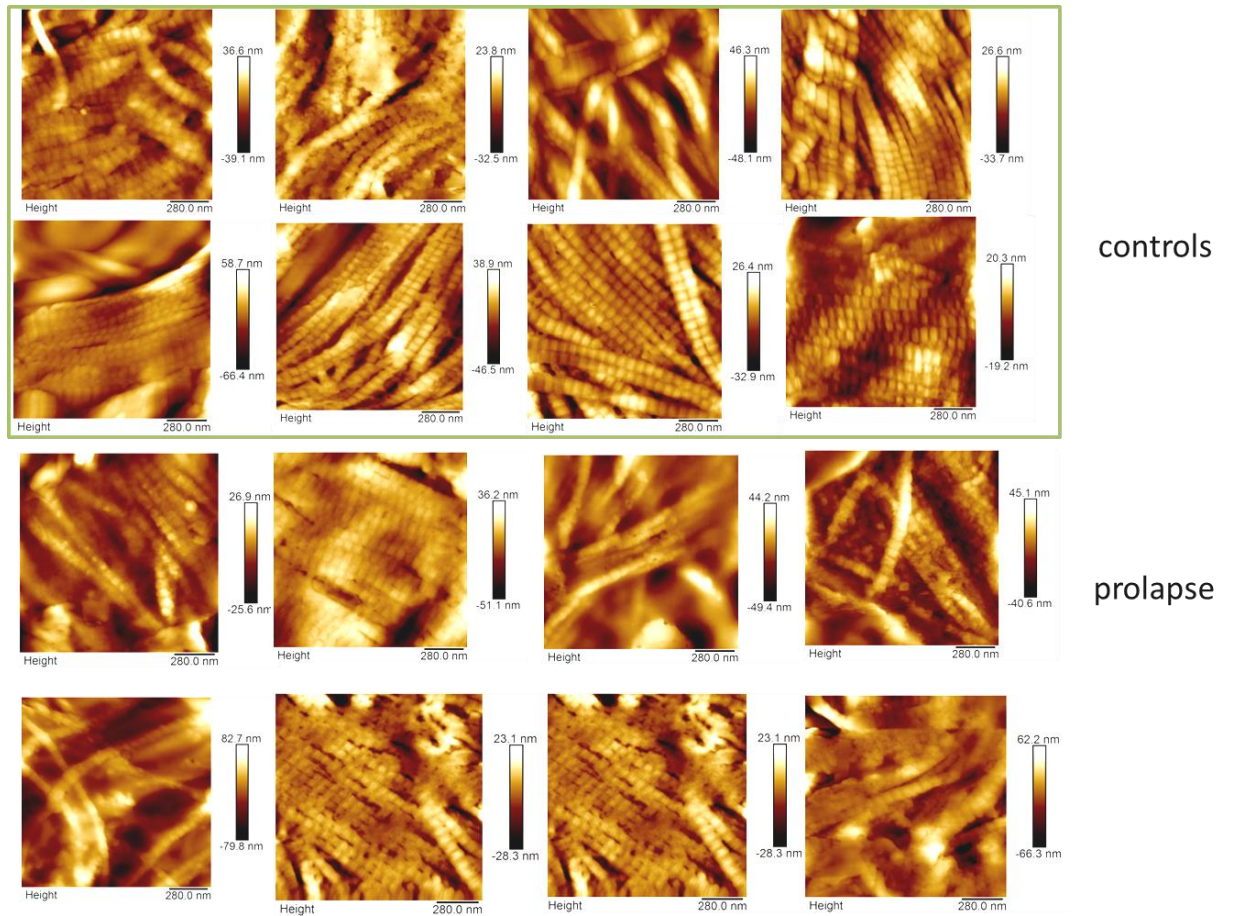


Figure 6.16: Representative AFM images showing collagen fibril organization in $1.4 \mu\text{m}^2$ areas of prolapsed and control tissues within the LP region.

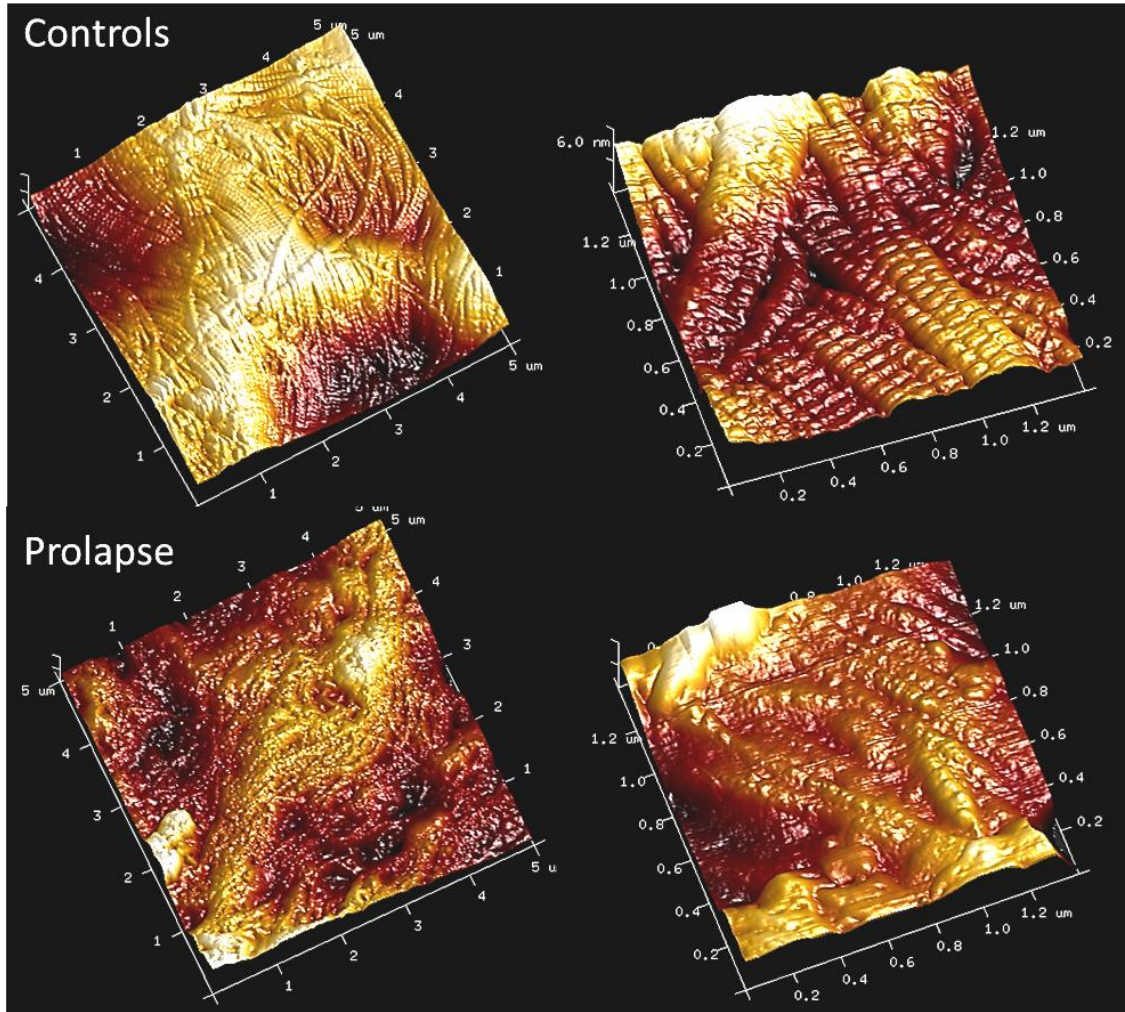


Figure 6.17: Representative 3-D AFM images illustrating ultrastructural organisation within the LP region of prolapsed and control tissues. $5 \mu\text{m}^2$ and $1.4 \mu\text{m}^2$ images are shown on the left and right respectively. The collagen bundling and compaction is more evident in control samples but appears lost in the prolapsed tissues.

In the adventitial region, Figure 6.18, the same bundling of collagen fibers and ‘basket weave’ appearance was noted in the controls samples. In prolapsed tissues, residual bundles were observable but disorganization was more evident and some tissues had a webbed appearance. The characteristic D-banding was also present in collagen fibrils in the region, enabling

identification visible in the $5 \mu\text{m}^2$ and $1.4 \mu\text{m}^2$ images (Figures 6.18 and 6.19). Within groups of collagen, alignment was preserved in the control samples but this was lost in the prolapsed tissues. Some prolapsed tissues had fibrils crossing through others in a disorderly manner. 3-D images (figure 6.20) further confirmed observations. The control tissues were organised into clear bundles which was not appreciable in the prolapsed tissues.

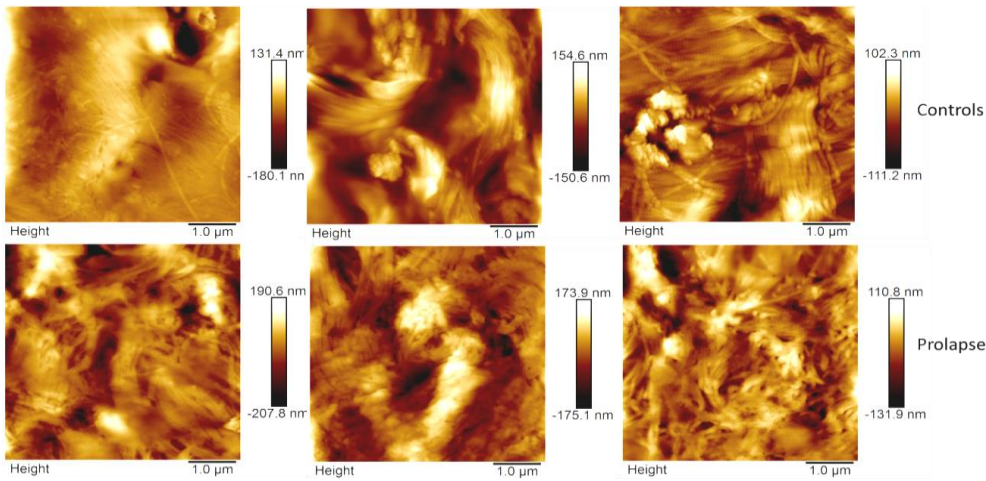


Figure 6.18: Representative AFM height images showing collagen fibril organization in $5.0 \mu\text{m}^2$ areas of prolapsed and control tissues' adventitial region.

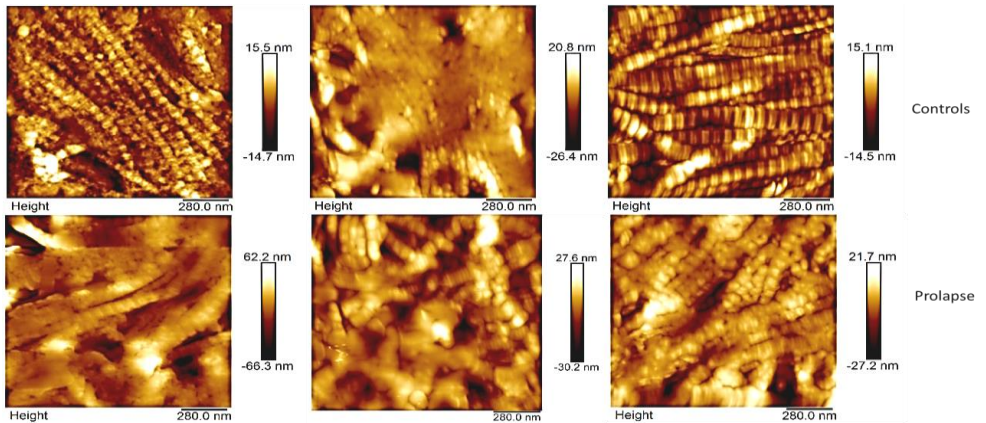


Figure 6.19: Representative AFM height images showing collagen fibril organization in $1.4 \mu\text{m}^2$ areas of prolapsed and control tissues in the adventitial regions.

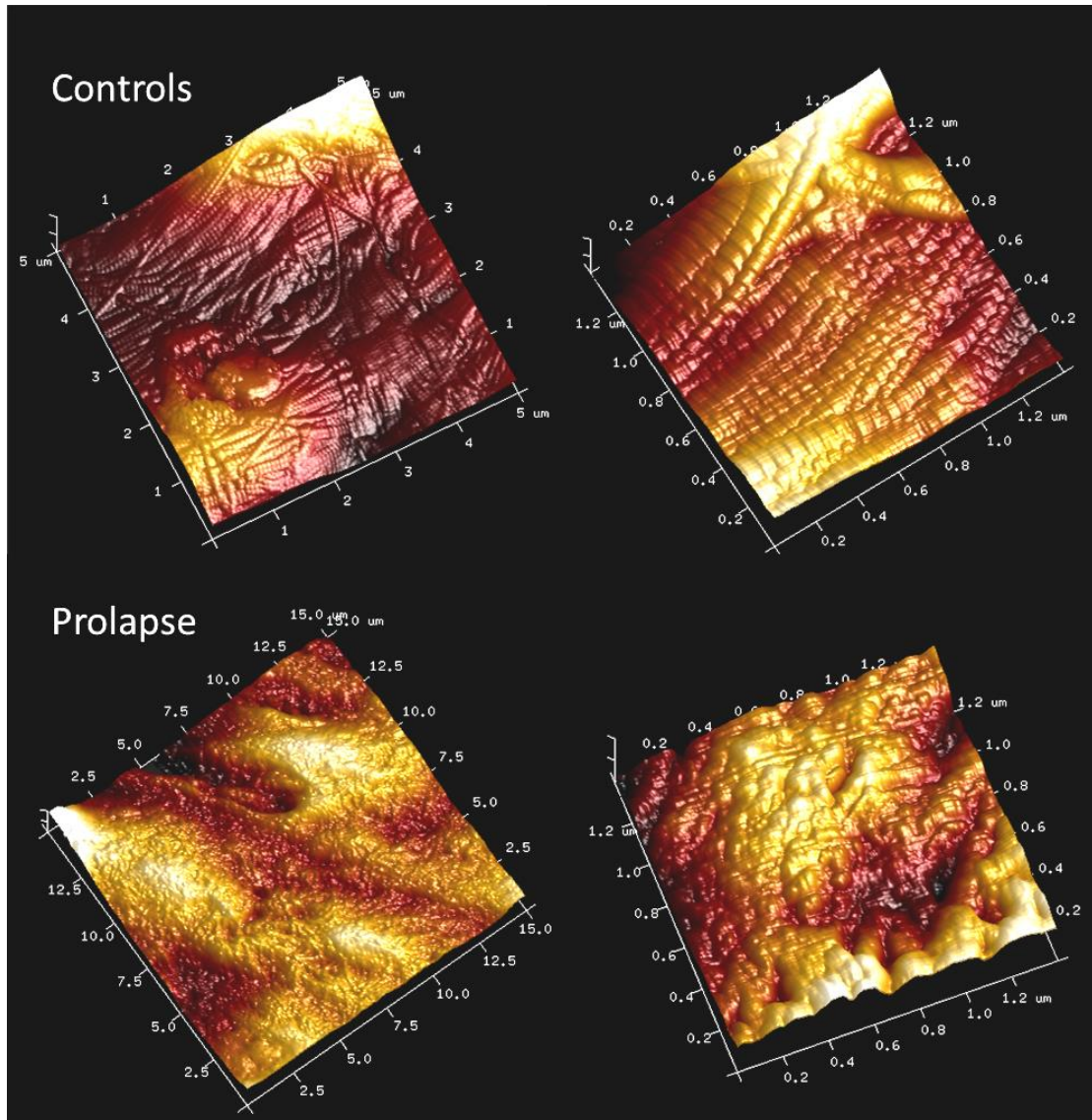


Figure 6.20: Representative 3-D AFM images illustrating ultrastructural organisation within the adventitial region of prolapsed and control tissues. $5 \mu\text{m}^2$ and $1.4 \mu\text{m}^2$ images are shown on the left and right respectively. More obvious bundling of collagen fibrils is seen in the control samples but the prolapsed tissue exhibits a completely disorganized architecture.

Further quantification of the sizes of gaps between the collagen fibrils revealed wider average gap in prolapsed tissues compared to controls (figure 6.21). There was more variability in the sizes of gaps between the fibrils within prolapsed tissues with a range of 12 nm unlike in controls, which had more uniformly sized gaps within a range of 1 nm. The standard errors of mean were 4.5 and 0.5 respectively. At the micron level, the gap between collagen fibrils in prolapsed vaginal wall was five times that of normal vaginal tissue, Figure 6.21. There was minimal variability in collagen fibril size in both control and prolapsed tissues (figure 6.22). The average collagen fibril diameter in prolapsed tissues was also significantly smaller than for controls (p=0.00).

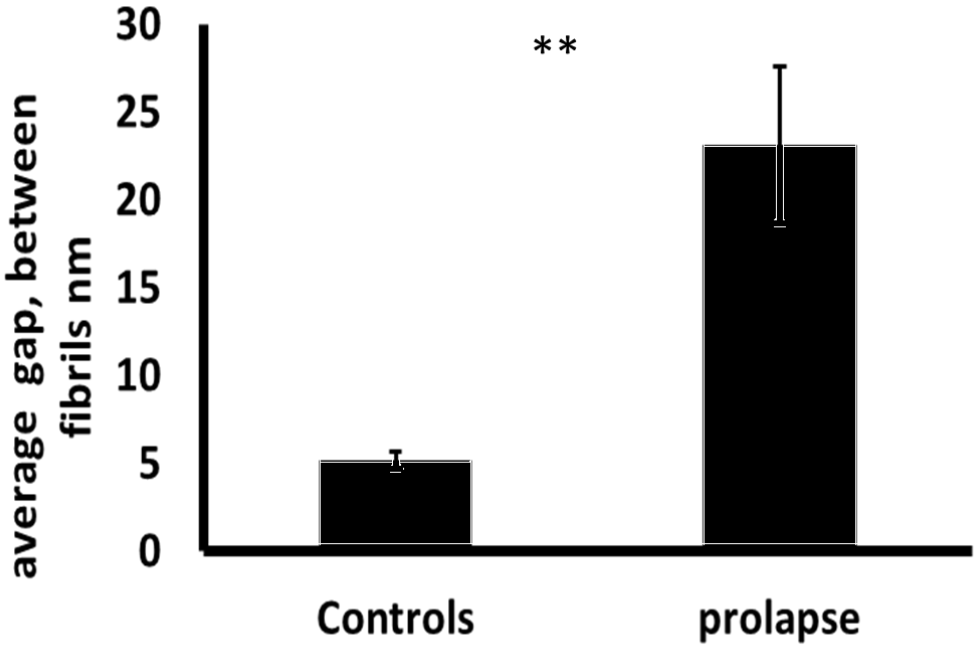


Figure 6.21: Average gap between collagen fibrils in $1.4 \mu\text{m}^2$ areas of control and prolapsed vaginal tissue sections (n=8 per group). The difference is statistically significant (p=0.005)**

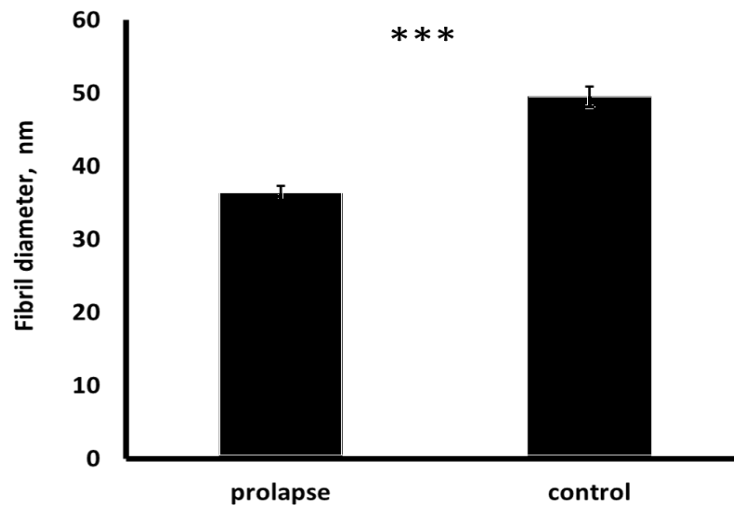


Figure 6.22: Average collagen fibril diameter in $1.4 \mu\text{m}^2$ areas of prolapsed and control vaginal tissues (n=8 per group with each n number representing the average of diameters of all visible collagen fibers in representative prolapse and control images). Significant difference is noted between both groups (p=0.00).**

There was reasonable distribution of collagen fibrils within each measured area but the number of fibrils was less in the prolapsed tissues (figure 6.23). There were significantly more collagen fibrils in the same area of control vaginal tissues. The alignment of collagen fibrils to the dominant axis of the tissues was significantly better in control tissues (figure 6.24). There was more deviation or increased angulation of collagen fibrils in the prolapsed tissues away from the predominant axis.

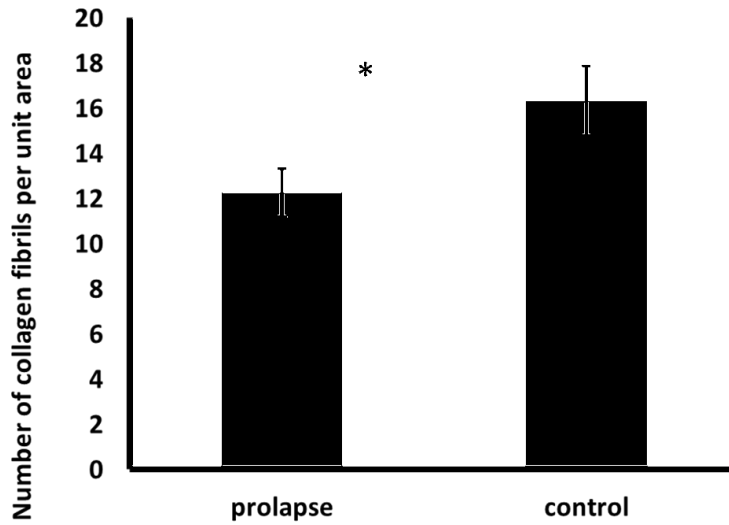


Figure 6.23: Collagen fibril count in $1.0 \mu\text{m}^2$ per unit area in prolapsed and control samples, * $p=0.038$. $n=8$ per group)

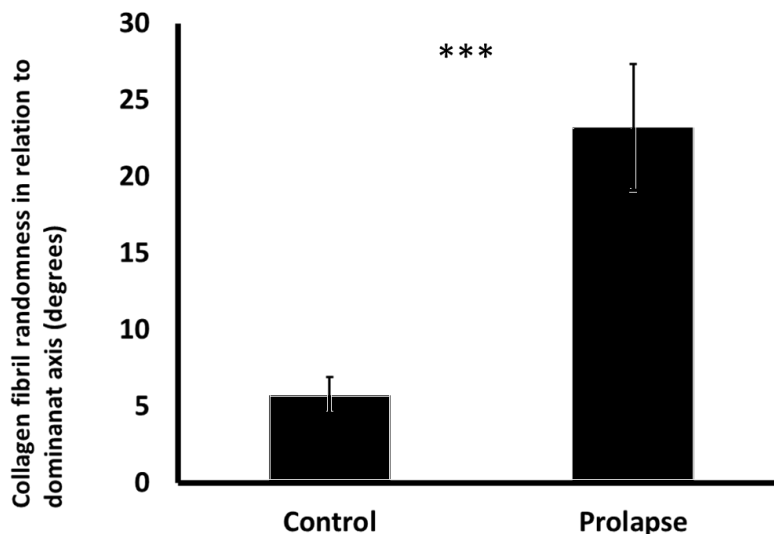


Figure 6.24: Collagen fibril alignment in control and prolapsed tissues ($n=8$ per group, with each n number representing average alignment of all visible collagen fibrils in representative images of each sample). Average alignment of each fibril to dominant axis in the LP and adventitial regions ($p=0.00$).**

6.4.4 RELATIONSHIP BETWEEN GLYCATION AND PROLAPSED TISSUE MECHANICS (FROM BALL INDENTATION DATA)

6.4.4.1 Thickness of tissues using slicing methods 1 and 2

The average thickness of tissues obtained using slicing methods 1 and 2 differed significantly as depicted in figure 6.25. The average size of tissues using methods 1 and 2 were 1.8mm and 0.7mm respectively. Inter specimen variability was minimal using both techniques (standard errors of means of 0.07 and 0.04 respectively).

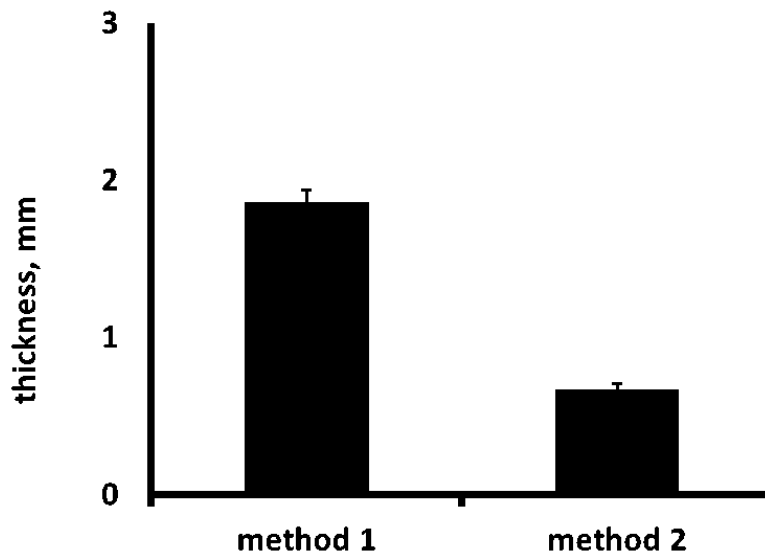


Figure 6.25: Thickness of tissues obtained using the two methods of slicing (n=10 and 9 respectively).

6.4.4.2 Modulus and Creep results using methods 1 and 2

The modulus and creep of prolapsed samples have been measured by ball indentation method. The modulus values were within 43-110 kPa region and 24 creep were in 0.4-1.2 mm region by method 1, and 3-120 kPa and 0.1-1.5 mm region by method 2. It was impossible to

undertake a comparative study (with control samples) using the ball indentation measurement because the control sample sizes were approximately 4 mm² in dimension and as a result could not be mounted on the ball indentation ring. However, plots of the creep or modulus against associated pentosidine value in the samples, revealed a consistent relationship between pentosidine content of the tissues, the tissues' creep and modulus using both slicing techniques. This has been presented in Figures 6.26 and 6.27. From both experiments, an inverse correlation is noted between pentosidine content of the tissues and creep, while a direct relationship exists with tissue modulus as expected. The strength of correlation was however stronger in method 1 ($r^2 = 0.8$) than in method 2 ($r^2 = 0.7$).

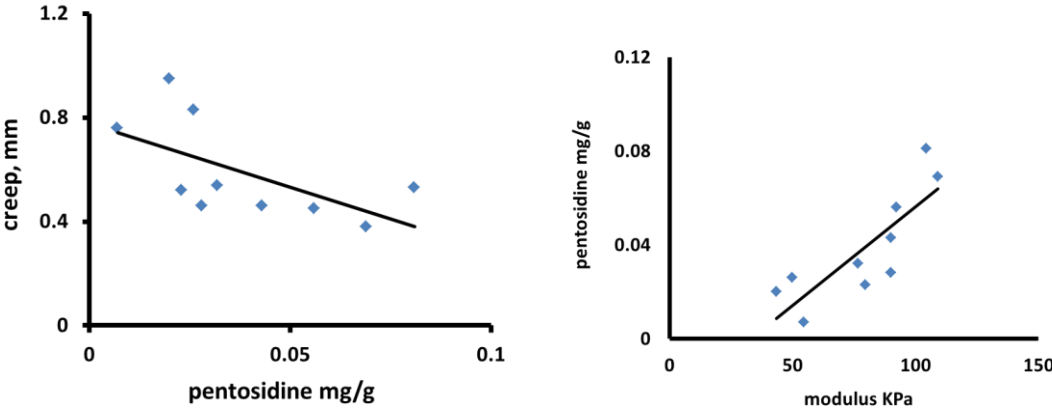


Figure 6.26: Correlation of creep and modulus of adventitial layer of prolapsed tissues sliced using method 1 with pentosidine content. ($r^2=0.8$)

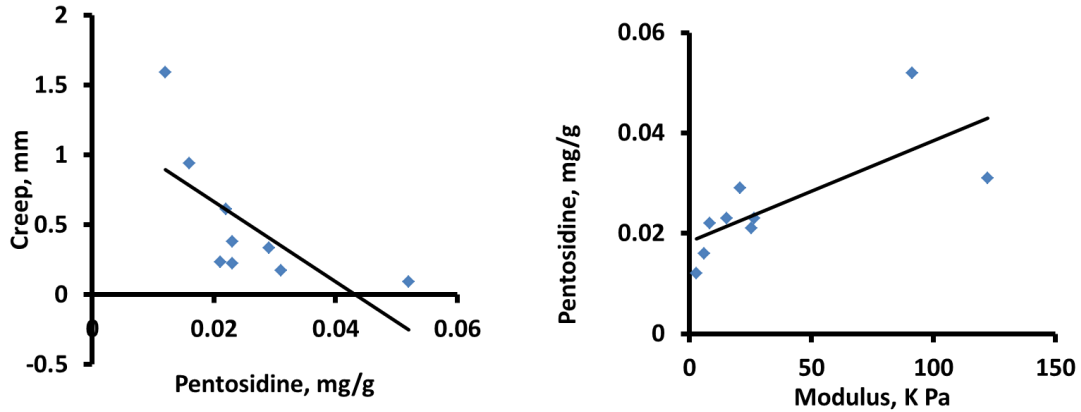


Figure 6.27: Correlation of creep and modulus of adventitial layer of prolapsed tissues sliced using method 2 with their pentosidine content. ($r^2=0.8$)

6.4.5 OCE (MECHANICS AT TISSUE SCALE)

To obtain mechanical property differences in the prolapse and control samples, OCE measurements were carried out on whole tissue segments in air and embedded in the agar phantom for reference. The sample size for OCE measurement was around 4.0 mm^3 . Images of specimen set up were obtained as shown in figure 6.28 for an understanding of sample orientation during data interpretation.

There was noticeably more uniform modulus distribution within control tissues, seen in figure 6.29. From the pictographic scale, modulus appeared to exist between the 200-350 relative modulus range through the different layers of the tissues. Prolapse tissues show ‘demarcation’ between layers with highest modulus in epithelial and LP zone. The first four prolapse samples in Figure 6.29 show weaker muscularis (middle zone/darker blue) regions.

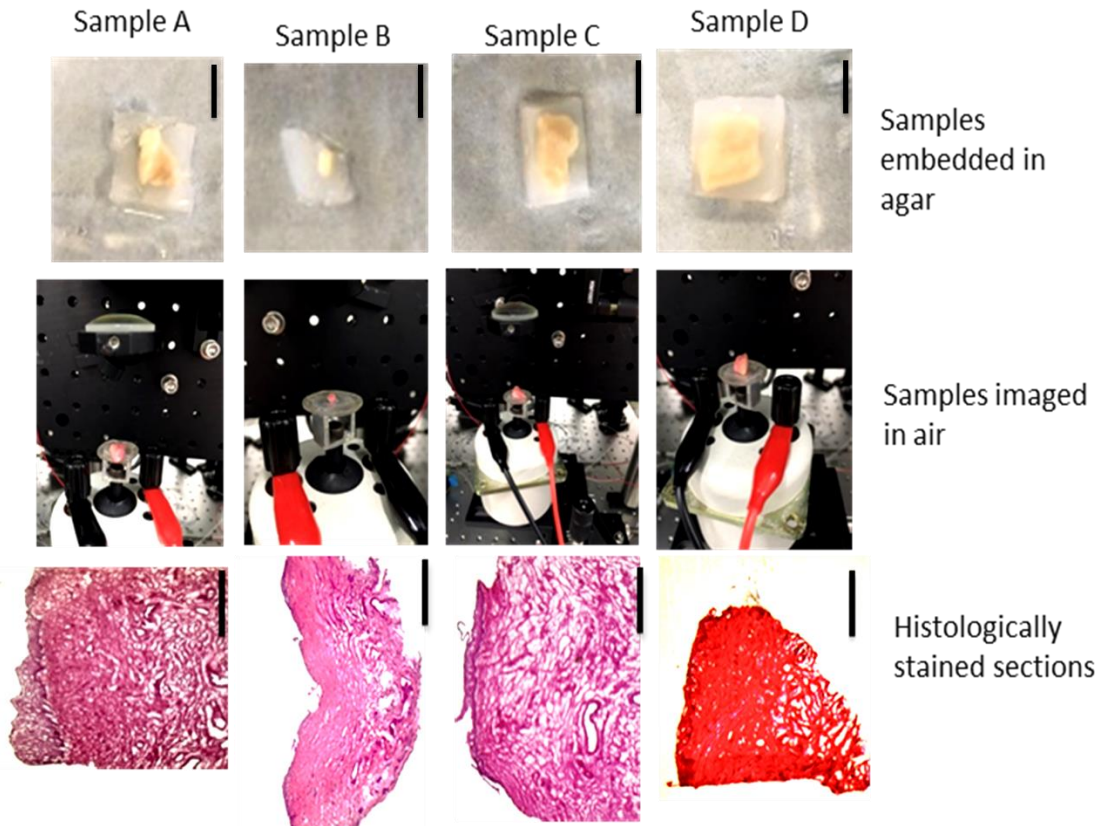


Figure 6.28: OCE tissue set up with and without embedding in agar for image acquisition. The orientation of each sample tested (LP and adventitial zones) was noted to ensure accurate data interpretation. Scale bars for samples embedded in agar = 4000 μm ; Scale bars for H & E stained images = 1000 μm

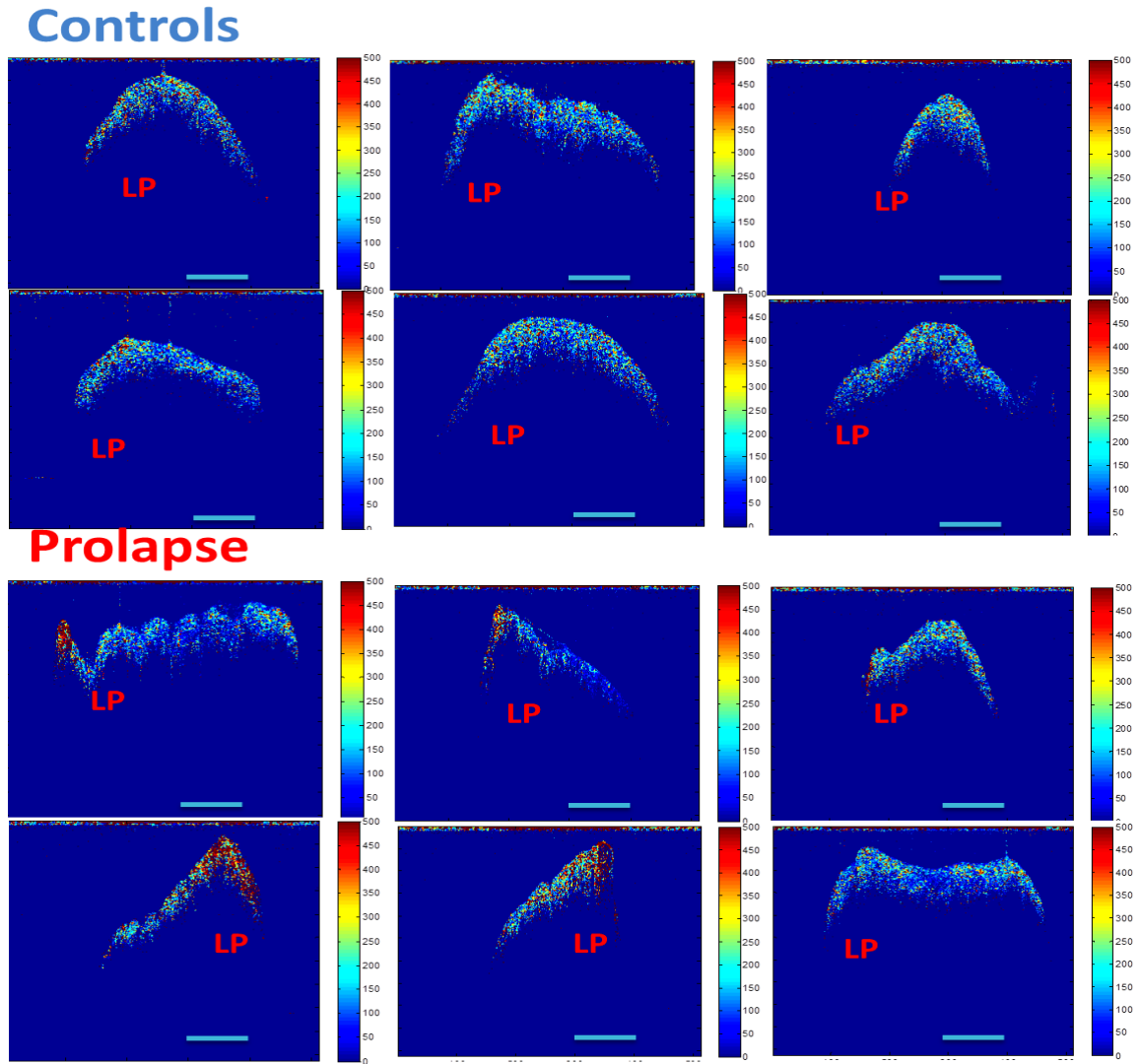
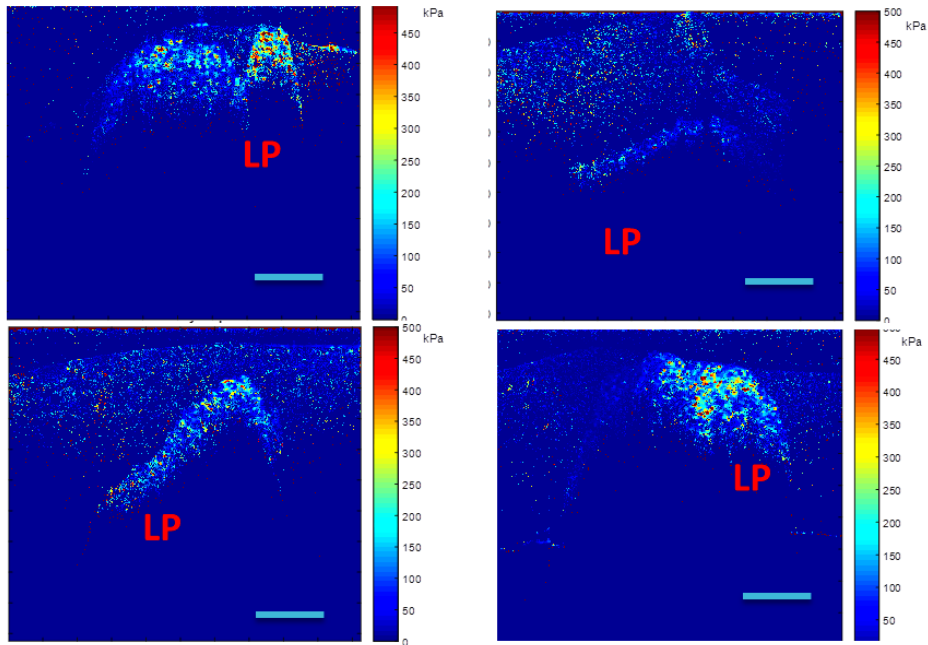


Figure 6.29: Elasticity map of Control and Prolapsed tissues imaged in air. Cross-sectional views along the y-axis of horizontally placed tissues are shown. The colour bars represent the relative modulus of the tissues. Scale bar= 1000 μm LP = Lamina Propria

Images obtained following immersion in agar, figure 6.30, revealed the same trend. The prolapsed tissues have appreciable regions with modulus around 500KPa based on the colour coding. This however was not the case with controls, which were mostly within 200-250 KPa in modulus. Within agar, the tissue stiffness was more extensive but predominantly localised

to the LP regions. More uniformity in modulus was noted within the control samples which appeared to have overall lower modulus than prolapse. Both OCE experiments strongly suggest that prolapsed tissues have heterogeneous distribution of stiffness within the tissue, confirming AFM findings of higher modulus in prolapsed LP region compared with adventitial layers.

Controls



Prolapse

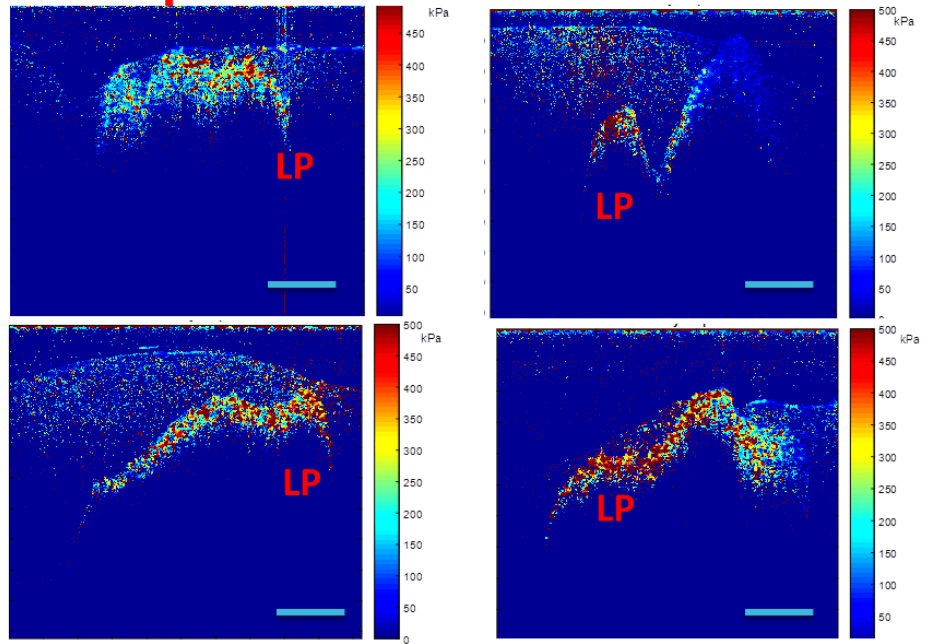


Figure 6.30: Elasticity map of Prolapsed and control tissues imaged immersed in agar.

Scale bar =1000 μ m LP = Lamina Propria

6.5 DISCUSSION

6.5.1 HISTOLOGY

Understanding the histological changes that are present in prolapsed tissue may not immediately answer the ‘cause or effect question’ but can influence clinical decision making in terms of completely removing prolapsed areas or supporting them (268,269). The histology of prolapsed vaginal wall has been poorly studied and understood. Previous studies have had varying results (8) but common trends can be seen. Many studies have used localized biopsies which are poorly characterised and do not allow evaluation of histology across the full thickness of the vaginal wall (268). In this present study, we investigated full thickness prolapsed and control tissues with most prolapsed tissues obtained from the middle vaginal regions and the majority of the controls from apical regions. The prolapsed tissues exhibited disorganized connective tissue structure with notable changes in the basal cell count, tissue integrity and connective tissue collagen densifications. Quantitatively, total collagen was increased in prolapsed vaginal tissues. Our findings can be better understood by taking cognizance of findings from other studies. For example, research comparing histology and histological zones of vaginal tissues in different regions (apical, middle and distal thirds) of the vaginal wall have found no significant difference in composition of collagen in the human vagina (270). This implies that the consistent differences we observed in the collagen composition of prolapsed tissues (predominantly middle vaginal segment) and controls (largely apical segments) are differences associated with the disease and hence, noteworthy.

Structural and morphological studies have revealed more disorganized architecture in prolapsed tissues (271). The majority of research has noted a thinned out muscularis layer in prolapsed tissue and increased numbers of enlarged venous vasculature but reduced amounts of capillaries (272). Some studies have also noted decreased innervation of prolapsed anterior vaginal wall compared with controls (270). In this study, there was less oestrogen expression in the prolapsed tissues. Since, oestrogen induces an increase or growth in the vaginal layers of normal vagina (269), its decline in prolapse may explain the thinning of the superficial epithelial zone of the prolapsed tissues observed in this study.

In 2006, Lin et al studied elastin expression in the anterior vaginal wall by immunohistochemistry in 23 prolapsed tissues and 15 controls and found no significant difference (273). In 1996 Jackson et al also had similar findings from studying the vaginal epithelium of 8 premenopausal women with prolapse and 10 controls (23). Some studies on localized histological zones of the tissues and a few with staining carried out for specific types of elastin have found decreased expression in prolapsed tissues (268,274). A study by Zong et al investigating eighty-seven full thickness vaginal biopsies void of epithelium in premenopausal controls and women with prolapse (premenopausal, menopausal not on HRT and on HRT) for tropoelastin (elastin precursor) and mature elastin found an increase in both in prolapse with more increase in postmenopausal women with prolapse but not on HRT (275). These suggest that although elastin content may vary across layers of prolapsed tissues there is an inverse influence of hormones on elastin content. The varied findings in these studies may be the result of biopsy taken from different histological layers, differing methods of analysis and non-discrimination between tropoelastin and mature elastin in some studies. Our study observes differential expression of elastin in the various tissue layers with more

expression in the epithelial and muscularis layers. By qualitative observation, elastin was more expressed in the prolapsed tissue sections. This is in keeping with findings by Zong et al (275). The differential distribution in the various histological zones may explain the varied results from other studies on elastin content in prolapsed tissues depending on the histological zone of the vaginal wall studied. Overall, the existing literature on elastin content of prolapsed tissues is inconclusive and requires further investigation.

There are indications that pelvic tissue innervation is impaired in prolapse (91). In a cohort study to assess the sensory and motor innervation of genitals in women with prolapse, an abnormal genital vibration sensation was noted in women with prolapse. This worsened with age but was uninfluenced by surgical repair (276). Neuropeptide Y, a brain and autonomic nervous system neurotransmitter was found to decrease in pelvic prolapse with decrease correlating with severity prolapse (277). Another study that investigated the innervation pattern of vaginal tissues using immunostaining observed localization of nerve bundles at the adventitial and muscularis region with reduced size and frequency of nerve bundles in prolapsed tissues. We noted increased expression of neural processes in vaginal tissue sections from women with prolapse compared to control tissues. These findings in addition to existing literature consistently suggest affectation of the nerves as a significant pathology in prolapsed tissues.

Cells recreate tissue matrix and remodel these when necessary. Therefore changes in tissue structure and histology should warrant the study of inherent cells. The few studies that have investigated cells in the prolapsed vaginal wall have focused on the fibroblasts (268). Fibroblasts from prolapsed vaginal wall have been shown to decline in number and become less functional by contracting less, and producing altered ECM proteins (115). For the first

time, we have observed increased number of cells in the basal lamina region of prolapsed tissues. Basal epithelial cells, in different body tissues, are poorly differentiated cells or stem cells which give rise to the more specialized cells of the epithelium (278). They enable replenishing or renewal of the epithelium (258). Mechanical stimulus such as constant friction or repeated stretching has been shown to lead to proliferation of epithelial cells. In a study in which controlled friction was applied to hamster cheek pouch epithelium, the cells increased in size and number (279). Another study in which mouse epithelial skin was stretched to observe for effects on proliferation, noted an increase in mitotic index maintained after 4 days and an increase in basal progenitor cells (280). The increase in the basal vaginal epithelial cells noted in our study may be therefore be induced by the constant abrasion the prolapsed vaginal wall is exposed to and indicative of a tissue undergoing mechanical stress.

6.5.2 STRUCTURE AND COMPOSITION

Our study revealed that the connective tissue of prolapsed vaginal wall had remarkably dissimilar properties from controls. At the micro scale, prolapsed vaginal tissues contained less or patchy muscularis layer which was infiltrated with connective tissue, notable in trichrome stained images. There was also a disorganized architecture of prolapsed tissues. Collagen, a connective tissue component, was visibly increased in prolapsed vaginal tissues as revealed in picrosirius red stained images. This was confirmed by hydroxyproline assay. In published literature, inconsistent outcomes have been obtained from various studies on collagen and elastin content of prolapsed tissues (251,268). A study involving 10 anterior pre-cervical vaginal fascia samples from women with prolapse and 10 from the control group and

another study using samples from the precervical vaginal fascia of 24 women with prolapsed and 21 controls noted increased total collagen in prolapsed tissue (109,273). Another study on samples from women with stress urinary incontinence and prolapse, 32 women with prolapse and 28 controls using tissues obtained from the same region of the vagina as the previous study found decreased collagen III (281). Some studies have found no significant difference in amounts of collagen types III and I in the prolapsed and control tissues (109,281). Fewer studies have used full thickness vaginal tissues. Kocku in 2002 found an increase in total collagen in full thickness prolapsed vaginal tissues from a study involving 24 premenopausal women with prolapse and 21 controls (273). In 2005, Moalli et al investigated full thickness vaginal tissue from the apical region of 16 premenopausal women and 15 controls and found an increase in total collagen in the premenopausal women with prolapse and non-use of HRT (108). Jackson et al in 1996 studied 8 premenopausal women with prolapse and 15 controls and found a decrease in total collagen in the epithelial region (23). These suggest that the different outcomes may be due to the different histological regions tested and other factors such as HRT use. Many studies have not described the histological zones of the tissues tested. Therefore variations in outcomes could be due to differences in aspects of the tissues biopsied and improper characterisation of the tissues. We studied full-thickness vaginal tissue samples and found significantly increased total collagen content in prolapsed tissues. This is collaborated by studies that have made use of full thickness tissues (108,273). Despite differences in study outcomes, it is likely that prolapsed tissues have overall increased total collagen content.

In a recent study aimed at investigating morphological and immunohistochemical changes of tissues in 14 women with prolapse by investigating Collagen I and Collagen III, α -Smooth

Muscle Actin (α -SMA), Platelet-Derived-Growth-Factor (PDGF), matrix metalloproteinase 3 (MMP3), tissue inhibitors metalloproteinase 1 (TIMP1), Caspase3 immunochemically and histologically and making comparisons with ten controls obtained from women admitted for plastic surgery, a similar finding of poorly organized myocytes, displaced by increased collagen III deposition leading to altered organization of the LP was noted (282). Another study also utilizing trichrome staining to assess smooth muscle content of the anterior apical aspect of the vaginal wall in women with prolapse and controls observed decreased fractional area of non-vascular smooth muscle in prolapsed tissues (283). Furthermore, an increase in the fractional area of connective tissue in prolapsed vaginal tissues was noted. These strongly corroborate our findings. Another histological study carried out using samples from 33 women with prolapse and nine controls found significantly altered smooth muscle actin expression and altered morphology of prolapsed tissues (284). In our study, the prolapsed tissues had reduced and less organised muscularis layers, which were infiltrated with connective tissue. The extra connective tissue was likely to be collagen as noted by the significantly increased collagen content and increased picrosirius red staining of the prolapsed tissues' muscularis layers. These findings are highly suggestive of changed or displaced phenotype within the vaginal wall of women with prolapse and such changes may be important pathological changes leading to altered vaginal wall functionality and prolapse.

The altered tissue structure and composition of prolapsed tissues is reflected in the genetic expression. In a study investigating the expression of genes encoding smooth muscle proteins in prolapsed tissues a procontractile gene, SM-myosin heavy chain (MHY11) was noted to have up to five times down-regulation in women with prolapse compared with controls of similar menopausal status (285). Other genes encoding such as caldesmon (CALD 1), SM

gamma-actin (ACTG2), and tropomyosin (TPM1) were down-regulated in controls but not in prolapsed tissues. These altered genes could be the effectors of observed muscularis changes in prolapsed tissues or responses to the changes. Although detailed genetic studies would be required to better understand this, the findings strongly suggest that a dysfunctional muscularis region contributes to the observed pathology of prolapse.

The organisational changes observed in the light microscopy images were more evident at the nano-scale. AFM studies are useful in revealing mechanical properties and structural changes in vaginal tissue structure and interaction with ECM (286). Our AFM results show morphological signs of prolapse at the micro and nano scale. There were disorganized collagen fibrils with significantly wider gaps between fibrils and less bundling unlike in control tissues. This disorganization was noticeable in LP and adventitial regions of the prolapsed tissues. Notable loss of collagen bundling, disintegration and misalignment were evident. There are a few other AFM studies of the vaginal wall in women with prolapse and these have varied findings. A study on periurethral tissues in young women with prolapse revealed 30% less collagen than in age-matched controls (287). Another study investigating the uterosacral ligaments in women with prolapse observed no difference in collagen I but correlation of higher collagen III content with the presence of prolapsed (288). An AFM study in the organization of collagen fibrils in skin tissue of women with prolapse revealed changes in the collagen fibril bundle organization and mechanical properties in women with prolapse (243). It noted loosening of collagen fibers, disorganization and disintegration of the fibers in skin tissues of women with prolapse. This suggests that changes observed in prolapsed tissues are present or occur similarly in other tissues (as also noted in 4.3). Another study investigating early changes in prolapsed vaginal wall, observed bulkier and stiffer collagen

fibrils with variable width and higher amounts of the wider collagen I than III (289). This study also noted loose arrangement and reduced total collagen in prolapsed tissues. Some other studies however have revealed increased amounts of collagen III and total collagen in prolapsed tissues. A study investigating the remodeling of vaginal connective tissues in prolapse found predominant collagen in the vaginal wall to be type III and increased total collagen in women with prolapse (108). In the various studies, the observed variation in outcome may be the result of different age groups, vaginal regions and status of menopause of women studied. The most consistent outcomes however are the stiffening and disorganisation of the collagen fibrils in the vaginal wall of women with prolapse.

6.5.3 MECHANICS AND GLYCATION

The studies of the mechanical property of the vaginal tissues at the nano, micro and tissue level confirmed the heterogeneous modulus distribution in prolapsed samples with the presence of a higher modulus region in LP area of prolapsed tissues compared to more homogenous controls. There are a few other studies on the mechanics of prolapse. They commonly note the increased stiffening of prolapsed vaginal wall compared to controls. Research by Chen et al in 2007 revealed higher Young's modulus of prolapsed tissues, more so in conjunction with menopause (164). The control tissues also exhibited higher maximum elongation and maximum fracture suggestive of a more resilient tissue. This implies that increase in modulus noted in prolapse does not contribute to improved mechanical properties. Changes in prolapse were similar to menopausal changes in the same study (164), suggesting a similar underlying mechanism for vaginal wall changes in prolapse and menopause. A vaginal tactile imaging study however revealed a contrary result of lower elastic modulus in stage III prolapsed tissue (290). Although results from other prolapsed stages were not reported in that

study, it is interesting to note that measurement was carried out *in vivo*. The study made use of a probe used to assess vaginal wall modulus with the women in anatomical position. Another *in vivo* study noted reduced modulus in the vaginal wall of women with prolapse (130). These *in vivo* tests reflect a non-isolated study of the vaginal wall. Results may thus be representative of vaginal wall and surrounding pelvic tissues. The prolapsed vaginal tissue, though stiffer than normal vaginal tissue when isolated from its anatomical surrounding, may exhibit overall inferior mechanical properties *in vivo*.

Due to the direct role of the vaginal wall in the support of other pelvic organs (291), changes in vaginal tissue mechanics will affect pelvic organs. Hence the importance of investigating changes in vaginal tissue mechanics. There are however no other studies that investigate the mechanical properties of the prolapsed tissues from the nano and micro scale to the tissue level. We have demonstrated this for the first time through a series of experiments that confirm that ultrastructural changes in the tissues' mechanics at the nano level are also evident on a much larger scale. Our investigation of nanomechanical properties of the prolapsed tissues focused on the collagen fibrils suggesting that the overall stiffness noticed in prolapsed tissues is largely due to collagen modifications. This is further supported by results from a study carried out with the aim of investigating the mechanical properties of the vaginal wall in fibulin-5 knockout mice with prolapse. These were compared with the vaginal wall of non-pregnant mice and found to have decreased maximum stress, strain and stiffness (13), suggesting that prolapse caused by genetically induced elastin changes may have a different effect on the tissue's modulus. Altered elastin in this case resulted in reduced stiffness of the vaginal wall.

In investigating the cause of observed stiffening of prolapsed tissues, findings of increased amounts of collagen type III (which is associated with reduced tissue modulus) (108,251) in prolapsed tissues yet higher modulus in prolapsed tissues further point to a cause other than the type of collagen. Glycation modifications are believed to be the cause of vaginal wall stiffening in prolapse as findings from previous research suggest this (8,23,245). The correlation of glycation and mechanical properties has been previously demonstrated in the vaginal wall in pregnancy (237) but not in prolapse. In the present study, we demonstrate for the first time that increased modulus of the vaginal tissues of women with prolapse directly correlates with tissue glycation content. This has previously been observed in other tissues but not in the human vaginal wall. In a study investigating the glycation in the Achilles tendon of rabbits, it was found that increased maximum load, stress, strain and Young's modulus occurred in association with non-enzymatic glycation (208). Pentosidine and insoluble collagen were observed to correlate positively with the tissues' modulus (208). In aortic intima, stiffening has also been correlated with pentosidine and non-fluorescent crosslinks (292). A strong positive correlation has also been noted between the equilibrium modulus of cortical bone and advanced glycation accumulation within the tissue (293). These findings emphasize the relationship between biochemical and mechanical properties of tissues. We have demonstrated this relationship in prolapsed vaginal tissues using an adaptation of the ball indentation technique. The ball indentation device has been successfully used in characterizing hydrogels and thin tissues but for the first time it has been adapted for the study of the human vaginal wall in vitro and revealed the relationship between vaginal wall glycation and increased stiffness of the same in prolapse. Although there was the disadvantage of tissue slicing, the ball indentation method is minimally destructive and enables the application of

multiaxial force to the tissue. This implies that it reasonably simulates the multidirectional force received by the tissue in vivo (11,168).

Furthermore, in our study, modulus assessment revealed a discrepancy between LP and adventitial layers of the prolapsed tissues. The LP layer was stiffer in prolapsed tissues when compared with LP regions of control samples and adventitial layers of prolapsed samples. This heterogeneity in stiffness observed in histological sections of prolapsed tissues was confirmed with OCE. OCE can provide both 2 and 3 dimensional elastographic images of tissues and this mechanical property has been found useful in distinguishing between disease and healthy states in some conditions (196) and also quantification of tissue mechanical property (199). Compared to techniques like AFM, OCE is minimally destructive (196). It has been used in the study of other diseases such as prostate cancer, where histological findings in the tissues correlate with OCE findings (294) and myocardial infarction but for the first time, it has been applied to the study of prolapse. In a research investigating the use of OCE in the study of carcinogenic changes in prostate tissues, OCE findings were shown to correlate with histological findings. OCE is able to detect within tissue, changes such as localized alterations in mechanical properties or mechanical property mapping of the individual samples.

In our study of full thickness control and prolapsed vaginal tissue segments, notable heterogeneity in the stiffening of prolapsed tissues was observed. In the prolapsed tissues, stiffening was localized to the top zones of the tissues, particularly around the LP region. This is an interesting observation with noteworthy implications on the pathology of prolapse. Although it is known that prolapsed tissues are stiffer than controls, no previous study has observed this “within-tissue” modulus difference in prolapsed tissue. In a weight bearing tissue such as the bone, intra tissue variation in modulus can negatively impact on the tissues’

overall strength and function. A study carried out to determine the effect of tissue heterogeneity in modulus on trabecular bone mechanics revealed that significant intra tissue variation in modulus can lead to overall lowering of the tissue's modulus (295). Another study investigating strength and modulus of trabecular bone noted that heterogeneity of the tissue played an important role in preventing failure and fragility (296). It was suggested that a heterogeneous tissue architecture would negatively impact on strain concentration, promotion and accumulation of damage. For materials of the same geometry and composition, homogeneity results in overall improved mechanical property (295) and this is important in load bearing tissues.

This is an important observation with implications in prolapse aetiology and may also explain the findings from the *in vivo* study by Egorov et al discussed earlier (290). The stiffening of the more superficial LP regions may lead to a downward and outward pull of the tissue in the anatomical position (illustrated in figure 6.31) or propagate intra tissue damage leading to overall tissue weakness that enables prolapse.

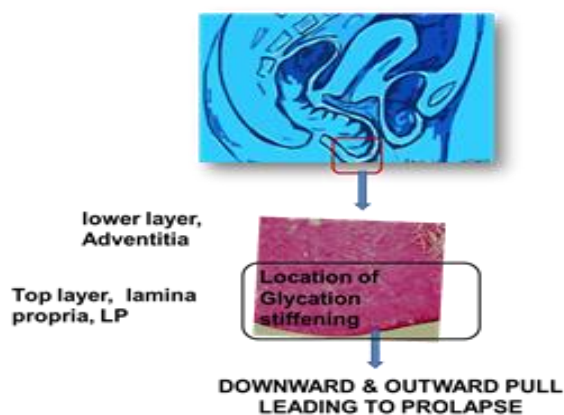


Figure 6.31: Illustration of glycation stiffening in prolapsed tissues and potential to initiate prolapse.

Taken together, these research findings imply that the prolapsed tissue is stiffer than control tissues and this stiffening is more notable in specific regions but the associated higher modulus does not translate to superior mechanical properties of the prolapsed tissue. As noted from studies by Jaasma et al and Zysset et al , within tissue heterogeneity may negatively affect the functional mechanics of the tissue (295,296). Homogeneity of the vaginal wall as observed in the control tissues is more likely to result in a mechanically strengthened vaginal wall.

The agar based OCE study also confirms overall higher moduli of prolapsed tissues compared to controls. Although the stiffness of tissues has the potential to vary based on the nature of the load applied and whether or not different elements of a tissue are investigated or aggregates are studied, the rate of deformation and whether or not it is cyclic or monotonic (297), our study of vaginal tissue stiffness across the nano, micro and macro levels of tissue organisations using three different mechanical tests has revealed a consistent trend. At nano, micro and macro scale, the prolapsed tissues were stiffer than the controls *in vitro*. AFM and OCE studies also noted the heterogeneity within prolapsed tissues. In addition to this heterogeneity being a likely cause of overall inferior effective mechanical properties of the prolapsed tissues, tissue ageing is implicated. The age-related stiffening of soft tissues further limits its mechanical protection as stiffer tissues are likely to have less deformation before failure (298). This increases the risk of injury, mechanical weakening and potentially, prolapse.

6.6 CONCLUSION

6.6.1 MAIN FINDINGS

By studying the structure and mechanical changes within prolapsed tissues using histological techniques, various soft tissue mechanical test devices and adaptations of the same, notable

differences have been identified. The ultra-structural organisation and regional modulus of the prolapsed tissues were significantly altered in comparison to controls. Prolapsed tissues exhibited disorganized connective tissue structure with notable histological and biochemical changes. For the first time, prolapsed tissue mechanics has been investigated at multiple levels of tissue organization – nano, micro and macro levels - and our study confirms that prolapsed tissues are stiffer than controls as reflected by the higher modulus of prolapsed tissues. The correlation of glycation and modulus was also studied for the first time in human prolapsed tissues. The consistent positive correlation obtained between glycation and tissue modulus suggests that glycation changes are responsible for the increase in modulus noted in prolapsed tissues. Improved insights into changes that lead to prolapse were obtained by localising collagen fibril stiffening within the tissues to the LP regions and understanding of the role of glycation in tissues.

A novel observation of remarkable heterogeneity existing within the prolapsed tissues has been made using two different mechanical techniques. This finding suggests that glycation induced stiffening of the vaginal wall in prolapsed tissues may be asymmetrically increased in the superficial regions of the tissue compared to other aspects of the tissue, making it a mechanically less homogeneous tissue than normal vaginal tissue. This loss of homogeneity may lead to easy overall inferior strength and increased susceptibility to damage and ultimately prolapse. Findings were also congruent between multiple techniques used suggesting that these were genuine trends in the tissues observable at all levels of structural organization.

A method of tissue slicing has been developed and adapted for use with vaginal tissue assessed via the ball indentation technique. Using this method, it was confirmed that pentosidine

content of the prolapsed tissues using two methods of tissue preparation was strongly predictive of changes in the tissues' mechanical property.

6.6.2 STUDY IMPLICATIONS

Although these observations do not directly answer the question of cause and effect, review of other research on the effects of heterogeneity on tissue mechanical strength strongly suggests that the observed differences in prolapsed tissues would lead to inferior mechanical strength and further prolapse at the least. Mechanical inhomogeneity is therefore a potential cause or propagator of the prolapse disease process. The data in Chapters 4 and 5 have highlighted the role of oestrogen in preventing glycation accumulation and it is known that oestrogen levels are lower with menopause, a largely age-dependent process. It is therefore possible to experimentally modulate glycation accumulation in animal models (for example) and look for alterations in tissue mechanics. Further studies along these lines may be useful in answering the question of cause and effect. Nonetheless, the outcome of the present study is a significant step towards unraveling the aetio-pathogenesis of prolapse.

7 CHAPTER 7: GENERAL DISCUSSION AND
CONCLUSIONS

7.1 OVERVIEW

Prolapse incidence increases with age and glycation markers of ageing are higher in prolapsed tissues (5, 23). This has led to an interest in the effect of age, especially age-linked changes that take place in the prolapsed tissues, with the aim of understanding prolapse pathology and proffering better treatment. Prolapse manifests as a change in the mechanical properties of the connective tissue of these pelvic organs which results from mechanical or biochemical damage in the tissue (5). There are also known biochemical changes in prolapsed tissues such as higher glycation and variable amounts of collagen but minimal understanding of the interplay between all these factors leading to prolapse. Ageing and notably, glycation-associated ageing in particular is being investigated to obtain a better understanding of the cause and progression of prolapse (8,23,91,245). Characterizing these biochemical effects in the prolapsed vaginal tissues with a view towards understanding the role the ageing process has in disease development is crucial.

Pregnancy is another biological state in which the mechanics and structure of vaginal tissue is altered but the changes are physiological and occur in preparation for delivery of the baby with minimal injury and return to pre-delivery states by the end of puerperium in most women (1,2,4, 30). Oestrogen, a notable pregnancy related hormone influences fibroblasts and pelvic connective tissues metabolism and remodelling (5-7). These actions may influence the proportion of old and new collagen within the tissues, thereby altering their mechanical properties. Therefore studying the vaginal tissue in pregnancy should provide an improved understanding of the biomechanical behaviour of the vaginal wall in relation to ovarian hormonal influence and glycation changes.

The present study uniquely characterizes vaginal tissues in pregnancy and prolapse and fills current knowledge gaps on why glycation is higher in prolapsed tissues and why the stiffer prolapsed vaginal wall exhibits overall inferior mechanical properties. Multiple mechanical test methods have been applied in the characterisation of the vaginal tissue in pregnancy and prolapse, with consistent outcomes where the same property was observed for. The effect of glycation on the vaginal wall's mechanics has been demonstrated in pregnancy and prolapse with corroborative outcomes. A relationship between ER- α , GLO-I and glycation has been demonstrated. An age-dependent significant increase in vaginal tissue glycation content was noted in the entire population and between the 6th and 7th decades in the prolapse group.

7.2 NOVEL APPLICATION OF MECHANICAL MEASUREMENT MODALITIES IN THE STUDY OF THE VAGINAL TISSUE

The quest for better prolapse treatment has been ongoing for over 400 years [1]. Many researches investigating prolapse seek to gain a better understanding of its cause, with the aim of improving current treatment options. Described as a multifactorial disease, the cause of prolapse has remained elusive for decades. The early studies focused on pelvic floor weakness, looking mainly at supporting ligaments and structures in the pelvis. Some of these studies made use of non-invasive imaging techniques such as MRI to assess tissue weakness. MRI imaging has been used to assess the function of pelvic floor before and after surgical repair (299) and also pre and post vaginal delivery (300). Dynamic imaging had gained particular usefulness in the grading of prolapse but is of little use in understanding its cause (301). The present study demonstrates the role of some newer imaging techniques in the study of prolapse. We have utilized three different mechanical tests in the characterization and visualisation of vaginal tissues. OCE and ball indentation methods have not previously been

used in the study of human vaginal tissue and only few past studies have investigated the vaginal wall using PFQNAFM. This AFM technique has the advantage of obtaining the nanomechanical properties of tissue sections as well as revealing structural properties and organization of the collagen fibrils in nanoscopic and microscopic areas (302). The test tissue is clearly visualized at the ultrastructural level and some ECM changes responsible for the disease phenotype are identified. OCE and ball indentation enable further characterization of tissue bulk mechanical properties in a non-destructive manner (168,196). With ball indentation and tissue adaptation we have been able to demonstrate the creep property and modulus of segments of the vaginal wall and relate this to the pentosidine content. OCE revealed within-tissue changes in whole intact full thickness vaginal wall segments. By using these three techniques to study the same tissue in the case of prolapse, it has been possible to observe the build-up of tissue mechanical property at all levels of tissue organization, noting the nanoscopic changes responsible for the disease phenotype.

7.3 RELATIONSHIP BETWEEN AGEs, GLYCATION AND THE PRESENCE OF PROLAPSE

Our study further investigated the observed higher accumulation of the glycation marker, pentosidine in prolapsed vaginal wall. Prolapse is described as a multifactorial disease caused by a combination of factors such as age, vaginal delivery, trauma, connective tissue disorders, obesity and neurovascular damage (303). The focus of many of such studies has been the pelvic floor as an entity. Whilst this is a holistic approach towards understanding the disease process, it is also important to acknowledge the central role of the vaginal tissue in pelvic support. This means that changes to the vaginal wall would impact on the entire pelvis. With the mean age of prolapse development as 56 and 50% of women 80 years of age having pelvic

floor disorders, age can be considered a vital factor in prolapse development. Many studies have consistently noted higher amounts of advanced glycation markers in prolapsed vaginal wall (8,23,245). In the present study we observed a similar increase in glycation content of prolapsed vaginal tissues. We also noted a steady non-significant increase in vaginal wall glycation with age in the control group and for the first time, a significant difference in glycation content of tissues in women with prolapse was observed between the 6th and 7th decade of life. This implies that the average age at which most women develop prolapse falls within the decade of life in which a significant increase in glycation occurs in the prolapse population. In the present study, prolapse was also commoner in older women but within the same age groups the vaginal wall glycation content in women with prolapse was higher than in controls. Our findings corroborate other studies (6,82) on the importance of age as a risk factor in prolapse development and also suggest a role of accelerated advanced glycation accumulation in the process.

7.4 NEW UNDERSTANDING ON THE RELATIONSHIP BETWEEN GLYCATION LEVEL, OESTROGEN AND GLYOXALASE I EXPRESSION

In the past decade, since the discovery of increased amounts of pentosidine in prolapsed vaginal tissues, the focus of investigative studies has shifted towards the composition and mechanics of prolapsed tissues, including the vaginal wall. Researchers have studied the amounts and presence of physiologic and non-physiologic protein modifications and cellular changes in various pelvic tissues in women with prolapse (8,251). Despite the consistent findings of elevated glycation content of prolapsed tissues and association of the disease with age, many questions remained unanswered. We aimed to elucidate the role of oestrogen and glyoxalase I in glycation accumulation. The present study has resulted in key outcomes that

lay a foundation for an improved understanding of prolapse. In both pregnancy and prolapse, ER- α was more expressed in inverse relation to the pentosidine content of the tissue. We sought for a link between ER- α and advanced glycation reduction to better understand the pathophysiology of the process and observed higher amounts of the antioxidant, glyoxalase I in the controls and in pregnancy, states of higher ER- α receptor expression. Studies have shown that oestrogen reduces pelvic tissue glycation (41,42). Oestrogen also up regulates the activity of glyoxalase I, a glycation lowering antioxidant (218,219). A review of the known role of oestrogen in improving the activity of glycation lowering antioxidant, glyoxalase I has led to the proposal of a pathway for the accumulation of glycation in prolapsed tissues. This provides an understanding of why glycation is commoner in prolapsed tissues and is suggestive of a role of oestrogen in the mechanical changes, particularly the stiffness noted in prolapsed tissues.

7.5 CORRELATION OF GLYCATION AND VAGINAL TISSUE MECHANICS IN PREGNANCY AND PROLAPSE

Furthermore, this study revealed a good correlation between the prolapsed tissues' mechanical property with their glycation content. Our case-control study cannot directly address the cause and effect question regarding the role of glycation in prolapse development but it brings to light the result of glycation on vaginal wall mechanics. In pregnancy, where the glycation marker was reduced, the tissue exhibited higher creep and lower modulus but in prolapse where the glycation content of the tissues was elevated, the tissues were stiffer and had less 24-hour creep. We also noted that glycation inversely correlated with the stiffness of the vaginal wall in pregnancy. This proves that the modulation of vaginal wall glycation affects its mechanical property. Whilst this correlation between glycation and tissue mechanics has been

demonstrated previously in other body tissues including lens and blood vessels (239–241), it is demonstrated in vaginal tissues of female Sprague-Dawley rats and humans for the first time. In the rat study, vaginal wall glycation in pregnancy correlated well with skin glycation in the same subjects in pregnant and non-pregnant states. Due to the private nature of the vaginal tissue and potential inconvenience vaginal tissue screening poses to women, skin glycation detection would be useful in predicting vaginal wall glycation. In this way, the mechanical and functional property of the vaginal wall can be predicted and potentially detect early signs of prolapse. Such predictions would also be useful in pregnancy, where higher glycation content would signify stiffer vaginal wall and potentially difficult delivery.

7.6 NEW CO-MORBIDITIES IN PROLAPSE: HYPERTENSION, SMOKING, CHOLESTEROL

Hypertension could be a noteworthy co-morbidity in women with prolapse. It has been associated with an increased risk of prolapse or higher prolapse stage (260,261). Increased glycation is also known to be implicated in the development of stiffer blood vessels and hypertension (263) but no previous study has quantified glycation in the vaginal wall of women in relation to hypertension as a comorbidity. We quantified glycation in the vaginal wall of women with and without prolapse and found that pentosidine content was higher in women with both prolapse and hypertension. The strong association of both hypertension and prolapse with glycation and the tendency for both diseases to co-exist in the same women places hypertension as a possible risk factor of prolapse. Smoking, a highly prevalent condition is also associated with higher glycation. Smoking promotes systemic inflammation which has also been implicated in prolapse (81,266). Our research notes higher presence of glycation in the vaginal wall of women with prolapse who were smokers or had elevated

cholesterol. There are few studies on the relationship between smoking and prolapse (266) but the recent findings warrant further research on these potential new associations of the disease or its underlying pathology.

7.7 IMPROVED KNOWLEDGE OF HISTOPATHOLOGY AND ULTRASTRUCTURAL CHANGES IN THE VAGINAL WALL IN PREGNANCY AND PROLAPSE

In pregnancy, the vaginal tissue had higher creep and lower stiffness as also noted in previous studies (4). This is thought to be a delivery adaptation to prevent injury (1,2,4). The lower modulus and higher creeping of the vaginal wall in pregnancy was also in keeping with lower glycation since crosslinking results in stiffening of tissues (19). Collagen fibrils within the vaginal wall also undergo progressive disorganisation and remodelling through the middle and later stages of pregnancy (48). We also noted merging of collagen fibrils in pregnancy, a process which did not result in overall higher modulus of the fibers (209) but may be linked to higher amounts of sGAG present in the pregnant tissues. sGAG was significantly higher in the vaginal wall of the pregnant rats. This has also been noted in previous studies (48,211). sGAG are known to modulate collagen fibrillogenesis (27,28,227) and may function to prevent completed fiber disorganisation during stretching. Our in vitro collagen engineering study confirmed that collagen fibrillogenesis is altered in the presence of sGAG. We noted faster kinetics and more merged fibrils and tenency towards bundling when the collagen fibers were formed in the presence of sGAG. This confirmed that observations in the native tissue of merged collagen fibrils in pregnancy were likely due to the higher sGAG content of the tissues in pregnancy.

The prolapsed vaginal wall exhibited significantly different histology from control tissues. They has reduced epithelial cell count, reduced muscularis region with connective tissue infiltrates and collagen content when compared with controls. Biochemical quantification and histological staining noted higher connective tissue and collagen in prolapsed tissues than in controls.

This is in keeping with outcomes from other studies (271). The majority of research has noted thinned out muscularis layer in prolapsed tissues and increased numbers of enlarged venous vasculature but reduced amounts of capillaries (272). Prolapsed tissues had reduced neural tissue expression, as also noted in other studies (91,270). Several other studies have noted a decrease in neurone expression or neurotransmitters in the prolapse vaginal tissue (276,277). Studies using full thickness vaginal tissues, as was used in this study also noted increased total collagen in prolapse vaginal tissues (108,273).

Light microscopy and AFM revealed organizational differences between prolapse and control tissues but these were more evident at the nano scale. Collagen fibrils were scattered within the ECM and had notably wider gaps between fibrils. Bundling was less evident in prolapsed tissues, which also had poorly aligned fibrils. Changes were present in both LP and adventitial regions of the tissues. Similar changes in the skin collagen fibrils of women with prolapse were noted in another study (243). The skin tissue of the women with prolapse contained loose, disintegrated and disorganized fibers. Another study revealed loose arrangement and reduced total collagen in prolapsed vaginal tissues (289). Taken together, the histological and ultrastructural changes noted in the present study contribute to the present understanding of prolapse pathology as a foundation for future therapies.

7.8 MECHANICAL CHANGES IN PROLAPSED TISSUES: NEW INSIGHT ON HETEROGENEITY OF PROLAPSED TISSUES

We studied the mechanical changes in prolapsed tissues, building up from nano, micro to macro scale and made consistent striking observations. Multiple mechanical test devices were utilized in this study, with consistent outcomes. The prolapsed vaginal wall was found to be stiffer at all levels of tissue organisation. Other in vitro studies have made similar observations (12,164). AFM revealed overall stiffer collagen fibrils with higher modulus noted at the LP region. This was confirmed with OCE which revealed the within tissue modulus of whole tissue segments. A novel finding of within-tissue heterogeneity was noted in prolapsed tissue, while controls were more homogenous. These observations have significant implications to the present understanding of prolapse pathology. Previous studies have noted that heterogeneity within tissues results in overall inferior functional mechanical property (295,296). This new observation might explain the apparent contradiction that currently exists in literature, which notes that prolapsed tissues are of higher modulus or stiffness but inferior support function. Taking cognizance of our recent finding of a positive correlation between the glycation content of prolapsed tissues and tissue stiffness, this heterogeneity may also imply differential location of the glycation compound within the prolapsed tissues and warrants further research to unravel this. However, the understanding of differential stiffening within prolapsed tissues adds to the current understanding of the disease and can inform mechanical changes required in future therapies.

7.9 CONCLUSIONS AND FUTURE CONSIDERATIONS

Pregnancy significantly alters the pelvic tissues in adaptation for delivery. The pelvic tissues are exposed to higher levels of female hormones like oestrogen, which decline as women age and approach menopause. This makes the state of pregnancy a condition that potentially contrasts the biological state of the ageing woman. In this project, pregnancy has been studied in parallel with prolapse and key outcomes, implications and findings were consistent.

This study revealed that vaginal tissue pentosidine in pregnancy and prolapse is inversely related to their oestrogen receptor and glyoxalase I expression. In view of the influence of glycation on tissue mechanics, this study suggests a vital role of oestrogen in vaginal tissue mechanics and has important implications in our understanding of prolapse pathology. We have demonstrated for the first time, in the human and rat vaginal wall, relationships between mechanical changes in prolapse and pregnancy and glycation changes. A direct correlation has been demonstrated between glycation and vaginal tissue modulus in both human and animal tissues. Using our rat model in conjunction with *in vitro* collagen fibrillogenesis study, we have demonstrated the role of sGAG in vaginal tissue collagen ultrastructure in pregnancy. We have also demonstrated a relationship between skin and vaginal tissue glycation for the first time, providing a foundation for further research into glycation screening and prolapse prediction.

Pelvic organ prolapse was confirmed to be a disease of ageing with higher occurrence with age and higher glycation content and age-related glycation increase of prolapsed tissues. For the first time, the glycation content of the vaginal wall in control and prolapsed cases from various age-groups was quantified and compared. Within the same age-group, the vaginal tissues from women with prolapse had higher glycation marker levels and a significant difference in glycation content of tissues in the 6th and 7th decade of life was noted in the prolapse group but

not in controls. Whilst this did not prove that glycation is a causative factor in prolapse development, accelerated vaginal tissue ageing cannot be excluded as a potential cause and is worth investigating further. A summary of the proposed relationship between ageing, glycation and prolapse has been shown in figure 33, which also highlights the understood role of oestrogen and glyoxalase I in limiting tissue glycation.

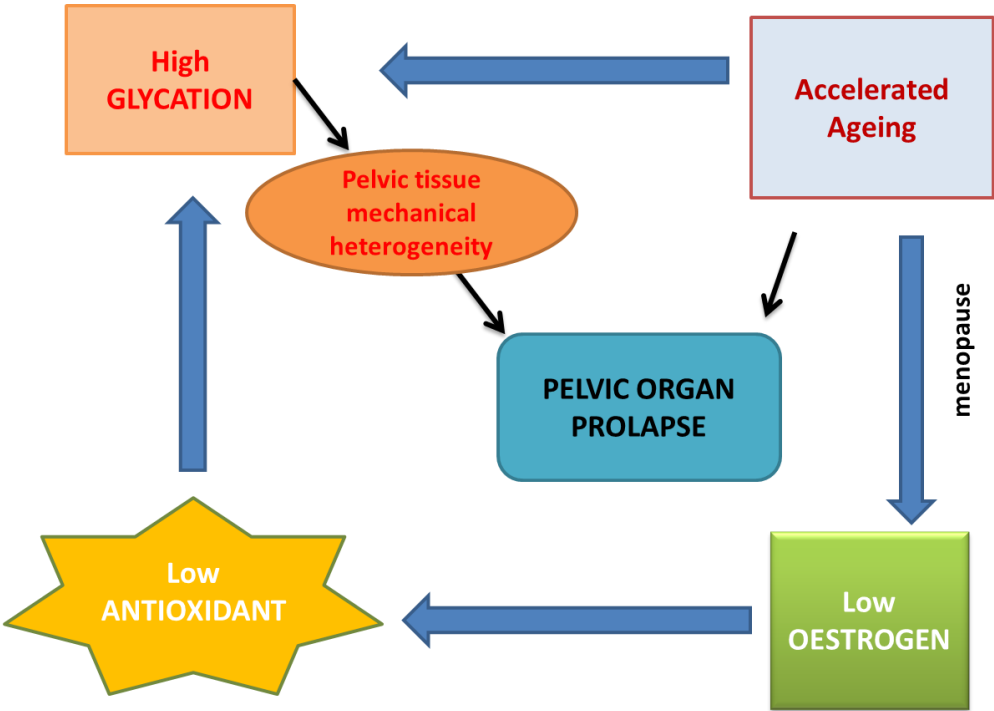


Figure 7.1: Proposed relationship between glycation, oestrogen, GLO-I antioxidant, accelerated ageing, altered tissue mechanics and pelvic organ prolapse.

Further co-morbidities of prolapse in association with glycation have been noted. Hypertension, smoking and elevated cholesterol were all associated with higher vaginal tissue glycation and prolapse. Although further studies will be needed to better understand this, it further emphasizes a pivotal role of glycation in not only the initial screening but also the follow up of patients with prolapse. Further investigations tracking glycation accumulation or effects of

such in relation to prolapse-induced tissue mechanics would give further insight to the development of non-traumatic vaginal wall prolapse.

The prolapsed tissues also had ultrastructural organisational differences and different histological composition. They had disorganised ECM and were notably higher in collagen content and lower in neural expression. This is in keeping with the observed stiffening of the tissues at the nano, micro and macro scale. Prolapsed vaginal tissues were particularly stiffer in the LP region. This heterogeneity was observed for the first time using PFQNM AFM and OCE, and may account for overall inferior functioning of the tissues (figure 7.1) despite higher modulus when compared with controls.

This study has utilized various techniques, some applied for the first time in the study of vaginal tissues in pregnancy and prolapse. It has resulted in an improved understanding of the pregnancy-induced vaginal wall changes and relevance in understanding prolapse. New insights have been gained into the vaginal wall pathology in prolapse. Skin glycation was shown to be reflective of vaginal wall glycation making it a potential marker for non-invasive prediction of or early diagnosis of prolapse. OCE revealed within tissue changes that have functional implications in prolapsed vaginal tissue segments. This device can also be adapted as a screening tool for vaginal wall heterogeneity. Overall, the findings in this work add to the current understanding of the disease and help to direct future research.

The findings from the present study have direct implications for future studies and clinical practise. For example, the outcomes in chapters 5 and 6 suggest that oestrogen receptor expression would be inversely related to the mechanical changes observed in prolapsed tissues. Results from this research would inform further pre-clinical studies on oestrogen's

effect on tissue mechanics. Future use of locally applied oestrogen and glycation breakers in changing vaginal tissue mechanics may be considered as a medical treatment for prolapse. This research is a case-control study and hence does not demonstrate a cause and effect relationship between all observed changes in the prolapsed tissues but is a good foundation for future prospective or interventional studies following adequate safety and ethical considerations. Due to difficulties obtaining control vaginal tissues, fewer and smaller sized control samples were obtained and this limited the use of control tissue for ball indentation mechanical study. Future work should focus on obtaining more and, if possible, larger control samples and re-adapting the ball indentation device for use with smaller samples.

8 REFERENCES

1. Wei JT, De Lancey JO. Functional anatomy of the pelvic floor and lower urinary tract. *Clin Obstet Gynecol.* 2004;47(1):3–17.
2. Shahryarinejad A., Vardy MD. Comparison of Human to Macaque Uterosacral-Cardinal Ligament Complex and Its Relationship to Pelvic Organ Prolapse. *Toxicol Pathol.* 2008; 36(7 Suppl):101S–107S.
3. Herschorn S. Female pelvic floor anatomy: the pelvic floor, supporting structures, and pelvic organs. *Rev Urol.* 2004;6 Suppl 5:S2–10.
4. Ashton-Miller J A, DeLancey JOL. Functional anatomy of the female pelvic floor. *Ann New York.* 2007;1101:266–96.
5. Goh JTW. Biomechanical and biochemical assessments for pelvic organ prolapse. *Curr Opin Obstet Gynecol.* 2003;15(5):391–4.
6. Kuncharapu I, Majeroni BA, Johnson DW. Pelvic organ prolapse. *Am Fam Physician.* 2010;81(9):1111–7.
7. DeLancey JO. Fascial and muscular abnormalities in women with urethral hypermobility and anterior vaginal wall prolapse. *Am J Obstet Gynecol.* 2002;187(1):93–8.
8. Kerkhof MH, Hendriks L, Brölmann HAM. Changes in connective tissue in patients with pelvic organ prolapse--a review of the current literature. *Int Urogynecol J Pelvic Floor Dysfunct.* 2009;20(4):461–74.

9. Slomianka L. Blue Histology - female Reproductive System. Sch Anat Hum Biol - Univ West Aust. The University of Western Australia; 2009; Available from: <http://www.lab.anhb.uwa.edu.au/mb140/corepages/malerepro/malerepro.htm>
10. Egorov V, van Raalte H, Lucente V. Quantifying vaginal tissue elasticity under normal and prolapse conditions by tactile imaging. *Int Urogynecol J*. 2012 Apr;23(4):459–66.
11. Abramowitch SD, Feola A, Jallah Z, Moalli P A. Tissue mechanics, animal models, and pelvic organ prolapse: a review. *Eur J Obstet Gynecol Reprod Biol*. 2009;144:S146-58.
12. Feola A, Duerr R, Moalli P, Abramowitch S. Changes in the rheological behavior of the vagina in women with pelvic organ prolapse. *Int urogynecology*. 2013;24(7):1221–7.
13. Rahn DD, Ruff MD, Brown S A, Tibbals HF, Word RA. Biomechanical properties of the vaginal wall: effect of pregnancy, elastic fiber deficiency, and pelvic organ prolapse. *Am J Obstet Gynecol*. 2008;198(5):590.e1-6.
14. Pierce LM, Coates KW, Kramer LA, Bradford JC, Thor KB, Kuehl TJ. Effects of bilateral levator ani nerve injury on pelvic support in the female squirrel monkey. *Am J Obstet Gynecol*. 2008;198(5):585.e1-8.
15. DeLancey JO, Morgan DM, Fenner DE, Kearney R, Guire K, Miller JM, et al. Comparison of levator ani muscle defects and function in women with and without pelvic organ prolapse. *Obs Gynecol*. 2007];109(2 Pt 1):295–302.
16. Alperin M, Moalli PA. Remodeling of vaginal connective tissue in patients with prolapse. *Curr Opin Obstet Gynecol*. 2006;18(5):544–50.
17. Kielty CM, Sherratt MJ, Shuttleworth CA. Elastic fibres. *J Cell Sci*. 2002;115(Pt

- 14):2817–28.
18. Davis EC, Mecham RP. Intracellular trafficking of tropoelastin. *Matrix Biol.* Elsevier; 1998;17(4):245–54.
 19. Bailey A J. Molecular mechanisms of ageing in connective tissues. *Mech Ageing Dev.* 2001;122(7):735–55.
 20. Woessner J, Brewer T. Formation and breakdown of collagen and elastin in the human uterus during pregnancy and post-partum involution. *Biochem J.* 1963;89:75–82.
 21. Shoulders MD, Raines RT. Collagen Structure and Stability. *Annu Rev Biochem.* 2009;78(1):929–58.
 22. Bailey AJ, Paul RG, Knott L. Mechanisms of maturation and ageing of collagen. *Mech Ageing Dev.* 1998;106(1–2):1–56.
 23. Jackson SR, Avery NC, Tarlton JF, Eckford SD, Abrams P, Bailey AJ. Changes in metabolism of collagen in genitourinary prolapse. *Lancet.* 1996;347(9016):1658–61.
 24. Nemoto T, Kubota R, Murasawa Y, Isogai Z. Viscoelastic Properties of the Human Dermis and Other Connective Tissues and Its Relevance to Tissue Aging and Aging-Related Disease. In: *Viscoelasticity - From Theory to Biological Applications.* InTech open access; 2012.
 25. Niyibizi C, Eyre DR. Structural Characteristics of Cross-Linking Sites in type V Collagen of Bone. Chain Specificities and Heterotypic Links to Type I Collagen. *Eur J Biochem.* 1994 Sep;224(3):943–50.

26. Ulmsten U, Falconer C. Connective tissue in female urinary incontinence. *Curr Opin Obs Gynecol.* 1999;11(5):509–15.
27. Rigozzi S, Müller R, Stemmer A, Snedeker JG. Tendon glycosaminoglycan proteoglycan sidechains promote collagen fibril sliding—AFM observations at the nanoscale. *J Biomech.* 2013;46(4):813–8.
28. Reese SP, Underwood CJ, Weiss JA. Effects of decorin proteoglycan on fibrillogenesis, ultrastructure, and mechanics of type I collagen gels. *Matrix Biol.* 2013 Oct;32(7–8):414–23.
29. Alperin M, Kaddis T, Pichika R, Esparza MC, Lieber RL. Pregnancy-induced adaptations in intramuscular extracellular matrix of rat pelvic floor muscles. *Am J Obstet Gynecol.* NIH Public Access; 2016;215(2):210.e1-e7.
30. Dietz HP, Lanzarone V. Levator Trauma After Vaginal Delivery. *Obstet Gynecol.* 2005;106(4):707–12.
31. Harkness MLR, Harkness RD. The collagen content of the reproductive tract of the rat during pregnancy and lactation. *J Physiol.* 1954;123(3):492–500.
32. Zhao L, Samuel CS, Tregear GW, Beck F, Wintour EM. Collagen studies in late pregnant relaxin null mice. *Biol Reprod.* World Scientific Publishing Co. Pte. Ltd., Singapore; 2000;63:697–703.
33. Willy Davila G. Hormonal Influences on the Pelvic Floor. In: *Pelvic Floor Dysfunction.* 2009; 295–9.
34. Kumar P, Magon N. Hormones in pregnancy. *Niger Med J.* Wolters Kluwer Medknow

Publications; 2012;53(4):179–83.

35. Mattsson R, Mattsson A, Holmdahl R, Whyte A, Rook GAW. Maintained pregnancy levels of oestrogen afford complete protection from post-partum exacerbation of collagen-induced arthritis. *Clin Exp Immunol*. Blackwell Publishing Ltd; 2008;85(1):41–7.
36. Pessina MA, Hoyt RF, Goldstein I, Traish AM. Differential effects of estradiol, progesterone, and testosterone on vaginal structural integrity. *Endocrinology*. 2006;147(1):61–9.
37. Falconer C, Ekman-Ordeberg G, Blomgren B, Johansson O, Ulmsten U, Westergren-Thorsson G, et al. Paraurethral connective tissue in stress-incontinent women after menopause. *Acta Obstet Gynecol Scand*. 1998;77(1):95–100.
38. Edwall L. Female stress incontinence and uterovaginal prolapse: Collagen turnover and hormone sensitivity in urogenital tissue. 2009.
39. Edwall L, Carlström K, Jonasson AF. Endocrine status and markers of collagen synthesis and degradation in serum and urogenital tissue from women with and without stress urinary incontinence. *Neurourol Urodyn*. 2007;26(3):410–5.
40. Chen B, Wen Y, Wang H, Polan ML. Differences in estrogen modulation of tissue inhibitor of matrix metalloproteinase-1 and matrix metalloproteinase-1 expression in cultured fibroblasts from continent and incontinent women. *Am J Obstet Gynecol*. 2003 Jul;189(1):59–65.
41. Jackson S, James M, Abrams P. The effect of oestradiol on vaginal collagen

- metabolism in postmenopausal women with genuine stress incontinence. *BJOG An Int J Obstet Gynaecol.* 2002;109(3):339–44.
42. Robinson D, Cardozo LD. The role of estrogens in female lower urinary tract dysfunction. *Urology.* 2003;62(4):45–51.
 43. DeAngelis CD, Berwick DM. Author in the Room. *JAMA.* 2005;293(8):1004.
 44. Cody JD, Richardson K, Moehrer B, Hextall A, Glazener CM. Oestrogen therapy for urinary incontinence in post-menopausal women. *Cochrane database Syst Rev.* 2009;(4):CD001405.
 45. Chen B, Wen Y, Li H, Polan M. Collagen metabolism and turnover in women with stress urinary incontinence and pelvic prolapse. *Int Urogynecol J.* 2002;80–7.
 46. Shynlova O, Bortolini MAT, Alarab M. Genes responsible for vaginal extracellular matrix metabolism are modulated by women's reproductive cycle and menopause. 2013;39(2):257–67.
 47. Skala CE, Petry IB, Albrich SB, Puhl A, Naumann G, Koelbl H. The effect of hormonal status on the expression of estrogen and progesterone receptor in vaginal wall and periurethral tissue in urogynecological patients. *Eur J Obstet Gynecol Reprod Biol.* 2010;153(1):99–103.
 48. Daucher JA, Clark KA, Stolz DB. Adaptations of the Rat Vagina in Pregnancy to Accommodate Delivery. 2007;109(1):128–35.
 49. Stadtman ER. Protein Oxidation in Aging and Age-Related Diseases. *Ann N Y Acad Sci.* 2006;928(1):22–38.

50. Hayflick L. The limited in vitro lifetime of human diploid cell strains. *Exp Cell Res.* 1965;37(3):614–36.
51. Smith JG, Finlayson GR, D M. Dermal Connective Tissue Alterations with Age and Chronic Sun Damage. *J Soc Cosmet Chem.* 1965;535:527–35.
52. Carrino DA, Calabro A, Darr AB, Dours-Zimmermann MT, Sandy JD, Zimmermann DR, et al. Age-related differences in human skin proteoglycans. *Glycobiology.* Oxford University Press; 2011;21(2):257–68.
53. Cattell MA, Anderson JC, Hasleton PS. Age-related changes in amounts and concentrations of collagen and elastin in normotensive human thoracic aorta. *Clin Chim Acta.* 1996;245(1):73–84.
54. Di Lullo G a, Sweeney SM, Korkko J, Ala-Kokko L, San Antonio JD. Mapping the ligand-binding sites and disease-associated mutations on the most abundant protein in the human, type I collagen. *J Biol Chem.* 2002;277(6):4223–31.
55. Gkogkolou P, Böhm M. Advanced glycation end products: Key players in skin aging? *Dermatoendocrinol.* 2012 Jul 1;4(3):259–70.
56. Luevano-Contreras C, Chapman-Novakofski K. Dietary advanced glycation end products and aging. *Nutrients.* 2010;2(12):1247–65.
57. Singh R, Barden A, Mori T, Beilin L. Advanced glycation end-products: A review. *Diabetologia.* 2001;44(2):129–46.
58. DeGroot J, Verzijl N, Wenting-Van Wijk MJ, Bank R a, Lafeber FP, Bijlsma JW, et al. Age-related decrease in susceptibility of human articular cartilage to matrix

- metalloproteinase-mediated degradation: the role of advanced glycation end products. *Arthritis Rheum.* 2001;44(11):2562–71.
59. Yamauchi M, Woodley DT, Mechanic GL. Aging and cross-linking of skin collagen. *Biochem Biophys Res Commun.* 1988 Apr;152(2):898–903.
60. Siegel RC, Pinnell SR, Martin GR. Cross-linking of collagen and elastin. Properties of lysyl oxidase. *Biochemistry.* 1970 Nov;9(23):4486–92.
61. Ledl F, Schleicher E. New Aspects of the Maillard Reaction in Foods and in the Human Body. *Angew Chemie Int Ed English.* 1990 Jun;29(6):565–94.
62. Cerami A, Vlassara H, Brownlee M. Glucose and aging. 1987.
63. Słowik-Zyłka D, Safranow K, Dziedziejko V, Bukowska H, Ciechanowski K, Chlubek D. A sensitive and specific HPLC method for the determination of total pentosidine concentration in plasma. *J Biochem Biophys Methods.* 2004;30(61):313–29.
64. Chemistry C, Tak M, Kazuhiro T, Kushida I, Kawana K, Hplc U. Direct quantification of pentosidine in urine and serum by HPLC with column switching. *Clin Chem.* 1996;1444:1439–44.
65. Sell DR, Monnier VM. Structure Elucidation of a Senescence Cross-link from Human Extracellular Matrix. 1989;264:21597–602.
66. Alan R, Belen L. A new assay for quantifying pentosidine levels in avian species. 2009. Available from: http://www.wpi.edu/Pubs/E-project/Available/E-project-031209-205737/unrestricted/Final_MQP.pdf

67. Uchiyama A, Ohishi T. Fluorophores from aging human articular cartilage. *J. Biochem* 1991 718:714–8.
68. Hudson BI, Stickland MH, Grant PJ. I d e n t i f i c a t i o n of Polymorphisms in the Receptor for Advanced Glycation End Products (RAGE) Gene Brief Genetics Report. *Dibetes*. 1998;47:1155–7.
69. Inagi R, Miyata T, Ueda Y, Yoshino A, Nangaku M, van Ypersele de Strihou C, et al. Efficient in vitro lowering of carbonyl stress by the glyoxalase system in conventional glucose peritoneal dialysis fluid. *Kidney Int*. 2002;62(2):679–87.
70. Xue M, Rabbani N, Momiji H, Imbasi P, Anwar MM, Kitteringham N, et al. Transcriptional control of glyoxalase 1 by Nrf2 provides a stress-responsive defence against dicarbonyl glycation. *Biochem J*. 2012;443(1):213–22.
71. Yasui T, Yonetsu M, Tanaka R, Tanaka Y, Fukushima S, Yamashita T, et al. In vivo observation of age-related structural changes of dermal collagen in human facial skin using collagen-sensitive second harmonic generation microscope equipped with 1250-nm mode-locked Cr:Forsterite laser. *J Biomed Opt*. 2013 Mar;18(3):31108.
72. Nyman J, Roy A, Acuna R, Gayle H. Age-related effect on the concentration of collagen crosslinks in human osteonal and interstitial bone tissue. *Bone*. 2006;39(6):1210–7.
73. Wilson SL, Guilbert M, Sulé-Suso J, Torbet J, Jeannesson P, Sockalingum GD, et al. A microscopic and macroscopic study of aging collagen on its molecular structure, mechanical properties, and cellular response. *FASEB J*. Federation of American

Societies for Experimental Biology; 2014;28(1):14–25.

74. Brownlee M. Advanced protein glycosylation in diabetes and aging. *Annu Rev Med.* 1995;46:223–34.
75. Mizutari K, Ono T, Ikeda K, Kayashima K, Horiuchi S. Photo-Enhanced Modification of Human Skin Elastin in Actinic Elastosis by NE-(Carboxymethyl)lysine, One of the Glycoxidation Products of the Maillard Reaction. *J Invest Dermatol.* 1997 May;108(5):797–802.
76. Bucala R, Model P, Cerami A. Modification of DNA by reducing sugars: a possible mechanism for nucleic acid aging and age-related dysfunction in gene expression. *Proc Natl Acad Sci U S A.* 1984 Jan;81(1):105–9.
77. Strinić T, Buković D, Roje D, Milić N, Pavić M, Turčić P. Epidemiology of pelvic floor disorders between urban and rural female inhabitants. *Coll Antropol.* 2007 Jul;31(2):483–7.
78. Chanda A, Unnikrishnan V, Roy S, Richter HE. Computational Modeling of the Female Pelvic Support Structures and Organs to Understand the Mechanism of Pelvic Organ Prolapse: A Review. *Appl Mech Rev. American Society of Mechanical Engineers;* 2015;67(4):40801.
79. Barber MD, Maher C. Epidemiology and outcome assessment of pelvic organ prolapse. *Int Urogynecol J.* 2013;24(11):1783–90.
80. Cooper J, Annappa M, Dracocardos D, Cooper W, Muller S, Mallen C. Prevalence of genital prolapse symptoms in primary care: a cross-sectional survey. *Int Urogynecol J.*

2014;26(4):505–10.

81. Olsen A, Smith V, Bergstrom J, Colling J, Clark A. Epidemiology of surgically managed pelvic organ prolapse and urinary incontinence. *Obstet Gynecol.* 1997;89(4):501–6.
82. Swift S, Woodman P, O’Boyle A, Kahn M, Valley M, Bland D, et al. Pelvic Organ Support Study (POSST): the distribution, clinical definition, and epidemiologic condition of pelvic organ support defects. *Am J Obstet Gynecol.* 2005;192(3):795–806.
83. Hendrix SSL, Clark A, Nygaard I, Aragaki A, Barnabei V, McTiernan A. Pelvic organ prolapse in the women’s health initiative: Gravity and gravidity. *Am J Obstet Gynecol.* 2002;186(6):1160–6.
84. Ellerkmann RM, Cundiff GW, Melick CF, Nihira MA, Leffler K, Bent AE. Correlation of symptoms with location and severity of pelvic organ prolapse. *Am J Obstet Gynecol.* 2001;185(6):1332-7-8.
85. Maher C, Baessler K. Surgical management of pelvic organ prolapse in women. *Database Syst Rev.* 2010;(4).
86. Price N, Jackson SR, Avery K, Brookes ST, Abrams P. Development and psychometric evaluation of the ICIQ Vaginal Symptoms Questionnaire: The ICIQ-VS. *BJOG An Int J Obstet Gynaecol.* 2006;113(6):700–12.
87. Persu C, Cr C, Cauni V, Gutue S, Geavlete P. Pelvic Organ Prolapse Quantification System (POP-Q) – a new era in pelvic prolapse staging. 2011;4(1):75–81.
88. Shah HN, Badlani GH. Mesh complications in female pelvic floor reconstructive

- surgery and their management: A systematic review. *Indian J Urol*. Wolters Kluwer Medknow Publications; 2012;28(2):129–53.
89. Clark AL, Gregory T, Smith VJ, Edwards R. Epidemiologic evaluation of reoperation for surgically treated pelvic organ prolapse and urinary incontinence. *Am J Obstet Gynecol*. 2003;189(5):1261–7.
90. Tsai H, Hong M, Wu M. The Alteration of Collagen Subtypes and Myofibroblasts may Account for Pelvic Organ Prolapse Clinical pearls — Research in brief. *Incont Pelvic Floor Dysfunct*. 2011;5(2):47–8.
91. Jelovsek J, Maher C, Barber M. Pelvic organ prolapse. *Lancet*. 2007;369(9566):1027–38.
92. Gyhagen M, Bullarbo M, Nielsen TF, Milsom I. Prevalence and risk factors for pelvic organ prolapse 20 years after childbirth: A national cohort study in singleton primiparae after vaginal or caesarean delivery. *BJOG An Int J Obstet Gynaecol*. 2013;120(2):152–60.
93. Buchsbaum GM, Duecy EE, Kerr LA, Huang L-S, Perevich M, Guzick DS. Pelvic organ prolapse in nulliparous women and their parous sisters. *Obstet Gynecol [Internet]*. 2006;108(6):1388–93.
94. Moalli PA, Howden NS, Lowder JL, Navarro J, Debes KM, Abramowitch SD, et al. A rat model to study the structural properties of the vagina and its supportive tissues. *Am J Obstet Gynecol*. 2005 Jan;192(1):80–8.
95. Okonkwo JEN, Obiechina NJ a, Obionu CN. Incidence of pelvic organ prolapse in

- Nigerian women. *J Natl.* 2003;95(2):132–6.
96. Zong W, Jallah ZC, Stein SE, Abramowitch SD, Moalli PA. Repetitive Mechanical Stretch Increases Extracellular Collagenase Activity in Vaginal Fibroblasts. Vol. 16, *Female Pelvic Medicine & Reconstructive Surgery*. 2010. p. 257–62.
 97. Spence-Jones C, Kamm MA, Henry MM, Hudson CN. Bowel dysfunction: a pathogenic factor in uterovaginal prolapse and urinary stress incontinence. *BJOG An Int J Obstet Gynaecol*. Blackwell Publishing Ltd; 1994;101(2):147–52.
 98. Arya LA, Novi JM, Shaunik A, Morgan MA, Bradley CS. Pelvic organ prolapse, constipation, and dietary fiber intake in women: A case-control study. *Am J Obstet Gynecol*. Elsevier; 2005;192(5 SPEC. ISS.):1687–91.
 99. Chiaffarino F, Chatenoud L, Dindelli M, Meschia M, Buonaguidi A, Amicarelli F, et al. Reproductive factors, family history, occupation and risk of urogenital prolapse. *Eur J Obstet Gynecol Reprod Biol*. 1999;82(1):63–7.
 100. Tinelli A, Malvasi A, Rahimi S, Negro R, Vergara D, Martignago R, et al. Age-related pelvic floor modifications and prolapse risk factors in postmenopausal women. Vol. 17, *Menopause*. 2010; 204–12.
 101. Sun B, Zhou L, Wen Y, Wang C, Baer TM, Pera RR, et al. Proliferative behavior of vaginal fibroblasts from women with pelvic organ prolapse. *Eur J Obstet Gynecol Reprod Biol*. 2014;183:1–4.
 102. M. Nauli A. Calorie Restriction: The Natural Way of Slowing Down Aging. *J Biosaf Heal Educ*. OMICS International; 2013;1(1).

103. Olsen, A L, Smith V J, Bergstrom J O, Colling J C Clark AL. Epidemiology of Surgically Managed Pelvic Organ Prolapse and Urinary Incontinence. Vol. 89, Obstetrics & Gynecology. 1997:501–6.
104. Mant J, Painter R, Vessey M. Epidemiology of genital prolapse: observations from the Oxford Family Planning Association study. BJOG An Int J Obstet Gynaecol. 1997;104(5):579–85.
105. Whitcomb EL, Rortveit G, Brown JS, Creasman JM, Thom DH, Van Den Eeden SK, et al. Racial Differences in Pelvic Organ Prolapse. Obstet Gynecol. 2009;114(6):1271–7.
106. Brizzolara SS, Killeen J, Urschitz J. Gene expression profile in pelvic organ prolapse. Mol Hum Reprod. 2009;15(1):59–67.
107. Ewies AA, Al-Azzawi F, Thompson J. Changes in extracellular matrix proteins in the cardinal ligaments of post-menopausal women with or without prolapse: A computerized immunohistomorphometric analysis. Hum Reprod. 2003;18(10):2189–95.
108. Moalli P, Shand S, Zyczynski H, Gordy S, Meyn L. Remodeling of vaginal connective tissue in patients with prolapse. Obstet Gynecol. 2005;106(5):953–63.
109. Makinen J, Soderstrom KO, Kiilholma P et al., Mäkinen J, Söderström K-OO, Kiilholma P, Hirvonen T. Histological changes in the vaginal connective tissue of patients with and without uterine prolapse. Arch Gynecol. 1986;239(1):17–20.
110. Takano CC, Girão MJBC, Sartori MGF, Castro RA, Arruda RM, Simões MJ, et al. Analysis of collagen in parametrium and vaginal apex of women with and without uterine prolapse. Int Urogynecol J Pelvic Floor Dysfunct. 2002;13(6):342–5.

111. Moalli PA, Talarico LC, Sung VW, Klingensmith WL, Shand SH, Meyn LA, et al. Impact of menopause on collagen subtypes in the arcus tendineous fasciae pelvis. *Am J Obstet Gynecol.* 2004;190(3):620–7.
112. Goepel C, Hefler L, Methfessel HH-D, Koelbl H. Periurethral connective tissue status of postmenopausal women with genital prolapse with and without stress incontinence. *Acta Obstet Gynecol Scand.* 2003;82(7):659–64.
113. Gabriel B, Watermann D, Hancke K, Gitsch G, Werner M, Tempfer C, et al. Increased expression of matrix metalloproteinase 2 in uterosacral ligaments is associated with pelvic organ prolapse. *Int Urogynecol J.* 2006;17(5):478–82.
114. Murphy M, Shrestha R, Haff R, Van Raalte H, Devakumar H, Lucente VR. Vaginal hysterectomy at the time of transvaginal mesh placement. *Female Pelvic Med Reconstr Surg.* 2010;16(5):272–7.
115. Ruiz-Zapata AM, Kerkhof MH, Zandieh-Doulabi B, Brölmann HAM, Smit TH, Helder MN. Functional characteristics of vaginal fibroblastic cells from premenopausal women with pelvic organ prolapse. *Mol Hum Reprod.* 2014;20(11):1135–43.
116. Ruiz-Zapata AM, Kerkhof MH, Ghazanfari S, Zandieh-Doulabi B, Stoop R, Smit TH, et al. Vaginal Fibroblastic Cells from Women with Pelvic Organ Prolapse Produce Matrices with Increased Stiffness and Collagen Content. *Sci Rep. Nature Publishing Group;* 2016;6:22971.
117. Zong W, Zyczynski HM, Meyn LA, Gordy SC, Moalli PA. Regulation of MMP-1 by sex steroid hormones in fibroblasts derived from the female pelvic floor. *Am J Obstet*

Gynecol. 2007;196(4):349.e1-11.

118. Baah-Dwomoh A, McGuire J, Tan T, De Vita R. Mechanical Properties of Female Reproductive Organs and Supporting Connective Tissues: A Review of the Current State of Knowledge. *Appl Mech Rev. American Society of Mechanical Engineers*; 2016;68(6):60801.
119. Malmström E, Sennström M, Holmberg A, Frielingsdorf H, Eklund E, Malmström L, et al. The importance of fibroblasts in remodelling of the human uterine cervix during pregnancy and parturition. *Mol Hum Reprod. 2007;13(5):333–41.*
120. Zhao S, Fields PA, Sherwood OD. Evidence That Relaxin Inhibits Apoptosis in the Cervix and the Vagina during the Second Half of Pregnancy in the Rat 1. *Endocrinology. Oxford University Press*; 2001;142(6):2221–9.
121. Lowder J, Debes K, Moon D, Howden N, Abramowitch S, PA. M. Biomechanical adaptations of the rat vagina and supportive tissues in pregnancy to accommodate delivery. *Obs Gynecol. 2007;109(1):136–43.*
122. Feola A, Moalli P, Alperin M, Duerr R, Gandley RE, Abramowitch S. Impact of Pregnancy and Vaginal Delivery on the Passive and Active Mechanics of the Rat Vagina. *Ann Biomed Eng. 2011;39(1):549–58.*
123. Rundgren A. Physical properties of connective tissue as influenced by single and repeated pregnancies in the rat. *Acta Physiol Scand Suppl. 1974;417:1–138.*
124. Moalli PA, Debes KM, Meyn LA, Howden NS, Abramowitch SD. Hormones restore biomechanical properties of the vagina and supportive tissues after surgical menopause

- in young rats. *Am J Obstet Gynecol*. 2008;199(2):544–50.
125. Wen Y, Zhao YY, Li S, Polan ML, Chen BH. Differences in mRNA and protein expression of small proteoglycans in vaginal wall tissue from women with and without stress urinary incontinence. *Hum Reprod*. 2007;22(6):1718–24.
126. Cosson M, Lambaudie E, Boukerrou M, Lobry P, Crépin G, Ego A. A biomechanical study of the strength of vaginal tissues. *Eur J Obstet Gynecol Reprod Biol*. 2004;112(2):201–5.
127. Rubod C, Boukerrou M, Brieu M, Jean-Charles C, Dubois P, Cosson M. Biomechanical properties of vaginal tissue: preliminary results. *Int Urogynecol J Pelvic Floor Dysfunct*. 2008;19(6):811–6.
128. Jean-Charles C, Rubod C, Brieu M, Boukerrou M, Fasel J, Cosson M. Biomechanical properties of prolapsed or non-prolapsed vaginal tissue: Impact on genital prolapse surgery. *Int Urogynecol J*. 2010;21(12):1535–8.
129. Epstein LB, Graham CA, Heit MH. Systemic and vaginal biomechanical properties of women with normal vaginal support and pelvic organ prolapse. *Am J Obstet Gynecol*. Mosby; 2007;197(2):165.e1-165.e6.
130. Chuong CJ, Ma M, Eberhart RC, Zimmern P. Viscoelastic properties measurement of the prolapsed anterior vaginal wall: A patient-directed methodology. *Eur J Obstet Gynecol Reprod Biol*. 2014;173(1):106–12.
131. Chantreau P, Brieu M, Kammal M, Farthmann J, Gabriel B, Cosson M. Mechanical properties of pelvic soft tissue of young women and impact of aging. *Int Urogynecol J*

- Pelvic Floor Dysfunct. 2014;25(11):1547–53.
132. Bozzola JJ, Russell LD. Electron microscopy : principles and techniques for biologists. Jones and Bartlett; 1999. 670.
 133. Mazia D, Schatten G, Sale W. Adhesion of cells to surface coated with polylysine. J Cell Biol. 1975;66(1):198–200.
 134. Smith KCA, Oatley CW. The scanning electron microscope and its fields of application. Br J Appl Phys. IOP Publishing; 1955;6(11):391–9.
 135. Kohl H, Reimer L. Transmission Electron Microscopy: Physics of Image Formation. New York, NY: Springer New York; 2008. 601.
 136. Grossman M, Ben-Chetrit N, Zhuravlev A, Afik R, Bassat E, Solomonov I, et al. Tumor cell invasion can be blocked by modulators of collagen fibril alignment that control assembly of the extracellular matrix. Cancer Res. American Association for Cancer Research; 2016;76(14):4249–58.
 137. Melo RCN, Dvorak AM. Lipid body-phagosome interaction in macrophages during infectious diseases: Host defense or pathogen survival strategy? Chitnis CE, editor. Vol. 8, PLoS Pathogens. Public Library of Science; 2012:6.
 138. Goldberg MW, Fišerová J. Immunogold labeling for scanning electron microscopy. In: Methods in Molecular Biology. Springer-Verlag; 2016:309–25.
 139. Ottersen OP. Postembedding immunogold labelling of fixed glutamate: an electron microscopic analysis of the relationship between gold particle density and antigen concentration. J Chem Neuroanat. 1989;2(1):57–66.

140. Lucocq J. Quantitation of gold labelling and antigens in immunolabelled ultrathin sections. *J Anat.* Wiley-Blackwell; 1994;184(Pt 1):1–13.
141. Birrell GB, Hedberg KK, Griffith OH. Pitfalls of immunogold labeling: analysis by light microscopy, transmission electron microscopy, and photoelectron microscopy. *J Histochem Cytochem.* SAGE PublicationsSage CA: Los Angeles, CA; 1987;35(8):843–53.
142. Anisotropy of collagen fibre alignment in bovine cartilage: comparison of polarised light microscopy and spatially resolved diffusion-tensor measurements. *Histochemistry and Cell Biology.* Springer-Verlag; 1996; 106:41–58.
143. de Visser SK, Bowden JC, Wentrup-Byrne E, Rintoul L, Bostrom T, Pope JM, et al. Anisotropy of collagen fibre alignment in bovine cartilage: comparison of polarised light microscopy and spatially resolved diffusion-tensor measurements. *Osteoarthritis Cartil.* W.B. Saunders; 2008;16(6):689–97.
144. Torok P, Higdon PD, Wilsö T. On the general properties of polarised light conventional and confocal microscopes. *Optics Communications.* North-Holland; 1998. 148:300–15.
145. Whittaker DM, Culshaw IS. Scattering-matrix treatment of patterned multilayer photonic structures. *Phys Rev B.* American Physical Society; 1999;60(4):2610–8.
146. Rieppo J, Hallikainen J, Jurvelin JS, Kiviranta I, Helminen HJ, Hyttinen MM. Practical considerations in the use of polarized light microscopy in the analysis of the collagen network in articular cartilage. *Microsc Res Tech.* Wiley Subscription Services, Inc., A Wiley Company; 2008;71(4):279–87.

147. Murphy DB, Davidson MW. Differential Interference Contrast Microscopy and Modulation Contrast Microscopy. *Fundam Light Microsc Electron Imaging*. Hoboken, NJ, USA: John Wiley & Sons, Inc.; 2013;173–98.
148. Changoor A, Tran-Khanh N, Méthot S, Garon M, Hurtig MB, Shive MS, et al. A polarized light microscopy method for accurate and reliable grading of collagen organization in cartilage repair. *Osteoarthr Cartil*. W.B. Saunders; 2011;19(1):126–35.
149. Dayan D, Hiss Y, Hirshberg A, Bubis JJ, Wolman M. Are the polarization colors of Picrosirius red-stained collagen determined only by the diameter of the fibers? *Histochemistry*. Springer-Verlag; 1989;93(1):27–9.
150. Rich L, Whittaker P. Collagen and Picrosirius Red Staining : A Polarized Light Assessment of Fibrillar Hue and Spatial Distribution. *Braz J Morphol Sci*. 2005;22(2):97–104.
151. Blanchard CR. Atomic Force Microscopy. *Chem Educ*. Springer-Verlag; 1996;1(5):1–8.
152. Binnig G, Quate CF, Gerber C. Atomic Force Microscope. *Phys Rev Lett* [Internet]. American Physical Society; 1986;56(9):930–3.
153. Adamcik J, Berquand A, Mezzenga R. Single-step direct measurement of amyloid fibrils stiffness by peak force quantitative nanomechanical atomic force microscopy. *Appl Phys Lett*. 2011;98(19):193701.
154. Bozec L, Horton M. Topography and Mechanical Properties of Single Molecules of Type I Collagen Using Atomic Force Microscopy. *Biophys J*. Cell Press;

- 2005;88(6):4223–31.
155. Williams RM, Zipfel WR, Webb WW. Interpreting second-harmonic generation images of collagen I fibrils. *Biophys J. Elsevier*; 2005;88(2):1377–86.
 156. Zoumi A, Yeh A, Tromberg BJ. Imaging cells and extracellular matrix in vivo by using second-harmonic generation and two-photon excited fluorescence. *Proc Natl Acad Sci.* 2002;99(17):11014–9.
 157. Freund I, Deutsch M, Sprecher A. Connective tissue polarity. Optical second-harmonic microscopy, crossed-beam summation, and small-angle scattering in rat-tail tendon. *Biophys J. Cell Press*; 1986;50(4):693–712.
 158. Guilbert M, Said G, Happillon T, Untereiner V, Garnotel R, Jeannesson P, et al. Probing non-enzymatic glycation of type I collagen: A novel approach using Raman and infrared biophotonic methods. *Biochim Biophys Acta - Gen Subj. Elsevier*; 2013;1830(6):3525–31.
 159. Roy R, Boskey A, Bonassar LJ. Processing of type I collagen gels using nonenzymatic glycation. *J Biomed Mater Res - Part A. Wiley Subscription Services, Inc., A Wiley Company*; 2010;93(3):843–51.
 160. Parker PS. Application of Infrared, Raman and Resonance Raman spectroscopy in biochemistry. 1983: 21-25
 161. Pietrabissa R, Quaglini V, Villa T. Experimental methods in testing of tissues and implants. In: *Meccanica. Kluwer Academic Publishers*; 2002: 477–88.
 162. Larrabee WF. A finite element model of skin deformation. *Laryngoscope. John Wiley*

& Sons, Inc.; 1986;96(4):399-405.

163. Larrabee WF, Sutton D. A finite element model of skin deformation. II. An experimental model of skin deformation. *Laryngoscope* John Wiley & Sons, Inc.; 1986;96(4):406-412.
164. Lei L, Song Y, Chen R. Biomechanical properties of prolapsed vaginal tissue in pre- and postmenopausal women. *Int Urogynecol J Pelvic Floor Dysfunct*. 2007;18(6):603–7.
165. Ulrich D, Edwards SL, Letouzey V, Su K, White JF, Rosamilia A, et al. Regional variation in tissue composition and biomechanical properties of postmenopausal ovine and human vagina. *PLoS One*. 2014;9(8).
166. Gu WY, Yao H, Huang CY, Cheung HS. New insight into deformation-dependent hydraulic permeability of gels and cartilage, and dynamic behavior of agarose gels in confined compression. *J Biomech*. Elsevier; 2003;36(4):593–8.
167. Koob TJ, Hernandez DJ. Mechanical and thermal properties of novel polymerized NDGA-gelatin hydrogels. *Biomaterials*. Elsevier; 2003;24(7):1285–92.
168. Ahearne M, Yang Y, El Haj AJ, Then KY, Liu K. Characterizing the viscoelastic properties of thin hydrogel-based constructs for tissue engineering applications. *J R Soc Interface*. 2005;2(5):455–63.
169. Kenedi RM, Gibson T, Evans JH, Barbenel JC. Tissue mechanics. *Phys Med Biol*. IOP Publishing; 1975;20(5):699–717.
170. Cosson M, Lambaudie E, Boukerrou M, Lobry P, Crépin G, Ego A. A biomechanical

- study of the strength of vaginal tissues: Results on 16 post-menopausal patients presenting with genital prolapse. *Eur J Obstet Gynecol Reprod Biol.* 2004 Feb;112(2):201–5.
171. Drury JL, Dennis RG, Mooney DJ. The tensile properties of alginate hydrogels. *Biomaterials.* Elsevier; 2004;25(16):3187–99.
172. Ranta-Eskola AJ. Use of the hydraulic bulge test in biaxial tensile testing. *Int J Mech Sci.* Pergamon; 1979;21(8):457–65.
173. Reddy GK, Enwemeka CS. A simplified method for the analysis of hydroxyproline in biological tissues. *Clin Biochem.* 1996 Jun;29(3):225–9.
174. Tullberg-Reinert H, Jundt G. In situ measurement of collagen synthesis by human bone cells with a sirius red-based colorimetric microassay: effects of transforming growth factor beta 2 and ascorbic acid 2-phosphate. *Histochem Cell Biol.* 1999;112(4):271–6.
175. Lin Y-K, Kuan C-Y. Development of 4-hydroxyproline analysis kit and its application to collagen quantification. *Food Chem.* Elsevier Ltd; 2010 Apr;119(3):1271–7.
176. Gordon MK, Hahn RA. *Collagens. Cell and Tissue Research.* Springer-Verlag; 2010.339:247–57.
177. Haus JM, Carrithers JA, Trappe SW, Trappe TA. Collagen, cross-linking, and advanced glycation end products in aging human skeletal muscle. *J Appl Physiol.* American Physiological Society; 2007;103(6):2068–76.
178. Stegemann H, Stalder K. Determination of hydroxyproline. *Clin Chim Acta [Internet].* 1967;18(2):267–73.

179. Stimler NP. High-performance liquid chromatographic quantitation of collagen biosynthesis in explant cultures. *Anal Biochem.* 1984 Oct;142(1):103–8.
180. Green, G.D.; Reagan K. Determination of hydroxyproline by high pressure liquid chromatography. *Anal Biochem.* 1992;201(2):265–9.
181. Malkusch W, Rehn B, Bruch J. Advantages of Sirius Red staining for quantitative morphometric collagen measurements in lungs. *Exp Lung Res.* 1995;21(1):67–77.
182. Kume S, Takeya M, Mori T, Araki N, Suzuki H, Horiuchi S, et al. Immunohistochemical and ultrastructural detection of advanced glycation end products in atherosclerotic lesions of human aorta with a novel specific monoclonal antibody. *Am J Pathol.* 1995 147(3):654–67.
183. American Society of Biological Chemists. WH, Rockefeller Institute for Medical Research. S, American Society for Biochemistry and Molecular Biology. *The Journal of biological chemistry. Journal of Biological Chemistry.* American Society for Biochemistry and Molecular Biology; 1954. 211;915-926
184. Slowik-Zylka D, Safranow K, Dziedziejko V, Ciechanowski K, Chlubek D. Association of plasma pentosidine concentrations with renal function in kidney graft recipients. *Clin Transplant.* Blackwell Publishing Ltd; 2010;24(6):839–47.
185. Sakata N. Modification of elastin by pentosidine is associated with the calcification of aortic media in patients with end-stage renal disease. *Nephrol Dial Transplant.* 2003;18(8):1601–9.
186. Pataridis S, Eckhardt A, Mikulíková K, Sedláková P, Mikšík I. Identification of

- collagen types in tissues using HPLC-MS/MS. *J Sep Sci*. WILEY-VCH Verlag; 2008;31(20):3483–8.
187. Reddy PH, Beal MF. Amyloid beta, mitochondrial dysfunction and synaptic damage: implications for cognitive decline in aging and Alzheimer's disease. *Trends Mol Med*. 2008;14(2):45–53.
188. Yu S, Tozzi C, Babiarz J, Leppert P. Collagen changes in rat cervix in pregnancy-- polarized light microscopic and electron microscopic studies. *Proc Soc Exp Biol Med*. 1995;209(4):360–8.
189. Wilson T, Sheppard C. Theory and practice of scanning optical microscopy. London Academic Press; 1984: 213
190. Papi M, Paoletti P, Geraghty B, Akhtar R. Nanoscale characterization of the biomechanical properties of collagen fibrils in the sclera. *Appl Phys Lett*. 2014;104(10):103703.
191. Hoemann CD, Sun J, Chrzanowski V, Buschmann MD. A multivalent assay to detect glycosaminoglycan, protein, collagen, RNA, and DNA content in milligram samples of cartilage or hydrogel-based repair cartilage. *Anal Biochem*. 2002;300(1):1–10.
192. Uchiyama A, Ohishi T, Takahashi M, Kushida K, Inoue T, Fujie M, et al. Fluorophores from aging human articular cartilage. *J Biochem*. 1991;110(5):714–8.
193. Colgrave ML, Allingham PG, Jones A. Hydroxyproline quantification for the estimation of collagen in tissue using multiple reaction monitoring mass spectrometry. *J Chromatogr A*. Elsevier; 2008;1212(1–2):150–3.

194. Forchheimer D, Platz D, Tholén EA, Haviland DB. Model-based extraction of material properties in multifrequency atomic force microscopy. *Phys Rev B - Condens Matter Mater Phys.* 2012;85(19):1–7.
195. Huang D, Swanson EA, Lin CP, Schuman JS, Stinson WG, Chang W, et al. Optical coherence tomography. *Science. NIH Public Access;* 1991;254(5035):1178–81.
196. Wang S, Larin K V. Optical coherence elastography for tissue characterization: A review. *Journal of Biophotonics. WILEY-VCH Verlag;* 2015;8:279–302.
197. Schmitt JM. OCT elastography: imaging microscopic deformation and strain of tissue. *Opt Express. Optical Society of America;* 1998;3(6):199.
198. Kennedy BF, Kennedy KM, Sampson DD. A review of optical coherence elastography: Fundamentals, techniques and prospects. *IEEE Journal on Selected Topics in Quantum Electronics.* 2014. 20:272–88.
199. Guan G, Li C, Ling Y, Yang Y, Vorstius JB, Keatch RP, et al. Quantitative evaluation of degenerated tendon model using combined optical coherence elastography and acoustic radiation force method. *J Biomed Opt. International Society for Optics and Photonics;* 2013;18(11):111417.
200. Chang K-C, Hsu K-L, Tseng C-D, Lin Y-D, Cho Y-L, Tseng Y-Z. Aminoguanidine prevents arterial stiffening and cardiac hypertrophy in streptozotocin-induced diabetes in rats. *Br J Pharmacol.* 2006;147(8):944–50.
201. Goldin A, Beckman J A, Schmidt AM, Creager M A. Advanced glycation end products: sparking the development of diabetic vascular injury. *Circulation.* 2006;114(6):597–

605.

202. de Ranitz-Greven WL, Kaasenbrood L, Poucki WK, Hamerling J, Bos DC, Visser GHA, et al. Advanced glycation end products, measured as skin autofluorescence, during normal pregnancy and pregnancy complicated by diabetes mellitus. *Diabetes Technol Ther.* 2012;4(12):1134–9.
203. Walsh BA, Busch BL, Mullick AE, Reiser KM, Rutledge JC. 17 β -Estradiol Reduces Glycooxidative Damage in the Artery Wall. *Arterioscler Thromb Vasc Biol.* 1999;19(4):840–6.
204. Lin J, Zuo G, Xu Y, Xiong J. Estrogen Reduces Advanced Glycation End Products Induced HUVEC Inflammation Via NF-kappa B Pathway. *Lat Am J Pharm.* 2014;33(1):2383.
205. Lee S, Sakurai T, Ohsako M, Saura R, Hatta H, Atomi Y. Tissue stiffness induced by prolonged immobilization of the rat knee joint and relevance of AGEs (pentosidine). *Connect Tissue Res.* 2010;51(6):467–77.
206. Yoshida N, Okumura K, Aso Y. High serum pentosidine concentrations are associated with increased arterial stiffness and thickness in patients with type 2 diabetes. *Metabolism.* 2005;54(3):345–50.
207. Wagner DR, Reiser KM, Lotz JC. Glycation increases human annulus fibrosus stiffness in both experimental measurements and theoretical predictions. *J Biomech.* 2006;39(6):1021–9.
208. Reddy GK. Cross-Linking in Collagen by Nonenzymatic Glycation Increases the

- Matrix Stiffness in Rabbit Achilles Tendon. *Exp Diabetes Res.* 2004;5(2):143–53.
209. Yang Y, Leone LM, Kaufman LJ. Elastic Moduli of Collagen Gels Can Be Predicted from Two-Dimensional Confocal Microscopy. *Biophys J* 2009;97(7):2051–60.
210. Christiansen DL, Huang EK, Silver FH. Assembly of type I collagen: Fusion of fibril subunits and the influence of fibril diameter on mechanical properties. *Matrix Biol.* 2000;19(5):409–20.
211. Osmers RGW, Adelman-Grill BC, Rath W, Stuhlsatz HW, Tschesche H, Kuhn W. Biochemical Events in Cervical Ripening Dilatation during Pregnancy and Parturition. *J Obstet Gynaecol (Lahore).* 1995;21(2):185–94.
212. Neame PJ, Kay CJ, McQuillan DJ, Beales MP, Hassell JR. Independent modulation of collagen fibrillogenesis by decorin and lumican. *Cell Mol Life Sci.* 2000 57(5):859–63.
213. Yang Y, Rupani A, Bagnaninchi P, Wimpenny I, Weightman A. Study of optical properties and proteoglycan content of tendons by polarization sensitive optical coherence tomography. *J Biomed Opt.* 2012;17(8):81417.
214. Goh S-Y, Cooper ME. Clinical review: The role of advanced glycation end products in progression and complications of diabetes. *J Clin Endocrinol Metab.* 2008;93(4):1143–52.
215. Lee H, Chi SW, Lee PY, Kang S, Cho S, Lee C-K, et al. Reduced formation of advanced glycation endproducts via interactions between glutathione peroxidase 3 and dihydroxyacetone kinase 1. *Biochem Biophys Res Commun.* 2009;389(1):177–80.
216. Hammes HP. Pathophysiological mechanisms of diabetic angiopathy. *J Diabetes*

Complications. 2003;17(2 Suppl):16–9.

217. Mizutani K, Ikeda K, Kawai Y, Yamori Y. Protective Effect Of Resveratrol On Oxidative Damage In Male And Female Stroke-Prone Spontaneously Hypertensive Rats. *Clin Exp Pharmacol Physiol*. 2001;28(1–2):55–9.
218. Lean JM, Davies JT, Fuller K, Jagger CJ, Kirstein B, Partington GA, et al. A crucial role for thiol antioxidants in estrogen-deficiency bone loss. *J Clin Invest*. 2003;112(6):915–23.
219. Rulli A, Antognelli C, Prezzi E, Baldracchini F, Piva F, Giovannini E, et al. A possible regulatory role of 17 β -estradiol and tamoxifen on glyoxalase I and glyoxalase II genes expression in MCF7 and BT20 human breast cancer cells. *Breast Cancer Res Treat*. 2006;96(2):187–96.
220. Miyata T, van Ypersele de Strihou C, Imasawa T, Yoshino A, Ueda Y, Ogura H, et al. Glyoxalase I deficiency is associated with an unusual level of advanced glycation end products in a hemodialysis patient. *Kidney Int*. 2001;60(6):2351–9.
221. Mailankot M, Padmanabha S, Pasupuleti N, Major D, Howell S, Nagaraj RH. Glyoxalase I activity and immunoreactivity in the aging human lens. *Biogerontology*. 2009;10(6):711–20.
222. Bednarek-Tupikowska G, Bohdanowicz-Pawlak A, Bidzińska B, Milewicz A, Antonowicz-Juchniewicz J, Andrzejak R. Serum lipid peroxide levels and erythrocyte glutathione peroxidase and superoxide dismutase activity in premenopausal and postmenopausal women. *Gynecol Endocrinol*. 2001;15(4):298–303.

223. Smedsrød B, Melkko J, Araki N, Sano H, Horiuchi S. Advanced glycation end products are eliminated by scavenger-receptor-mediated endocytosis in hepatic sinusoidal Kupffer and endothelial cells. *Biochem J.* 1997 Mar 1;322 (Pt 2):567–73.
224. Bucciarelli LG, Wendt T, Rong L, Lalla E, Hofmann MA, Goova MT, et al. RAGE is a multiligand receptor of the immunoglobulin superfamily: implications for homeostasis and chronic disease. *Cell Mol Life Sci.* 2002;59(7):1117–28.
225. Dehkordi RF, Parchami A. Effect of Hormonal Manipulations on the Pattern of the Vaginal Tissue Structure. *waset.org.* 2012;4(6):249–52.
226. Williams BR, Gelman RA, Poppke DC, Piez KA. Collagen fibril formation optimal in vitro conditions and preliminary kinetic results*. 1978;253(18):6578-85
227. Paderi JE, Sistiabudi R, Ivanisevic A, Panitch A. Collagen-binding peptidoglycans: a biomimetic approach to modulate collagen fibrillogenesis for tissue engineering applications. *Tissue Eng Part A.* Mary Ann Liebert, Inc.; 2009;15(10):2991–9.
228. Sidhu SS, Yuan S, Innes AL, Kerr S, Woodruff PG, Hou L, et al. Roles of epithelial cell-derived periostin in TGF-beta activation, collagen production, and collagen gel elasticity in asthma. *Proc Natl Acad Sci U S A.* National Academy of Sciences; 2010;107(32):14170–5.
229. Boer GJ. Ethical guidelines for the use of human embryonic or fetal tissue for experimental and clinical neurotransplantation and research. *J Neurol.* Springer-Verlag; 1994;242(1):1–13.
230. Antoni D, Burckel H, Josset E, Noel G. Three-dimensional cell culture: a breakthrough

- in vivo. *Int J Mol Sci. Multidisciplinary Digital Publishing Institute (MDPI)*; 2015;16(3):5517–27.
231. McPherson JM, Wallace DG, Sawamura SJ, Conti A, Condell RA, Wade S, et al. Collagen Fibrillogenesis In Vitro: A Characterization of Fibril Quality as a Function of Assembly Conditions. *Coll Relat Res.* 1985;5(2):119–35.
232. Brightman AO, Rajwa BP, Sturgis JE, McCallister ME, Robinson JP, Voytik-Harbin SL. Time-lapse confocal reflection microscopy of collagen fibrillogenesis and extracellular matrix assembly in vitro. *Biopolymers.* John Wiley & Sons, Inc.; 2000;54(3):222–34.
233. Garg AK, Berg RA, Silver FH, Garg HG. Effect of proteoglycans on type I collagen fibre formation. *Biomaterials.* 1989;10(6):413–9.
234. Reed CC, Iozzo R V. The role of decorin in collagen fibrillogenesis and skin homeostasis. *Glycoconjugate Journal.* Kluwer Academic Publishers; 2002. 19:249–55.
235. Kadler KE, Hill A, Canty-Laird EG. Collagen fibrillogenesis: fibronectin, integrins, and minor collagens as organizers and nucleators. *Current Opinion in Cell Biology.* Elsevier Current Trends; 2008. 20:495–501.
236. Donald AM. The use of environmental scanning electron microscopy for imaging wet and insulating materials. *Nat Mater.* Nature Publishing Group; 2003;2(8):511–6.
237. Weli HK, Akhtar R, Chang Z, Li W-W, Cooper J, Yang Y. Advanced glycation products' levels and mechanical properties of vaginal tissue in pregnancy. *Eur J Obstet Gynecol Reprod Biol.* 2017;214:78–85.

238. Cerami C, Founds H, Nicholl I, Mitsuhashi T, Giordano D, Vanpatten S, et al. Tobacco smoke is a source of toxic reactive glycation products. *Med Sci*. 1997;94:13915–20.
239. Mikulikova K, Eckhardt A, Kunes J. Advanced glycation end-product pentosidine accumulates in various tissues of rats with high fructose intake. *Physiol*. 2008;57(1):89–94.
240. Genuth S, Sun W, Cleary P, Sell DR, Dahms W, Malone J, et al. Glycation and carboxymethyllysine levels in skin collagen predict the risk of future 10-year progression of diabetic retinopathy and nephropathy in the diabetes control and complications trial and epidemiology of diabetes interventions and complications. *Diabetes*. NIH Public Access; 2005;54(11):3103–11.
241. Sternberg M, M'bemba J, Urios P, Borsos A-M, Selam J-L, Peyroux J, et al. Skin collagen pentosidine and fluorescence in diabetes were predictors of retinopathy progression and creatininemia increase already 6years after punch-biopsy. *Clin Biochem*. 2016;49(3):225–31.
242. Yamagishi SI, Fukami K, Matsui T. Evaluation of tissue accumulation levels of advanced glycation end products by skin autofluorescence: A novel marker of vascular complications in high-risk patients for cardiovascular disease. *Int J Cardiol*. 2015.15;185:263–8.
243. Kotova SL, Timashev PS, Guller AE, Shekhter AB, Misurkin PI, Bagratashvili VN, et al. Collagen Structure Deterioration in the Skin of Patients with Pelvic Organ Prolapse Determined by Atomic Force Microscopy. *Microsc Microanal*. 2015;21(2):324–33.

244. Phillips CH, Anthony F, Benyon C, Monga AK. Collagen metabolism in the uterosacral ligaments and vaginal skin of women with uterine prolapse. *BJOG An Int J Obstet Gynaecol*. Blackwell Science Ltd; 2006;113(1):39–46.
245. Chen Y, Huang J, Hu C, Hua K. Relationship of advanced glycation end products and their receptor to pelvic organ prolapse. 2015;8(3):2288–99.
246. Ramasamy R, Yan SF, Schmidt AM. Advanced glycation endproducts: from precursors to RAGE: round and round we go. *Amino Acids*. 2012;42(4):1151–61.
247. Lucey GM, Wei B, Singer EJ, Mareninov S. A review of room temperature storage of biospecimen tissue and nucleic acids for anatomic pathology laboratories and biorepositories. 2015;47(0):267–73.
248. Karlsson JOM, Toner M. Long-term storage of tissues by cryopreservation: critical issues. *Biomaterials*. 1996;17(3):243–56.
249. Bravo D, Rigley TH, Gibran N, Strong DM, Newman-Gage H. Effect of storage and preservation methods on viability in transplantable human skin allografts. *Burns*. 2000;26(4):367–78.
250. Zhu ZM. The stretching of mouse skin in vivo: effect on epidermal proliferation and thickness. *Zhonghua Wai Ke Za Zhi*. 1989;27(3):169–72, 190.
251. Kerkhof MH, Ruiz-Zapata AM, Bril H, Bleeker MCG, Belien JAM, Stoop R, et al. Changes in tissue composition of the vaginal wall of premenopausal women with prolapse. *Am J Obstet Gynecol*. 2014;210(2):168.e1-9.
252. Koshy SSKG, Reddy HK, Shukla HH. Collagen cross-linking: new dimension to

- cardiac remodeling. *Cardiovasc.* 2003;57(3):594–8.
253. Verzijl N, DeGroot J, Thorpe SR, Bank RA, Shaw JN, Lyons TJ, et al. Effect of collagen turnover on the accumulation of advanced glycation end products. *J Biol Chem.* 2000;275(50):39027–31.
254. Mott JD, Khalifah RG, Nagase H, Shield CF, Hudson JK, Hudson BG. Nonenzymatic glycation of type IV collagen and matrix metalloproteinase susceptibility. *Kidney Int. Elsevier Masson SAS*; 1997;52(5):1302–12. 5
255. Chaney R, Blemings K, Bonner J, Klandorf H. Pentosidine as a Measure of Chronological Age in Wild Birds. *Am Ornithol Soc.* 2003;120(2):394–9.
256. Waanders F, Greven WL, Baynes JW, Thorpe SR, Kramer AB, Nagai R, et al. Renal accumulation of pentosidine in non-diabetic proteinuria-induced renal damage in rats. *Nephrol Dial Transplant.* 2005;20(10):2060–70.
257. Yoshida K, Jiang H, Kim M, Vink J, Cremers S, Paik D, et al. Quantitative Evaluation of Collagen Crosslinks and Corresponding Tensile Mechanical Properties in Mouse Cervical Tissue during Normal Pregnancy. Kreplak L, editor. *PLoS One.* 2014;9(11):e112391.
258. Wang S, Zhang Z, Lü D, Xu Q. Effects of mechanical stretching on the morphology and cytoskeleton of vaginal fibroblasts from women with pelvic organ prolapse. *Int J Mol Sci.* 2015;16(5):9406–19.
259. Thornalley PJ. Glyoxalase I – structure, function and a critical role in the enzymatic defence against glycation. *Biochem Soc Trans.* 2003;31(6):1343–8.

260. Isik H, Aynioglu O, Sahbaz A, Selimoglu R, Timur H, Harma M. Are hypertension and diabetes mellitus risk factors for pelvic organ prolapse? *Eur J Obstet Gynecol Reprod Biol.* 2016;197:59–62.
261. Swift SE, Pound T, Dias JK. Case–Control Study of Etiologic Factors in the Development of Severe Pelvic Organ Prolapse. *Int Urogynecol J.* 2001;12(3):187–92.
262. Landahl S, Bengtsson C, Sigurdsson J A., Svanborg a., Svardsudd K. Age-related changes in blood pressure. *Hypertension.* 1986;8(11):1044–9.
263. Bakris G, Bank A, Kass D, Neutel J, Preston R, Oparil S. Advanced glycation end-product cross-link breakersA novel approach to cardiovascular pathologies related to the aging process. *Am J Hypertens.* 2004;17(12):S23–30.
264. Hegab Z. Role of advanced glycation end products in cardiovascular disease. *World J Cardiol.* 2012;4(4):90.
265. Singh VP, Bali A, Singh N, Jaggi AS. Advanced Glycation End Products and Diabetic Complications. *Korean J Physiol Pharmacol.* 2014;18(1):1.
266. Badi SS, Foarfa MC, Rica N, Grosu F, Stanescu C. Etiopathogenic, therapeutic and histopathological aspects upon the anterior vaginal wall prolapse. *Rom J Morphol Embryol.* 2015;56(2):765–70.
267. Scotti RJ, Lazarou G, Greston WM. Anatomy of the pelvic floor. In: *Female Pelvic Medicine and Reconstructive Pelvic Surgery.* 2006; 25–36.
268. De Landsheere L, Munaut C, Nusgens B, Maillard C, Rubod C, Nisolle M, et al. Histology of the vaginal wall in women with pelvic organ prolapse: a literature review.

Int Urogynecol J. 2013;24(12):2011–20.

269. Kannan K, McConnell A, McLeod M, Rane A. Microscopic alterations of vaginal tissue in women with pelvic organ prolapse. *J Obstet Gynaecol (Lahore)*. 2011;31(3):250–3.
270. Inal HA, Kaplan PB, Usta U, Taştekin E, Aybatlı A, Tokuc B. Neuromuscular morphometry of the vaginal wall in women with anterior vaginal wall prolapse. *Neurourol Urodyn*. 2009; 29(3):458-63
271. Suzme R, Yalcin O, Gurdol F, Gungor F, Bilir A. Connective tissue alterations in women with pelvic organ prolapse and urinary incontinence. *Acta Obstet Gynecol Scand*. 2007;86(7):882–8.
272. Boreham MK, Wai CY, Miller RT, Schaffer JI, Word RA. Morphometric analysis of smooth muscle in the anterior vaginal wall of women with pelvic organ prolapse. *Am J Obstet Gynecol*. 2002;187(1):56–63.
273. Kökçü A, Yanik F, Çetinkaya M, Alper T, Kandemir B, Malatyalioglu E. Histopathological evaluation of the connective tissue of the vaginal fascia and the uterine ligaments in women with and without pelvic relaxation. *Arch Gynecol Obstet*. 2002;266(2):75–8.
274. Karam JA, Vazquez D V., Lin VK, Zimmern PE. Elastin expression and elastic fibre width in the anterior vaginal wall of postmenopausal women with and without prolapse. *BJU Int*. 2007;100(2):346–50.
275. Zong W, Stein SE, Starcher B, Meyn LA, Moalli PA. Alteration of Vaginal Elastin Metabolism in Women With Pelvic Organ Prolapse. *Obstet Gynecol*. 2010;115(5):953–

- 61.
276. North C, Creighton S, Smith A. A comparison of genital sensory and motor innervation in women with pelvic organ prolapse and normal controls including a pilot study on the effect of vaginal prolapse surgery on genital sensation: a prospective study. *BJOG An Int J Obstet Gynaecol.* 2013;120(2):193–9.
277. Li Z-G. Neuropeptide Y innervation in the vaginal mucosa among patients with pelvic organ prolapse. *Mol Med Rep.* 2011;5(2):444-8
278. Cotsarelis G, Cheng S-Z, Dong G, Sun T-T, Lavker RM. Existence of slow-cycling limbal epithelial basal cells that can be preferentially stimulated to proliferate: Implications on epithelial stem cells. *Cell.* 1989;57(2):201–9.
279. Mackenzie IC, Miles AEW. The effect of chronic frictional stimulation on hamster cheek pouch epithelium. *Arch Oral Biol. Pergamon;* 1973;18(11):1341–IN1.
280. Squier C A The stretching of mouse skin in vivo: effect on epidermal proliferation and thickness. *The Journal of investigative dermatology. Elsevier;* 1980. 74;68–71.
281. Liapis A, Bakas P, Pafiti A, Frangos-Plemenos M, Arnoyannaki N, Creatsas G. Changes of collagen type III in female patients with genuine stress incontinence and pelvic floor prolapse. *Eur J Obstet Gynecol Reprod Biol.* 2001;97(1):76–9.
282. Kotova SL, Shekhter AB, Timashev PS, Guller AE, Mudrov AA, Timofeeva VA, et al. AFM study of the extracellular connective tissue matrix in patients with pelvic organ prolapse. *J Surf Investig X-ray, Synchrotron Neutron Tech.* 2014;8(4):754–60.
283. Badiou W, Granier G, Bousquet P-J, Monrozies X, Mares P, de Tayrac R. Comparative

- histological analysis of anterior vaginal wall in women with pelvic organ prolapse or control subjects. A pilot study. *Int Urogynecol J*. 2008;19(5):723–9.
284. Meijerink AM, Van Rijssel RH, Van Der Linden PJQ. Tissue composition of the vaginal wall in women with pelvic organ prolapse. *Gynecol Obstet Invest*. 2013;75(1):21–7.
285. Bortolini MAT, Shynlova O, Drutz HP, Castro RA, Girao MJ, Lye S, et al. Expression of genes encoding smooth muscle contractile proteins in vaginal tissue of women with and without pelvic organ prolapse. *Neurourol Urodyn*. 2012;31(1):109–14.
286. Sridharan I, Ma Y, Kim T, Kobak W, Rotmensch J, Wang R. Structural and mechanical profiles of native collagen fibers in vaginal wall connective tissues. *Biomaterials*. 2012;33(5):1520–7.
287. Söderberg MW, Falconer C, Bystrom B, Malmström A, Ekman G. Young women with genital prolapse have a low collagen concentration. *Acta Obstet Gynecol Scand*. Munksgaard International Publishers; 2004;83(12):1193–8.
288. Falconer C, Ekman-Ordeberg G, Ulmsten U, Westergren-Thorsson G, Barchan K, Malmström A. Changes in paraurethral connective tissue at menopause are counteracted by estrogen. *Maturitas*. 1996;24(3):197–204.
289. Kim T, Sridharan I, Ma Y, Zhu B, Chi N, Kobak W, et al. Identifying distinct nanoscopic features of native collagen fibrils towards early diagnosis of pelvic organ prolapse. *Nanomedicine Nanotechnology, Biol Med*. 2016;12(3):667–75.
290. Egorov V, Urogynecology P, Street E, B- S. Quantifying vaginal tissue elasticity under

normal and prolapse conditions by tactile imaging. 2013;23(4):459–66.

291. DeLancey JOL. Anatomy and Biomechanics of Genital Prolapse. *Clinical obstetrics and gynecology*. 1993;30:897–909.
292. Sims TJ, Rasmussen LM, Oxlund H, Bailey AJ. The role of glycation cross-links in diabetic vascular stiffening. *Diabetologia*. 1996;39(8):946–51.
293. Vashishth D, Gibson G., Khoury J., Schaffler M., Kimura J, Fyhrie D. Influence of nonenzymatic glycation on biomechanical properties of cortical bone. *Bone*. 2001;28(2):195–201.
294. Li C, Guan G, Ling Y, Hsu YT, Song S, Huang JTJ, et al. Detection and characterisation of biopsy tissue using quantitative optical coherence elastography (OCE) in men with suspected prostate cancer. *Cancer Lett* 2015;357(1):121–8.
295. Jaasma MJ, Bayraktar HH, Niebur GL, Keaveny TM. Biomechanical effects of intraspecimen variations in tissue modulus for trabecular bone. *J Biomech*. 2002;35(2):237–46.
296. Zysset PK, Edward Guo X, Edward Hoffler C, Moore KE, Goldstein SA. Elastic modulus and hardness of cortical and trabecular bone lamellae measured by nanoindentation in the human femur. *J Biomech*. 1999;32(10):1005–12.
297. Krouskop TA, Wheeler TM, Kallel F, Garra BS, Hall T. Elastic Moduli of Breast and Prostate Tissues under Compression. *Ultrason Imaging*. SAGE PublicationsSage CA: Los Angeles, CA; 1998;20(4):260–74.
298. Pawlaczyk M, Lelonkiewicz M, Wieczorowski M. Age-dependent biomechanical

- properties of the skin. *Postepy Dermatologii i Alergologii*. Termedia Publishing; 2013 30;302–6.
299. Goodrich M, Webb M, King B, Bampton A, Campeau N, Riederer S. Magnetic Resonance Imaging of Pelvic Floor Relaxation Dynamic Analysis and Evaluation of Patients Before and After Surgical Repair. 1993. 883–91.
300. Manuscript A, Images R, Vaginal A. The Appearance of Levator Ani Muscle Abnormalities in Magnetic Resonance Images After Vaginal Delivery. 2005;101(1):46–53.
301. Comiter C, Vasavada S, Barbaric Z, Gousse A, S R. Grading pelvic prolapse and pelvic floor relaxation using dynamic magnetic resonance imaging. *Urology*. 1999;54(3):454–457.
302. Chlanda A, Rebis J, Kijeńska E, Wozniak MJ, Rozniatowski K, Swieszkowski W, et al. Quantitative imaging of electrospun fibers by PeakForce Quantitative NanoMechanics atomic force microscopy using etched scanning probes. *Micron*. 2015 May;72:1–7.
303. Gill EJ, Hurt WG. Pathophysiology of Pelvic Organ Prolapse. *Obstet Gynecol Clin North Am*. Elsevier; 1998;25(4):757–69.

9 APPENDICES

APPENDIX 1: CAP STUDY PROFORMA

Participant Number:

CAP STUDY DATA FORM (CONFIDENTIAL)

Participant questions:

1. Age:

2. a. Number of deliveries:

0 1 2 3 4 5 6 7 8 >8

b. Mode of deliveries

(Please indicate mode of delivery by ticking appropriate box in table below)

SVD = spontaneous Vaginal Delivery, VD = ~~Ventouse~~ Instrumental Delivery,

FD = Forceps Instrumental Delivery, C/S = Cesarean Section

	SVD	VD	FD	C/S
1 st delivered pregnancy				
2 nd delivered pregnancy				
3 rd delivered pregnancy				
4 th delivered pregnancy				
5 th delivered pregnancy				
6 th delivered pregnancy				
7 th delivered pregnancy				
8 th delivered pregnancy				

3. Smoking: Yes No

Participant Number:

If no, have you ever smoked previously: yes no

4. Do you experience any of these symptoms?

- Urinary dribbling: Yes No
- Fecal incontinence: Yes No
- Painful intercourse Yes No
- Feeling of fullness in vagina: Yes No
- Dragging sensation in pelvis: Yes No
- Other symptoms (please specify): _____

5. Have you ever had Hormonal Replacement Therapy (HRT)? Yes No

If yes: When did you start using it? _____

For how long did you use it? _____

6. Previous surgeries:

- Removal of ovaries: Yes No
- Removal of uterus/womb: Yes No
- Other surgeries (please specify): _____

7. Use of Medications:

- Steroids: Yes No
- Oestrogen cream: Yes No
- Others (please specify): _____

-----Thank you for taking time to answer these questions-----

Participant Number:

Surgeon questions:

1. Medical history:

• Diabetes? Yes No

• Hypertension Yes No

• Other medical

conditions _____

2. ICIQ-VS assessment:

• Total vaginal symptoms score

• Sexual matters score

• Quality of life score

3. Urinary Incontinence: Stress Urge Mixed

4. Type and Grade of Prolapse: _____

5. Type of surgery performed: _____

6. Reason for surgery: Prolapse heavy bleeding Cancer

APPENDIX 2: ICIQVS QUESTIONNAIRE

Initial number

ICIQ-VS 10/05

CONFIDENTIAL

VAGINAL SYMPTOMS QUESTIONNAIRE

Many people experience vaginal symptoms some of the time. We are trying to find out how many people experience vaginal symptoms, and how much they bother them. We would be grateful if you could answer the following questions, thinking about how you have been, on average, over the PAST FOUR WEEKS.

Please write in today's date:

DAY MONTH YEAR

Please write in your date of birth:

DAY MONTH YEAR

Vaginal symptoms

1a.	Are you aware of dragging pain in your lower abdomen?	never	<input type="text"/>	0								
		occasionally	<input type="text"/>	1								
		sometimes	<input type="text"/>	2								
		most of the time	<input type="text"/>	3								
		all of the time	<input type="text"/>	4								
1b.	How much does this bother you? <i>Please ring a number between 0 (not at all) and 10 (a great deal)</i>											
		0	1	2	3	4	5	6	7	8	9	10
		not at all										a great deal

2a.	Are you aware of soreness in your vagina?	never	<input type="text"/>	0								
		occasionally	<input type="text"/>	1								
		sometimes	<input type="text"/>	2								
		most of the time	<input type="text"/>	3								
		all of the time	<input type="text"/>	4								
2b.	How much does this bother you? <i>Please ring a number between 0 (not at all) and 10 (a great deal)</i>											
		0	1	2	3	4	5	6	7	8	9	10
		not at all										a great deal

3a. Do you feel that you have reduced sensation or feeling in or around your vagina?

not at all 0
a little 1
somewhat 2
a lot 3

3b. How much does this bother you?
Please ring a number between 0 (not at all) and 10 (a great deal)

0 1 2 3 4 5 6 7 8 9 10
not at all a great deal

Prolapse is a common condition affecting the normal support of the pelvic organs, which results in descent or 'dropping down' of the vaginal walls and/or the pelvic organs themselves. This can include the bladder, the bowel and the womb. Symptoms are usually worse on standing up and straining (e.g. lifting, coughing or exercising) and usually better when lying down and relaxing.

Prolapse may cause a variety of problems. We are trying to find out how many people experience prolapse, and how much this bothers them. We would be grateful if you could answer the following questions, thinking about how you have been, on average, over the **PAST FOUR WEEKS**.

4a. Do you feel that your vagina is too loose or lax?

not at all 0
a little 1
somewhat 2
a lot 3

4b. How much does this bother you?
Please ring a number between 0 (not at all) and 10 (a great deal)

0 1 2 3 4 5 6 7 8 9 10
not at all a great deal

5a. Are you aware of a lump or bulge coming down in your vagina?

never 0
occasionally 1
sometimes 2
most of the time 3
all of the time 4

5b. How much does this bother you?
Please ring a number between 0 (not at all) and 10 (a great deal)

0 1 2 3 4 5 6 7 8 9 10
not at all a great deal

6a. Do you feel a lump or bulge come out of your vagina, so that you can feel it on the outside or see it on the outside?

never 0
occasionally 1
sometimes 2
most of the time 3
all of the time 4

6b. How much does this bother you?
Please ring a number between 0 (not at all) and 10 (a great deal)

0 1 2 3 4 5 6 7 8 9 10
not at all a great deal

7a. Do you feel that your vagina is too dry?

never 0
occasionally 1
sometimes 2
most of the time 3
all of the time 4

7b. How much does this bother you?
Please ring a number between 0 (not at all) and 10 (a great deal)

0 1 2 3 4 5 6 7 8 9 10
not at all a great deal

8a. Do you have to insert a finger into your vagina to help empty your bowels?

never 0
occasionally 1
sometimes 2
most of the time 3
all of the time 4

8b. How much does this bother you?
Please ring a number between 0 (not at all) and 10 (a great deal)

0 1 2 3 4 5 6 7 8 9 10
not at all a great deal

9a. Do you feel that your vagina is too tight?

never
occasionally
sometimes
most of the time
all of the time

9b. How much does this bother you?
Please ring a number between 0 (not at all) and 10 (a great deal)

0 1 2 3 4 5 6 7 8 9 10
not at all a great deal

Sexual matters

We would be grateful if you could answer the following questions, thinking about how you have been, on average, over the **PAST FOUR WEEKS**.

10. Do you have a sex life at present?	yes	<input type="checkbox"/>	1
	no, because of my vaginal symptoms	<input type="checkbox"/>	0
	no, because of other reasons	<input type="checkbox"/>	2
If NO, please go to question 14			

11a. Do worries about your vagina interfere with your sex life?	not at all	<input type="checkbox"/>	0								
	a little	<input type="checkbox"/>	1								
	somewhat	<input type="checkbox"/>	2								
	a lot	<input type="checkbox"/>	3								
11b. How much does this bother you? <i>Please ring a number between 0 (not at all) and 10 (a great deal)</i>	0	1	2	3	4	5	6	7	8	9	10
	not at all										a great deal

12a. Do you feel that your relationship with your partner is affected by vaginal symptoms?	not at all	<input type="checkbox"/>	0								
	a little	<input type="checkbox"/>	1								
	somewhat	<input type="checkbox"/>	2								
	a lot	<input type="checkbox"/>	3								
12b. How much does this bother you? <i>Please ring a number between 0 (not at all) and 10 (a great deal)</i>	0	1	2	3	4	5	6	7	8	9	10
	not at all										a great deal

13. How much do you feel that your sex life has been spoilt by vaginal symptoms? <i>Please ring a number between 0 (not at all) and 10 (a great deal)</i>	0	1	2	3	4	5	6	7	8	9	10
	not at all										a great deal

Quality of life

We would be grateful if you could answer the following questions, thinking about how you have been, on average, over the **PAST FOUR WEEKS**.

14. Overall, how much do vaginal symptoms interfere with your everyday life? <i>Please ring a number between 0 (not at all) and 10 (a great deal)</i>	0	1	2	3	4	5	6	7	8	9	10
	not at all										a great deal

Thank you very much for answering these questions.

APPENDIX 3: ETHICAL APPROVAL FOR STUDY



Health Research Authority

NRES Committee London - Hampstead

Skipton House
Ground Floor, NRES/HRA
80 London Road
London SE1 6LH

Telephone: 020 7972 2554
Facsimile: 020 7972 2592

21 October 2013

Dr Ying Yang
Reader
Keele University
Thornburrow Drive
Hartshill
Stoke on Trent ST4 7QB

Dear Dr Yang

Study title: Investigation of the effect of ageing and alteration in connective tissue metabolism on pelvic organ prolapse
REC reference: 13/LOH1655
Protocol number: 1
IRAS project ID: 128131

The Proportionate Review Sub-committee of the NRES Committee London - Hampstead reviewed the above application on 16 October 2013.

We plan to publish your research summary wording for the above study on the NRES website, together with your contact details, unless you expressly withhold permission to do so. Publication will be no earlier than three months from the date of this favourable opinion letter. Should you wish to provide a substitute contact point, require further information, or wish to withhold permission to publish, please contact the Co-ordinator Mrs Alka Bhayani, NRESCommittee.London-Hampstead@nhs.net.

Ethical opinion

The members of the PR subcommittee did not have any ethical issues with the study.

On behalf of the Committee, the sub-committee gave a favourable ethical opinion of the above research on the basis described in the application form, protocol and supporting documentation, subject to the conditions specified below.

Ethical review of research sites

The favourable opinion applies to all NHS sites taking part in the study, subject to management permission being obtained from the NHS/HSC R&D office prior to the start of the study (see "Conditions of the favourable opinion" below).

Conditions of the favourable opinion

The favourable opinion is subject to the following conditions being met prior to the start of the study.

Management permission or approval must be obtained from each host organisation prior to the start of

the study at the site concerned.

Management permission ("R&D approval") should be sought from all NHS organisations involved in the study in accordance with NHS research governance arrangements.

Guidance on applying for NHS permission for research is available in the Integrated Research Application System or at <http://www.nrforum.nhs.uk>.

Where a NHS organisation's role in the study is limited to identifying and referring potential participants to research sites ("participant identification centre"), guidance should be sought from the R&D office on the information it requires to give permission for this activity.

For non-NHS sites, site management permission should be obtained in accordance with the procedures of the relevant host organisation.

Sponsors are not required to notify the Committee of approvals from host organisations.

Registration of Clinical Trials

All clinical trials (defined as the first four categories on the IRAS filter page) must be registered on a publically accessible database within 6 weeks of recruitment of the first participant (for medical device studies, within the timeline determined by the current registration and publication trees).

There is no requirement to separately notify the REC but you should do so at the earliest opportunity e.g. when submitting an amendment. We will audit the registration details as part of the annual progress reporting process.

To ensure transparency in research, we strongly recommend that all research is registered but for non-clinical trials this is not currently mandatory.

If a sponsor wishes to contest the need for registration they should contact Catherine Blewett (catherineblewett@nhs.net), the HRA does not, however, expect exceptions to be made. Guidance on where to register is provided within IRAS.

You should notify the REC in writing once all conditions have been met (except for site approvals from host organisations) and provide copies of any revised documentation with updated version numbers. The REC will acknowledge receipt and provide a final list of the approved documentation for the study, which can be made available to host organisations to facilitate their permission for the study. Failure to provide the final versions to the REC may cause delay in obtaining permissions.

It is the responsibility of the sponsor to ensure that all the conditions are complied with before the start of the study or its initiation at a particular site (as applicable).

Approved documents

The documents reviewed and approved were:

Document	Version	Date
Covering Letter		
Evidence of Insurance or Indemnity		23 July 2013
Investigator CV		
Other: CV of students Jason Cooper (19/09/2013) and Homayemem Well (10/08/2013)		
Other: Letter from Keele University		02 August 2013
Participant Consent Form	1	26 September 2013
Participant Information Sheet	1	26 September 2013

A Research Ethics Committee established by the Health Research Authority

Protocol	1	19 March 2013
REC application	128131/510250/1/716	

Membership of the Proportionate Review Sub-Committee

The members of the Sub-Committee who took part in the review are listed on the attached sheet.

Statement of compliance

The Committee is constituted in accordance with the Governance Arrangements for Research Ethics Committees and complies fully with the Standard Operating Procedures for Research Ethics Committees in the UK.

After ethical review

Reporting requirements

The attached document "After ethical review – guidance for researchers" gives detailed guidance on reporting requirements for studies with a favourable opinion, including:

- Notifying substantial amendments
- Adding new sites and investigators
- Notification of serious breaches of the protocol
- Progress and safety reports
- Notifying the end of the study

The NRES website also provides guidance on these topics, which is updated in the light of changes in reporting requirements or procedures.

Feedback

You are invited to give your view of the service that you have received from the National Research Ethics Service and the application procedure. If you wish to make your views known please use the feedback form available on the website.

Information is available at National Research Ethics Service website > After Review

13/LON1655:	Please quote this number on all correspondence
-------------	--

We are pleased to welcome researchers and R & D staff at our NRES committee members' training days – see details at <http://www.hra.nhs.uk/hra-training/>

With the Committee's best wishes for the success of this project.

Yours sincerely
PP



Miss Stephanie Ellis
Chair

Email: NRESCommittee.London-Hampstead@nhs.net

Enclosures: *List of names and professions of members who took part in the review*

"After ethical review – guidance for researchers" [SL-AR2]

A Research Ethics Committee established by the Health Research Authority